Oncothermia Journal

PUBLICATION OF ONCOTHERM | ISSN 2191-6438

VOLUME 38. | AUGUST 2026

www.oncothermia-journal.com

Imprint

Editorial

Dear reader, Dear colleagues, Dear hyperthermia specialists,

Our newspaper has been working on publishing a new edition for some time. However, economic challenges and the retirement of Editorial Board members have caused delays.

This volume includes materials from 2024, which are likely of interest to our readers.

The initial article discusses a novel phenomenon and a cutting-edge advancement in Oncothermia. The pulsed and modulated RF signal, derived from recent research, shows potential to enhance clinical practice and yield better results.

The review of preclinical verifications of oncothermia is divided into three parts, providing compelling evidence to doctors and patients about the method's exceptional capabilities and clear excellence, highlighting the shift toward immuno-oncology.

These expectations are fulfilled in clinical practice, as illustrated by Dr. Nair's article on successfully treating high-grade glioma. Additionally, his other article emphasizes the significance of integrative medicine in managing breast cancer, specifically through Oncothermia.

Dr. Kim's article offers a clear summary of the fundamentals and key applications of Oncothermia, presenting an informative and well-structured review of this fast-evolving subject.

I believe this material offers an excellent update on the successes of the mEHT method. You will find this issue of Oncothermia Journal useful in your daily medical practice. Recent preclinical and clinical data highlight the superiority of mEHT, confirming its expected benefits and validating its role in oncology.

Dr. Andras Szasz
Professor, Chair, Biotechnics Department of Hungarian University of Agriculture and Life Sciences

Liebe Leser, liebe Kollegen, liebe Hyperthermie-Experten,

Unsere Zeitung arbeitet seit einiger Zeit daran, eine neue Ausgabe zu veröffentlichen. Wirtschaftliche Herausforderungen und der Ruhestand von Mitgliedern des Redaktionsausschusses haben jedoch zu Verzögerungen geführt.

Diese Ausgabe enthält Materialien aus dem Jahr 2024, die für unsere Leser von Interesse sein dürften.

Der erste Artikel befasst sich mit einem neuartigen Phänomen und einer bahnbrechenden Weiterentwicklung in der Oncothermie. Das aus jüngsten Forschungsergebnissen hervorgegangene gepulste und modulierte HF-Signal zeigt das Potenzial, die klinische Praxis zu verbessern und bessere Ergebnisse zu erzielen.

Die Übersicht über die präklinischen Verifizierungen der Oncothermie ist in drei Teile gegliedert und liefert Ärzten und Patienten überzeugende Belege für die außergewöhnlichen Möglichkeiten und die klare Überlegenheit der Methode. Dabei wird insbesondere die Entwicklung hin zur Immunonkologie hervorgehoben.

Diese Erwartungen werden in der klinischen Praxis erfüllt, wie der Artikel von Dr. Nair über die erfolgreiche Behandlung eines hochgradigen Glioms zeigt. Darüber hinaus unterstreicht sein weiterer Artikel die Bedeutung der integrativen Medizin bei der Behandlung von Brustkrebs, insbesondere durch den Einsatz der Oncothermie.

Der Artikel von Dr. Kim bietet eine klare Zusammenfassung der Grundlagen und der wichtigsten Anwendungen der Oncothermie und stellt eine informative und gut strukturierte Übersicht über dieses sich schnell entwickelnde Gebiet dar.

Ich bin der Meinung, dass dieses Material eine ausgezeichnete Aktualisierung über die Erfolge der mEHT-Methode bietet. Sie werden diese Ausgabe des Oncothermia Journal für Ihre tägliche medizinische Praxis als nützlich empfinden. Die aktuellen präklinischen und klinischen Daten unterstreichen die Überlegenheit der mEHT, bestätigen ihre erwarteten Vorteile und belegen ihre Rolle in der Onkologie.

Rules of submission

As the editorial team we are committed to a firm and coherent editorial line and the highest possible printing standards. But it is mainly you, the author, who makes sure that the Oncothermia Journal is an interesting and diversified magazine. We want to thank every one of you who supports us in exchanging professional views and experiences. To help you and to make it easier for both of us, we prepared the following rules and guidelines for abstract submission.

Als redaktionelles Team vertreten wir eine stringente Linie und versuchen, unserer Publikation den höchst möglichen Standard zu verleihen. Es sind aber hauptsächlich Sie als Autor, der dafür Sorge trägt, dass das Oncothermia Journal zu einem interessanten und abwechslungsreichen Magazin wird. Wir möchten allen danken, die uns im Austausch professioneller Betrachtungen und Erfahrungen unterstützen. Um beiden Seiten die Arbeit zu erleichtern, haben wir die folgenden Richtlinien für die Texterstellung entworfen.

1. Aims and Scope

The Oncothermia Journal is an official journal of the Oncotherm Group, devoted to supporting those who would like to publish their results for general use. Additionally, it provides a collection of different publications and results. The Oncothermia Journal is open towards new and different contents but it should particularly contain complete study-papers, case-reports, reviews, hypotheses, opinions and all the informative materials which could be helpful for the international Oncothermia community. Advertisement connected to the topic is also welcome.

- Clinical studies: regional or local or multilocal Oncothermia or electro cancer therapy (ECT) treatments, case-reports, practical considerations in complex therapies, clinical trials, physiological effects, Oncothermia in combination with other modalities and treatment optimization
- Biological studies: mechanisms of Oncothermia, thermal- or non-temperature dependent effects, response to electric fields, bioelectromagnetic applications for tumors, Oncothermia treatment combination with other modalities, effects on normal and malignant cells and tissues, immunological effects, physiological effects, etc.
- Techniques of Oncothermia: technical development, new technical solutions, proposals
- Hypotheses, suggestions and opinions to improve Oncothermia and electro-cancer-therapy methods, intending the development of the treatments

Further information about the journal, including links to the online sample copies and content pages can be found on the website of the journal: www.oncothermia-journal.com

Umfang und Ziele

Das Oncothermia Journal ist das offizielle Magazin der Oncotherm Gruppe und soll diejenigen unterstützen, die ihre Ergebnisse der Allgemeinheit zur Verfügung stellen möchten. Das Oncothermia Journal ist neuen Inhalten gegenüber offen, sollte aber vor allem Studienarbeiten, Fallstudien, Hypothesen, Meinungen und alle weiteren informativen Materialien, die für die internationale Oncothermie-Gemeinschaft hilfreich sein könnten, enthalten. Werbung mit Bezug zum Thema ist ebenfalls willkommen.

- Klinische Studien: regionale, lokale oder multilokale Oncothermie oder Electro Cancer Therapy (ECT) Behandlungen, Fallstudien, praktische Erfahrungen in komplexen Behandlungen, klinische Versuche,

physiologische Effekte, Oncothermie in Kombination mit anderen Modalitäten und Behandlungsoptimierungen

- Biologische Studien: Mechanismen der Oncothermie, thermale oder temperaturunabhängige Effekte, Ansprechen auf ein elektrischesFeld, bioelektromagnetische Anwendungen bei Tumoren, Kombination von Oncothermie und anderen Modalitäten, Effekte auf normale und maligne Zellen und Gewebe, immunologische Effekte, physiologische Effekte etc.
- Oncothermie-Techniken: technische Entwicklungen, neue technische Lösungen
- Hypothesen undMeinungen, wie die Oncothermie- und ECT-Methoden verbessert werden können, um die Behandlung zu unterstützen

Weitere Informationen zum Journal sowie Links zu Online-Beispielen und Inhaltsbeschreibung sind auf der Website zu finden: www.oncothermia-journal.com

2. Submission of Manuscripts

All submissions should be made online via email: info@oncotherm.org

Manuskripte einreichen

Manuskripte können online eingereicht werden: info@oncotherm.org

3. Preparation of Manuscripts

Manuscripts must be written in English, but other languages can be accepted for special reasons, if an English abstract is provided.
Texts should be submitted in a format compatible with Microsoft Word for Windows (PC). Charts and tables are considered textual and should also be submitted in a format compatible with Word. All figures (illustrations, diagrams, photographs) should be provided in JPG format.

Manuscripts may be any length, but must include:

- Title Page: title of the paper, authors and their affiliations, 1-5 keywords, at least one corresponding author should be listed, email address and full contact information must be provided
- Abstracts: Abstracts should include the purpose, materials, methods, results and conclusions.
- Test: unlimited volume
- Tables and Figures: Tables and figures should be referred to in the text (numbered figures and tables). Each table and/or figure must have a legend that explains its purpose without a reference to the text. Figure files will ideally be submitted as a jpg-file (300dpi for photos).
- References: Oncothermia Journal uses the Vancouver (Author-Number) system to indicate references in the text, tables and legends, e.g. [1], [1-3]. The full references should be listed numerically in order of appearance and presented following the text of the manuscript.

Manuskripte vorbereiten

Manuskripte müssen in englischer Sprache vorliegen. Andere Sprachen können in Ausnahmefällen akzeptiert werden, wenn ein englisches Abstract vorliegt.
Texte sollten in einem mit Microsoft Word für Windows (PC) kompatiblen Format eingereicht werden. Tabellen sollten in einem Word-kompatiblen Format eingefügt werden. Alle Graphiken (Illustrationen, Diagramme, Photographien) sollten im jpg Format vorliegen.

Manuskripte können jede Länge haben, müssen aber die folgenden Punkte erfüllen:

- Titelseite: Titel der Arbeit, Autor, Klinikzugehörigkeit, 1-5 Schlüsselworte, mindestens ein Autor muss genannt werden, E-Mail-Adresse und Kontaktdetails des Autors

- Abstracts: Abstracts müssen Zielsetzung, Material und Methoden, Ergebnisse und Fazit enthalten.
- Text: beliebige Länge
- Abbildungen und Tabellen: Abbildungen und Tabellen sollten im Text erläutert werden (nummeriert). Jede Abbildung / Tabelle muss eine erklärende Bildunterschrift haben. Bilder sollten als jpg eingereicht werden (300 dpi).
- Zitate: Das Oncothermia Journal verwendet die Vancouver Methode (Autornummer), um Zitate auszuweisen, z.B. [1], [1-3]. Die Bibliographie erfolgt numerisch in Reihenfolge der Erwähnung im Text.

4. Copyright

It is a condition of publication that authors assign copyright or license the publication rights in their articles, including abstracts, to the publisher. The transmitted rights are not exclusive, the author(s) can use the submitted material without limitations, but the Oncothermia Journal also has the right to use it.

Copyright

Es ist eine Publikationsvoraussetzung, dass die Autoren die Erlaubnis zur Publikation ihres eingereichten Artikels und des dazugehörigen Abstracts unterschreiben. Die überschriebenen Rechte sind nicht exklusiv, der Autor kann das eingereichte Material ohne Limitation nutzen.

5. Electronic Proofs

When the proofs are ready, the corresponding authors will receive an e-mail notification. Hard copies of proofs will not be mailed. To avoid delays in the publication, corrections to proofs must be returned within 48 hours, by electronic transmittal or fax.

Elektronische Korrekturfahne

Wenn die Korrekturfahnen fertig gestellt sind, werden die Autoren per E-Mail informiert. Gedruckte Kopien werden nicht per Post versandt. Um Verzögerungen in der Produktion zu verhindern, müssen die korrigierten Texte innerhalb von 48 Stunden per E-Mail oder Fax zurückgesandt werden.

6. Offprints and Reprints

Author(s) will have the opportunity to download the materials in electronic form and use it for their own purposes. Offprints or reprints of the Oncothermia Journal are not available.

Sonderdrucke und Nachdrucke

Die Autoren haben die Möglichkeit, das Material in elektronischer Form herunterzuladen, Sonderdrucke und Nachdrucke des Oncothermia Journals sind nicht erhältlich.

7. Advertisement

The Oncothermia Journal accepts advertising in any language but prefers advertisements in English or at least partially in English. The advertising must have a connection to the topics in the Oncothermia Journal and must be legally correct, having checked that all information is true.

Werbung

Das Oncothermia Journal akzeptiert Werbeanzeigen in allen Sprachen, bevorzugt, aber die zumindest teilweise Gestaltung in englischer Sprache. Die Werbung muss eine Beziehung zu den Themen des Oncothermia Journals haben und der Wahrheit entsprechende Inhalte aufweisen.

8. Legal responsibility

Authors of any publications in the Oncothermia Journal are fully responsible for the material which is published. The Oncothermia Journal has no responsibility for legal conflicts due to any publications. The editorial board has the right to reject any publication if its validity has not been verified enough or the board is not convinced by the authors.

Haftung

Die Autoren aller im Oncothermia Journal veröffentlichten Artikel sind in vollem Umfang für ihre Texte verantwortlich. Das Oncothermia Journal übernimmt keinerlei Haftung für die Artikel der Autoren. Die Redaktion hat das Recht Artikel abzulehnen.

9. Reviewing

The Oncothermia Journal has a special peer-reviewing process, represented by the editorial board members and specialists, to whom they are connected. To avoid personal conflicts the opinion of the reviewer will not be released and her/his name will be handled confidentially. Papers which are not connected to the topics of the journal could be rejected without reviewing.

Bewertung

Die Texte für das Oncothermia Journal werden durch die Redaktion kontrolliert. Um Konflikte zu vermeiden, werden die Namen des jeweiligen Korrektors nicht öffentlich genannt. Artikel, die nicht zu den Themen des Journals passen, können abgelehnt werden

Content

Heat shock factor 1 inhibition enhances the effects of modulated electro hyperthermia in a triple negative breast cancer mouse model

Pedro H. L. Viana[1], Csaba A. Schvarcz[1,2], Lea O. Danics[1], Balázs Besztercei[1], KenanAloss[1], Syeda M. Z. Bokhari[1], Nino Giunashvili[1], Dániel Bócsi[1] , Zoltán Koós[1] , Zoltán Benyó[1,2] & Péter Hamar[1*]

[1] Institute of Translational Medicine, Semmelweis University, Tűzoltó Utca 37 47, Budapest 1094, Hungary.

2 HUN-REN-SU Cerebrovascular and Neurocognitive Diseases Research Group, Tűzoltó Utca 37 47, Budapest 1094, Hungary.

*email: hamar.peter@semmelweis.hu

Citation

Viana,, P.H.L. et al (2024) Heat shock factor 1 inhibition enhances the effects of modulated electro hyperthermia in a triple negative breast cancer mouse model

Oncothermia Journal 38, August 2026., 9-33.
https://oncotherm.com/VianaPHL_2024_Heat_shock_factor_1_inhibitation

Modulated electrohyperthermia (mEHT) is a non-invasive complementary cancer therapy using an electromagnetic feld generated by amplitude modulated 13.56 MHz frequency that induces tumor cell destruction. However, we have demonstrated a strong induction of the heat shock response (HSR) by mEHT, which can result in thermotolerance. We hypothesized that inhibition of the heat shock factor 1 (HSF1) can synergize with mEHT and enhance tumor cell-killing. Thus, we either knocked down the HSF1 gene with a CRISPR/Cas9 lentiviral construct or inhibited HSF1 with a specifc small molecule inhibitor: KRIBB11 in vivo. Wild type or HSF1-knockdown 4T1 TNBC cells were inoculated into the mammary gland's fat pad of BALB/c mice. Four mEHT treatments were performed every second day and the tumor growth was followed by ultrasound and caliper. KRIBB11 was administrated intraperitoneally at 50 mg/kg daily for 8 days. HSF1 and Hsp70 expression were assessed. HSF1 knockdown sensitized transduced cancer cells to mEHT and reduced tumor growth. HSF1 mRNA expression was signifcantly reduced in the KO group when compared to the empty vector group, and consequently mEHT-induced Hsp70 mRNA upregulation diminished in the KO group. Immunohistochemistry (IHC) confrmed the inhibition of Hsp70 upregulation in mEHT HSF1-KO group. Demonstrating the translational potential of HSF1 inhibition, combined therapy of mEHT with KRIBB11 signifcantly reduced tumor mass compared to either monotherapy. Inhibition of Hsp70 upregulation by mEHT was also supported by qPCR and IHC. In conclusion, we suggest that mEHT-therapy combined with HSF1 inhibition can be a possible new strategy of TNBC treatment with great translational potential.

Keywords

Triple-negative breast cancer, Modulated electro-hyperthermia, Heat shock response, HSF1, Hsp70

Abbreviations

ER Estrogen receptor
EV Empty vector
HER2 Human epidermal growth factor receptor 2
HSF1 Heat shock factor 1
Hsp Heat shock protein
HSR Heat shock response
IHC Immunohistochemistry
KO Knockdown
mEHT Modulated electro-hypertermia
PR Progesterone receptor
RF Radiofrequency
shRNA Short hairpin RNA
TDR Tumor destruction ratio
TNBC Triple-negative breast cancer
Veh Vehicle
WT Wild-type

Female breast cancer is the most diagnosed cancer type and has surpassed lung cancer as the leading cause of global cancer incidence in 2020, with an estimated 2.3 million new cases, representing 11.7% of all cancer cases[1] . Triple-negative breast cancer (TNBC) lacks expression of estrogen receptor (ER), progesterone receptor (PR), and human epidermal growth factor receptor 2 (HER2), and is the most aggressive type accounting for 15–20% of all breast cancer cases[2] with poor prognosis[3] . As TNBC lacks targetable receptor expression, there is no endocrine or targeted

therapy available at present. Tus, efective TNBC treatment regimens are still lacking[4] . Terefore, development of new TNBC treatment strategies is an unmet clinical need[5].

Modulated electro-hyperthermia (mEHT) treatment (Oncothermia) is a non-invasive complementary cancer therapy applied in the clinics successfully [6–10]. mEHT uses an electromagnetic feld generated by amplitude modulated 13.56 MHz frequency that induces tumor cell destruction[11]. Te modulated radiofrequency (RF) energy is directed to the tumor area and creates a heat fow that triggers biochemical processes in the malignant cell membrane, causing apoptotic cell death[12,13]. Te cell killing efects are targeted due to diferences between the electromagnetic properties of lipid rafs (electrical conductivity and permeability) of cancer cells and surrounding normal tissue[14]. Unlike convetional hyperthermia the surrounding normal tissues are minimally damaged during mEHT treatments[15]. Te specifc radiofrequency has been clinically used to treat tumors for approximately 20 years[16].

The mEHT-induced energy absorbed by tumor tissues results in temperature elevation, hence inducing the heat shock response (HSR)[17]. Te HSR, initiated by its master regulator, the heat shock transcription factor 1 (HSF1), protects cells from a wide range of stresses, including heat stress[18]. As described before, cell survival is achieved through the activation of anti-apoptotic proteins and the inhibition of pro-apoptotic proteins, such as Hsp70, a phenomenon known as thermotolerance, which enables cancer cells to withstand the efects of heat[19]. Hsp70 is a molecular chaperone able to restore the balance of cell proteome by protecting proteins and refolding unfolded proteins under a variety of stress conditions [20,21]. Hsp70 is upregulated in various cancer cells promoting survival and proliferation[22]. Terefore, blocking or silencing the HSR by targeting HSF1 or Hsps can be an efective way to reverse thermotolerance in cancer cells.

We previously demonstrated in vitro that inhibition of Hsp70 synergized with mEHT and enhanced its anticancer therapeutic effects [17,23]. Moreover, we observed in vivo a strong Hsp70 signal in mEHT-treated tumors around the apoptotic, damaged area17. It has been demonstrated that overexpression of Hsp70 in cancer cells is a consequence of the disruption in HSF1 transcriptional activity [24,25], although Hsp70 might be also expressed regardless of HSF gene[26]. Constitutive activation of HSF1 during tumorigenesis is one possible explanation of the enhanced Hsp70 expression in several cancers[24]; however, the mechanism remains unclear. Te inhibition of HSF1 using short hairpin RNAs (shRNAs) or small synthetic molecules, such as KRIBB11, decreased the expression of HSF1 downstream proteins[27]. Furthermore, we also demonstrated in vitro the enhancement of mEHT-4T1 cancer cell killing efect by KRIBB1123. KRIBB11 has abolishing activity on the heat shock-dependent induction of Hsp70 gene through inhibition of HSF1, causing signifcant decrease of tumor growth[28]. Terefore, reducing HSF1 could signifcantly inhibit the growth of cancer cells and promote their apoptosis[29]. Despite of several HSF1 inhibitors have been investigated[25], KRIBB11 is the frst specifc inhibitor of HSF1[28].

Another way to block the HSR is by gene-silencing its master regulator: HSF1. Tis strategy has been successfully applied in many studies to demonstrate the pro-oncogenic efects of HSF1[30]. Indeed, it has been demonstrated that HSF1 knockout (KO) mice had decreased susceptibility to spontaneous lymphoma[31] and survival of tumor bearing mice increased[32]. Furthermore, HSF1-KO prevented tissue hyperplasia and cancer development in a mouse mammary gland-specifc HSF1-KO model[33]. An in vitro model using cervical cancer cells has proposed that silencing HSF1 by gene-editing or inhibiting HSF1 by chemical inhibitors sensitizes cancer cells to chemotherapeutic

reagents or hyperthermia, in which an incubator was used for heating procedures[34]. Tus, in the present study, we investigated the hypothesis that downregulation of the heat shock response by gene-editing knockdown of HSF1, or by a specifc chemical inhibitor of HSF1: KRIBB11, enhances the therapeutic efciency of mEHT in breast cancer treatment.

1. Material and Methods

Cell culture and reagents

For both in vitro and in vivo studies, the 4T1 murine mammary carcinoma cell line, provided by Judy Lieberman (Lieberman Laboratory, Harvard University, Boston, MA, USA), was used. Te 4T1 cells were grown as adherent culture in Dulbecco's Modifed Eagle Medium (DMEM high glucose, 4.5 g/L without lglutamine and Phenol Red, Capricorn Scientifc, Ebsdorfergrund, Germany, Cat-No. DMEM-HXRXA) supplemented with 10% Fetal Bovine Serum (FBS—South America Origen, EU approved, EuroClone S.p.A., Pero, Italy, CatNo. ECS0180L), l-glutamine 200 mM (Capricorn Scientifc, Ebsdorfergrund, Germany, Cat-No. GLN-B), and penicillin/streptomycin 100x (Capricorn Scientifc, Ebsdorfergrund, Germany, Cat-No. PS-B). Cells were submitted to passages every 2 or 3 days. Trypsin 10x (Lonza A. G., Basel, Switzerland, Cat-No. 17-160E) was used to release cells from sub-confuent monolayers. The detached cells were seeded back into cell culture flasks or prepared for experiments. KRIBB11 was purchased from MedChemExpress (Monmouth Junction, NJ, USA, Cat-No. HY-100872).

Construction and verification of stable HSF1-knockdown by flow cytometry

CRISPR gRNA Lentiviral Transduction particles from Sigma-Aldrich® (St. Louis, MO, USA) was used for knockdown of HSF1. The plasmid sequences for HSF1 gene are listed in Fig. 1. The lentiviral structure consisted of (1) the target region to knockdown HSF1-gene; (2) a puromycin resistance gene; and (3) GFP gene. Murine 4T1 cells were seeded at 1.4× 104 cells/well in triplicate into a 96-well plate and incubated for 24 h at 37 °C. After the cells were adherent to the bottom, 8 µg/mL of hexadimethrine bromide (SigmaAldrich/Merck, St. Louis, MO, USA, Cat-No. H9268-5G) were added to each well to enhance transduction. The lentiviral particles or the negative particles were added to appropriate wells. Cells were further cultured for 24 h, and then the medium containing the lentiviral particles were replaced. Next, transfected cells were selected by culturing in a medium containing 6 µg/ml puromycin (Sigma-Aldrich/Merck, St. Louis, MO, USA, Cat-No. 540411-25MG) to kill nontransfected cells as established earlier[23]. Surviving cells were considered successfully transfected cells. Forty-eight hours after transduction, fluorescence of successful transduced cells was assessed by fluorescent microscope. Puromycin-resistant colonies were selected and expanded to assay for expression of the construct. Cells were sorted by Fluorescence-activated single cell sorting (FACS) (Sony Corp. San Jose, CA, USA, Sony SH800) in three cell types: 4T1 wild type, 4T1 empty vector, and 4T1 HSF1-KO. Flow cytometry was used to check for GFP-positiveness in transduced cells after expansion. For that, cells were harvested at 1× 106 cells/mL, washed with cold PBS (without Ca & Mg, without Phenol Red, Capricorn Scientifc, Ebsdorfergrund, Germany, CatNo. PBS-1A), and centrifuged for 5 min at 300g. The supernatant was removed, and fresh, cold PBS was added. The suspended cells were transferred to FACS tubes and were kept on ice. Cells

were analyzed based on GFPexpression by using a CytoFLEX Flow Cytometer (Beckman Coulter, Inc. Brea, CA, USA). The expression of HSF1 and Hsp70 was determined by qPCR.

In vitro HSF1-KO model

Knockdown-, empty vector-, and wild type 4T1 cells were counted and seeded onto 60 mm petri dishes at a density of 1× 106 cells per petri dish in DMEM medium with 10% FBS. After 24 h, cells were treated with water bath hyperthermia, 42 °C for 30 min. Two hours after hyperthermia treatment, the medium was discarded and 500 µL TRI Reagent® RT (Molecular Research Center, Inc. Cincinnati, OH, USA, Cat-No. RT 111) was added for RNA collection. The cells were homogenized and transferred to pre-labeled Eppendorf tubes. The Eppendorf tubes were immediately frozen in liquid nitrogen.

In vivo HSF1-KO model

Six-to-eight-weeks old female BALB/c mice were kept under 12 h dark/light cycles with ad libitum access to food and water in the Animal Facility Department of Basic Medical Center, Semmelweis University—Budapest, Hungary. The mice were anesthetized with isoflurane (Baxter International Inc., Deerfeld, IL, USA). Anesthesia was induced with 5% concentration and maintained with 2–2.5% concentration in 0.6–0.8 l/min compressed airflow. 4T1 cells were kept in cell culture flasks, trypsinized, counted, suspended in Dulbecco's PBS 1x (without Ca & Mg, without Phenol Red, Capricorn Scientifc, Ebsdorfergrund, Germany, Cat-No. PBS-1A). 1× 106 4T1 cells suspended in 50 µL PBS were subcutaneously inoculated into the 4th mammary gland's fat pad of each mouse[35] using a 50 µL Hamilton syringe (Hamilton Company, Reno, NV, USA). Eight days after inoculation, tumor size was measured with digital caliper (Fine Science Tools Inc., Foster City, CA, USA) and ultrasound (Phillips Sonos 5500, Philips, Amsterdam, Netherlands) as described earlier[23]. Mice were randomized into treatment groups (Table 1) according to their tumor volume and body mass, to achieve similar average for all groups. Animals exhibiting disproportionate tumor measures, such as irregular shapes, twin tumors, or those where the size significantly deviated from the average, were excluded from the experiment. mEHT treatments were started the day after randomization. In total, four mEHT treatments were performed every two days. In the days between treatments, tumor size was followed by both digital caliper and ultrasound (US). The correlation between tumor mass and US or caliper was collected in the Supplementary Fig. S1. Figure 2 shows a schematic overview of HSF1-KO and mEHT treatments schedule. Mice were kept under isoflurane anesthesia for all procedures described here. For tumor sample collection 24 h after the last treatment, heparin 10x (Teva, Debrecen, Hungary, Cat-No. OGYI-T-2216/01) was injected intraperitoneally.

a

Vector	Clone ID	Digest	Pasmid sequence verified	P24 antigen ELISA titer ≥ 10^6 VP/ml
LV01	NEGATIVECONTROL1	PASS	CGCGATAGCGCGAATATATT	3.7x10^7 VP/mL
LV01	MMPD0000018544	PASS	GCTCGCCTCCAGTACCCGA	1.6x10^7 VP/mL

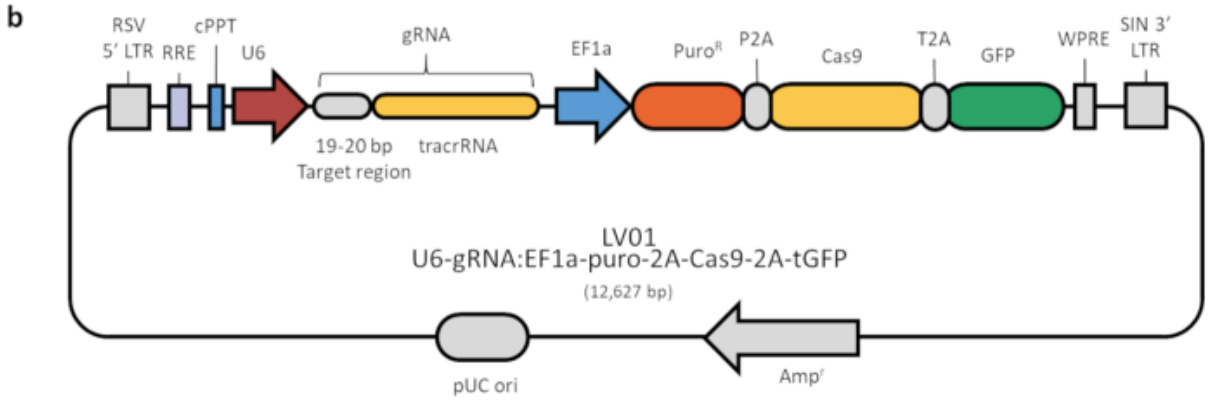

Figure 1. CRISPR/Cas 9 lentiviral constructs. (a) Plasmid sequence of the negative control (empty vector) and the HSF1 knockdown, which contains the target gene. (b) Scheme showing the structure of HSF1-KO lentiviral particles. (Modified from Sigma-Aldrich® (St. Louis, MO, USA)).

Mice physical body condition was checked, and mice were terminated by cervical dislocation. The abdominal cavity was opened, blood was taken, and tumors were harvested, cleaned (from adjacent connective tissues), weighed, and halved in two similar halves: one half was placed in 4% formaldehyde solution (Semmelweis Pharmacy, Budapest, Hungary) and sent to histological processing; the other half was frozen in liquid nitrogen for molecular analysis. Interventions and housing of the animals conformed to the Hungarian Laws No. XXVIII/1998 and LXVII/2002 about the protection and welfare of animals, and the directives of the European Union. All animal procedures were approved by the National Scientific Ethical Committee on Animal Experimentation under the No. PE/EA/50-2/2019.

In vivo KRIBB11 model

KRIBB11 (MedChemExpress, Monmouth Junction, NJ, USA, CatNo. HY-100872) was dissolved in 10% dimethylacetamide (MedChemExpress, New Jersey, USA, Cat-No. HY-W042416), 50% PEG300 (MedChemExpress, Monmouth Junction, NJ, USA, Cat.No.: HY-Y0873), and 40% nuclease-free water (Invitrogen, Carlsbad, CA, USA, Cat-No. 10977-035), as described previously[28]. Following randomization as described above, KRIBB11 or vehicle was administrated intraperitoneally at a dose of 50 mg/kg/day for 8 days according to each group (Table 2). Figure 3 depicts a schematic overview of mEHT+KRIBB11 experiment. Tumor volume was followed as described above. Supplementary Fig. S2 shows the correlation between tumor mass and US (S2a) or caliper (S2b). In total, four mEHT treatments were performed every two days. On day 16, the mice were sacrificed, and the tumors were removed, halved, and analysed by: (1) immunohistochemistry (IHC) and (2) qRT-PCR.

	Empty vector	HSF1-KO
Sham	6	5
mEHT	8	8

Table 1. HSF-KO experiment number of mice per group.

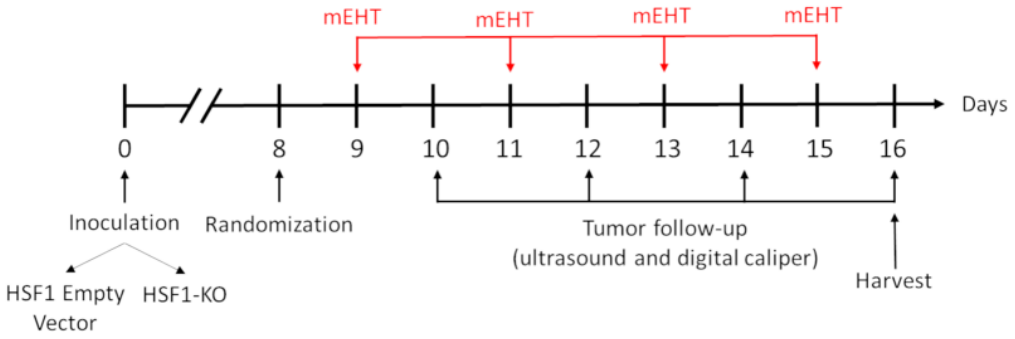

Figure 2. Experimental scheme of the 4T1 HSF1 knockdown model. 4T1 TNBC cells, containing either the HSF1 empty vector (EV) lentiviral construct or the HSF1 knockdown (HSF1-KO) lentiviral construct, were inoculated at day zero. Mice were randomized into groups (Sham EV or mEHT EV, and Sham HSF1-KO or mEHT HSF1-KO) at day 8. mEHT treatments were performed every two days. Tumor volume was monitored by ultrasound and digital caliper between mEHT treatments. The study was terminated on day 16 with the harvest of tumors.

	Vehicle	KRIBB11
Sham	4	7
mEHT	4	8

Table 2. KRIBB11 experiment number of mice per group.

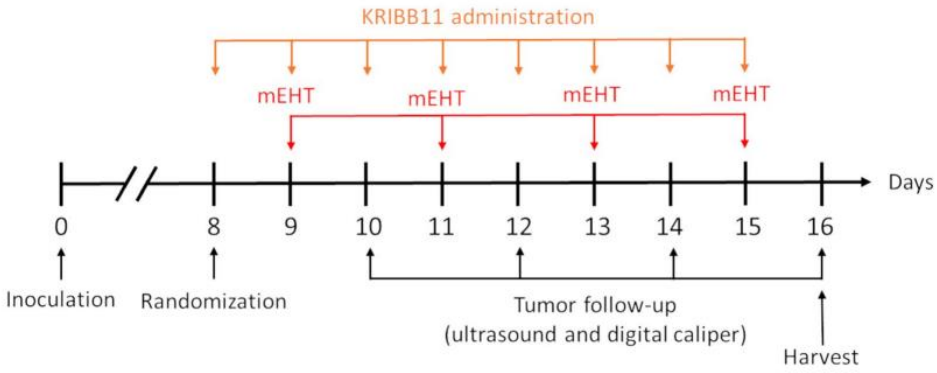

Figure 3. Experimental scheme of the mEHT+KRIBB11 experiment. 4T1 cells were inoculated at day zero. Mice were randomized into groups, as depicted in Table 2, at day 8 together with the first KRIBB11 injection. KRIBB11 was administered every day for 8 days. mEHT treatments were performed every two days. Tumor volume was monitored by ultrasound and digital caliper between mEHT treatments. The study was terminated on day 16 with the harvest of tumors.

In vivo mEHT treatments

Tumor-bearing mice were treated with modulated electro-hyperthermia (mEHT) device as described in detail earlier[17]. Briefly, electromagnetic heating was generated by capacitive coupled, amplitude modulated 13.56 MHz radiofrequency (LabEHY 200, Oncotherm kft., Budaors, Hungary). The mice were mEHT-treated four times every two days for 30 min plus maximum 5 min for device stabilization with 0.2–1.0 W. Temperature monitoring was performed with optical sensors (Luxtron FOT Lab Kit, LumaSense Technologies, Inc., CA, USA). The optical sensors were calibrated before

each treatment and were placed (1) on the skin right above the tumor, (2) into the rectum for body temperature monitoring, (3) on the heating pad, and (4) near the treatment setup for room temperature monitoring. Te skin temperature was kept at 40±0.5 °C during the treatments, as it assured the required 42 °C inside the tumor. Rectal temperature was kept in the physiologic range (37.0±0.5 °C), and the heating pad was set at the same temperature. Room temperature was 25±1 °C. For Sham treatments, cables were disconnected, therefore, no electromagnetic field was generated, and no energy was transferred (no heating).

Histopathology and immunohistochemistry

Formalin-fixed cancer samples were dehydrated and embedded in paraffin. Serial secrions (2.5 μm) were cut for hematoxylin–eosin (H&E) staining or dewaxed and rehydrated for immunohistochemistry (IHC) using a polymerperoxidase system (Histols, Histopathology Ltd., Pécs, Hungary). H&E and stained slides were digitalized using Pannoramic Scan and analyzed with the HistoQuant module of CaseViewer image-analysis software (all from 3DHISTECH, Budapest, Hungary) based on image color and intensity segmentation. The tumor area was digitally annotated and the damaged and living areas were delimited. The ratio between the damaged area per the whole tumor area was used for calculating the tumor destruction ratio (TDR%) on H&E slides.

$$TDR(\%) = \frac{\text{Damaged area}}{\text{Whole tumor area}}$$

Slide samples used in IHC were deparaffinized and incubated for 20 min with 3% H2O2 in methanol to block endogenous peroxidase activity. For antigen retrieval, slide samples were soaked in citrate buffer and heated for 20 min using an Avair electric pressure cooker (ELLA 6 LUX(D6K2A), Bitalon Kft, Pécs, Hungary), followed by 30 min cooling step. 3% bovine serum albumin (BSA, Millipore Corp., Kankakee, IL, USA, CatNo. 82–100-6) solution was used to block non-specific proteins for 20 min. The sections were incubated with the primary antibodies diluted in 1% BSA/TBS+TWEEN (TBST, pH 7.4) (Table 3) overnight in humidity chamber. Peroxidaseconjugated anti-rabbit & anti-mouse IgGs (HISTOLS-MRT, micropolymer-30011.500T, Histopathology Ltd., Pécs, Hungary) were used for 40 min incubation and the enzyme activity was revealed in 3,3′diaminobenzidine (DAB) chromogen/hydrogen peroxide kit (DAB QuantoTA-060-QHDX-Termo Fischer Scientific, Waltham, MA, USA, Cat-No. 12623957) under optical microscope. All incubations were at room temperature with sample washings between incubations in TBST buffer for 3×5 min. Slides were digitalized and the reactions were evaluated. The tumor area was digitally annotated and the area containing positive immune reaction was masked by setting the intensity, color, and saturation in the annotated area on each staining using the QuantCenter module of CaseViewer. Te ratio of the masked area to the annotated area (relative mask area=rMA) was used to estimate the expression of the target molecule. rMA of HSF1 and Hsp70 were measured in the intact tumor area. Important to mention, due to technical problems there is no data about Hsp70 staining of three samples from KRIBB11 experiment: one in Sham vehicle, one in Sham KRIBB11, and one in mEHT KRIBB11.

Antigen	Type	Reference no	Dilution	Vendor1
HSF1	Rabbit, pAb	#4356	1:100	Cell signaling
Hsp70	Rabbit, pAb	#4872	1:100	Cell signaling

Table 3. Antibodies and conditions used for immunohistochemistry.

RNA isolation and mRNA RT-PCR

RNA was isolated with the TRI reagent® RT (Molecular Research Center Inc., Cincinnati, OH, USA, Cat-No. RT111) according to the manufacturer's instructions. RNA integrity was analyzed by agarose gel electrophoresis, sample purity and concentration were measured by a Nanodrop spectrophotometer (Thermo Fisher Scientific Inc., Waltham, MA, USA). Reverse transcription of isolated RNA was performed by High-Capacity cDNA Reverse Transcription Kit (Applied Biosystems Inc., Foster City, CA, USA, Cat-No. 4368814). The amplified cDNA was used as a template for RT-PCR. Gene expression was measured according to standard qPCR procedures with SYBER Green based RT-PCR with SsoAdvanced™ Universal SYBER® Green Supermix (Bio Rad Laboratories, Inc., Hercules, CA, USA, Cat-No. 1725271) on CFX Connect Real-Time PCR Detection System (Bio Rad Laboratories, Inc., Hercules, CA, USA). The relative expression values for the target mRNAs were calculated after normalization using GAPDH. The primers used are listed in Table 4.

Statistical analysis

All statistical analyses were performed using the statistical software program GraphPad Prism software (v.6.01; GraphPad Software, Inc., La Jolla, CA, USA). Comparisons among groups were made with one-way ANOVA. Differences were considered statistically significant at *$p<0.05$, **$p<0.01$, ***$p<0.001$, ****$p<0.0001$, ns=not significant. Data are given as mean± Standard Deviation (SD).

Ethical approval

Our study was conducted in accordance with Animal Research: Reporting of In Vivo Experiments (ARRIVE) guidelines. Interventions and housing of the animals conformed to the Hungarian Laws No. XXVIII/1998 and LXVII/2002 about the protection and welfare of animals, and the directives of the European Union. All animal procedures were approved by the National Scientific Ethical Committee on Animal Experimentation under the No. PE/EA/50-2/2019.

2. Results

Successful transfection of TNBC cell-lines with the HSF1-gene editing lentiviral construct

The HSF1-knockdown (HSF1-KO) CRISPR/Cas9 construct included a GFP encoding sequence for the selection of transfected cells. As expected, non-transfected wild type (WT) 4T1 cells did not express GFP (Fig. 4a and d). In contrast, more than 95% of 4T1 cells transfected with the active HSF1-KO CRISPR/Cas9 construct successfully expressed GFP, confirming successful transfection (Fig. 4c and f). Transfection with the empty vector (EV) was less effective, resulting in 62.8% of cells being GFP-positive, while 37.2% remained non-transfected (Fig. 4b and e). These non-transfected cells were removed through fluorescent sorting, followed by subsequent propagation in cell culture media supplemented with puromycin.

Successful reduction of HSF1 and HSP70 expression in transfected TNBC cell-lines

HSF1 mRNA levels were comparable in both WT and EV cells, whether maintained at 37 °C or exposed to 42 °C in cell culture (Fig. 5a). Notably, the lentiviral construct led to a substantial downregulation of HSF1 mRNA in the knockdown group (HSF1-KO), as compared to both the wild type and empty vector groups (Fig. 5a). Baseline expression of Hsp70 at 37 °C remained low across all groups (Fig. 5b). Elevating the culture temperature to 42 °C significantly induced Hsp70 upregulation in WT and EV cells. However, this heat-induced response was significantly diminished in the HSF1-KO group (Fig. 5b).

mEHT-induced tumor growth reduction was enhanced in HSF1-KO tumors

The Sham EV tumors nearly doubled in volume over the course of the experiment (Fig. 6a and b—red). In contrast, Sham HSF1-KO were smaller and their growth rate was slower than EV tumors (rose). Remarkably, mEHT treated tumors did not grow and their size was reduced after the 4th treatment. The tumor growth rate was significantly slower in the HSF1-KO mEHT-treated group (light blue) compared to mEHT-treated EV group (dark blue). Despite having similar initial tumor volumes, mEHT KO tumors were notably smaller than mEHT EV tumors by the end of the study. Furthermore, supporting the tumor volume data, tumor mass was reduced by both mEHT and HSF-1 KO; yet, the smallest tumors were observed in the mEHT KO group (Fig. 6c and d) by the study termination.

Gene symbol	Gene name	Primer pairs
GAPDH	Glyceraldehyde-3phosphate-dehydrogenase [*Mus musculus*]	Fwd: CTCCCACTCTTC-CACCTTCG Rev: GCCTCTCTTGCTC-AGTGTCC
Hsp70	Heat shock protein 70 [*Mus musculus*]	Fwd: CTTCACCTCCAA-GTTCACCAA Rev: GACTCTGCT-GCTTCTCCTTG
HSF1	Heat shock factor 1 [*Mus musculus*]	Fwd:CTGAGAAGTGCCT-CAGCGTA Rev: CTCCTGAATGTCCA-GCAGGG

Table 4. Primers used for RT-PCR.

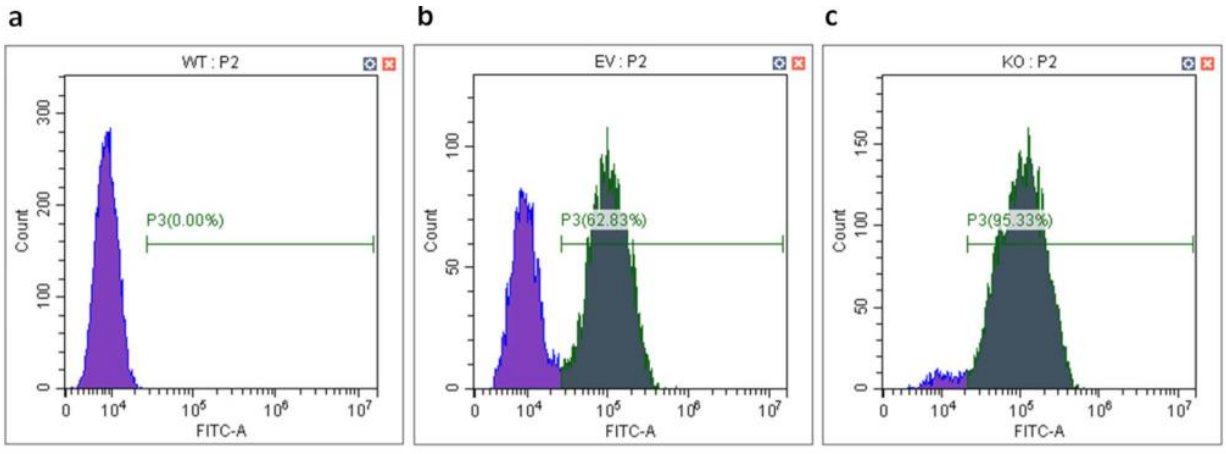

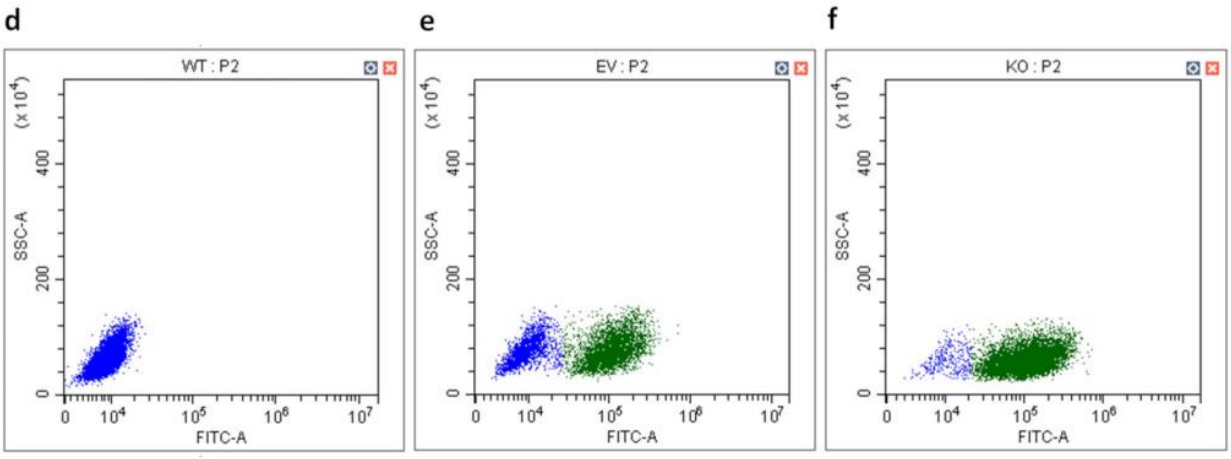

Figure 4. Flow cytometric analysis of transfected 4T1 cells. Flow cytometry histograms (upper row) and dot plots (lower row) (**a,d**) wild type (WT), (**b,e**) empty vector (EV) and (**c,f**) HSF1-KO (KO). The GFP positive cells are indicated with green, and the GFP-negative population is blue. SSC: Side Scatter; P2: second gate; FITC: Fluorescein Isothiocyanate.

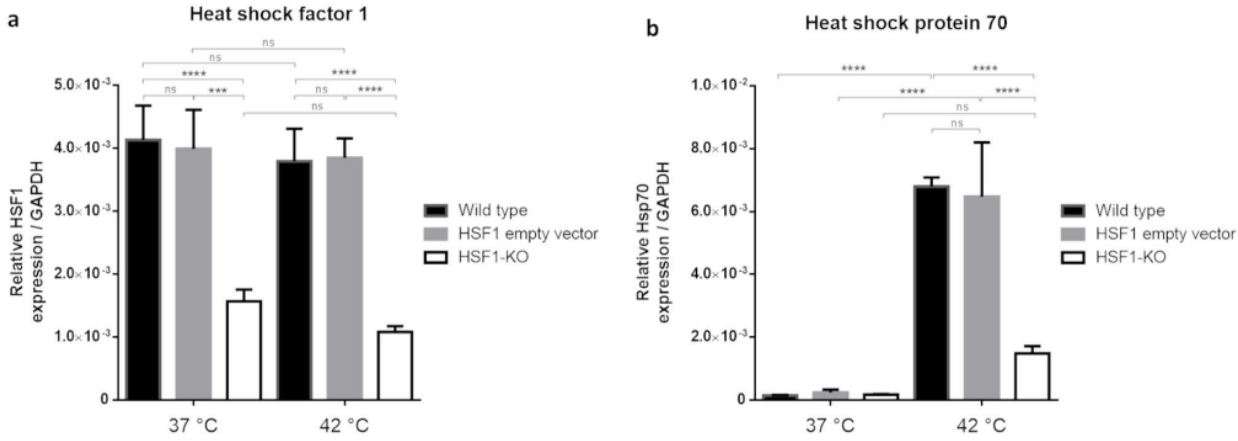

Figure 5. HSF1 and Hsp70 mRNA relative expression at 37 °C and 42 °C in the 4T1 cell line. (**a**) HSF1. (**b**) Hsp70. GAPDH: Glyceraldehyde 3-phosphate dehydrogenase: housekeeping gene. One-way ANOVA, Mean±SD, n=3/group, ***p<0.001, ****p<0.0001.

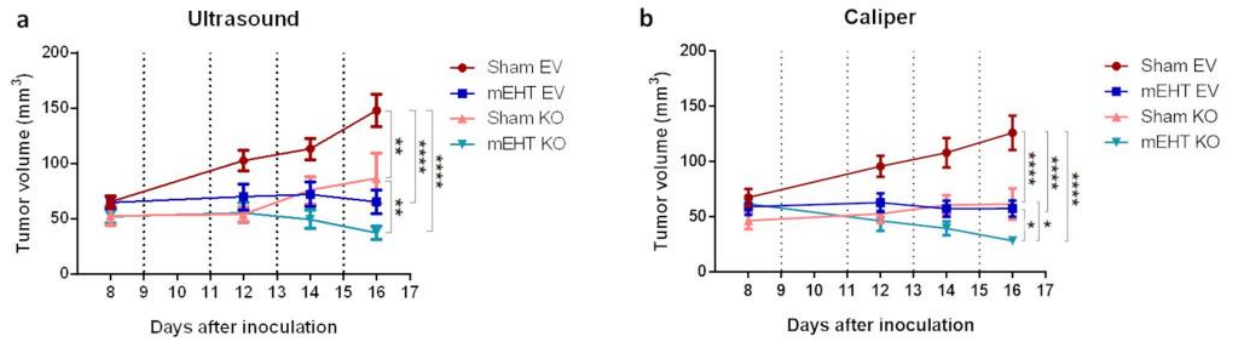

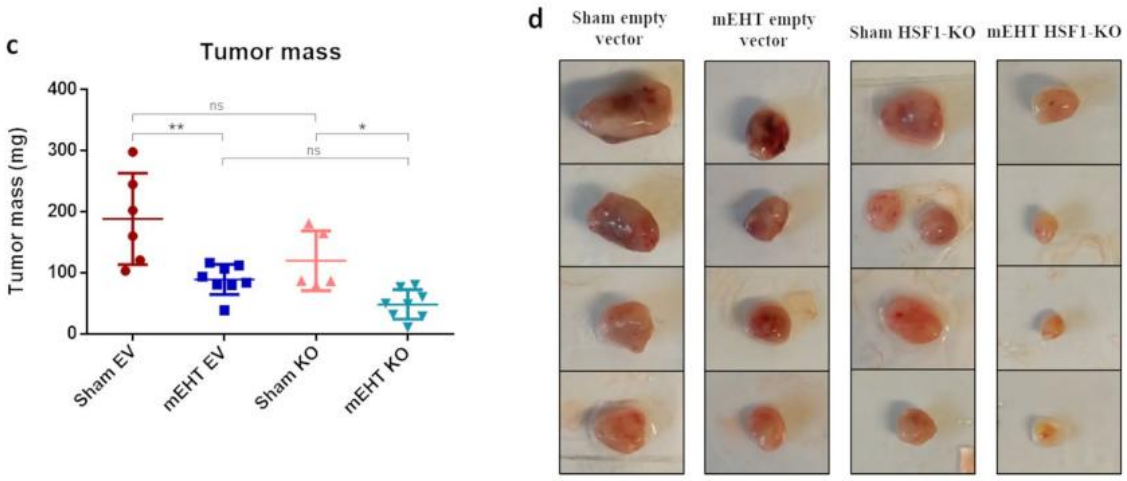

Figure 6. Tumor volume time-course and tumor mass at study termination after 4 mEHT treatments. Tumor growth inhibition as measured by (a) ultrasound and (b) digital caliper. (c) Tumor mass and (d) Four representative tumor images of each group (columns) by experiment termination. Mean±SD, One-Way and TwoWay Anova, Mean±SD, n=6–8/group, *p<0.05, **p<0.01, ***p<0.001, ****p<0.0001.

mEHT-induced tumor destruction was enhanced in HSF1-KO tumors

The area of tumor destruction, quantified as the tumor destruction ratio (TDR), was consistently minimal in all sham tumors, regardless of whether they were EV or KO transfected (Fig. 7a—red marked area). In contrast, mEHT-treated tumors exhibited a substantial increase in tissue damage compared to the sham group (Fig. 7a and b). Notably, there was an increased tendency toward severe tumor damage induced by mEHT in the mEHT treated HSF1-KO group (mEHT EV: 74.6 ±11%; mEHT HSF1-KO: 84.1 ±10.6%, p=0.52, ns). It is important to mention that histopathological data is unavailable for one Sham KO and one mEHT KO sample due to their small tumor size.

HSF1-KO prevented HSF1 and Hsp70 upregulation after mEHT treatment

Relative HSF1 mRNA baseline level, as assessed after four sham or mEHT treatments in EV-treated tumors, was significantly reduced in the KO groups, demonstrating effective silencing (Fig. 8a). HSF1 mRNA was not significantly influenced by mEHT. Contrarily, relative Hsp70 mRNA baseline level, as assessed after four sham treatments, increased significantly in mEHT-treated groups (Fig. 8b). As expected, mEHT stimulated Hsp70 mRNA significantly only in the EV-treated tumors. mEHT did not induce a significant Hsp70 response in HSF1- KO mEHT tumors. Immunohistochemistry (IHC) staining specific for HSF1 was present in most nuclei of empty vector treated tumors (Fig. 9a and b—upper row). Such specific HSF1 staining was not identified in HSF1-KO tumors (Fig. 9b— lower row). HSF1 protein expression was not influenced by mEHT (Fig. 9b—right column). Hsp70 specific protein staining was intense cytoplasmic staining in mEHT treated tumors. Such specific staining was absent in sham treated tumors (Fig. 9c and d—left column), demonstrating only background staining. Four mEHT treatments induced significant upregulation of Hsp70 specific staining in mEHT treated EV tumors (Fig. 9c and d). Such Hsp70 induction was not significant in the mEHT KO group vs sham-KO demonstrating that HSF1-KO was able to reduce the mEHT induced Hsp70 expression. Hsp70 induction was signifcantly inhibited in the HSF1-KO vs EV mEHT-treated group (Fig. 9c).

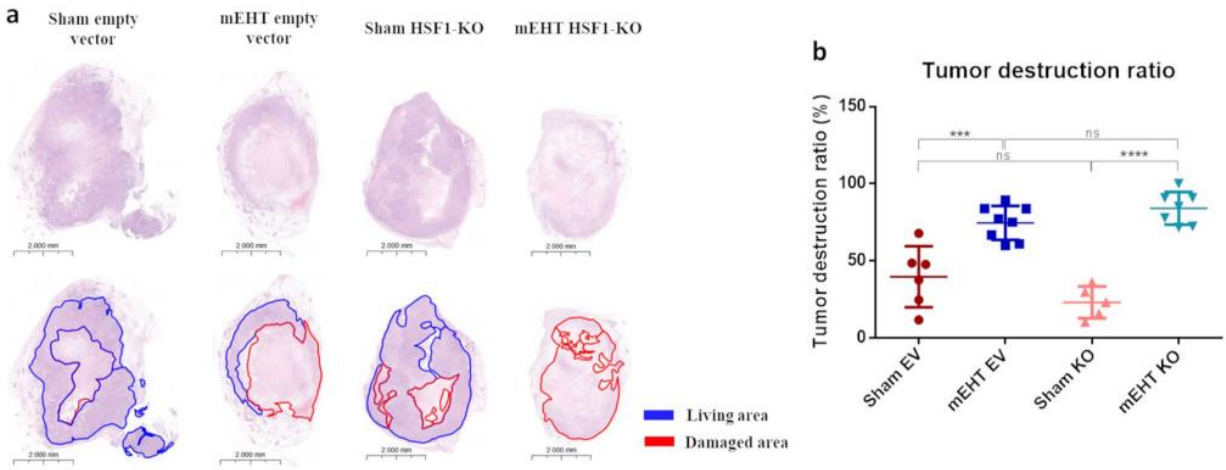

Figure 7. Tumor destruction ratio (TDR) afer 4 mEHT treatments. (**a**) Representative tumor images (H&E, 1.0x). (**b**) Quantification of TDR on H&E-stained tumors. One-way ANOVA test, Mean±SD, n=5–8/group, ***p<0.001, ****p<0.0001.

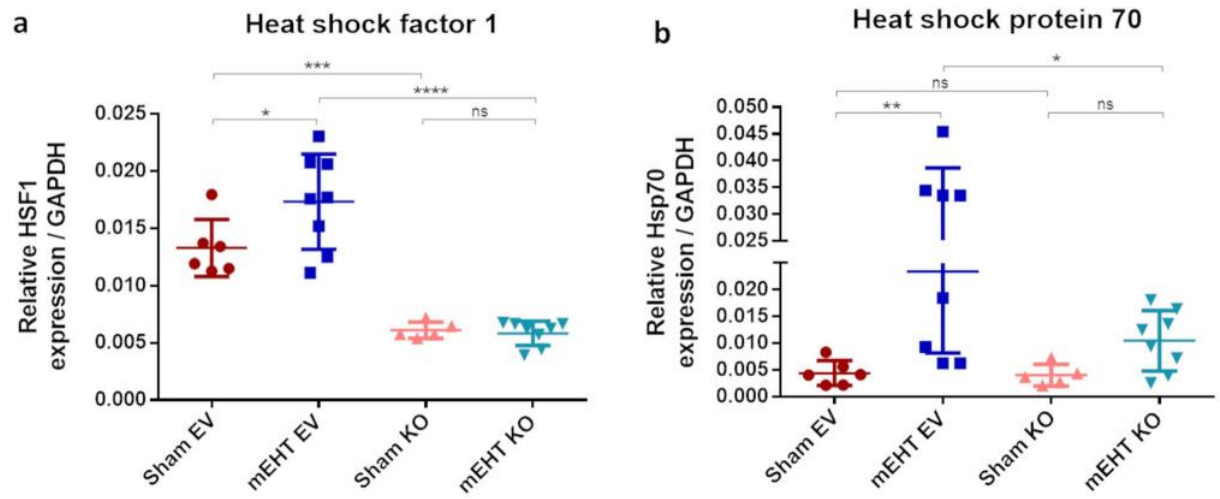

Figure 8. HSF1 and Hsp70 mRNA relative expression after 4 mEHT treatments. (**a**) HSF1. (**b**) Hsp70. GAPDH: Glyceraldehyde 3-phosphate dehydrogenase: housekeeping gene. Oneway ANOVA, Mean±SD, n=6–8/group, ns=not significant, *p<0.05, **p<0.01, ***p<0.001, ****p<0.0001.

mEHT-tumor growth reduction was synergistically enhanced by the heat shock inhibitor, KRIBB11, after 4 mEHT treatments

The volume of Sham + Veh tumors increased almost 4-times during the experiment (Fig. 10a and b—red). KRIBB11 monotherapy did not influence tumor growth significantly (rose). However, mEHT treated tumors grew slower (dark blue) and their size was significantly reduced after the 4th treatment (Fig. 10c). Tumor growth rate was further reduced significantly in the KRIBB11+mEHT co-treated group (light blue). Despite similar tumor volumes at the beginning of the treatments mEHT tumors were significantly smaller than sham tumors at the end of the study. Supporting tumor volume data, tumor mass was reduced only by mEHT but not by KRIBB11 alone. The tumors were

significantly the smallest in the KRIBB11+mEHT co-treated group (Fig. 10c and d) by study termination.

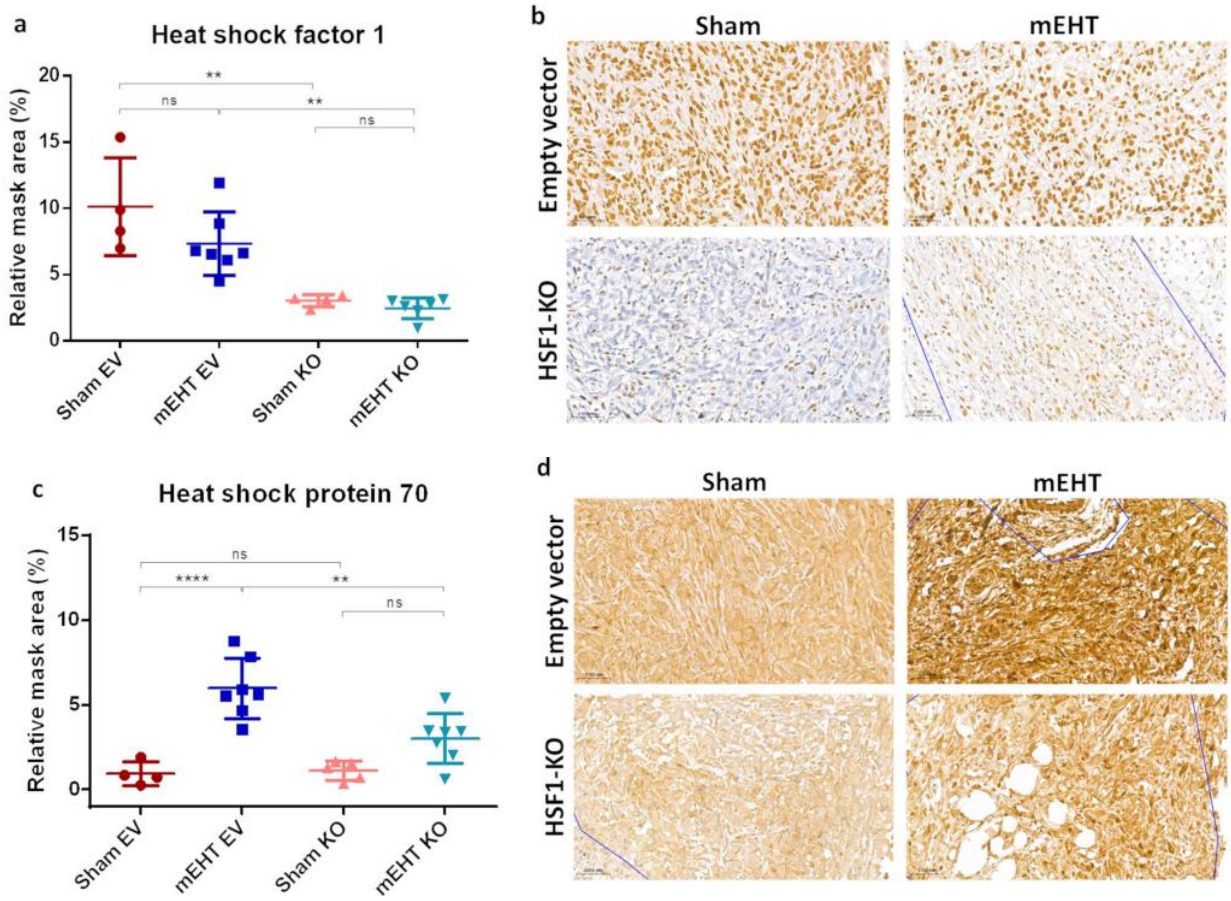

Figure 9. HSF1 and Hsp70 protein detection and quantification with immunohistochemistry after 4 mEHT treatments. (a) HSF1 and (c) Hsp70 protein quantification. Representative sections of (b) HSF1 and (d) Hsp70 , 40×magnifcation. One-way ANOVA, Mean±SD, n=4–7/group, ns=not significant, *p<0.05, **p<0.01, ***p<0.001.

KRIBB11 prevented Hsp70 upregulation after 4 mEHT treatments

Relative HSF1 mRNA baseline level as assessed after four sham or mEHT treatments was significantly reduced in the KRIBB11 treated groups demonstrating effective inhibition of the heat shock response in KRIBB11 treated tumors (Fig. 11a). HSF1 mRNA was not influenced significantly by mEHT. Relative Hsp70 mRNA baseline level was assessed after four sham treatments. Although mEHT induced an increase in Hsp70 mRNA compared to the sham group, this difference did not reach statistical significance (Fig. 11b). In contrast, Hsp70 elevation was absent in KRIBB11 treated tumors receiving mEHT, and Hsp70 mRNA levels were significantly lower in the mEHT+KRIBB11 group compared to the mEHT+Veh group. In tumors treated with mEHT+ Veh, Immunohistochemistry (IHC) staining specific for HSF1 displayed prominent nuclear staining (Fig. 12a and b—upper right panel). In contrast, such specific HSF1 staining was notably less prevalent in KRIBB11 and sham-mEHT treated tumors (Fig. 12b—lower panel). Remarkably, mEHT treatment did not significantly alter HSF1 protein expression levels (Fig. 12b). Intense cytoplasmic staining specific to Hsp70

protein was observed exclusively in tumors treated with mEHT monotherapy (Fig. 12c and d—right columns). In contrast, such distinctive staining was notably absent in shamtreated tumors, indicating only background levels of Hsp70 (Fig. 12c and d—left columns). The mEHT-induced upregulation of Hsp70 was significantly attenuated by co-treatment with KRIBB11, emphasizing the inhibitory effect of HSF1 on mEHT-induced Hsp70 expression (Fig. 12c).

Slightly increased tumor destruction tendency was observed in tumors treated with combined therapy

The Tumor Destruction Ratio (TDR) was relatively small in all sham tumors (Fig. 13c—red marked area). Notably, there was significant tissue damage observed in mEHT-treated tumors (Fig. 13a and c). While a subset of mEHT+KRIBB11 treated tumors demonstrated enhanced damage, another subset exhibited a smaller TDR, resulting in a non-statistically significant overall effect. It is worth noting that the core damaged area in the tumors exhibited a negative correlation with tumor mass, with larger tumors demonstrating a higher TDR (Fig. 13b). The most pronounced tumor destruction relative to tumor size was observed in the mEHT+KRIBB11 combination therapy group, highlighted by light blue dots.

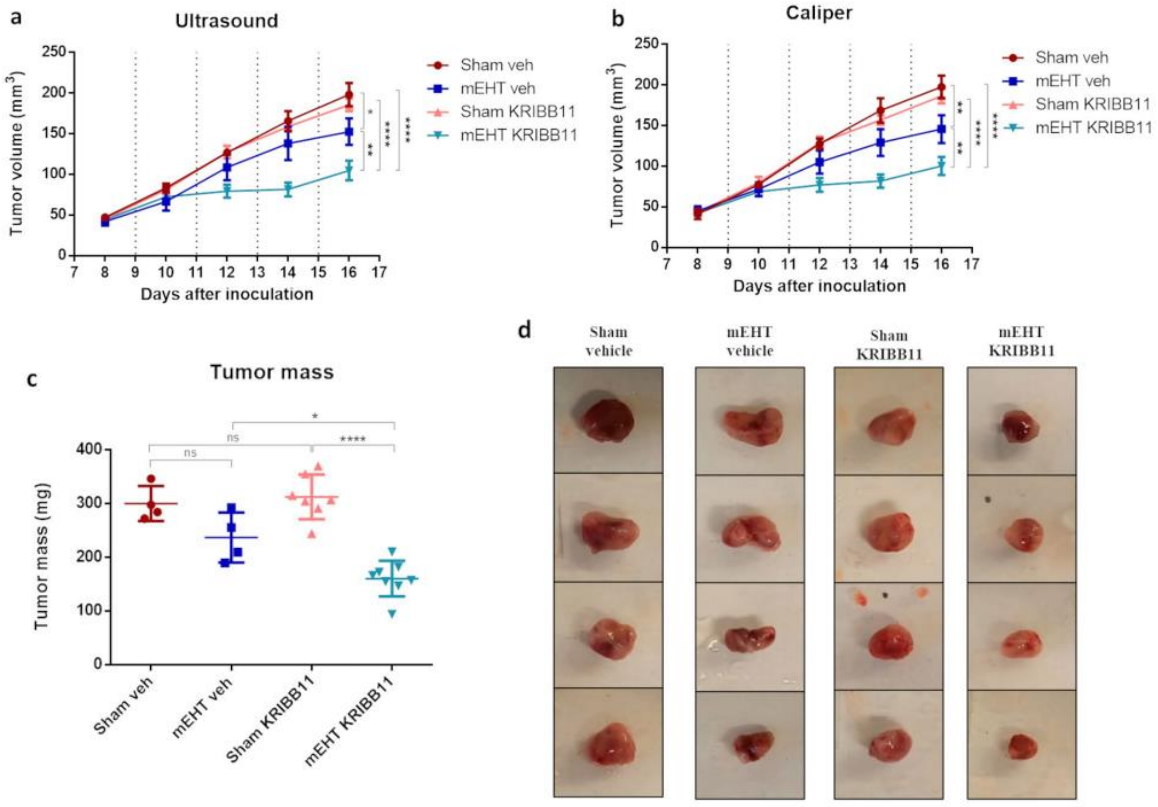

Figure 10. Tumor volume time-course and tumor mass at study termination in the combination therapy experiment. Tumor growth inhibition as measured by (a) ultrasound and (b) digital caliper. (c) Tumor mass and (d) Four representative tumor images of each group (columns) by experiment termination. Mean±SD, OneWay and Two-Way Anova, Mean±SD, n=4–8/group, ns=not significant, *p<0.05, **p<0.01, ****p<0.0001.

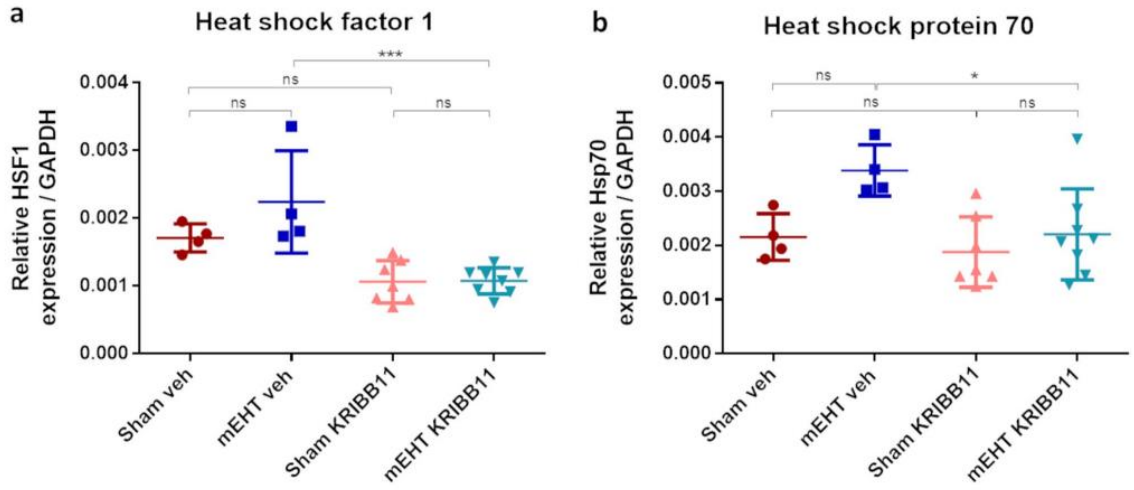

Figure 11. HSF1 and Hsp70 mRNA relative expression after 4 mEHT treatments. (a) HSF1. (b) Hsp70. GAPDH: Glyceraldehyde 3-phosphate dehydrogenase: housekeeping gene. Oneway ANOVA, Mean±SD, n=4–8/group, ns=not significant, *p<0.05, ***p<0.001.

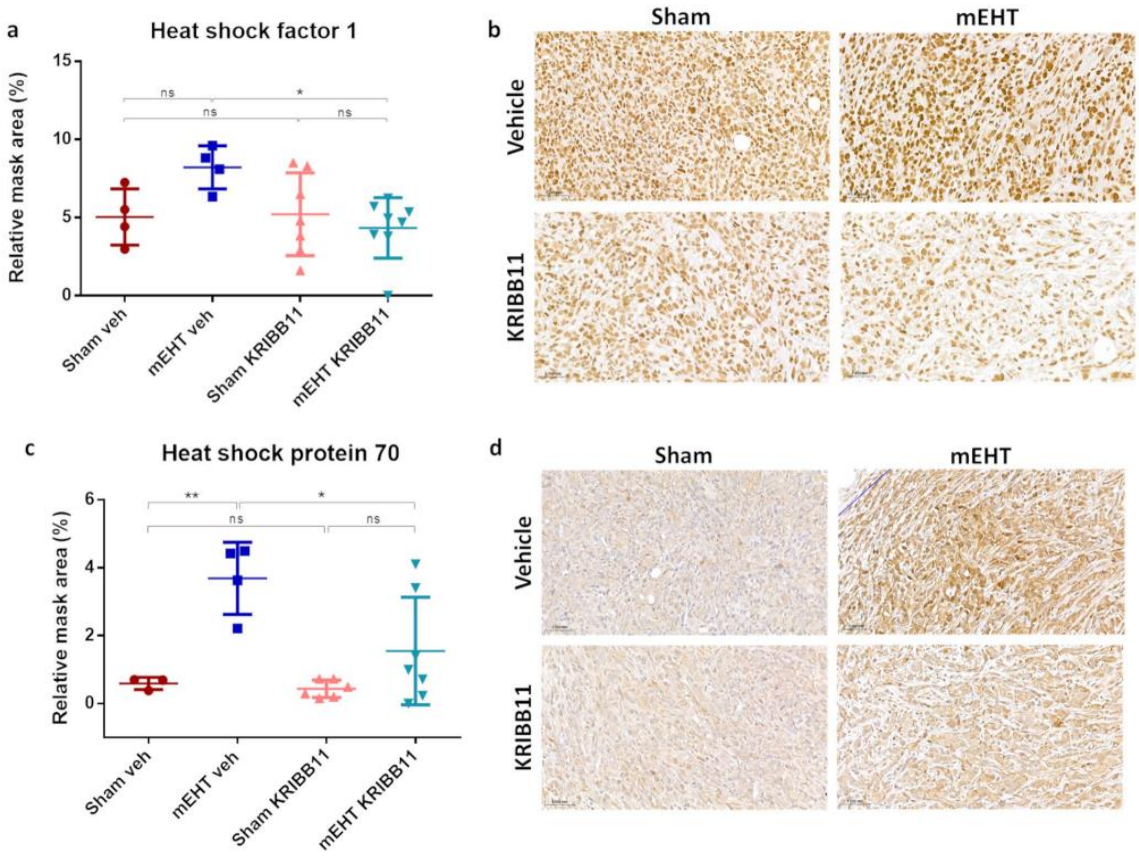

Figure 12. HSF1 and Hsp70 protein detection and quantification with immunohistochemistry after 4 mEHT treatments. (a) Heat shock factor 1 (HSF1) and (c) Heat shock protein 70 (Hsp70) protein quantification. Representative sections of (b) HSF1 and (d) Hsp70, 40×magnifcation. One-way ANOVA, Mean±SD, n=3–8/ group, ns=not significant, *p<0.05, ***p<0.001.

3. Discussion

Modulated eletcro-hyperthermia (mEHT) is a loco-regional non-invasive cancer therapy which has been successfully applied in vitro, in vivo, and in the clinics for over 20 years[15]. The mEHT treatment triggers apoptosis and necrosis of cancer cells via non-thermal effects such as membrane perturbations (similarly to electrophoresis), and the radiofrequency field also induces temperature increase to 42 °C[16]. The high energy absorbed by cancer cells and specifically cancer cell membranes lipid rafts consequently disrupts membrane arrangement and integrity on the basis of its elevated oxidative glycolysis (Warburg effect), ion concentration, and conductivity compared to adjacent normal tissues[36] and inducing anti-cancer responses[12]. However, it is known that mEHT provokes cell- and heat-stress activating the heat shock response11. In our previous studies, we demonstrated that mEHT induced the heat shock response in our mouse cancer model, resulting in strong upregulation of Hsp70 [17,23]. Indeed, massive induction of Hsp70 has been reported in other cancer models treated with mEHT such as colorectal37, and melanoma[38] models. It is worth noting that Hsp70, a crucial molecular chaperone, typically maintains low or undetectable levels in unstressed cells[39]. Te transcription of Hsp70 is triggered by the nuclear translocation of heat shock factor 1 (HSF1), a master regulator of the heat shock response[40]. When activated, HSF1 binds to the heat shock response elements (HSEs) within promoters of several Hsps and initiates Hsp transcription[41]. It has been demonstrated in a wide range of cancer types that HSF1 has a cytoprotective activity and supports cancer cell proliferation, survival, invasion, and metastasis[42]. Targeting HSF1 in cancer therapy has been suggested before[27], and in HSF1-knockdown experiments, mammary[43], liver[44], and skin[32] carcinogenesis was inhibited. We therefore hypothesized that the inhibition of mEHT-induced heat shock response by inhibiting HSF1 would enhance the therapeutic potential of mEHT. As a proof-of-concept, we used genome editing tools to knockdown HSF1. To investigate the translational potential, we also studied a small molecule inhibitor (KRIBB11), aiming to inhibit HSF1 and thus enhance the anticancer effects of mEHT treatment.

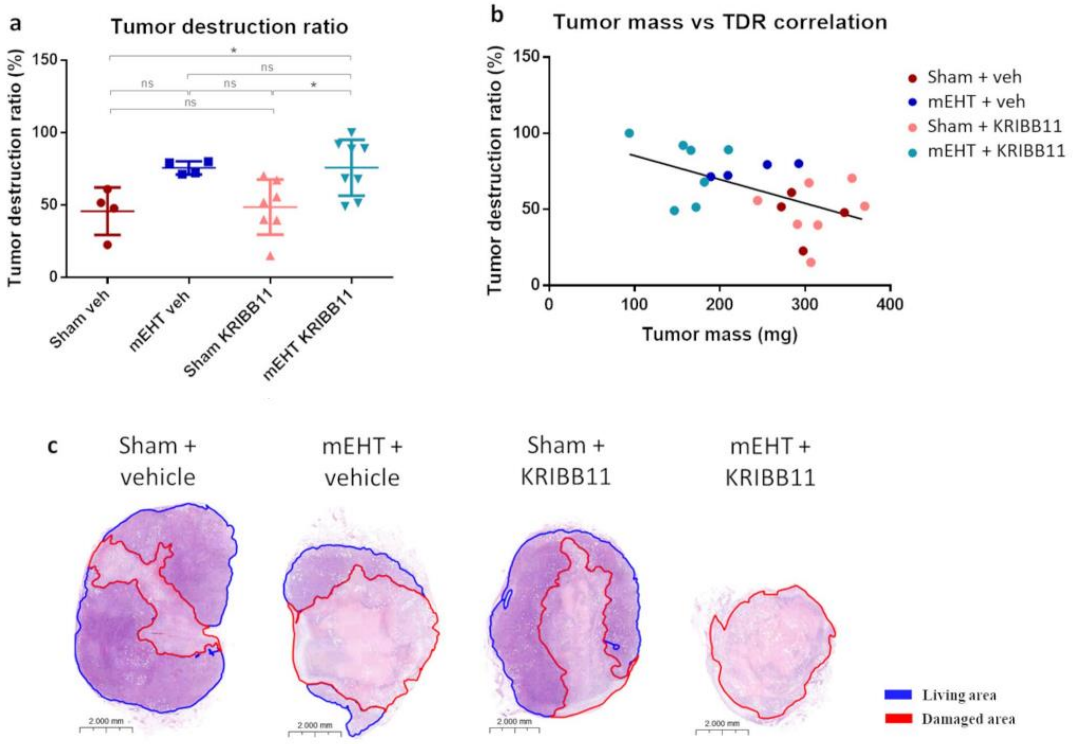

Figure 13. Tumor destruction ratio (TDR) afer 4 mEHT treatments. (**a**) Quantifcation of TDR on H&Estained tumors. (**b**) Scatter diagram and linear regression line showing negative correlation between tumor destruction ratio (TDR: Y axis) and tumor mass (X axis). (**c**) Representative tumor images (H&E, 1.0x). Oneway ANOVA test, Mean±SD, n=4–8/group, ns=not significant *p<0.05.

The integration of mEHT with conventional cancer treatment modalities presents a promising avenue in the quest for enhanced therapeutic efficacy. mEHT, known for its ability to selectively elevate temperatures in tumor tissues, can act synergistically and complementarily to radiotherapy and chemotherapy. A slight temperature elevation is expected to enhance blood flow, facilitating improved oxygenation in the affected area. Tis, in turn, can augment the efficacy of gold-standard cancer treatments[45]. The synergistic interplay of ionizing, thermal, and non-thermal effects promotes immunogenic cell death in malignant cells. This is achieved by exciting lipid rafts through mEHT-induced heating and inducing double-strand DNA breaks with radiotherapy[46]. Furthermore, studies have demonstrated the additional benefits of mEHT in conjunction with conventional therapies, leading to increased treatment response, improved overall survival, and a lack of side effects [47–49]. Therefore, this combinatorial strategy holds the promise of not only improving the local control of tumors but also potentially minimizing side effects.

In the present study, CRISPR/Cas9-mediated HSF1 knockdown was successful in 4T1 murine breast cancer cells. While the use of CRISPR to completely ablate genes can be challenging, as this system rarely eliminates the expression of a target gene entirely, leading to low knockdown efficiencies (<80%)[50–54], we achieved an impressive knockdown efficacy of over 95% (Fig. 4). Tis high efficacy was evidenced by the GFP-positivity of transduced cells after antibiotic selection (puromycin) and FACS sorting. However, these strategies seemed to be less effective in the empty vector group (62.83%). This group used a non-targeting guide RNA with no specific target site on the entire genome, designed to serve as a control group with a wild type phenotype. The genome editing using the CRISPR/Cas9 lentiviral empty vector did not enable gene truncation via polymerase chain reaction (PCR) (Fig. 5). On the other hand, we achieved a very strong HSF1 knockdown efficiency as demonstrated by flow cytometry and confirmed by real-time PCR (Fig. 8). Immunohistochemistry analysis of in vivo tumors further corroborated the HSF1 knockdown (Fig. 9a and b). Baseline HSF1 expression was reduced and hyperthermia induced Hsp70 upregulation was inhibited in HSF1-KO cells.

mEHT cancer selectivity and its inhibition of tumor growth have been reported in a wide range of cancer types[55]. Previously we also demonstrated inhibition of tumor growth by mEHT monotherapy in our murine breast cancer model [17,23]. In this study, we observed a significant enhancement in tumor growth inhibition with mEHT treatment in HSF1-KO cells. HSF1-KO tumors exhibited a size reduction of over 50% compared to non mEHT-treated empty vector tumors (Fig. 4). Tis aligns with previous findings suggesting the essential role of the HSF1 gene in cancer development, as HSF1-KO tumors naturally grow at a slower rate than empty vector tumors [33]. Despite this fact, mEHT further amplified the reduction in tumor growth in the KO group. Therefore, the importance of HSF1 supporting carcinogenesis can be demonstrated by the susceptibility reduction of HSF1-KO cells to cancer formation[56].

Based on our previous data[17] and the HSF1 knockdown study, we hypothesized that the inhibition of heat shock response (HSR) by KRIBB11, a specific inhibitor of HSF157, could potentiate the

anticancer effects of mEHT in tumor allograft. Mouse cancer xenograft studies have demonstrated reduction of cancer growth in samples treated daily with KRIBB11 dose in human colon cancer28, breast cancer [58,59], human myeloma60, bladder cancer61, and hepatocellular carcinoma62, both alone or in combination with other chemical compounds. When in combination, KRIBB11 efficacy was increased58. Indeed, we propose that KRIBB11 has translational potential when applied in combination with mEHT treatments, as the combined therapy demonstrated synergism in tumor growth inhibition (Fig. 10). Here we established the synergism between four-mEHT treatments and daily dose of KRIBB11 at 50 mg/kg for 8 days, as demonstrated by tumor volume and tumor mass reduction in the combined therapy group. Using the average of tumor masses for each treatment group (Sham+Vehicle: 300.0 mg, mEHT+Vehicle: 237.0 mg, Sham+KRIBB11: 312.3 mg, and mEHT+KRIBB11: 160.3 mg), we calaculated the expected combined effect based on individual mEHT and drug effects based on the Bliss Independence model63,64. Our analysis revealed that the observed effect of mEHT+KRIBBB11 ($E_{mEHT+KRIBB11}$=0.466) exceeded the expected combined effect (EBliss=0.243). Specifically, $E_{mEHT+KRIBB11} > E_{Bliss}$, indicating a potential synergistic interaction between mEHT and KRIBB11. This suggests that the combined treatment may exert a more pronounced inhibitory effect on tumor growth than anticipated based on the individual effects of each agent alone.

However, KRIBB11 alone was not able to reduce cancer growth in monotherapy (Fig. 10c). Carpenter et al. reported similar findings, stating that KRIBB11 did not significantly inhibit tumor growth in a breast cancer model unless combined with an AKT inhibitor58. In another study a dose of 50 mg/kg of KRIBB11 did not reduce myeloma xenograft growth, whereas a dose of 65 mg/kg proved efective[60].

The effects of KRIBB11 abovementioned were achieved by following the protocol established by Yoon et al. which involved daily administration of KRIBB11 over a period of 18 days[28]. Due to our experiment's shorter duration (8 days), our mice received fewer KRIBB11 injections. This decision was based on our previous findings, which demonstrated that prolonged mEHT treatments could lead to substantial damage in tumor tissue. Tis damage hinders the isolation and detection of RNA from treated tumors, thereby impeding molecular analysis[17]. This may also account for the observed lack of significant tumor growth inhibition with KRIBB11 monotherapy.

While previous studies have demonstrated that mEHT induces the heat shock response mainly by upregulation of Hsps [11,12], we observed that mEHT may not directly lead to significant changes in HSF1 mRNA (Fig. 11a) and protein levels (Fig. 12a). Instead, the regulation of HSF1 might primarily occur through its cellular localization, particularly its movement from the cytoplasm to the nucleus in response to stress[65]. This nuclear translocation of HSF1 is a crucial step in initiating the transcription of additional Hsps.

Corroborating with the HSF1-KO TDR data (Fig. 5), the damaged area observed in the combined mEHT and KRIBB11 therapy did not demonstrate statistically significant differences compared to mEHT + vehicle (Fig. 13). While tumor volume and mass reduction demonstrated synergistic enhancement of the mEHT effect with additional KRIBB11 therapy, the TDR results were not as pronounced. This could be attributed to the extensive destruction observed in Sham tumors, leading to spontaneous necrosis due to increased tumor size, as previously noted by our group[17]. The elevated mitochondrial metabolism of 4T1 cancer cells might contribute to necrosis development as a result of low oxygen levels and nutrient supply66. Therefore, the damage

magnitude may be related to tumor size. Indeed, our study revealed that larger tumors tended to have moderate TDR's (Fig. 13b). This trend was primarily due to their large size, with most of them belonging to the Sham groups (vehicle and KRIBB11). Consequently, the necrosis observed at the core of Sham tumors was a direct result of cancer outgrowth (Fig. 13b, red and pink dots). In contrast, mEHT-treated tumors exhibited a notably high TDR along with reduced mass (Fig. 13b, dark blue and light blue dots). From this, we infer that necrosis observed in mEHT groups (both vehicle and KRIBB11) arose from the cancer-killing effect of mEHT. Furthermore, this effect was amplified by administration of KRIBB11 (Fig. 13b, light blue dots). This suggests that the increase in cancer core destruction in Sham groups is primarily linked to tumor size, whereas in mEHT groups, it is more likely due to the treatment itself.

In conclusion, we have demonstrated that the combination of modulated electro-hyperthermia (mEHT) with the CRISPR/Cas9 gene-editing technique significantly enhances its anticancer effects in vivo. Specifically, the knockdown of heat shock transcription factor 1 (HSF1) led to the inhibition of tumor growth and a reduction in Hsp70 upregulation induced by mEHT. Moreover, the administration of the specific heat shock inhibitor, KRIBB11, further amplified the therapeutic impact of mEHT. These findings suggest a potential synergy between KRIBB11 and established clinical anticancer therapies like mEHT. Consequently, KRIBB11 holds promise for translation into clinical applications, offering a potentially impactful addition to cancer treatment modalities.

Data availability

All data associated with this study are presented in the paper. The data that support the findings of this study are available from the corresponding author upon reasonable request.
Received: 20 October 2023; Accepted: 20 March 2024
Published online: 08 April 2024

References

1. Sung, H. et al. Global cancer statistics 2020: GLOBOCAN estimates of incidence and mortality worldwide for 36 cancers in 185 countries. CA Cancer J. Clin. 71(3), 209–249 (2021).
2. Yin, L., Duan, J.-J., Bian, X.-W. & Yu, S.-C. Triple-negative breast cancer molecular subtyping and treatment progress. Breast Cancer Res. 22(1), 61 (2020).
3. Vagia, E., Mahalingam, D. & Cristofanilli, M. Te landscape of targeted therapies in TNBC. Cancers 12(4), 916 (2020).
4. Jhan, J.-R. & Andrechek, E. R. Triple-negative breast cancer and the potential for targeted therapy. Pharmacogenomics. 18(17), 1595–1609 (2017).
5. Won, K.-A. & Spruck, C. Triple-negative breast cancer therapy: Current and future perspectives (review). Int. J. Oncol. 57(6), 1245–1261 (2020).
6. Hegyi, G., Szigeti, G. P. & Szász, A. Hyperthermia versus oncothermia: Cellular efects in complementary cancer therapy. Evid. Based Complement. Alternat. Med. 2013, 672873 (2013).

7. Szasz, A. Current status of oncothermia therapy for lung cancer. Korean J. Torac. Cardiovasc. Surg. 47(2), 77–93 (2014).

8. Lee, S. Y., Kim, J. H., Han, Y. H. & Cho, D. H. Te efect of modulated electro-hyperthermia on temperature and blood fow in human cervical carcinoma. Int. J. Hyperthermia. 34(7), 953–960 (2018).

9. Minnaar, C. A. et al. Te efect of modulated electro-hyperthermia on local disease control in HIV-positive and -negative cervical cancer women in South Africa: Early results from a phase III randomised controlled trial. PLoS ONE. 14(6), e0217894 (2019).

10. Fiorentini, G. et al. Modulated electrohyperthermia in integrative cancer treatment for relapsed malignant glioblastoma and astrocytoma: Retrospective multicenter controlled study. Integr. Cancer Ter. 18, 1534735418812691 (2019).

11. Vancsik, T. et al. Modulated electro-hyperthermia induced loco-regional and systemic tumor destruction in colorectal cancer allografs. J. Cancer. 9(1), 41–53 (2018).

12. Yang, K.-L. et al. In vitro comparison of conventional hyperthermia and modulated electro-hyperthermia. Oncotarget. 7(51), 84082 (2016).

13. Szasz, A., Szasz, N. & Szasz, O. Oncothermia—A new kind of oncologic hyperthermia. In Oncothermia: Principles and Practices (eds Szasz, A. et al.) 173–392 (Springer, Netherlands, 2011).

14. Yang, W. et al. Combined treatment with modulated electro-hyperthermia and an autophagy inhibitor efectively inhibit ovarian and cervical cancer growth. Int. J. Hyperth. 36(1), 9–20 (2019).

15. Andocs, G. et al. Comparison of biological efects of modulated electro-hyperthermia and conventional heat treatment in human lymphoma U937 cells. Cell Death Discov. 2(1), 16039 (2016).

16. Andocs, G., Szasz, O. & Szasz, A. Oncothermia treatment of cancer: From the laboratory to clinic. Electromagn. Biol. Med. 28(2), 148–165 (2009).

17. Schvarcz, C. A. et al. Modulated electro-hyperthermia induces a prominent local stress response and growth inhibition in mouse breast cancer isografs. Cancers. 13(7), 1744 (2021).

18. Kim, J. A. et al. Fisetin, a dietary favonoid, induces apoptosis of cancer cells by inhibiting HSF1 activity through blocking its binding to the hsp70 promoter. Carcinogenesis. 36(6), 696–706 (2015).

19. Viana, P. & Hamar, P. Targeting the heat shock response induced by modulated electro-hyperthermia (mEHT) in cancer. Biochim. Biophys. Acta Rev. Cancer. 1879(2), 189069 (2024).

20. Tsang, Y.-W. et al. Improving immunological tumor microenvironment using electro-hyperthermia followed by dendritic cell immunotherapy. BMC Cancer. 15(1), 708 (2015).

21. Chtcheglova, L. A. & Hinterdorfer, P. Simultaneous AFM topography and recognition imaging at the plasma membrane of mammalian cells. Semin. Cell Dev. Biol. 73, 45–56 (2018).

22. Juhasz, K. et al. Te complex function of Hsp70 in metastatic cancer. Cancers. 6(1), 42–66 (2014).

23. Danics, L. et al. Exhaustion of protective heat shock response induces signifcant tumor damage by apoptosis afer modulated electro-hyperthermia treatment of triple negative breast cancer isografs in mice. Cancers. 12(9), 2581 (2020).

24. Powers, M. V. & Workman, P. Inhibitors of the heat shock response: Biology and pharmacology. FEBS Lett. 581(19), 3758–3769 (2007).

25. Whitesell, L. & Lindquist, S. Inhibiting the transcription factor HSF1 as an anticancer strategy. Expert Opin. Ter. Targets. 13(4), 469–478 (2009).

26. Wigmore, S. J. et al. De-repression of heat shock transcription factor-1 in interleukin-6-treated hepatocytes is mediated by downregulation of glycogen synthase kinase 3β and MAPK/ERK-1. Int. J. Mol. Med. 19(3), 413–420 (2007).

27. Lee, S. et al. Targeting HSF1 as a therapeutic strategy for multiple mechanisms of EGFR inhibitor resistance in EGFR mutant non-small-cell lung cancer. Cancers. 13(12), 2987 (2021).

28. Yoon, Y. J. et al. KRIBB11 inhibits HSP70 synthesis through inhibition of heat shock factor 1 function by impairing the recruitment of positive transcription elongation factor b to the hsp70 promoter*. J. Biol. Chem. 286(3), 1737–1747 (2011).

29. Wang, X. et al. A study on the biological function of heat shock factor 1 proteins in breast cancer. Oncol. Lett. 16(3), 3145–3149 (2018).

30. Dai, C. Te heat-shock, or HSF1-mediated proteotoxic stress, response in cancer: From proteomic stability to oncogenesis. Philos. Trans. R. Soc. Lond. B Biol. Sci. 373(1738), 20160525 (2018).

31. Min, J. N., Huang, L., Zimonjic, D. B., Moskophidis, D. & Mivechi, N. F. Selective suppression of lymphomas by functional loss of Hsf1 in a p53-defcient mouse model for spontaneous tumors. Oncogene. 26(35), 5086–5097 (2007).

32. Dai, C., Whitesell, L., Rogers, A. B. & Lindquist, S. Heat shock factor 1 is a powerful multifaceted modifer of carcinogenesis. Cell. 130(6), 1005–1018 (2007).

33. Gabai, V. L. et al. Heat shock transcription factor Hsf1 is involved in tumor progression via regulation of hypoxia-inducible factor 1 and RNA-binding protein HuR. Mol. Cell. Biol. 32(5), 929–940 (2012).

34. Rossi, A., Ciafrè, S., Balsamo, M., Pierimarchi, P. & Santoro, M. G. Targeting the heat shock factor 1 by RNA interference: A potent tool to enhance hyperthermochemotherapy efcacy in cervical cancer. Cancer Res. 66(15), 7678–7685 (2006).

35. Zhang, G. L., Zhang, Y., Cao, K. X. & Wang, X. M. Orthotopic injection of breast cancer cells into the mice mammary fat pad. J. Vis. Exp. 143, e58604 (2019).

36. Krenacs, T. et al. Modulated electro-hyperthermia-induced tumor damage mechanisms revealed in cancer models. Int. J. Mol. Sci. 21(17), 6270 (2020).

37. Vancsik, T., Forika, G., Balogh, A., Kiss, E. & Krenacs, T. Modulated electro-hyperthermia induced p53 driven apoptosis and cell cycle arrest additively support doxorubicin chemotherapy of colorectal cancer in vitro. Cancer Med. 8(9), 4292–4303 (2019).

38. Besztercei, B. et al. Stress-induced, p53-mediated tumor growth inhibition of melanoma by modulated electrohyperthermia in mouse models without major immunogenic efects. Int. J. Mol. Sci. 20(16), 4019 (2019).

39. Tsang, Y.-W. et al. Modulated electro-hyperthermia-enhanced liposomal drug uptake by cancer cells. Int. J. Nanomedicine. 14, 1269–1279 (2019).

40. Ahmed, K., Zaidi, S. F., Mati ur, R., Rehman, R. & Kondo, T. Hyperthermia and protein homeostasis: Cytoprotection and cell death. J. Term. Biol. 91, 102615 (2020).

41. Cyran, A. M. & Zhitkovich, A. Heat shock proteins and HSF1 in cancer. Front. Oncol. 12, 860320 (2022).

42. Dong, B., Jaeger, A. M. & Tiele, D. J. Inhibiting heat shock factor 1 in cancer: A unique therapeutic opportunity. Trends Pharmacol. Sci. 40(12), 986–1005 (2019).

43. Jiang, S. et al. Multifaceted roles of HSF1 in cancer. Tumor Biol. 36(7), 4923–4931 (2015).

44. Jin, X., Moskophidis, D. & Mivechi, N. F. Heat shock transcription factor 1 is a key determinant of HCC development by regulating hepatic steatosis and metabolic syndrome. Cell Metab. 14(1), 91–103 (2011).

45. Szasz, A., Szasz, N. & Szasz, O. Oncothermia: Principles and Practices (Springer Science & Business Media, 2010).

46. Szasz, A. Heterogeneous heat absorption is complementary to radiotherapy. Cancers. 14(4), 901 (2022).

47. Nagata, T. et al. Clinical study of modulated electro-hyperthermia for advanced metastatic breast cancer. Mol. Clin. Oncol. 14(5), 103 (2021).

48. Petenyi, F. G. et al. Modulated electro-hyperthermic (mEHT) treatment in the therapy of inoperable pancreatic cancer patients—A single-center case-control study. Diseases. 9(4), 81 (2021).

49. Fiorentini, G. et al. Modulated electro-hyperthermia as palliative treatment for pancreatic cancer: A retrospective observational study on 106 patients. Integr. Cancer Ter. 18, 1534735419878505 (2019).

50. Lu, X. et al. An efcient and precise method for generating knockout cell lines based on CRISPR-Cas9 system. Eng. Life Sci. 20(12), 585–593 (2020).

51. Guo, P., Yang, J., Huang, J., Auguste, D. T. & Moses, M. A. Terapeutic genome editing of triple-negative breast tumors using a noncationic and deformable nanolipogel. Proc. Natl. Acad. Sci. 116(37), 18295–18303 (2019).

52. Kenney, J., Ndoye, A., Lamar, J. M. & DiPersio, C. M. Comparative use of CRISPR and RNAi to modulate integrin α3β1 in triple negative breast cancer cells reveals that some pro-invasive/pro-metastatic α3β1 functions are independent of global regulation of the transcriptome. PLoS ONE. 16(7), e0254714 (2021).

53. Vydra, N. et al. Heat Shock Factor 1 (HSF1) as a new tethering factor for ESR1 supporting its action in breast cancer. bioRxiv. 2021.05.06.442900 (2021).

54. Han, X. et al. CRISPR-Cas9 delivery to hard-to-transfect cells via membrane deformation. Sci. Adv. 1(7), e1500454 (2015).

55. Alshaibi, H. F., Al-shehri, B., Hassan, B., Al-zahrani, R. & Assiss, T. Modulated electrohyperthermia: A new hope for cancer patients. BioMed Res. Int. 2020, 8814878 (2020).

56. Mendillo Marc, L. et al. HSF1 drives a transcriptional program distinct from heat shock to support highly malignant human cancers. Cell. 150(3), 549–562 (2012).

57. Sharma, C. & Seo, Y. H. Small molecule inhibitors of HSF1-activated pathways as potential next-generation anticancer therapeutics. Molecules. 23(11), 2757 (2018).

58. Carpenter, R. L. et al. Combined inhibition of AKT and HSF1 suppresses breast cancer stem cells and tumor growth. Oncotarget. 8(43), 73947–73963 (2017).

59. Yang, T. et al. Phosphorylation of HSF1 by PIM2 induces PD-L1 expression and promotes tumor growth in breast cancer. Cancer Res. 79(20), 5233–5244 (2019).

60. Fok, J. H. L. et al. HSF1 is essential for myeloma cell survival and a promising therapeutic target. Clin. Cancer Res. 24(10), 2395–2407 (2018).

61. Huang, M. et al. HSF1 facilitates the multistep process of lymphatic metastasis in bladder cancer via a novel PRMT5-WDR5- dependent transcriptional program. Cancer Commun. 42(5), 447–470 (2022). 62. Shen, Z. et al. Combined inhibition of AURKA and HSF1 suppresses proliferation and promotes apoptosis in hepatocellular carcinoma by activating endoplasmic reticulum stress. Cell Oncol. 44(5), 1035–1049 (2021).

62. Pomeroy, A. E., Schmidt, E. V., Sorger, P. K. & Palmer, A. C. Drug independence and the curability of cancer by combination chemotherapy. Trends Cancer. 8(11), 915–929 (2022).

63. Zhao, W. et al. A new bliss independence model to analyze drug combination data. J. Biomol. Screen. 19(5), 817–821 (2014).

64. Li, J., Labbadia, J. & Morimoto, R. I. Rethinking HSF1 in stress, development, and organismal health. Trends Cell Biol. 27(12), 895–905 (2017).

65. Simões, R. V. et al. Metabolic plasticity of metastatic breast cancer cells: Adaptation to changes in the microenvironment. Neoplasia. 17(8), 671–684 (2015).

Acknowledgements

The authors wish to thank Eva Mátrainé Balogh, Zsuzsanna Forgács, and Rita Uzseka for their expert technical assistance with the preparation of samples for immunohistochemistry. We also would like to thank Oncotherm Ltd. (Budapest, Hungary) for making the LabEHY-200 device available, together with its accessories, and for maintenance.

Author contributions

P.H.L.V. conceived and designed the study under the supervision of P.H.. P.H.L.V., C.A. S., K.A., S.M.Z.B., N.G., D.B. and Z.K. performed the animal experiments and processed the harvested animals for further analysis. P.H.L.V. conducted the immunohistochemistry, molecular and statistical analysis. L.O.D. prepared the HSF1- knockdown cells using CRISPR/Cas9. P.H.L.V. and B.B. performed the in vitro experiments. Z.B. contrebuted to the financing, initiation and theoretical supervision of the project. All authors reviewed and approved the manuscript.

Funding

Open access funding provided by Semmelweis University. This research was funded by: Semmelweis Science and Innovation Fund: (STIA-OTKA-2022) to P.H., Semmelweis Science and Innovation Fund: (STIA-MEC-2022) to P.H.L.V., Ministry for Innovation and Technology from the source of the National Research, Development and Innovation Fund, NVKP (National Competitiveness and Excellency Program), Improving the efficiency and market introduction of electromagnetic cancer therapy equipment, (NVKP 16-1-2016-0042), Tempus Foundation: Stipendium Hungaricum scholarship, Semmelweis University: SE 250+ Excellence PhD Scholarship (SE250 + EFOP-3.6.3-VEKOP-16-2017-00009), Ministry for Innovation and Technology, Hungary (National Research, Development and Innovation Fund): Bilateral Science and Technology (S&T) cooperation (Brazil relation), (2021-1.2.4-TÉT-2021-00060), New National Excellence Program of the Ministry for Innovation and Technology from the source of the National Research, Development and Innovation Office (ÚNKP-23-4-ISE-22), New National Excellence Program of the Ministry for Innovation and Technology from the source of the National Research, Development and Innovation Office (ÚNKP-23-3-II-SE-45).

Competing interests

The authors declare no competing interests.

Pulsing Addition to Modulated Electro-Hyperthermia

Andras Szasz

Department of Biotechnics, Hungarian University of Agriculture and Life Sciences, 2100 Gödöllő, Hungary

Email: biotech@gek.szie.hu

Citation

Szasz, A. (2024) Pulsing Addition to Modulated Electro-Hyperthermia

Oncothermia Journal 38, August 2026., 34-70.
https://oncotherm.com/SzaszA_2024_Pulsing_addition_to_mEHT

Abstract

Numerous preclinical results have been verified, and clinical results have validated the advantages of modulated electro-hyperthermia (mEHT). This method uses the nonthermal effects of the electric field in addition to thermal energy absorption. Modulation helps with precisely targeting and immunogenically destroying malignant cells, which could have a vaccination-like abscopal effect. A new additional modulation (high-power pulsing) further develops the abilities of the mEHT. My objective is to present the advantages of pulsed treatment and how it fits into the mEHT therapy. Pulsed treatment increases the efficacy of destroying the selected tumor cells; it is active deeper in the body, at least tripling the penetration of the energy delivery. Due to the constant pulse amplitude, the dosing of the absorbed energy is more controllable. The induced blood flow for reoxygenation and drug delivery is high enough but not as high as increasing the risk of the dissemination of malignant cells. The short pulses have reduced surface absorption, making the treatment safer, and the increased power in the pulses allows the reduction of the treatment time needed to provide the necessary dose.

Keywords

hyperthermia; tumor; electric-field; thermal; energy; pulse; nonthermal; apoptosis; cell-selection

1. Introduction

Hyperthermia as a cancer cure is one of the early medical practices that originated from ancient medicine. The medical processes using heat remain a vital “household remedy”, even nowadays. Electromagnetic heating techniques replaced the ineffective ancient heat delivery. The application of electromagnetic effects presented unique possibilities and renewed the hyperthermia methodology. In modern therapeutic practices, using electromagnetic processes (mainly radiation) to heat the whole body or its local volume developed rapidly over a century ago. Various technical solutions for oncologic hyperthermia (HT) attract growing attention among oncology professionals.

The technical development of electromagnetic heating methods in the early 1900s revolutionized heat application for therapeutic gains, including malignancies. The curative processes with electromagnetic methods became available in the first quarter of the 19th century [1]. A French doctor, Arsene D’Arsonval, introduced a pure electromagnetic treatment called “Darsonvalization”. The absorbed electromagnetic energy resulted in heating. However, the physiological effects of heating (change in blood perfusion, thermal homeostatic regulations, risk of malignant dissemination, etc.) were initially neglected. The starting process was not free from extreme exaggerations. The German Electric Belt Agency went far, advertising that practitioners should reduce or even stop using drugs, advocating for electricity treatment alone [2].

The research on electromagnetic heating effects has revealed a complex interplay of factors. The temperature increase caused by electromagnetic energy absorption and the additional chemical changes (molecular excitations) induced by the electromagnetic field are key aspects. The thermal

component is directly related to the square of the electric current, while the field component is proportional to that current. The bioelectromagnetic excitation alters the chemical bonds and the structure of compounds through direct electric forces, while some of the absorbed energy heats the target, raising its temperature. The thermal effect alone can also trigger chemical reactions, and the field excitation enhances these effects. This understanding has paved the way for therapeutic practices that combine electromagnetic molecular, cellular, and tissue excitation with heating.

A further push on the development was the discovery of microwaves, which began clinical practice working similarly to microwave ovens. The thermal effect of electromagnetic energy absorption was much more straightforward to understand and was more accessible to study; therefore, separating the heating and exciting (thermal and nonthermal) effects became dominant (Figure 1). Our present approach creates synergy between the thermal and nonthermal components of the electromagnetic energy absorption processes.

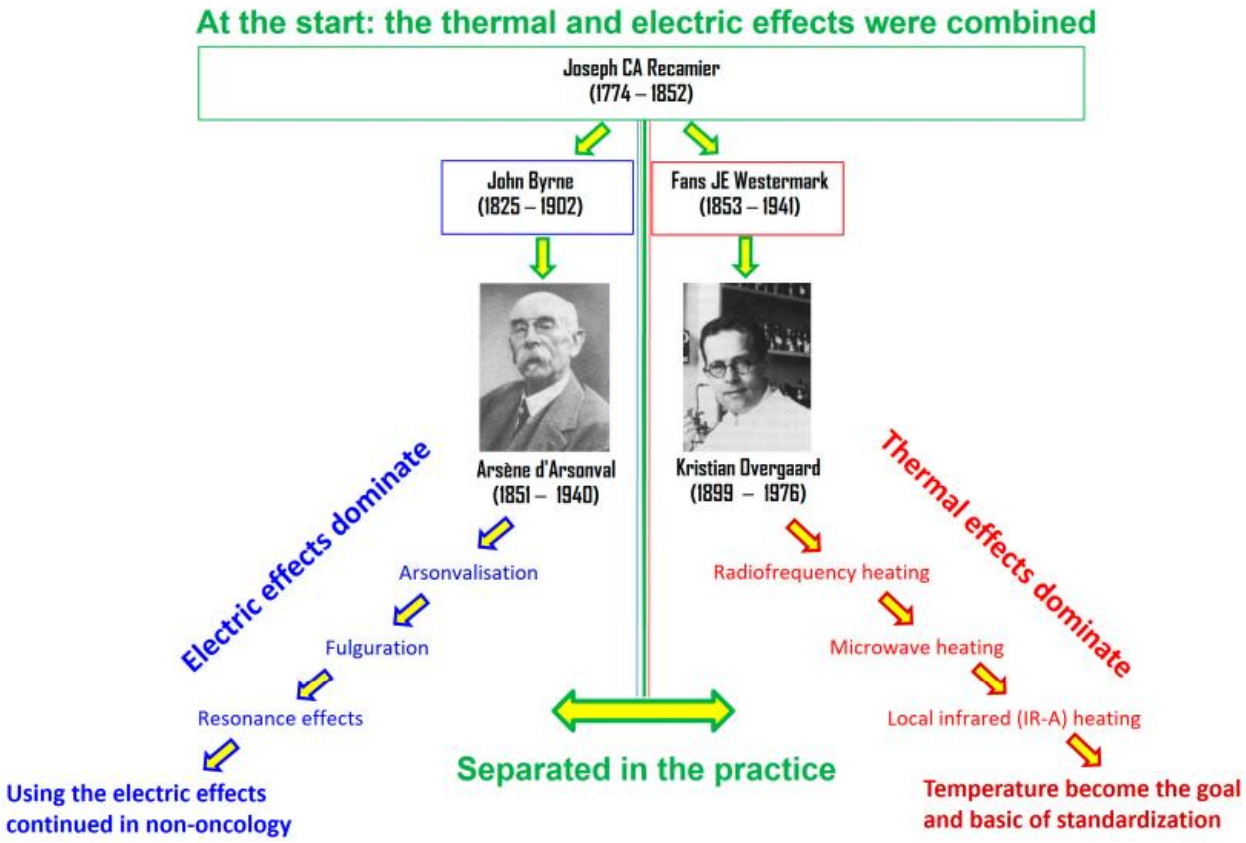

Figure 1. Arsene d'Arsonval (French) and Kristian Overgaard (Danish) are the leading doctors who divide the nonthermal field effects from heat, and the separation has widened over time.

The method's long history has not benefited it and has increased skeptical opposition, with varying positive and negative results. Infancy is standard for all developing systems but is abnormal when it is unusually long. Hyperthermia is mature for broad acceptance.

The currently known and accepted oncological hyperthermia effects can be divided into three categories, according to Figure 2:

1. It destroys the tumor cells by absorbing energy;
2. It has immunogenic effect;
3. In the most frequent application, it sensitizes the conventional oncotherapies, like radiotherapy and chemotherapy.

Two primary electromagnetic therapies are applied in medice: ionizing and nonionizing radiation. Ionizing radiation (e.g., radiotherapy) primarily has a nonthermal effect, breaking the DNA string with energy and causing more nonthermal radiative damage. At the same time, its thermal component is only tiny in most cases. The nonionizing radiation used in hyperthermia treatments is the opposite of the thermal/nonthermal ratio. It usually concentrates on the thermal component of the radiation, and the nonthermal component is a small part of conventional hyperthermia (Figure 3). The ratio of the thermal component effects looks at contrasts between the two methods, and direct cellular damage is also unlike. The direct cellular damage in the ionizing instance mostly breaks the DNA strands. At the same time, in nonionizing impact, the primary effect targets the cells as units, with concentration on the membrane damage at a temperature of about 42 ◦C. We discuss here the non-ablative applications, where the nonionizing has less energy than necessary for a direct burn.

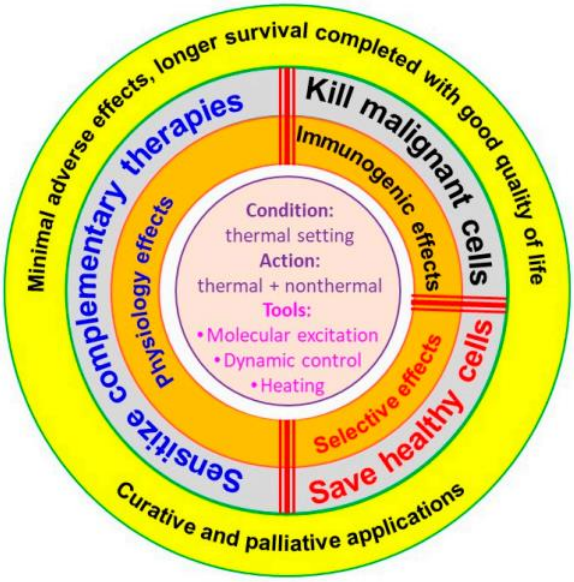

Figure 2. The hallmarks of hyperthermia's effects in oncology. The main tasks are connected to complementary applications, where the thermal conditions promote the parallel administration of other therapies.

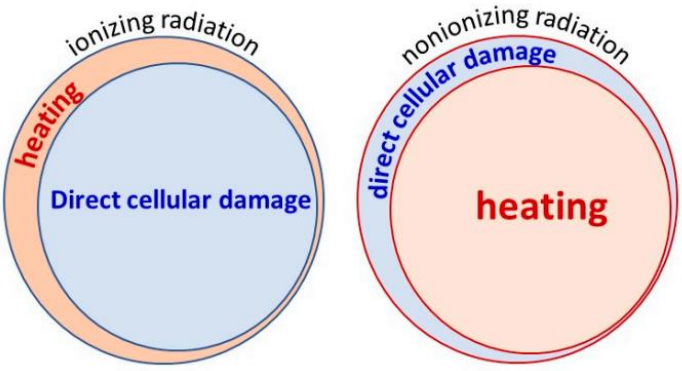

Figure 3. The treatments of electromagnetic radiation sharply differ in ionizing and nonionizing conditions.

2. Electrothermal Complexity

The electrothermal interactions are complex and can not be separated by thermal and nonthermal effects because their synergy does the job [3]. However, the ratio of these effects could be modified, forcing more nonthermal parts into the processes by the molecular excitation methods [4,5]. The primary selection mechanism uses the target's extended electric and thermal heterogeneity, which can be utilized to select the molecular groups and excite the appropriate signal patterns [6]. The electric field gives the best opportunity for selection, which can technically be achieved with capacitive coupling [7]. Capacitive coupling with the intent of homogenous mass heating was applied on deep-seated [8] and superficial tumors [9]. Multiple clinical trials were performed for many metastatic stages. Soft-tissue [10] and Ewing sarcomas [11], pancreas cancer [12], breast cancer [13], liver tumors [14], rectal [15] and colorectal [16,17] malignancies, metastatic gastric tumors [18], urinary bladder lesions [19,20], esophageal [21–23], and head & neck tumors [24,25] all have shown the feasibility of capacitive hyperthermia with remarkable results. Some studies were performed on non-small-cell lung cancer, too [26,27], but its efficacy was questioned [28]. Intraluminal capacitive application for the esophagus has also shown feasibility [21,29].

However, numerous challenges need solutions. The physiological thermal homeostasis, the thermal and electric inhomogeneity of the tumor, the complexity of the bioelectromagnetic processes, which are induced by the hyperthermia, the controllable dose, and the nearly exponential decay of the energy absorption, which overheats the surface, are all complications that need to be solved. The conventional dose is connected to the tumor's reached temperature, supporting isotherm homogeneity in the target. However, due to thermal and electric heterogeneity, the heating of biosystems is far from thermal equilibrium. Due to the physiological corrective feedback and the enormously inhomogeneous malignant target, fixing a homogeneous energy absorption in the tumor is impossible. The physiological feedback and thermodynamic processes destroy the possible homogeneous absorption part. The complex reality of living objects contradicts the macroscopic equilibrium. Moreover, the feedback processes deviate from the standard linearity of the specific absorption rate (SAR) and the temperature growth [30]. The isothermal expectation and the time-linearity in the heating process are only an illusion.

2.1. Temperature Development

The temperature development in the selected molecular group could be higher than their surroundings [31] and heat the area by the thermal convection of conduction, as is characteristically recognized in nanoparticle heating [32]. The extensively heated distance from the selectively heated small parts is small, less than 100 nm, and depends on how far it is from the artery, which cools it down. The heated molecular groups have relatively high temperatures due to the absorbed energy, and the larger volumes have gradually lower temperature averages (Figure 4). The concentrated energy absorption heats the transmembrane protein clusters (rafts), which heats the cell, but the average temperature will be less than in the raft. The cell heats the tumor, further lowering the average temperature. This thermal cascade makes it possible that the thermal effect, on average, remains safe and creates optimal conditions for the chemical reactions. Still, the micro-parts have enough energy to excite the necessary signal pathways.

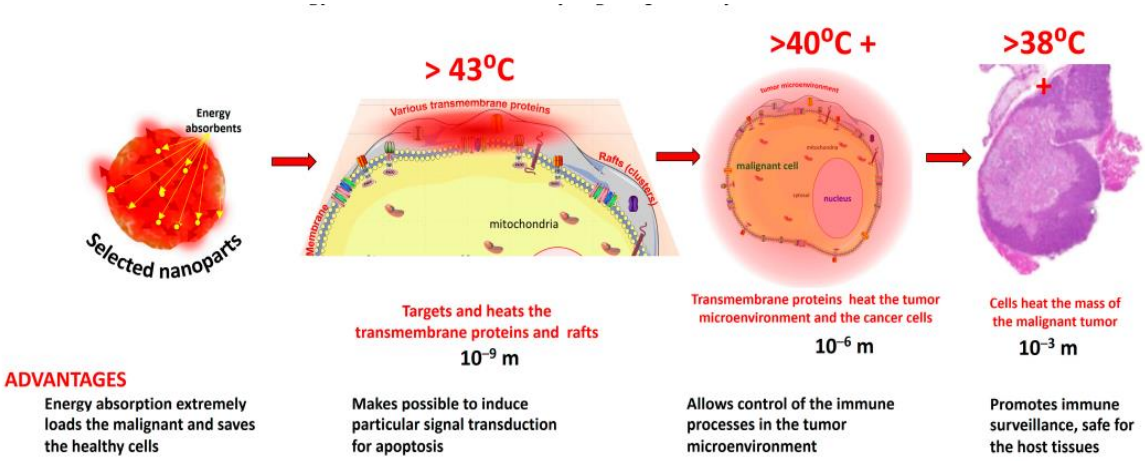

Figure 4. The thermal cascade of the averages for the heterogenic heating of the mEHT. The average sizes magnify about three orders of magnitudes in the different steps.

The heating by the small protein molecular groups (rafts) has limitations. When the energy is too large, the transmembrane proteins are dehydrated and decomposed, which does not serve the signal excitation demand. The selection no longer works, and the thermal component starts to overdominate the entire process.

2.2 Selection

The first selection step is based on the metabolic differences between cancer and healthy cells. The reprogrammed metabolism (Warburg effect) increases the ionic concentration in the tumor microenvironment, so the well-chosen RF current may prefer to flow through the tumor. The next selective factor finds the tumor cells, which will differ from their healthy counterpart because of their autonomy and the broken healthy network, which provides differentiation in the dielectric constant of the cell and offers a cellular selection. The selected malignant cells have transmembrane protein molecular clusters (membrane rafts) that are the target of the selection. These rafts are embedded in the well-isolating lipid membrane, so their relative conductivity is high, and they massively absorb the energy [31]. The energy absorption with the well-chosen modulation, delivered by the RF carrier frequency, induces signals leading the cell to immunogenic cell death (Figure 5).

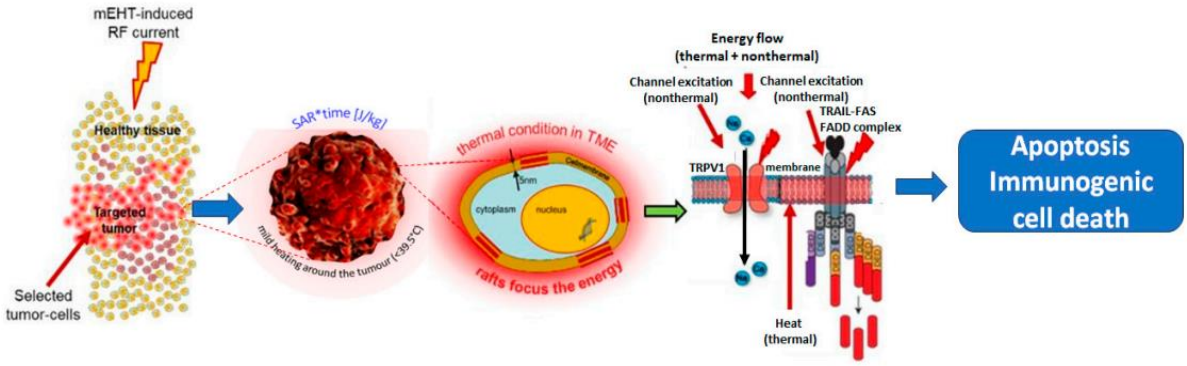

Figure 5. The cell is "gently" destroyed by the support of natural apoptotic signals, allowing the unhurt immunogenic information to be liberated during special apoptosis

The impedance matching allows an energy-dose measure, ensuring that mainly the selected molecules absorb the energy. The specific absorption rate and temperature are connected at the physiological level by the blood flow (vasodilatation and vasocontraction changes) [30], which has no relevance when the heating is nanoscopic but has an increased modification of the energy intake by the homogenization of the temperature, leading to overdosing. Applied fractal modulation is also a novel technical innovation in impedance matching solutions [33], helping to produce immunogenic cell death (ICD) with its dynamic synchronization for homeostatic demands. The modulation with impedance-matching cellular selection completes the modulated electro-hyperthermia (mEHT) method [34,35]. The technical solution to optimize the ratio of the thermal and nonthermal components of the RF current needs a precise fit to the individual case, which changes with every treatment. The electronic solution is tuning the system to the measured impedance of the treated individual. The tuning seeks to form a touching situation as a purely metallic electrode would be fitted to the skin directly. This matching situation calculates the actual energy loss carefully, controls the reflected power, and matches the resonant compensation of the surface capacitor of the adipose tissue. The active impedance-guided capacitive solution (like mEHT) can use the bioelectromagnetic specialties of the malignant cells directly by RF current flow when it is matched to the optimized current. Cancer cells have an intensive metabolism to supply their proliferation [36]. The metabolic rate in most of the tumors is higher than their healthy counterpart (by at least 15% higher [37,38]), which selectively increases their temperature. The process has positive feedback because the growing temperature decreases the impedance of the tissue [39]. The high metabolic rate is used to identify the proliferation by positron-emission tomography (PET) [40,41]. The high nutrient/waste transport increases the ion concentration of the electrolytes in the surroundings of the malignant cell. The increased ionic concentration means a higher microenvironment conductivity [42] in the tumor cells and lowers the resistivity of the whole tumor. It could distinguish between healthy and malignant situations [43]. Due to the lack of a healthy cellular network in malignancy, the extracellular matrix of malignant cells has high dielectric permittivity, which can be used for selection [44,45]. The permittivity and the conduction modify the total impedance in the microenvironment of the malignant cells [46], which allows their automatic selection, while the RF current flows in the direction of the low electric impedance. The RF current density (specially chosen frequency and modulation) will self-selectively flow toward the malignant cells, which is measurable by the MRI current density image [47,48]. This effect is entirely automatic and follows any movements of the cells in real-time, solving the challenge of focusing.

The amount of apoptosis could be regulated by the ratio of the heating (temperature grows) and keeping (temperature is stable) periods. In the heating-up period, the thermal effect grows, and the excitation (non-thermal effect) grows due to the better conditions of the molecular reaction rates. In the stable temperature period, the thermal and non-thermal factors are constant, and the absorbed energy replaces the heat loss in the system. It is observed that during the heating-up period by mEHT, the apoptosis rate is significantly higher than that of the temperature-keeping period [49]. Applied step-up heating uses this difference to improve apoptotic processes [50].

2.3 Nonthermal Effects

Living objects are profoundly heterogenic. This heterogeneity defines the nonthermal electromagnetic interactions and the final effect. Electromagnetism acts through the various molecular and cellular structures, making energy absorption by current flow, making the

polarization effect for polar molecules, exciting electrons between two energy levels, arranging the structure (order/disorder transition), making connected or separated clusters (percolation), breaking the cellular membrane (electroporation), inducing electrophoresis, electroosmosis, and excitation of the membrane channels. These effects are well-oriented, while the thermal effect primarily increases the kinetic energy of the molecules, which move faster and vibrate more intensely. The more considerable thermal energy may change the molecular interactions or cause phase changes (Figure 6).

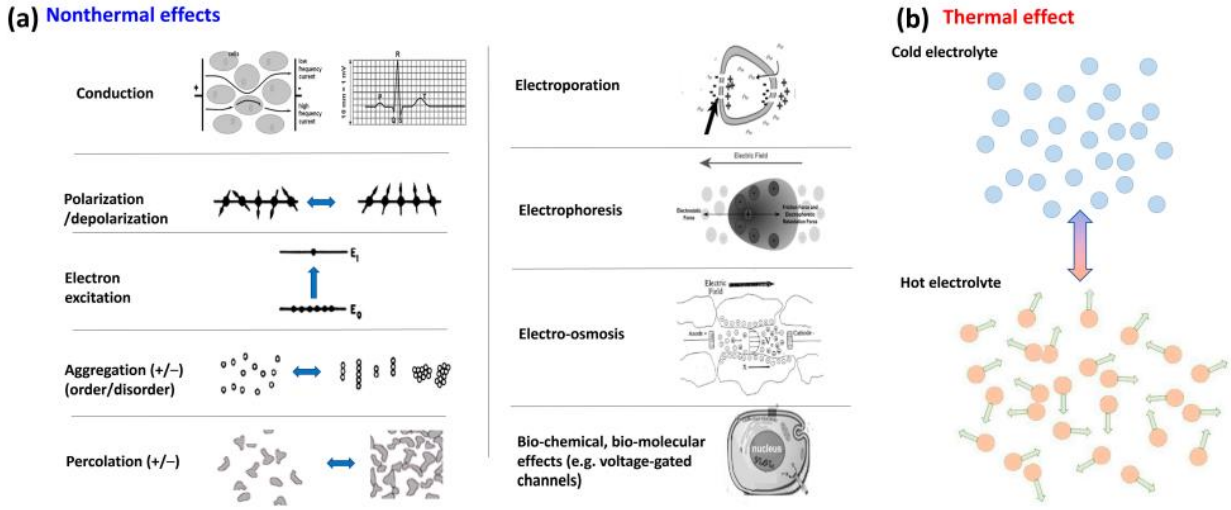

Figure 6. Nonthermal and thermal difference. (a) The nonthermal bioelectromagnetic effects vary widely in modifying energy absorption, allowing targeted manipulations of the chemical bonds in the body. (b) The thermal effects directly energize the target's electrolyte components (ions, molecules, cells), significantly increasing their kinetic energy.

The applied RF electric field changes the cells' polarization and has different current components caused by the target's impedance (Figure 7). The target's capacitive behavior declines a part of the current from the ohmic component, which is mainly responsible for thermal effects by its vectorial direction.

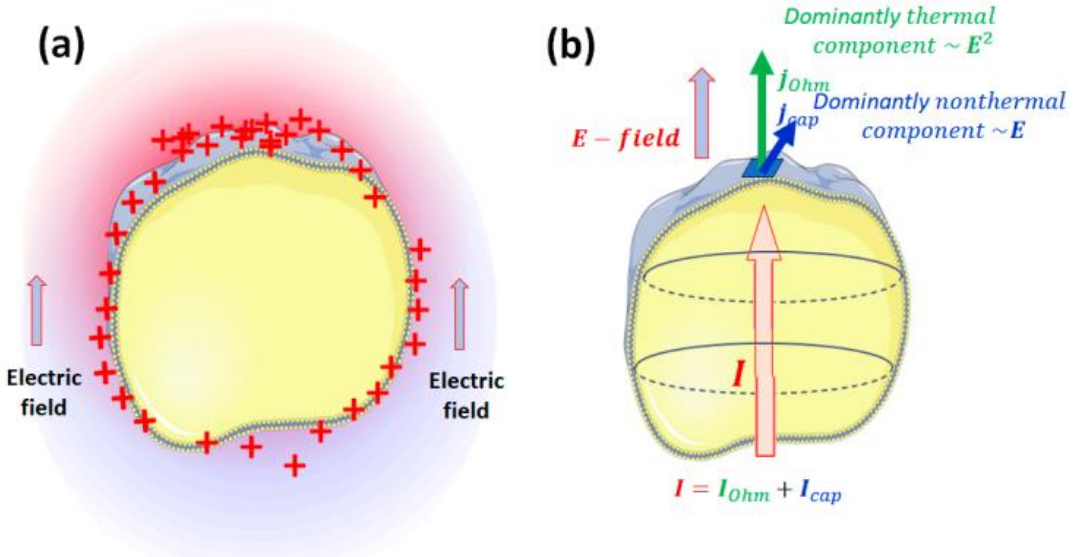

. **Figure 7**. The effects of the external RF field. (**a**) The intense polarization effect of the external field repolarizes the cells, causing hyperpolarization and depolarization states on the membrane. (**b**) The complex current has two components flowing through capacitors (membrane lipid layers).

Many molecular and physiological processes are determined by the heterogeneous lipid domains serving as molecular sorting platforms [51]. The malignant cells have a denser lipid-raft population on their membranes than their healthy counterparts [52]. Consequently, membrane heterogeneity is crucial in malignant cells' selective energy absorption (Figure 8) and appears to be a synergy of thermal effects with nonthermal electricity.

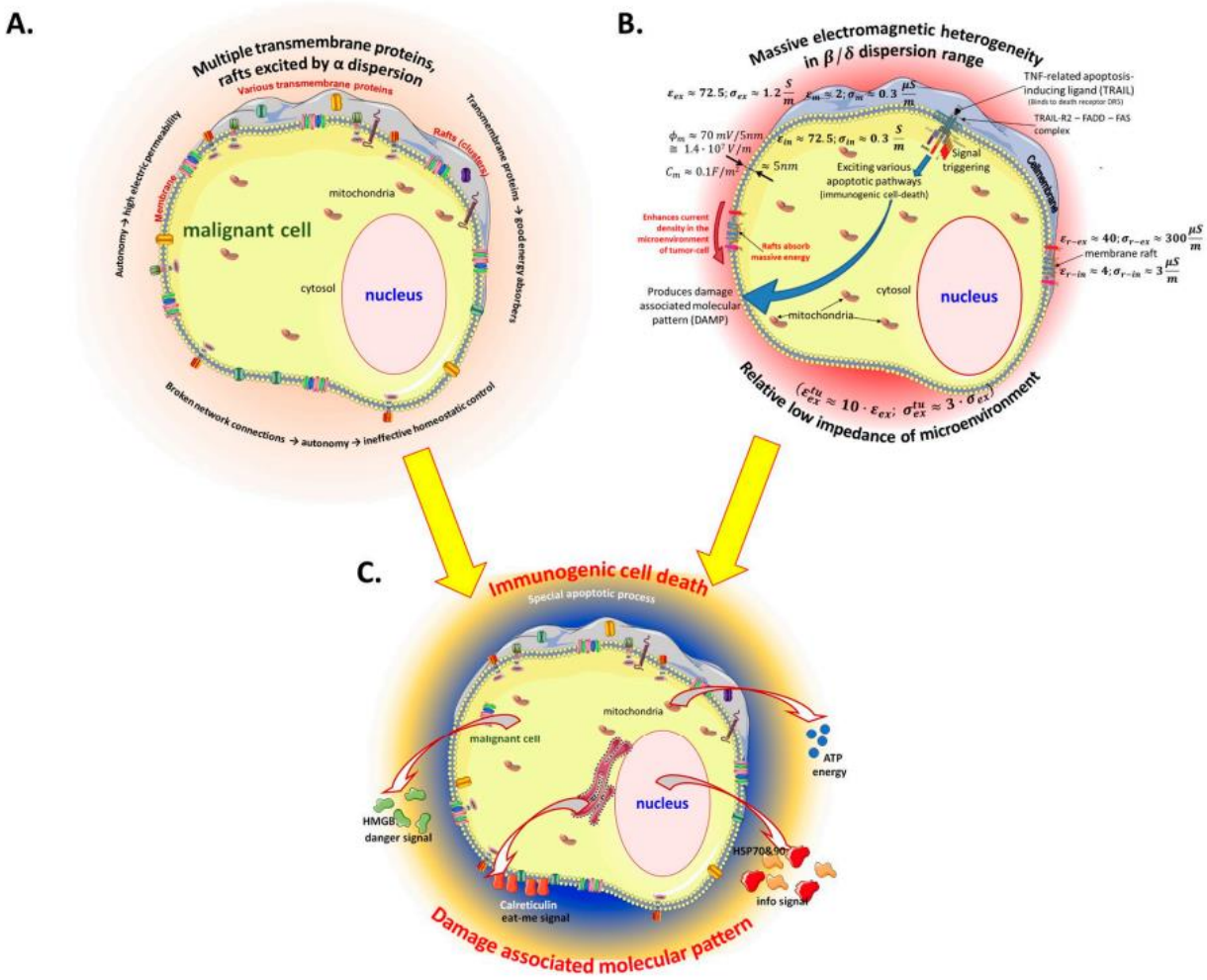

Figure 8. The electromagnetic heterogeneity of the selected tumor cell. (a) The transmembrane protein excitations are targeted by α-dispersion. (b) The electromagnetic heterogeneity is targeted by particular RF frequency (C). The result is the damage associated with molecular patterns induced by immunogenic cell death. Abbreviations/references: εex and σex are the relative permittivity and conductivity of extracellular electrolytes in the microenvironment of a cell [53]; ε tu ex and σ tu ex are the relative permittivity and conductivity of extracellular electrolytes in the microenvironment of a tumor cell: εm and σm are the relative permittivity and conductivity of the cell membrane [54]; εin and σin are the relative permittivity and conductivity of intracellular electrolytes of a cell [52]; εr-in and σr-in are the relative permittivity and

conductivity of the intracellular side of raft proteins [55,56]; εr-ex and σr-ex are the relative permittivity and conductivity of the extracellular side of raft proteins [57,58].

2.4 Thermal Homeostasis

The thermal processes have a complex nonlinear interaction with homeostatic regulation, which tries to keep thermal homeostasis. The hypothalamus receives thermal signals (primarily from TRP receptors) and acts to reduce the temperature. The principal effects are blood flow with vasodilation and sweating trying to cool using an evaporating process. The thermal regulation balances the incoming energy, which nonlinearly fluctuates in the equilibrium (Figure 9) of incoming energy [59]. The fluctuation has various physiological components, including the opposition sensory mechanisms [60] and the various relaxation times of the different processes. The basic relaxation times could be measured with NMR [61], and the complex processes by various physiological measurements [62,63].

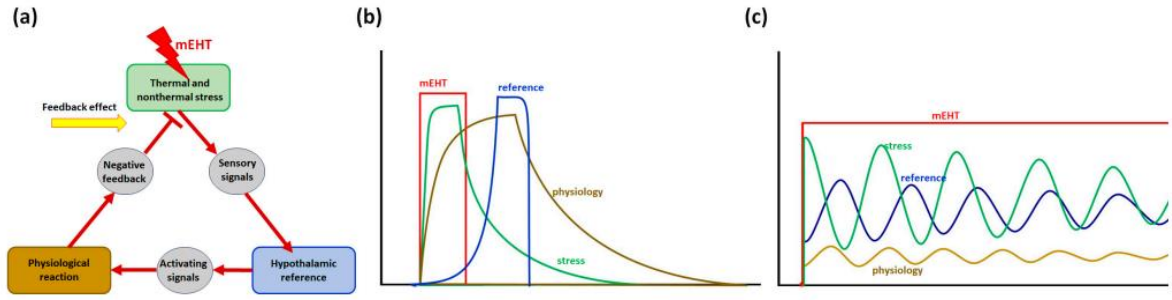

Figure 9. The temperature in the homeostatic range adapts to the new conditions, defining a new equilibrium state. (a) Thermal homeostasis has a negative feedback loop as the basis of regulation. (b) In a pulse of mEHT, the heat stress rises, and exponential decline returns to the baseline. The thermal reference (hypothalamus) and the physiological counter action (mainly the blood low) have a time lag, acting later. (c) In continuing the mEHT impact, the stress, physiology, and reference point fluctuate decreasingly.

The temperature growth of local tissue in depth has a well-known character in time at constant absorbed power, defined by the specific absorption rate $\left(SAR = \frac{Absorbed\ power\ [\mathrm{W}]}{Mass\ of\ absorber\ [\mathrm{kg}]}\right)$.

The absorbed energy (E_{absorb}) heats the local target, increasing its temperature (T). The physiological feedback process has a condition-dependent delay. Still, thermal homeostasis tries to restore equilibrium after the reaction time with intensive heat exchange and electrolyte transport $(E_{transport})$, like blood and lymph. Some absorbed energy also heats the surroundings, initially nontargeted issues (E_{tissue}). Consequently, the energy which increases the temperature (E_T) is less than the incident E_{absorb} value. The absorbed energy grows the target temperature energy, but a part of the energy is used up for thermal homeostatic control (primarily the blood flow regulation) and heat conductivity to the neighboring tissues:

Considering the energy balance, the Pennes equation [64] describes the heating process:

$$\rho_h c \frac{\partial T}{\partial t} = \rho_h SAR - c_b \rho_b w_b(T)(\Delta T) - k_h \nabla^2 T + q_0 \rho 1.1^{(\Delta T)} \quad (1)$$

The terms in the Equation (1) are as follows: $\rho_h c \frac{\partial T}{\partial t} = \begin{matrix} Energy\ for\ the \\ temperature\ grows, \\ in\ the\ target \end{matrix}$, $\rho_h SAR = \begin{matrix} Absorbed\ energy \\ from\ outside \\ incident\ power \end{matrix}$, $c_b \rho_b w_b(T)(\Delta T) = \begin{matrix} Energy\ loss\ by \\ homeostatic\ regulation \\ (blood,\ lymph\ transport) \end{matrix}$, and $\left(k_h \nabla^2 T + q_0 \rho 1.1^{(\Delta T)}\right) = \begin{matrix} Energy\ loss \\ by\ tissue \\ environment \end{matrix}$.

The c, ρ, and w are the specific heat, density, and perfusion. The subscripts denote the healthy tissue (h) and the blood (b) values. When the Pennes equation is applied to the tumor, the subscript will be t. The wb is the blood perfusion rate and T and t are the temperature and time, respectively. The analytical solution of this partial differential equation is a difficult task. The first approach uses the Green function [65,66] and the Green heat kernel function [67] and uses an analytical solution [68]. The point source Green function solution [69] can simulate the nanoparticle or thin needle with very local heating. The differential equation can be well approached with differences when the time changes. The homeostatic control is slow enough and does not allow rapid changes, so the differences in the values can be used to approach the solution of the differential equations with enough accuracy, neglecting the minority effects in (1) at constant SAR. Introducing the temperature difference instead of the differential, ΔT = T - Tb , we obtain the following:

$$\frac{\partial \Delta T}{\partial t} + \frac{1}{\tau} \Delta T = \frac{SAR}{c} \quad (2)$$

where $\tau_0 \cong \frac{1}{c_b w_b}$ is the relaxation time in the perfusion model according to the Pennes Equation (1). The solution to this difference-equation is as follows:

$$\Delta T = \frac{SAR}{c_b w_b}\left(1 - e^{-\frac{t}{\tau}}\right) \quad (3)$$

We must approximate the relaxation time in cancerous tissue. In rough approximations, the blood perfusion of the tumor is 0.833 kg/sm3 when the temperature is below 41 ◦C and 0.416 kg/sm3 when the temperature is above it [70]. Therefore, the following applies:

$$\begin{aligned} \tau_{<41} &\cong \frac{10^3}{0.833} = 1200\ \text{s} = 20\ \text{min}, \\ \tau_{>41} &\cong \frac{10^3}{0.416} = 40\ \text{min} \end{aligned} \quad (4)$$

However, the inflammatory reaction occurs in the surrounding tissues and not in the tumor itself, so the relaxation time in this constant perfusion model is as follows:

$$\tau_0 \cong \frac{10^3}{4} \cong 4.2 \text{ min} \quad (5)$$

It is the "wash-out" time of the heat perturbation in the tissue [71], depending on the blood flow of the studied tissue. This is the tissue relaxation after a heat shock by the blood-flow washout process. Healthy tissue is measured at ~ 4 - 7 min. The clinical standard average of SAR in the MHz range is 6 min [72], and we use it as a standard physiological average relaxation time, τ_{ave} = 6 min.

The time of thermal washout could be modified by changing the metabolic rate by lowering the temperature, and it will make the tail of the washout function longer in time. Consequently, a longer t ′ 0 > t0 a value will be added to the simple exponential, which depends on the decreased metabolism by the cooling process. This additional effect will cause a time lag because of the actual physiological time of the metabolic reaction. Due to the physiological self-time, which is about the same as the thermal washout physiological time, is approximately 6 min.

Thermal homeostasis regulates the temperature of the tissue. The absorbed energy drives temperature growth, but the increased blood flow, as an energy sink, counteracts. Over time, thermal homeostasis fixes the temperature in the thermal equilibrium, forming a steady-state process. The temperature, in this case, becomes constant. The absorbed energy substitutes the losses by $E_{transport}$ and E_{tissue}, without changing the temperature (Figure 10).

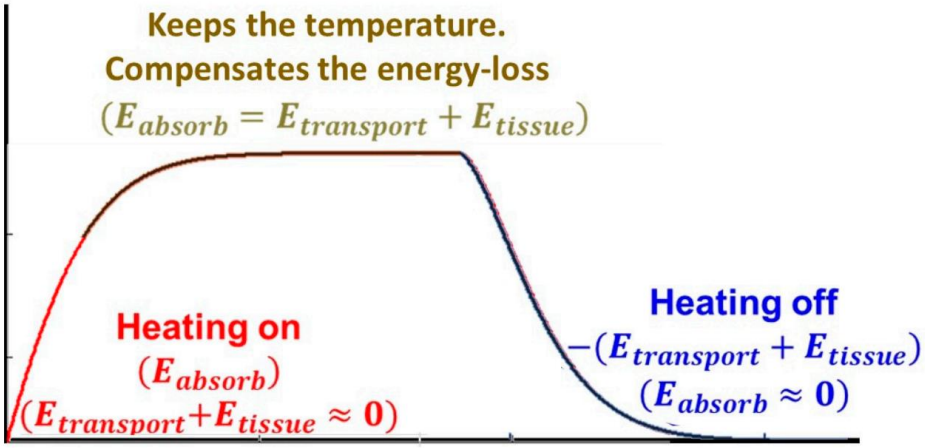

Figure 10. Figure 10. The phases of the temperature development while the absorption is on/off. The phases of the temperature development while the absorption is on/off.

All these dynamic changes depend sharply on personal homeostatic regulations, the electrolyte transport in the targeted volume, and the incident power. The dynamism of the heat delivery may also profoundly change the heating process [69]. Due to the physiological changes (first due to the blood-stream variation), the linear dependence breaks (Figure 11). When the SAR value is moderate, thermal surveillance develops an equilibrium [73]. However, a higher SAR (rapid temperature gain) could cause overshooting, compensated only after an overshooting, but the SAR could be as much

as the homeostatic regulation cannot fix the temperature. Notably, the tumors are usually hotter than their host due to the high proliferation and energy use, even in thermal equilibrium.

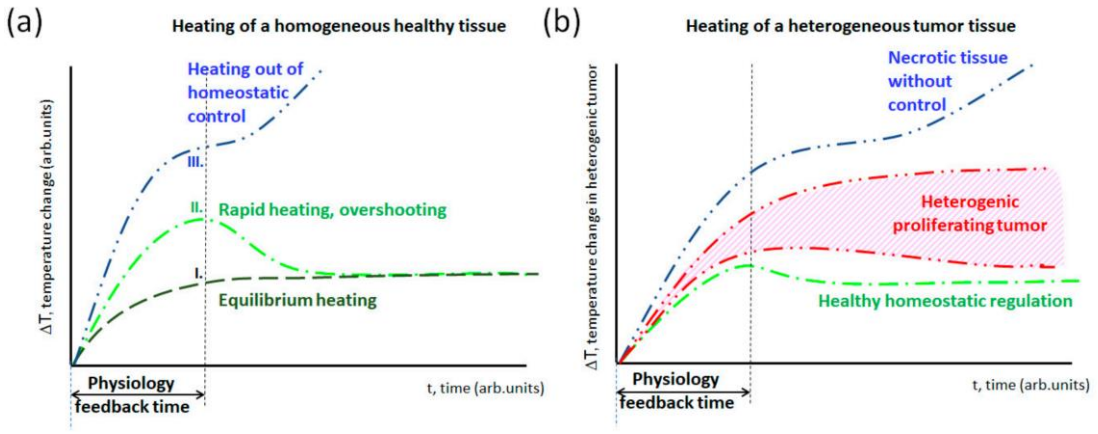

Figure 11. The incident heat could determine the different processes of the control process of thermal homeostasis. (a) (I) Is the simplest saturation, a steady state heating of a healthy tissue When the SAR is moderate, the temperature rise is relatively slow (this is the case in most regional treatments). (II) The SAR is high enough for sudden temperature changes, while the physiological thermal feedback only reacts later and regulates the saturation value (this is the case in high-energy local treatments). (III) The SAR is huge; feedback is not able to moderate the temperature, and it toxically burns (this is the case in most ablation treatments). (b) The tumor is highly heterogenic, and the temperature develops differently in its parts [71,74]. The high proliferation rate of the tumor enhances the deviation from the healthy equilibrium. A significant volume of the tumor could be necrotic without control.

The blood delivers the drugs for chemotherapies and oxygen for radiotherapy, so its behaviors are essential. The timing of the deliveries and washing out the toxic species are important factors to consider. In hyperthermia applications, the thermal washout time is driven by the BF and differs from the nonthermal clearance of molecules (like radiofarmacons, tracers, blood-delivered molecules, drugs, particles, or cells) from the tissues. The main difference is in the mechanisms of diffusion, which are different for various blood delivered particles or molecules and heat. The thermal washout is also a complex process mainly driven by the BF, but not determined by it alone. The investigations of the clearance of tracers clearly show that the clearance (wash-out) tightly depends on the BF but these parameters are not equal; instantaneous mixing with metabolic changes and diffusion breaks the unity. Also, the metabolic heat does not directly affect the clearance, while the thermal washout is directly modified by it.

A “similarity” could be observed in the washout of tracers [74], which is a rescaling of the time, showing a similar scaling behavior as we saw in the heat-up process. The washout scaling “similarity” is also present in the wash-in of the tracer [75]. An important observation in contrast material studies is that the enhancement of the contrast material decreases with the temperature growth while increasing with the thermal cooling coefficient [76]. The main message is the high variability of the BF with tumor entities, and the tumors have a massively heterogeneous BF, having a gradient from the center to the periphery.

Hyperthermia protocols usually apply step-up heating specialized to the patient's sensing. The heat pain effectively limits the hyperthermia dose. The patient senses the process and thus guides the personalized homeostatic heating-up dosing. It is more patient friendly, causing as little discomfort as possible because the patient's homeostatic control is active. The central task is to provide the proper dose. The actual protocol for the treated patient must be optimized to the given conditions and curatively effective with a high standard for safety, limiting the applied dose. This concept is entirely different from the conventional hyperthermia goals because instead of trying to produce isothermal volumes (equal temperature in the tumor), it uses heterogenic heating, following the heterogeneity of the tissue itself. This far-from-equilibrium heating keeps the driving force between the heated membrane rafts and its environment, pumping the heat from these nanoclusters to the cell interior.

When the intended dose is too much, it has to be corrected via personal notes. On the other hand, when the protocol presets a low energy dose, higher energy can be applied until the patient indicates the personalized limit. Overheating is practically impossible because the skin's surface has the highest thermal load, and heat sensing is also there. This personalized dose regulation is the main factor for safety and, together with this, for efficacy. In proper step-up heating, no continuous increase of the temperature is applied. The primary governing process is homeostasis, so the heating fits that equilibrium. A steady-state gradual heating is necessary. The physiological response time must be considered. This characteristic time is when the homeostatic equilibrium is re-established in the new conditions after a definite disturbance. The average wash-out time in humans is approx. five to seven minutes. Considering the transient "break" of six min, the step-up heating is shown in Figure 12. A detailed calculation shows the rise in temperature and its dependence on the power function in step-up heating [49,50].

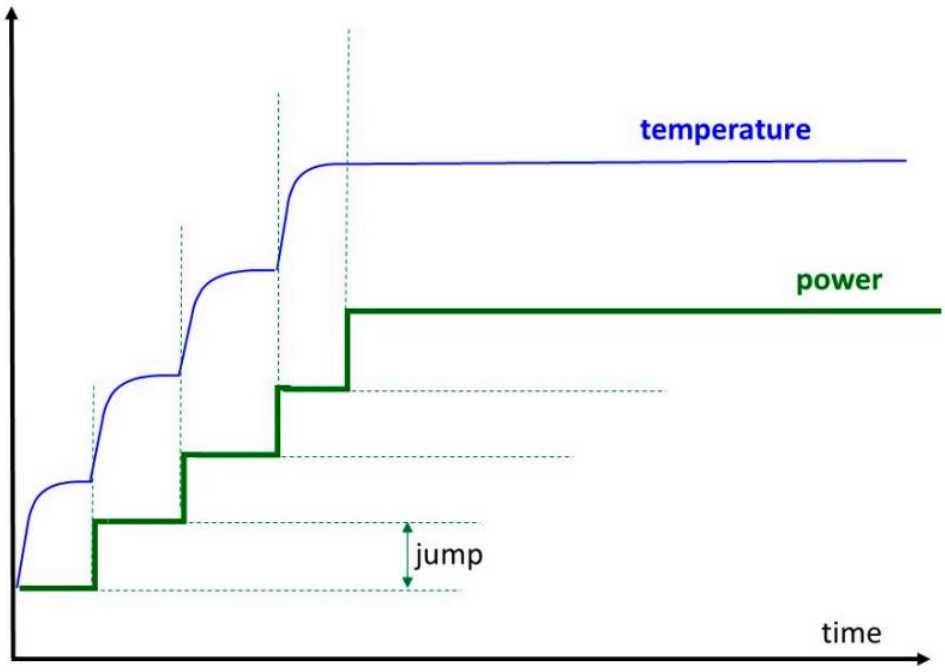

Figure 12. Step-up heating considers physiological adaptation. Step-up heating maintains the steps until homeostatic equilibrium. The provided cumulative energy could vary with the time intervals of the steps.

3. Semi-Adiabatic Synergy (SAR)

At the start of the heating, when the physiology does not impact ($E_{transport}$ = E_{tissue} = 0), the complete ET makes a temperature increase, so in this case, the following applies:

$$E_T = E_{absorb} = m_t \cdot c_t \cdot \Delta T \quad (6)$$

í

where m_t is the heated tumor mass, c_t is the specific heat of the tumor, and ΔT is the temperature increase. In a shorter time than the actual relaxation of the tissue, the thermal homeostasis does not modify the absorbed energy, and the SAR directly defines the temperature development. Using (6) in this initial stage as follows:

$$SAR = \frac{E_{absorb}}{m_t \cdot \Delta t} = \frac{m_t \cdot c_t \cdot \Delta T}{m_t \cdot \Delta t} = c_t \cdot \left(\frac{\Delta T}{\Delta t} \right) \quad (7)$$

This initial period is too short, causing a physiological reaction with blood perfusion. It is "semi-adiabatic", and only the SAR acts for temperature development, neglecting the thermal homeostatic processes led by blood perfusion, but additionally keeps away from the growing metabolic rate, the change of the absorbed power due to the variation of electric and thermal parameters with the temperature, etc. All the absorbed energy appears like it would be a non-living target, so the thermal and nonthermal synergy appears. Due to this period not dealing with the homeostatic processes, the nonthermal effects occur more than in the further heating when the thermal control works. So, the nonthermal impact is dominantly active in this period Figure 13.

The temperature profile after this semi-adiabatic period declines with the slope of the temperature change and seeks thermal equilibrium without changing the temperature (Figure 14). This equilibrium temperature requests an energy dose, which replaces the lost energy by cooling.

The equilibrium process could be described with a stochastic explanation [49], approximating the different heat transfer parts. When thermal homeostasis stabilizes the temperature, the absorbed energy replaces that lost by heat conduction, convection, and radiation to keep the equilibrium. When the temperature development deviates from the slope, going stationary, another so-called constant perfusion rate model could be introduced. We seek to equilibrate the dominant factors that remain in the Pennes Equation (1) as follows:

$$\rho_h c_h \frac{\partial T}{\partial t} = \rho_h SAR - c_b \rho_b w_b(T)(\Delta T) \quad (8)$$

The solution of (8) is as follows:

$$\Delta T = \frac{\rho_h SAR}{c_b \rho_b w_b(T)} \left(1 - e^{-\left(\frac{t}{\tau_0}\right)} \right) \quad (9)$$

where

$$\tau_0 = \frac{c_h \rho_h}{c_b \rho_b w_b(T)} \cong \frac{1}{w_b(T)} \quad (10)$$

is the time constant of the constant perfusion model. Using realistic parameters, we obtain $\tau_{cp} \sim =$ 6 min. When t is large, the system reaches thermal equilibrium, and no further rise in the temperature is observed:

$$0 = \rho_h SAR - c_b \rho_b w_b(T)(\Delta T) \quad (11)$$

From (11), the equilibrium temperature is as follows:

$$T_{eq} \cong 1.4 \frac{SAR}{c_b \cdot w_b(T_{eq})} = 1.4 \frac{SAR}{perfusion} \quad (12)$$

When the power is switched off, the target cools down, determined by the wash-out time.

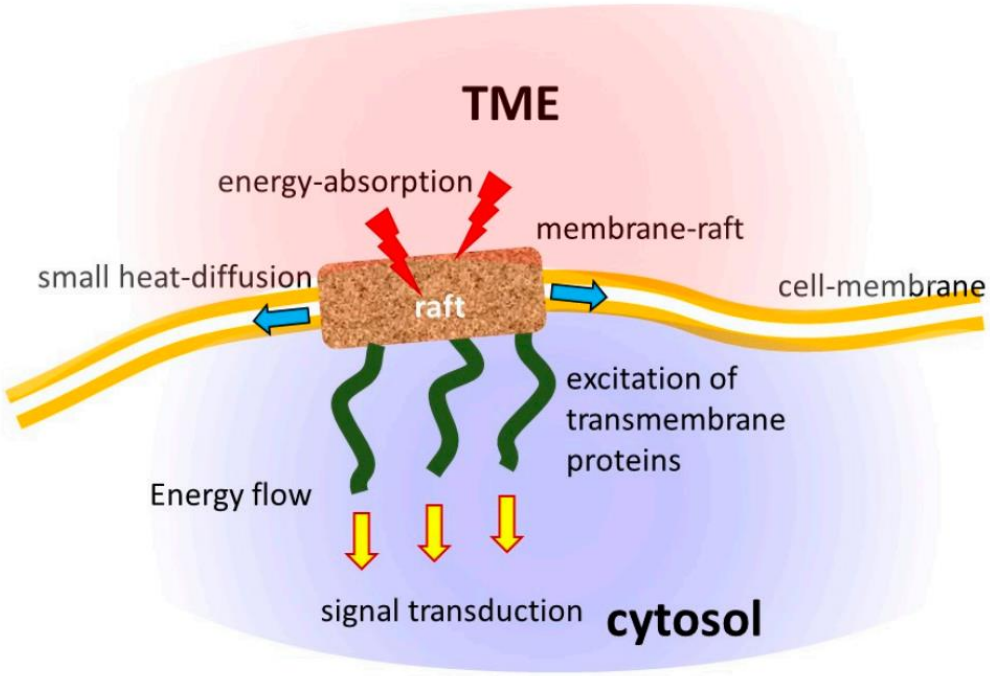

Figure 13. The semi-adiabatic heating of the raft structure. The energy absorption is focused on the rafts. They are embedded in a well-isolating lipid layer, which has bad heat conduction, increasing the time lag of the body's reaction to the heating process.

The impedance matching covers the cooling process and stabilizes the homeostatic control in the subcutis layer under the electrodes. Significant differences appear in the doses during the heating period, showing an increase in the temperature until it reaches the stable thermal equilibrium. The emphasis on the thermal or nonthermal processes makes the principal difference between the two heating periods. The nonthermal period primarily depends on the heating technique, the position of the tumor, and the initial power density $\left[\frac{W}{cm^2}\right]$

The semi-adiabatic period in radiation is between 10 and 15 min [77], which is about 20% of the complete session time. However, some protocol modifications could change the ratio. Step-up heating typically increases relative nonthermal dominance because the power proceeds before the thermal regulation becomes active. Of course, the thermal and nonthermal effects are strongly synergistic and tightly interact (Figure 15).

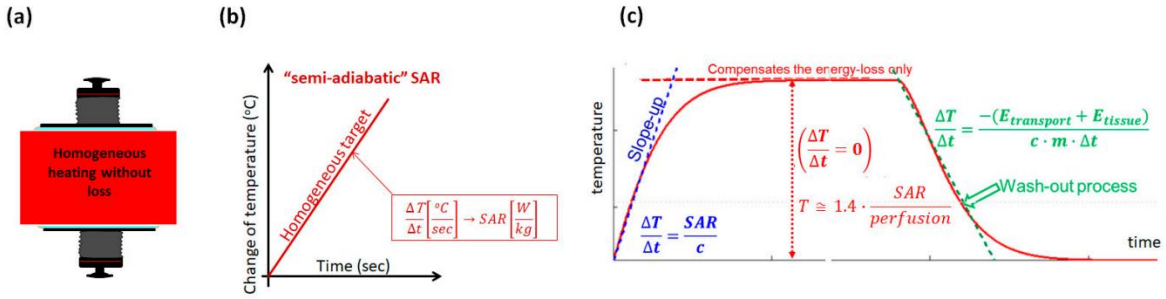

Figure 14. Heating process. (a) The target heated homogeneously. (b) The starting period heats only the target. It is semi-adiabatic. The physiological feedback has a conditional delay. (c) When the thermal regulation makes equilibrium, the temperature does not change, and the perfusion of the electrolyte transfer compensates for the incoming energy. When the power is switched off, the perfusion and tissue heat transfer defines the slope down (wash-out).

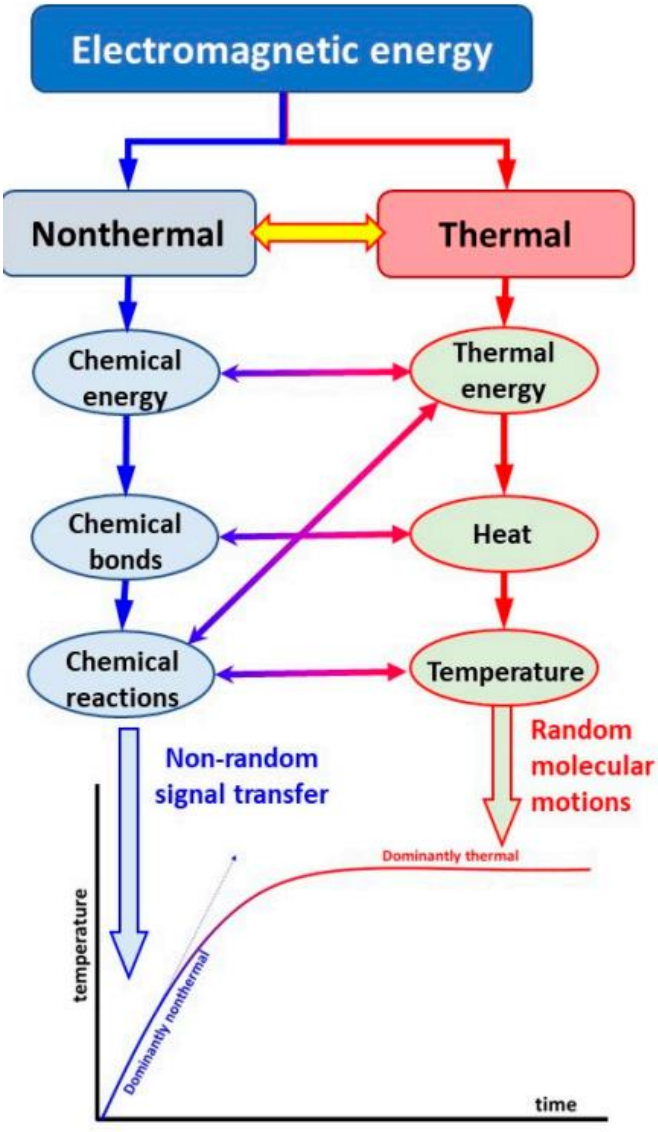

Figure 15. The thermal and nonthermal effects work in synergy. The nonthermal dominates the semi-adiabatic heating period, while the thermal dominates the equilibrium.

3.1 Semi-Adiabatic Synergy (SAS) Promotes Apoptosis

Two main categories (and many of their variants) cause cell death. Necrosis is the sudden rupture of the cell. The cytoplasm and the cellular organelles located freely in the extracellular matrix could cause inflammation or, in large quantities, could be toxic. Another major variant is apoptosis, where cell death is gentler. The cellular components became fragmented and could be embedded in lipid membranes for safe elimination. An extremely gentle fragmentation happens in immunogenic cell death when damage associated with a molecular pattern is released in an undestroyed form [78]. The unhurt molecules deliver information about the genetic structure of the cancer cell, which could be used to adapt the available dendritic cells for immune surveillance to overcome the evading capability of cancer [79,80]. The tumor-specific adaptive immune T cells (killer and helper cells) perform immune attacks on distant metastases to where the bloodstream delivers them [81], which was observed in human studies as well [82,83].

Nonthermal activity was widely studied [84,85], and its synergy with a thermal component of absorption is also studied [4,5]. The synergy of the thermal and nonthermal effects recognized in mEHT increases apoptosis compared to the only thermal conditions [86–88], which has been shown to be complementary to chemotherapy [89] and radiotherapy [90]. The effect of modulation as a purely nonthermal impact also increases apoptosis [91].

3.2. In Vitro Verification

In cell-line experimental conditions [49], it was proven that the increased temperature is proportional to the absorbed power (SAR) in semi-adiabatic states as shown in (7), while exponential declines from this linearity, as in (9), and equilibriums appear at constant temperature (12). The SAS conditions have nonthermal dominance. Apoptosis during this linear changing period may be compared to the equilibrium to study the thermal and nonthermal impact difference on the cellular level [49]. The experiment measured apoptosis during the two definite periods of energy absorption. The regular mEHT of the adenocarcinoma human alveolar basal epithelial cell line, A549 treatment, was performed at 42 ◦C starting from 25 ◦C. The heating details were studied by divided periods, as shown in Figure 17:

1. Phase 1. heated the cells from the room temperature (25 ◦C) to the usual starting temperature of the in vitro experiments, the human body temperature (37 ◦C);
2. Phase 2. heated the cell culture from 37 ◦C to 42 ◦C, which is the equilibrium temperature of many standard hyperthermia treatments expecting the thermal impact;
3. Phase 3. kept the equilibrium 42 ◦C for 30 min;
4. Phase 4. continued the equilibrium heating at 42 ◦C for the next 30 min

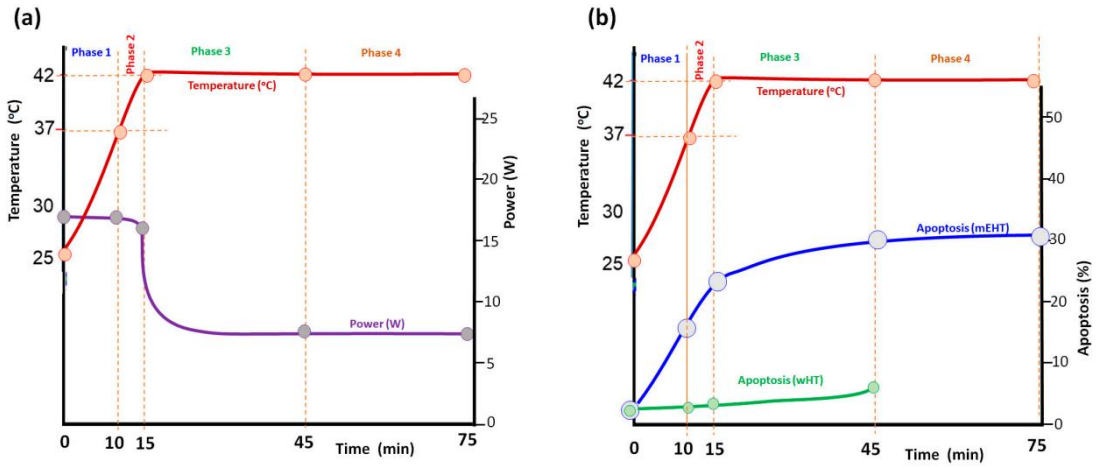

Figure 17. Analyzing the heating process in four phases: heat from 25 ℃ to 37 ℃, from 37 ℃ to 42 ℃, and keep the 42 ℃ for 30 and 60 min. (a) The power and temperature diagram: phase I and II 18 W, phase III and IV 7.5 W, and the absorbed energy in Phase I is 10.8 kJ, in Phase II 5.4 kJ in Phase III 13.5 kJ, and in Phase IV 13.5 kJ [49]. (b) The development of apoptosis in mEHT and wHT applications in the A549 cell line.

The SAS period was 15 min, (with 18 W power) the equilibrium period 30 min (7.5 W). In this case, the apoptosis (measured by Annexin V positive cells) was 31.18%. Remarkable apoptosis was measured in phases I and II, while in the longer phases III and IV, the apoptotic activity was low. Replacing the 1st phase with purely thermal water bath (WB) heating, apoptosis decreased to 22.6%, and when the 2nd phase was also replaced with WB, apoptosis decreased further to 7.2%, showing that the non-thermal effect in the heating up SAS period had produced the majority of apoptosis (Figure 18). Counting that the SAS had 18 W for 15 min (16.2 kJ), equilibrium needs only 7.5 W of power for 30 min (13.5 kJ). The energy-corrected expected apoptosis in the equilibrium period increased a little and became ~8.64%, but much smaller than the apoptosis in the SAS period. With the WB (42 ℃) and the incubation (37 ℃), applied for the same time when the mEHT treatment was performed, apoptosis was low at 2.61% and 2.42% respectively.

Numerous control experiments were performed [49], substituting the various phases with WB or incubation; the results showed the same dominance of the SAS period in apoptotic production. When the treatment time in the equilibrium temperature (42 ◦C) was doubled (added Phase 4.), apoptosis grew significantly from 31.18% to 31.63%. However, when the equilibrium period cooled down the cell line to 37 ◦C for 5 min and up again to 42 ◦C in the next 5 min, apoptosis significantly increased to 51% altogether (Figure 19). In this experiment, the pulsing increased apoptosis to more than two times more than the standard mEHT at the same time and same temperature. This remarkable result gave rise to the idea of the pulsed mEHT development.

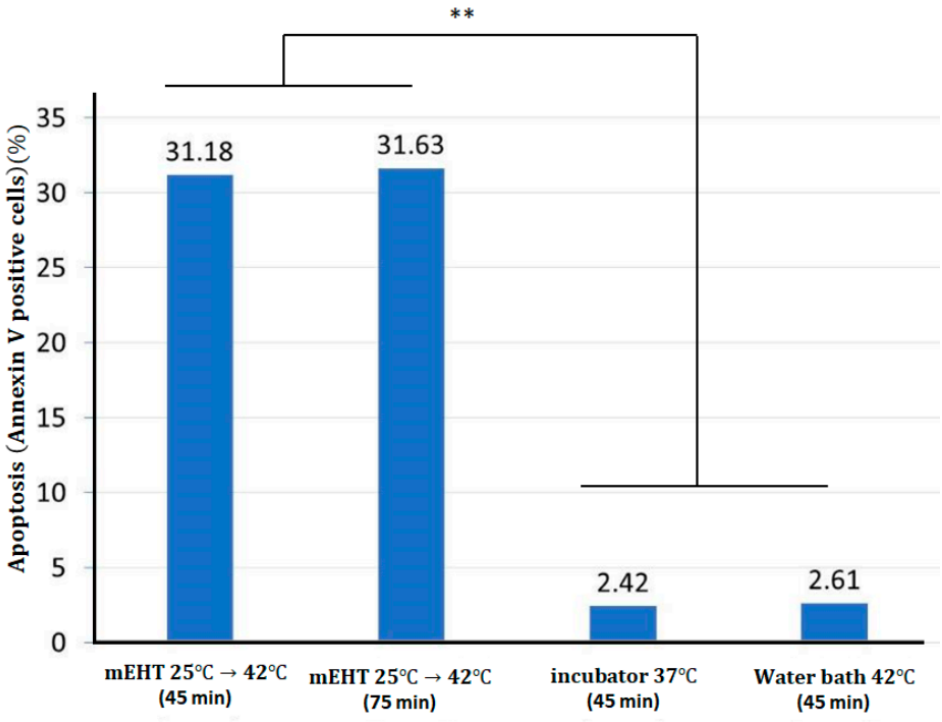

Figure 18. The apoptosis is high in the mEHT, keeping the treated adenocarcinoma human alveolar basal epithelial cell line, A549, at 42 ◦C, and statistically does not differ from the time of keeping the equilibrium (45 min or 75 min treatments), but the water bath with the same 42 ◦C has significantly less apoptosis in the same cell line and, at the same time [49]. This difference was observed by others, too [84,86]. It is noteworthy that the process in the incubator at 37 ◦C has statistically the same result as the water bath at 42 °C. Results are significant (**, $p < 0.005$).

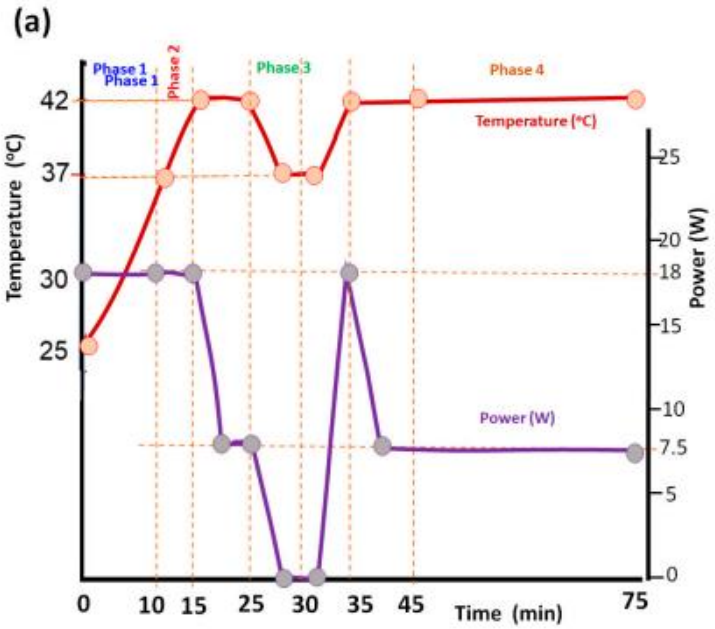

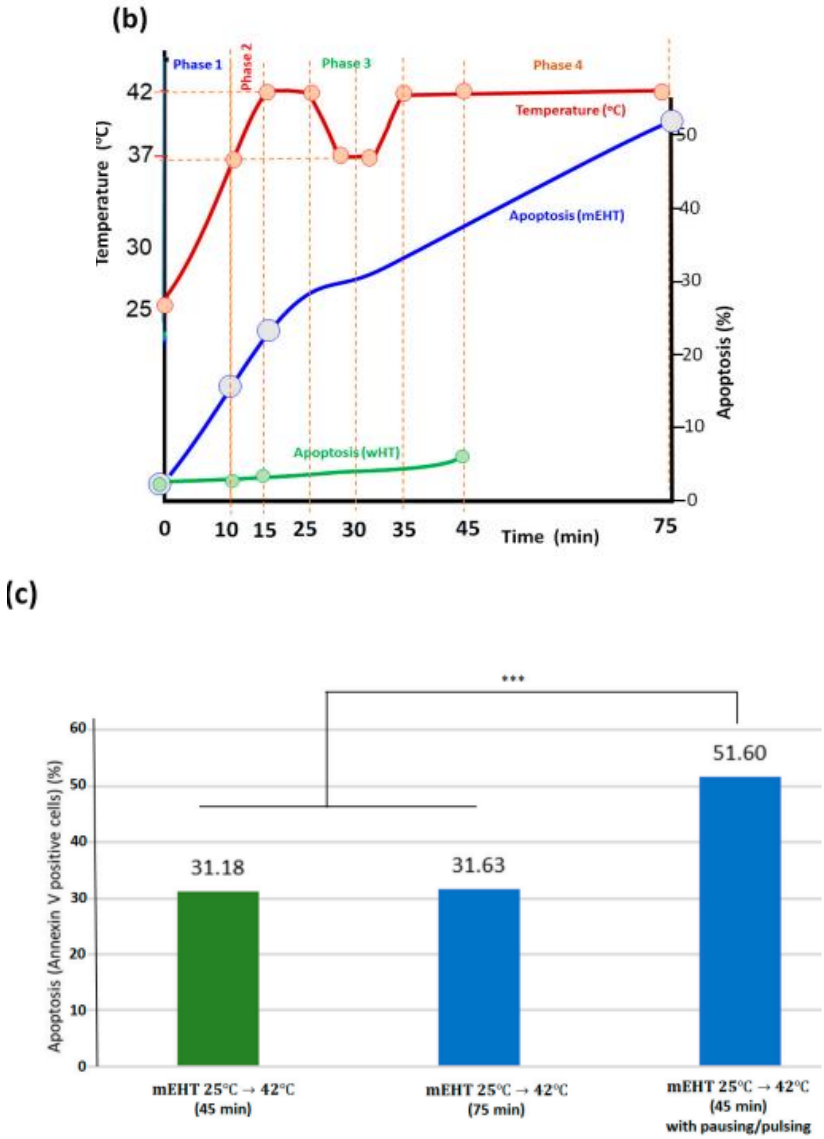

Figure 19. The interruption by pause/pulse power made a significant improvement in apoptosis. (a) the power impulse and the consequent temperature change in time. (b) The apoptosis development Figure 19. The interruption by pause/pulse power made a significant improvement in apoptosis. (a) the power impulse and the consequent temperature change in time. (b) The apoptosis development over time with mEHT and wHT is related to temperature. (c) Apoptosis in different treatment conditions. The difference between the continuous and pulsed treatment is highly significant (***, $p < 0.0005$).

The pulsing role in apoptosis well supports the importance of the semi-adiabatic heating period. At the same time, it proves the decisional role of the nonthermal effects on apoptosis. These experiences were verified in vivo.

3.3. In Vivo Verification

The in vitro rat model used immunocompetent animals [92]. An RG2 [D74] (ATCC®, CRL 2433™, Manassas, VA, USA) astrocytoma [93] was inoculated into the parietal lobe of syngeneic Fischer 344 rats. The inoculation was syngeneic, genetically sufficiently identical, and immunologically

compatible to allow for transplantation. There were three groups (three animals in each): (1) sham, (2) continuous mEHT, and (3) periodically stopped, pulsed mEHT treatments. The pulsing periods were 6 min with a 0.5 duty cycle, using the homeostatic relaxation time shown in Figure 20. A gadolinium-based MRI contrast agent (MAGNEVIST®, 0.5 mmol/mL, 0.2 mL/kg bdw) was used to detect lesions associated with an altered blood–brain barrier, and the volume of the tumor was quantified at the 8th and 15th days after inoculations. The brain temperature was evaluated indirectly by measuring the temperature in the middle ear and using a correlation curve set up in an earlier experiment.

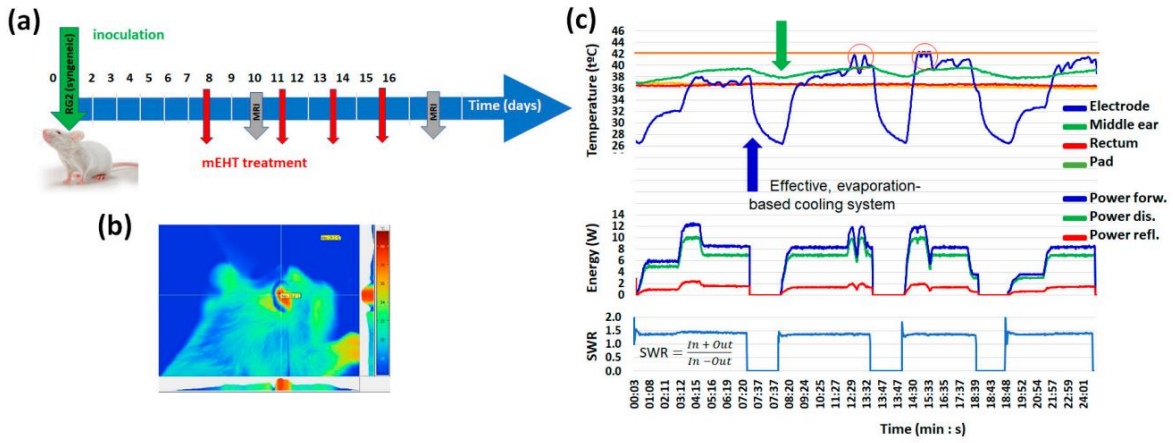

Figure 20. (a) The applied protocol. (b) Well-localized energy targeting on the head of the rat. (c) The parameters during the treatment [93].

The tumor growth rate between the 8th and 15th days after inoculations was, in the case of sham animals, 23.73 ± 12.15, in the treated with classical mEHT protocol, 19.08 ± 0.49, and in the treated with pulsing mEHT protocol, 6.83 ± 2.02 (Figure 21).

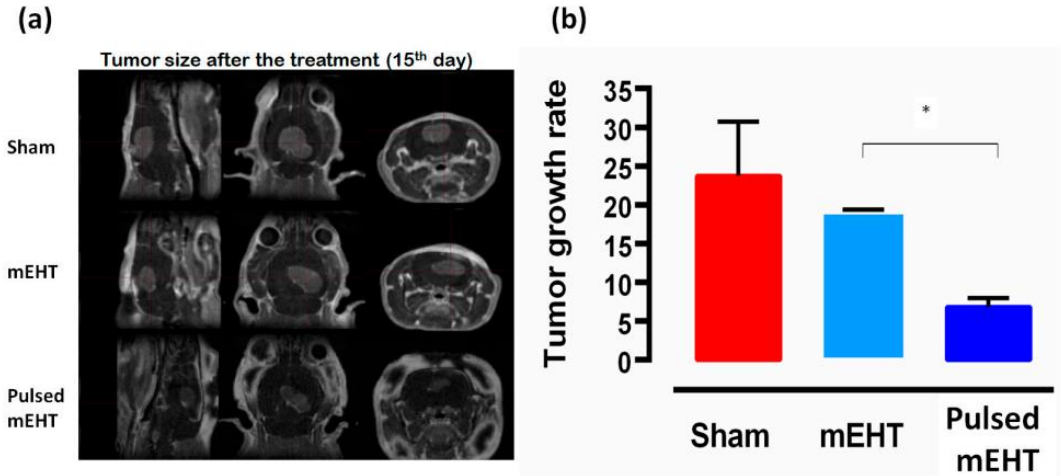

Figure 21. In vivo verification of the advantage of pulsed mEHT. (a) MRI imaging of the tumor 15th-day post-treatment with the Mediso nanoScan 1T small animal MRI system and a 3D image acquisition sequence MAGNEVIST®, 0.5 mmol/mL, 0.2 mL/kg body. (b) Tumor growth rate after the treatment (15th day) [92]. Results are significant (*, $p < 0.05$).

The immunohistochemical analysis shows the highest effects of the extracellular release of HSP70 in pulsed treatment. The extracellular HSP70 molecule has a decisional role [94] in tumor-specific immune reactions, delivering information for antigen-presenting and killer T cell priming [95,96]. The reduction of the Ki67 protein, which marks proliferation, shows the suppression of the malignant activity in the rat highest with pulsed mEHT, Figure 22.

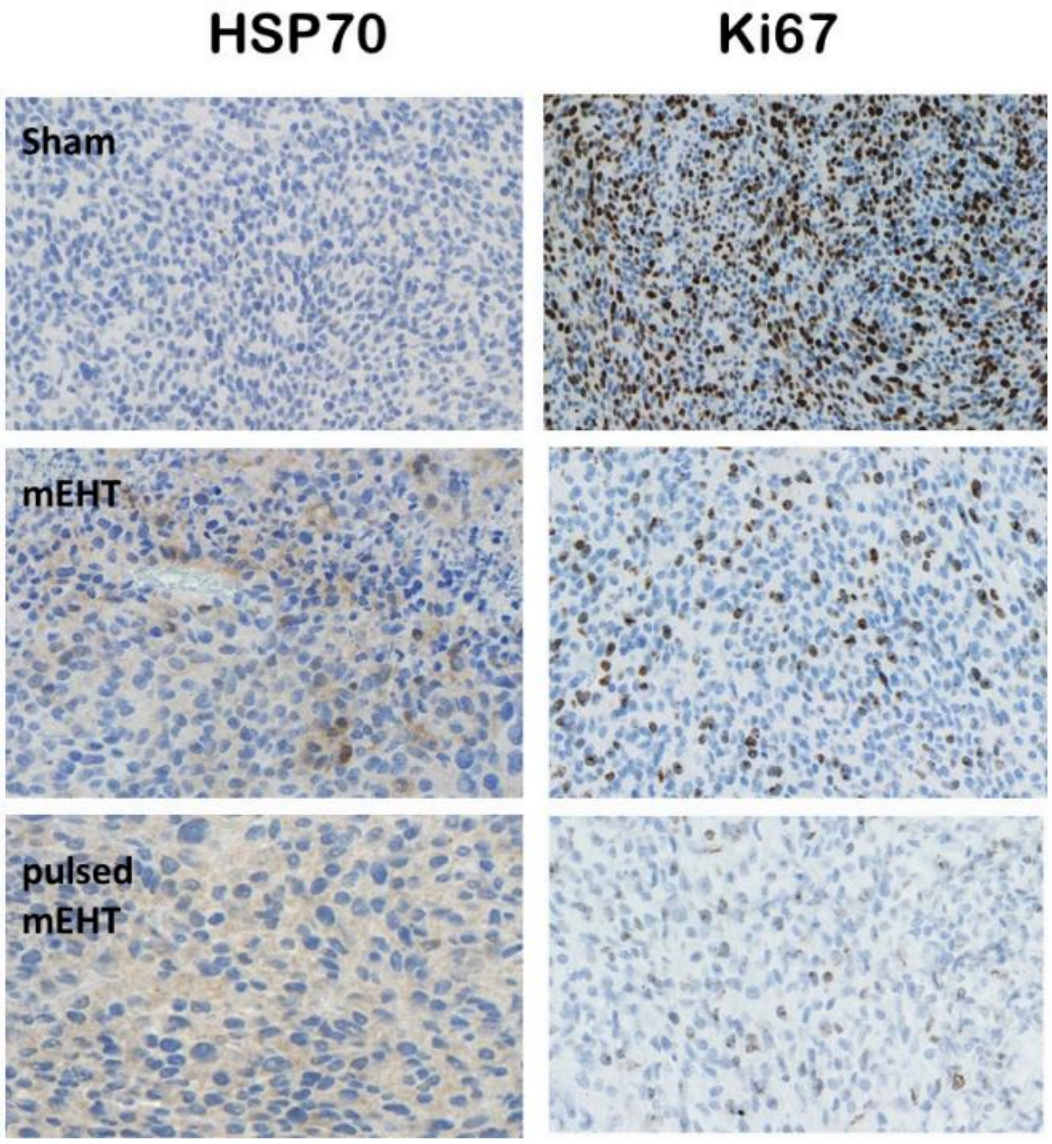

Figure 22. The increase of the extracellular HSP70 and the reduction of the Ki67 proliferation marker significantly increased in the pulsed experiment [92].

4. Pulsing Modulated Electro Hyperthermia

It is early knowledge that the blood flow and the speed of the heat delivery are connected. Rapid heating well differentiates the blood flow between the tumor and healthy host, while at slow heating, this difference tends to disappear [78], even when both were performed for 20 min at 43 ◦C. In an early experiment, a heating pulse (45 ◦C, 10 min) was used to treat experimental rhabdomyosarcoma BAll12 cells before continuous hyperthermia exposure for 3 h at 42.5 ◦C [97].

The starting pulse had a noticeable role in the results of the hyperthermia procedure. These observations emphasize the role of the semi-adiabatic heating period as one of the factors in the selection. Pulsed hyperthermia in cancer treatment refers to a technique where heat is applied to tumor tissue in short, controlled bursts rather than continuously. This approach can potentially enhance the effectiveness of cancer treatments while minimizing damage to healthy surrounding tissues. Pulsing is not a new heating technique. The precise temperature adjustment often uses pulsing for preciosity, like in the incubators [98]. Hyperthermia in cancer therapy also uses thermal cycling to enhance even the anticancer effect of natural compounds in pancreatic malignant cells [99], and it was also used in human treatment [100].

Continuous hyperthermia can also damage healthy tissues surrounding the tumor. Pulsed heating addresses this concern by delivering heat in cycles, having a heating phase (applied for a short duration and raising the temperature to the desired level), and following it with the resting phase (heating is stopped, allowing the tissue to cool down partially). This cycling provides for the following:

- Reduced risk of damage to healthy tissues: since healthy tissues cool down faster than tumors, they experience less heating during the resting phase
- Potentially enhanced tumor damage: some tumor cells might be more susceptible to heat when exposed to pulsed heating than continuous heat;
- Improved treatment tolerability: patients may experience fewer side effects due to reduced overall heat exposure.

The nonthermal effects of pulsed electromagnetic fields have also been investigated [101] and are shown to have a harmful nonthermal effect when the pulsing power is high. Damage by the pulsing heat treatment is also displayed in skin layer experiments [102] and well applicable for the chemical and thermal activation of the TRPV3 vanillin receptor [103], which otherwise has a role in immunogenic effects in mEHT applications because the mechanism of these channels could be modified by electric field [5]. An essential application of the pulsed electric treatment makes the transient reversible opening of the blood-brain barrier (BBB) [104–106]. This non-invasive method could be applied to promote drug delivery to the brain, which the BBB blocks. The opening mechanism is connected to the impact on tight junctions even without thermal effect [107]. When the power has a periodic increase, the applied step-up heating is also a pulsed process with very low frequency. The pulsed electric field (PEF) heating has particular applications in pain management [108,109]. The oncological applications have just started and have a good perspective [110]. The pulses are short (most nanoseconds) [111]. Longer heating times (50 s) by magnetic pulses shows the usual heating pattern for breast cancer hyperthermia treatment [112] and for induced damage of the tumor microcirculation. Electrochemotherapy (ECT) is developing on this basis. Continuous ECT (galvanic treatment) is an old therapy [113], also developed in the early 1990s in Bad Aibling (Germany) [114]. The PEF application is quickly developing in electroporation [115]. While the “pulsing technique” is commonly used in hyperthermia treatments, capacitive hyperthermia specifically does not utilize this technique broadly.

The new mEHT with a pulsing technique is thermally assisted and provides all the advantages of continuous mEHT operation. The above-described selective mechanisms target the membrane rafts and the membrane microdomains, which have a role in intracellular signal excitation and regulation, as well as the ICD processes. The targeting of membrane rafts helps to develop novel

complementary therapies to increase the sensitivity to chemotherapeutic compounds, opening the gate for drug penetration into the cell and reducing multidrug resistance [116]. The capacitive coupling could also give a unique advantage in modifying the membrane voltage [117] with a low electric field.

The personal sensing homeostatic step-up heating solves safety problems when the patient communicates about identifying any discomfort. The question naturally arises about the reliability of subjective sensing, but personal sensing is the best available method for monitoring the heating process. Personal sensing is typically used to drive many protocols active in today's medical treatments. When the patient cannot tolerate the prescribed dose, it is lowered, trying to fit it to the personal tolerance level. There is no reliable personalized dosing without controlling the guidance of personal sensing. In pulsed heat treatment, immense power can be tolerated for the short pulsing time when the time between the two pulses is long enough to return the temperature to the tolerable zone, at least partially. In these conditions, personal sensing will be the average time of the power. The slow thermal and physiologic reaction to the rapid power absorption makes averaging possible. By applying heat in pulses, healthy tissue surrounding the targeted area has more time to cool between pulses, potentially minimizing damage and side effects. This can be especially beneficial for tumors located near sensitive organs or nerves.

The duty cycle is as follows:

$$D = \frac{\langle P \rangle}{P_p} = \frac{t_p}{t_r} \qquad (13)$$

where ⟨P⟩ is the average, P_p is the pulsed power, t_p is the pulse width, and tr is the repetition time. While the pulse "window is rectangular, the resulting heating pattern differs. It all depends on the thermal parameters of the targeted mass (Figure 23).

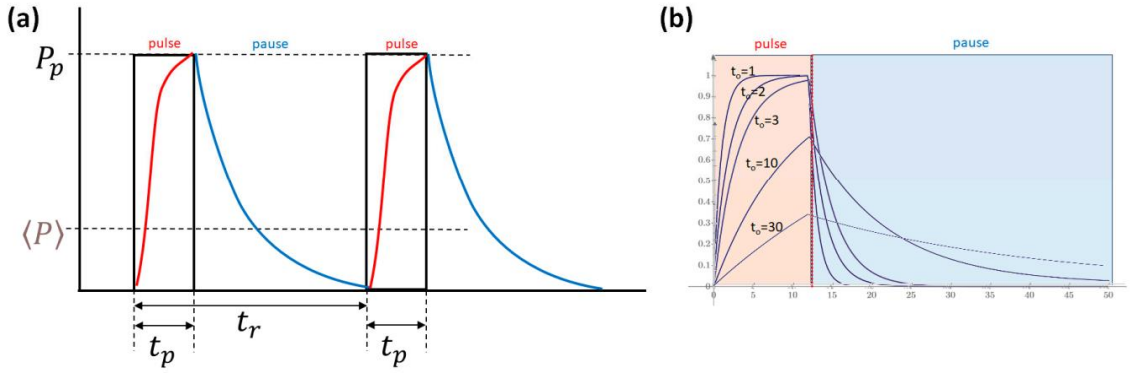

Figure 23. The electric pulsing and the thermal reaction differ. (a) The pulse heats the material, which is slower than the electric signal, and the end of the pulse starts a cooling process. (b) The thermal parameters of the target (t_0) define the relaxation time of heating–cooling phases. The change of t_0 may drastically change the thermal pulse at the same electric pulsing.

When the duty cycle is low, the average temperature is unchanged and remains on the baseline, having enough time to cool between the pulses. However, when the duty cycle grows, the cooling down period relatively shortens and could not be enough to reach the baseline again. In this case, the average temperature rises. The growing temperature follows roughly a cumulative Weibull

function [49] $W = exp\left(-\left(\frac{t}{t_0}\right)^n\right)$ where n is the is shape parameter, and t_0 is the time parameter. Both depend on the target material (Figure 24).

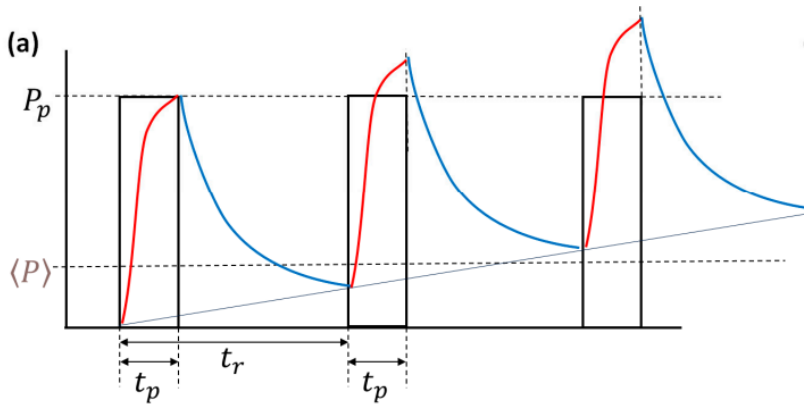

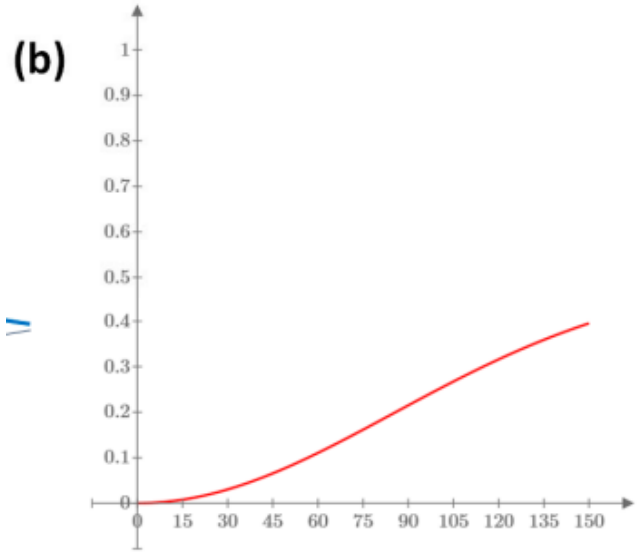

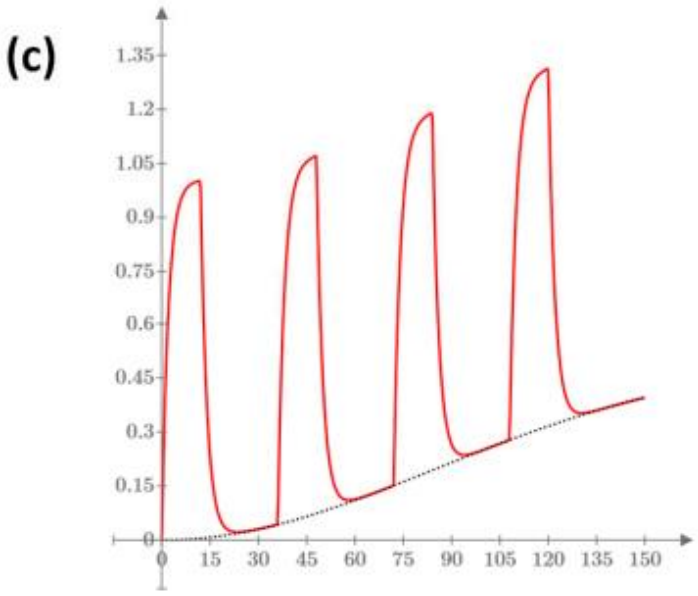

Figure 24. Effect of the duty cycle. (a) When the off-period of the pulsing is shorter than necessary for the thermal return to the baseline, the target cumulates the heat, and the overall average temperature grows. (b) The average temperature growth can usually be described with the Weibull function . (c) The pulsed heating process with Weibull heat-shape.

4.2. Advantages

The pulsing of mEHT has numerous advantages, as follows:

1. Enchanted Efficacy:

a. The active factor of the mEHT is the RF current, which selectively flows through the target. In pulsing conditions, the extreme power gives a proportionally sizeable current density, which causes an effect. Pulsed heating can be more effective at killing cancer cells than continuous heating at the same average temperature;

b. The pulsing induces he semi-adiabatic start of temperature growth, which accounts for the most significant part of apoptosis and induces immunogenic processes;

c. In a low-duty cycle, increased blood flow to the tumor during the off pulses can bring in more oxygen and nutrients needed for the heat to damage the cells.

d. The high-power pulse may induce reversible electroporation, increasing synergic efficacy with complementary chemo and immune therapies;

e. Pulsed heating does not drastically influence homeostatic regulation as continuous heating does. So, the treatment and natural regulations are more effective in cooperative harmony;

f. Studies show that pulsed electric fields effectively relieve pain, improving patients' quality of life.

2. Control and Flexibility:

a. Pulsed heating allows for finer control over the temperature delivered to the target area. The pulse duration, frequency, and power can be adjusted to achieve the desired therapeutic effect while minimizing the heating of surrounding tissue;

b. The power in the pulses may be kept constant; only the duty cycle changes the average power, which determines the temperature. Like digital technologies, the continuous power (and constant energy absorption in a pulse) makes the dose more controllable;

c. The associated side effects are reduced due to the pulsed heating and its relatively long relaxing time with a low-duty cycle;

d. The synergy of the thermal and nonthermal electric absorption is more reliable;

e. Despite the large pulse power, skin and adipose burns are less likely because the subcutaneous blood flow is active, may quickly reduce the heat stress in the pausing period, the pulse is short to burn, and the low-duty cycle ensures the low average temperature on the surface, too.

3. Potential Dose Reduction:
    a. Due to potentially higher efficacy, pulsed heating might require lower overall heat doses than continuous heating, potentially reducing treatment time;
    b. The specific benefits of pulsed heating may vary depending on the type of cancer, tumor size, location, and other factors.

4. Technical advantages;
    a. The reduced cooling facility makes designing a simpler and more efficient electrode system possible;
    b. Forcing step-up heating is unnecessary; choosing the semi-adiabatic phase is automatic and self-adjusted;
    c. The tuning is more accessible because the power (the pulse intensity) is constant during all the processes;
    d. Having 200 W in continuous heating, the power is at a 36 cm depth (the heaviest patient) and is ~ 15% of the incident field, which is ~ 30 W. In the pulsed case, reaching the same temperature with 800 cap W pulses with 0.24 duty cycle (average power is also 200 cap W like it was in the continuous case), the power at 36 cm will be 120 W in pulses, which is a significant increase. I propose the idea that this method treats all depths in humans equally.

4.3. Limitations

While pulsed mEHT shows significant advantages in cancer treatment, there are still potential limitations and adverse effects. The severity of the possible adverse effects depends on various factors, such as individual health, treatment parameters, and tumor characteristics.

1. Local tissue damage: Although pulsed heating reduces overall heating time, localized areas within the treatment zone may still experience high temperatures, potentially leading to extended tissue damage. The selection mechanisms on the tumor localize it, so the host tissues are likely safe. Still, we may lose part of the immunogenic advantages by the necrotic way of tumor cell death;
2. Pain: The heating process can cause discomfort, and individual sensitivity varies. Some patients might experience more intense pain with pulsed heating than continuous heating, but the overall pain reduction after the treatment likely works for all;
3. Nerve effect: Depending on the location, pulsed mEHT could lead to local numbness, tingling, or other nerve-related issues, depending on the patient's state;
4. Systemic effects: Like any hyperthermia treatment, pulsed heating can cause systemic effects like thirstiness, fever, chills, fatigue, nausea, and vomiting. The severity of these effects depends on factors like individual health, treatment parameters, underlying medical conditions, and complementary medical applications;

5. Tumor-specific risks: The significantly high-power intensity in the pulses may cause rapid tumor lysis syndrome, which is toxic;
6. Unforeseen complications: As with any new medical technology, unforeseen complications are always possible. More research is needed to fully understand the long-term effects and potential rare side effects of pulsed mEHT. Open communication and regular monitoring during treatment are crucial to identify and promptly manage any adverse effects;
7. Technical challenge:
    a. The pulsing power and temperature averages could differ depending on the tumor's thermal washout physiology, which patients may have differently.
    b. The average power depends on the duty-cycle, so it does not serve as a dose in the mEHT as it was in continuous power. The dose could be only the integrative absorbed energy.
    c. The pulsing can change the original 1/ f modulation depending on its duty cycle.

5. Conclusions

The pulsed mEHT treatment gives additional advantages to the standard modulated electro-hyperthermia. This type of treatment provides promising improvements in terms of safety and efficacy. The additional impulse modulation (high-power pulsing) increases the mEHT efficacy. The increased penetration depth supports the treatment of deep-seated tumors for heavy patients, and the decreased thermal load on the skin and the adipose tissues increases the patient's safety and quality of life.

Funding: This research was funded by Oncotherm GmbH, Troisdorf, Germany.
Conflicts of interest: The author is a consultant of Oncotherm GmbH, Troisdorf, Germany.

References

1. Lurito, P.W. The message was electric. IEEE Spectr. 1984, 21, 84–96. [CrossRef]
2. Advertisement of German Electric Appliance Agency. In Free Lance; 1902; II, p. 18. Available online: https://paperspast.natlib. govt.nz/newspapers/NZFL19020419.2.21.1 (accessed on 24 June 2024).
3. Andocs, G.; Renner, H.; Balogh, L.; Fonyad, L.; Jakab, C.; Szasz, A. Strong synergy of heat and modulated electro- magnetic field in tumor cell killing, Study of HT29 xenograft tumors in a nude mice model. Strahlenther. Onkol. 2009, 185, 120–126. [CrossRef] [PubMed]
4. Szasz, A. Thermal and nonthermal effects of radiofrequency on living state and applications as an adjuvant with radiation therapy. J. Radiat. Cancer Res. 2019, 10, 1–17. [CrossRef]

5. Szasz, A.M.; Lorant, G.; Szasz, A.; Szigeti, G. The immunogenic connection of thermal and nonthermal molecular effects in modulated electro-hyperthermia. Open J. Biophys. 2023, 13, 103–142. [CrossRef]
6. Szasz, A. Heterogeneous heat absorption is complementary to radiotherapy. Cancers 2022, 14, 901. [CrossRef] [PubMed]
7. Szasz, A. The capacitive coupling modalities for oncological hyperthermia. Open J. Biophys. 2021, 11, 252–313. [CrossRef]
8. Kakehi, M.; Ueda, K.; Mukojima, T.; Hiraoka, M.; Seto, O.; Akanuma, A.; Nakatsugawa, S. Multi-institutional Clinical Studies on hyperthermia combined with radiotherapy or chemotherapy or chemotherapy in advanced cancer of deep-seated organs. Int. J. Hyperth. 1990, 6, 719–740. [CrossRef]
9. Egawa, I.; Watanabe, S.; Ohno, Y.; Morita, K.; Tominaga, S.; Onoyama, Y.; Hashimoto, S. A randomized clinical trial of hyperthermia and radiation versus radiation alone for superficially located cancers. J. Jap. Soc. Ther. Radiol. Oncol. 1989, 1, 135–140.
10. Otsuka, T.; Yonezawa, M.; Kamiyama, F.; Matsushita, Y.; Matsui, N. Results of surgery and radio-hyperthemo-chemotherapy for patients with soft tissue sarcoma. Int. J. Clin. Oncol. 2001, 6, 253–258. [CrossRef]
11. Doi, O.; Kodama, K.; Tatsuta, M.; Higashiyama, M.; Aoki, Y.; Kuriyama, K.; Tateishi, R. Effectiveness of intrathoracic chemothermotherapy for malignant pleurisy due to Ewing's sarcoma: A case report. Int. J. Hyperth. 1990, 6, 947–963. [CrossRef]
12. Ishikawa, T.; Kokura, S.; Sakamoto, N.; Ando, T.; Imamoto, E.; Hattori, T.; Oyamada, H.; Yoshinami, N.; Sakamoto, M.; Kitagawa, K.; et al. Phase II trial of combined regional hyperthermia and Gemcitabine for locally advanced or metastatic pancreatic cancer. Int. J. Hyperth. 2012, 28, 597–604. [CrossRef] [PubMed]
13. Masunaga, S.; Hiraoka, M.; Takahashi, M.; Jo, S.; Akuta, K.; Nishimura, Y.; Nagata, Y.; Abe, M. Clinical results of thermoradiotherapy for locally advanced and/or recurrent breast cancer-comparison of results with radiotherapy alone. Int. J. Hyperth. 1990, 6, 487–497. [CrossRef] [PubMed]
14. Nagata, Y.; Hiraoka, M.; Nishimura, Y.; Masunaga, S.; Mitumori, M.; Okuno, Y.; Fujishiro, M.; Kanamori, S.; Horii, N.; Akuta, K.; et al. Clinical results of radiofrequency hyperthermia for malignant liver tumors. Int. J. Radiat. Oncol. Biol. Phys. 1997, 38, 359–365. [CrossRef]
15. Asao, T.; Sakurai, H.; Harashima, K.; Yamaguchi, S.; Tsutsumi, S.; Nonaka, T.; Shioya, M.; Nakano, T.; Kuwano, H. The synchronization of chemotherapy to circadian rhythms and irradiation in pre-operative chemoradiation therapy with hyperthermia for local advanced rectal cancer. Int. J. Hyperth. 2006, 22, 399–406. [CrossRef]
16. Nishimura, Y.; Hiraoka, M.; Akuta, K.; Jo, S.; Nagata, Y.; Masunaga, S.-I.; Takahashi, M.; Abe, M. Hyperthermia combined with radiation therapy for primarily unresectable and recurrent colorectal cancer. Int. J. Radiat. Oncol. Biol. Phys. 1992, 23, 759–768. [CrossRef] [PubMed]
17. Ohguri, T.; Imada, H.; Kato, F.; Yahara, K.; Morioka, T.; Nakano, K.; Korogi, Y. Radiotherapy with 8MHz radiofrequency-capacitive regional hyperthermia for pain relief of unresectable and recurrent colorectal cancer. Int. J. Hyperth. 2006, 22, 1–14. [CrossRef]

18. Mochiki, E.; Shioya, M.; Sakurai, H.; Andoh, H.; Ohno, T.; Aihara, R.; Asao, T.; Kuwano, H. Feasibility study of postoperative intraperitoneal hyperthermotherapy by radiofrequency capacitive heating system for advanced gastric cancer with peritoneal seeding. Int. J. Hyperth. 2007, 23, 493–500. [CrossRef]
19. Matsui, K.; Takebayashi, S.; Watai, K.; Kakehi, M.; Kubota, Y.; Yao, M.; Shuin, T. Combination radiotherapy of urinary bladder carcinoma with chemohyperthermia. Int J. Hyperth. 1991, 7, 19–26. [CrossRef]
20. Arends, T.J.H.; Nativ, O.; Maffezzini, M.; de Cobelli, O.; Canepa, G.; Verweij, F.; Moskovitz, B.; van der Heijden, A.G.; Witjes, J.A. Results of a randomized chemohyperthermia with Mitomycin C versus Bacillus Calmette-Guérin for adjuvant treatment of patients with intermediate—And high-risk non-muscle-invasive bladder cancer. Eur. Urol. 2016, 69, 1046–1052. [CrossRef]
21. Sugimach, K.; Kuwano, H.; Ide, H.; Toge, T.; Saku, M.; Oshiumi, Y. Chemotherapy combined with or without hyperthermia for patients with oesophagael carcinoma: A prospective randomized trial. Int. J. Hyperth. 1994, 10, 485–493. [CrossRef]
22. Ohguri, T.; Imada, H.; Yahara, K.; Morioka, T.; Nakano, K.; Terashima, H.; Korogi, Y. Radiotherapy with 8-MHz radiofrequencycapacitive regional hyperthermia for stage III non-small cell lung cancer: The radiofrequency-output power correlates with the intraesophageal temperature and clinical outcomes. Int. J. Radiat. Oncol. Biol. Phys. 2009, 1, 128–135. [CrossRef] [PubMed]
23. Ohguri, T.; Imada, H.; Yahara, K.; Morioka, T.; Nakano, K.; Terashima, H.; Korogi, Y. Deep regional hyperthermia for the whole thoracic region using 8MHz radiofrequency-capacitive heating device: Relationship between the radiofrequency-output power and the intra-oesophageal temperature and predictive factors for a good heating in 59 patients. Int. J. Hyperth. 2011, 27, 20–26.
24. Huilgol, N.G.; Gupta, S.; Sridhar, C.R. Hyperthermia with radiation in the treatment of locally advanced head and neck cancer: A report of randomized trial. J. Cancer Res. Ther. 2010, 6, 492–496. [CrossRef]
25. Datta, N.R.; Bose, A.K.; Kapoor, H.K.; Gupta, S. Head and neck cancers: Results of thermoradiotherapy versus radiotherapy. Int. J. Hyperth. 1990, 6, 479–486. [CrossRef] [PubMed]
26. Ohguri, T.; Imada, H.; Narisada, H.; Yahara, K.; Morioka, T.; Nakano, K.; Miyaguni, Y.; Korogi, Y. Systemic chemotherapy using paclitaxel and carboplatin plus regional hyperthermia and hyperbaric oxygen treatment for non-small cell lung cancer with multiple pulmonary metastases: Preliminary results. Int. J. Hyperth. 2009, 25, 160–167. [CrossRef] [PubMed]
27. Kodama, K.; Doi, O.; Tatsuta, M.; Kuriyama, K.; Tateishi, R. Development of postoperative intrathoracic chemo-thermotherapy for lung cancer with objective of improving local cure. Cancer 1989, 64, 1422–1428. [CrossRef] [PubMed]
28. Mitsumori, M.; Zeng, Z.-F.; Oliynychenko, P.; Park, J.H.; Choi, B.I.; Tatsuzaki, H.; Tanaka, Y.; Hitaoka, M. Regional hyperthermia combined with radiotherapy for locally advanced non-small cell lung cancers: A multi-institutional prospective randomized trial of the International Atomic Energy Agency. Int. J. Clin. Oncol. 2007, 12, 192–198. [PubMed]

29. Kitamura, K.; Kuwano, H.; Watanabe, M.; Nozoe, T.; Yasuda, M.; Sumiyoshi, K.; Saku, M.; Sugimachi, K. Prospective randomized study of hyperthermia combined with chemoradiotherapy for esophageal carcinoma. J. Surg Oncol. 1995, 60, 55–58. [CrossRef]

30. Szasz, O.; Szigeti, G.; Szasz, A. Connections between the specific absorption rate and the local temperature. Open J. Biophys. 2016, 6, 53–74. [CrossRef]

31. Papp, E.; Vancsik, T.; Kiss, E.; Szasz, O. Energy absorption by the membrane rafts in the modulated electro-hyperthermia (mEHT). Open J. Biophys. 2017, 7, 216–229. [CrossRef]

32. Govorov, A.O.; Richardson, H.H. Generating heat with metal nanoparticles. NanoToday 2007, 2, 30–38. [CrossRef]

33. Szasz, O.; Andocs, G.; Meggyeshazi, N. Modulation effect in oncothermia. Hindawi Publishing Corporation. Conf. Pap. Med. 2013, 2013, 395678.

34. Szasz, O. Bioelectromagnetic paradigm of cancer treatment—Modulated electro-hyperthermia (mEHT). Open J. Biophys. 2019, 9, 98–109. [CrossRef]

35. Szasz, A. Bioelectromagnetic Paradigm of Cancer Treatment Oncothermia. In Bioelectromagnetic and Subtle Energy Medicine; Paul, J.R., Ed.; CRC Press: Boca Raton, FL, USA; Taylor & Francis Group: Oxford, UK, 2015; pp. 323–336.

36. Semenza, G.L. Tumor metabolism: Cancer cells give and take lactate. J. Clin. Investig. 2008, 118, 3835–3837. [CrossRef] [PubMed]

37. Stoy, R.D.; Foster, K.R.; Schwan, H.P. Dielectric properties of mammalian tissues form 0.1 to 100 MHz: A summary of recent data. Phys. Med. Biol. 1982, 27, 501–513. [CrossRef]

38. Foster, K.R.; Schepps, J.L. Dielectric properties of tumor and normal tissues at radio through microwave frequencies. J. Microw. Power 1981, 16, 107–119. [CrossRef] [PubMed]

39. Gershing, E. Monitoring temperature-induced changes in tussue during hyperthermia by impedance methods. In Electrical Bioimpedance Methods; Riu, P.J., Ed.; New York Academy of Sciences: New York, NY, USA, 1999; Volume 873, pp. 13–20.

40. Oehr, P.; Biersack, H.J.; Coleman, R.E. PET and PET-CT in Oncology; Springer: Berlin/Heidelberg, Germany, 2004.

41. Larson, S.M. Positron Emission Tomography-Based Molecular Imaging in Human Cancer: Exploring the Link between Hypoxia and Accelerated Glucose Metabolism. Clin. Cancer Res. 2004, 10, 2203–2204. [CrossRef]

42. Sha, L.; Ward, E.R.; Story, B. A review of dielectric properties of normal and malignant breast tissue. In Proceedings of the IEEE SoutheastCon 2002 (Cat. No.02CH37283), Columbia, SC, USA, 5–7 April 2002; pp. 457–462.

43. Blad, B.; Wendel, P.; Jonsson, M.; Lindstrom, K. An electrical impedance index to distinguish between normal and cancerous tissues. J. Med. Eng. Technol. 1999, 23, 57–62. [CrossRef]

44. Szentgyorgyi, A. Electronic Biology and Cancer; Marcel Dekker: New York, NY, USA, 1998.

45. Szentgyorgyi, A. The Living State and Cancer; Marcel Dekker: New York, NY, USA, 1978.

46. Szigeti, G.P.; Szasz, O.; Hegyi, G. Connections between Warburg's and Szentgyorgyi's Approach about the Causes of Cancer. J. Neoplasm 2017, 1, 1–13.

47. Joy, M.L.G. MR current density and conductivity imaging: The state of the Art, Engineering in Medicine and Biology. In Proceedings of the IEMBS 26th Annual International Conference of the IEEE, San Francisco, CA, USA, 1–5 September 2004; Volume 2, pp. 5315–5319.

48. Muftuler, L.T.; Hamamura, M.J.; Birgul, O.; Nalcioglu, O. In vivo MRI electrical impedance tomography (MREIT) of tumors. Technol. Cancer Res. Treat. 2006, 5, 381–387.

49. Kao, P.H.-J.; Chen, C.-H.; Tsang, Y.-W.; Lin, C.-S.; Chiang, H.-C.; Huang, C.-C.; Chi, M.-S.; Yang, K.-L.; Li, W.-T.; Kao, S.-J.; et al. Relationship between energy dosage and apoptotic cell death by modulated electro-hyperthermia. Sci. Rep. 2020, 10, 8936. [CrossRef] [PubMed]

50. Szasz, O.; Szasz, A. Approaching complexity: Hyperthermia dose and its possible measurement in oncology. Open J. Biophys. 2021, 11, 68–132. [CrossRef]

51. Lee, I.-H.; Imanaka, M.Y.; Modahl, E.H.; Torres-Ocampo, A.P. Lipid raft phase modulation by membrane-anchored proteins with inherent phase separation properties. ACS Omega 2019, 4, 6551–6559. [CrossRef]

52. Staunton, J.R.; Agus, D.B.; Alexander, J.F.; Arap, W.; Ashili, S.; Aslan, J.E.; Bonneau, R. The Physical Sciences—Oncology Centers Network; A physical sciences network characterization of non-tumorigenic and metastatic cells. Sci. Rep. 2008, 3, 1449.

53. Kotnik, T. Theoretical Evaluation of the Distributed Power Dissipation in Biological Cells Exposed to Electric Fields. Bioelectromagnetics 2000, 21, 385–394. [CrossRef] [PubMed]

54. Campello, E.M.B.; Zohdi, T.I. Design Evaluation of a Particle Bombardment System Used to Deliver Substances into Cells. CMES 2014, 98, 221–245.

55. Lee, B.W.; Faller, R.; Sum, A.K.; Vattulainen, I.; Patra, M.; Karttunen, M. Structural Effects of Small Molecules on Phospholipid Bilayers Investigated by Molecular Simulations. Fluid Phase Equilibria 2004, 225, 63–68. [CrossRef]

56. Guest, W.C.; Cashman, N.R.; Plotkin, S.S. A theory for the anisotropic and inhomogeneous dielectric properties of proteins. Phys. Chem. Chem. Phys. 2011, 13, 6286–6295. [CrossRef] [PubMed]

57. Heikelä, M.; Vattulainen, I.; Hyvönen, M.T. Atomistic simulation studies of cholesteryl oleates: Model for the core of lipoprotein particles. J. Biophys. 2006, 90, 2247–2257. [CrossRef]

58. Waxham, M.N. Molecular mobility in cells examined with optical methods. In Protein Trafficking in Neurons; Bean, A.J., Ed.; Academic Press: Houston, TX, USA, 2007; pp. 3–27.

59. Cloutier, M.; Wang, E. Dynamic modeling and analysis of cancer cellular network motifs. Integr. Biol. 2011, 3, 724–732. [CrossRef] [PubMed]

60. Hernandez-Nunez, L.; Chen, A.; Budelli, G.; Berck, M.E.; Richter, V.; Rist, A.; Thum, A.S.; Cardona, A.; Klein, M.; Garrity, P.; et al. Synchronous and opponent thermosensors use flexible cross-inhibition to orchestrate thermal homeostasis. Sci. Adv. 2021, 7, eabg6707. [CrossRef] [PubMed] [PubMed Central]

61. Mathur-DeVre, R. Biomedical implications of the relaxation behaviour of water related to NMR imaging. Br. J. Radiol. 1984, 57, 955–976. [CrossRef]

62. Benson, H. The relaxation response: Its subjective and objective historical precedents and physiology. Trends Neurosci. 1983, 6, 281–284. [CrossRef]

63. Li, X.; Sun, S.; Yao, J.; Sun, Z. Using Relaxation Time to characterize biological effects of different mutagens. Sci. Rep. 2020, 10, 13941. [CrossRef] [PubMed]

64. Pennes, H.H. Analysis of tissue and arterial blood temperatures in the resting human forearm. J. Appl. Phys. 1948, 1, 93–122. [CrossRef] [PubMed]

65. Deng, Z.-S.; Liu, J. Analytical solutions to 3-D bioheat transfer problems with or without phase change. In Heat Transfer Phenomena and Applications; Intech: London, UK, 2012; Chapter 8; pp. 205–242.

66. Deng, Z.-S.; Liu, J. Analytical study on bioheat transfer problems with spatial or transient heating on skin surface or inside biological bodies. Trans. ASME 2002, 124, 638–649.

67. Cundin, L.X.; Roach, W.P.; Millenbaugh, N. Empirical comparison of Pennes' Bio-Heat equation. Proc. SPIE 2009, 7175, 238–246.

68. Lakhssassi, A.; Kengne, E.; Semmaoui, H. Modified Pennes' equation modelling bio-heat transfer in living tissues: Analytical and numerical analysis. Nat. Sci. 2010, 2, 1375–1385.

69. Gao, B.; Langer, S.; Corry, P.M. Application of the time-dependent Green's function and Fourier transforms to the solution of the bioheat equation. Int. J. Hyp. 1995, 11, 267–285. [CrossRef]

70. Erdman, B.; Lang, J.; Seebaas, M. Optimalisation of Temperature Distributions for Regional Hyperthermia Based on a Nonlinear Heat Transfer Model. Ann. N. Y. Acad. Sci. 1998, 858, 36–46. [CrossRef]

71. Hasegawa, T.; Gu, Y.-H.; Takahashi, T.; Hasegawa, T.; Yamamoto, I. Enhancement of hyperthermic effects using rapid heating. In Thermotherapy for Neoplasia, Inflammation, and Pain; Kosaka, M., Sugahara, T., Schmidt, K.L., Simon, E., Eds.; Springer: Tokyo, Japan; Berlin/Heidelberg, Germany, 2001; pp. 439–444.

72. IEEE C95.1; IEEE Standard for Safety Levels with Respect to Human Exposure to Radio Frequency Electromagnetic Fields, 3 kHz to 300 GHz. IEEE: Piscataway, NJ, USA, 2005.

73. Song, C.W.; Park, H.; Griffin, R.J. Theoretical and Experimental Basis of Hyperthermia, Thermotherapy for Neoplasia, Inflammation, and Pain; Kosaka, M., Sugahara, T., Schmidt, K.L., Simon, E., Eds.; Springer: Tokyo, Japan, 2001; pp. 394–407

74. 74. Bassingthwaighte, J.B. Physiology and theory of tracer washout techniques for the estimation of myocardial blood flow: Flow estimation from tracer washout. Prog. Cardiovasc. Dis. 1977, 20, 165–189. [CrossRef] [PubMed]

75. Bassingthwaighte, J.B.; Yipintosoi, T. Organ blood flow, wash-in, washout, and clearance of nutrients and metabolites. Mayo Clin. Proc. 1974, 49, 248–255. [PubMed]

76. Feldmann, H.J.; Molls, M.; Hoederath, A.; Krümpelmann, S.; Sack, H. Blood flow and steady state temperatures in deep-seated tumors and normal tissues. Int. J. Radiat. Oncol. Biol. Phys. 1992, 23, 1003–1008. [CrossRef] [PubMed]

77. Fatehi, D.; van der Zee, J.; Notenboom, A.; van Rhoon, G.C. Comparison of intratumor and intraluminal temperatures during loco-regional deep hyperthermia of pelvic tumors. Strahlenther. Und Onkol. 2007, 183, 479–486. [CrossRef] [PubMed]

78. Lee, S.Y.; Szasz, A. Immunogenic Effect of Modulated Electro-hyperthermia (mEHT) in Solid Tumors. In Interdisciplinary Cancer Research; Springer: Cham, Switzerland, 2022. [CrossRef]

79. Tsang, Y.-W.; Huang, C.-C.; Yang, K.-L.; Chi, M.-S.; Chiang, H.-C.; Wang, Y.-S.; Andocs, G.; Szasz, A.; Li, W.-T.; Chi, K.-H. Improving immunological tumor microenvironment using electro-hyperthermia followed by dendritic cell immunotherapy. BMC Cancer 2015, 15, 708. [CrossRef]

80. Qin, W.; Akutsu, Y.; Andocs, G.; Suganami, A.; Hu, X.; Yusup, G.; Komatsu-Akimoto, A.; Hoshino, I.; Hanari, N.; Mori, M.; et al. Modulated electro-hyperthermia enhances dendritic cell therapy through an abscopal effect in mice. Oncol. Rep. 2014, 32, 2373–2379. [CrossRef] [PubMed]

81. Vancsik, T.; Kovago, C.; Kiss, E.; Papp, E.; Forika, G.; Benyo, Z.; Meggyeshazi, N.; Krenacs, T. Modulated electro-hyperthermia induced loco-regional and systemic tumor destruction in colorectal cancer allografts. J. Cancer 2018, 9, 41–53. [CrossRef]

82. Minnaar, C.A.; Kotzen, J.A.; Ayeni, O.A.; Vangu, M.-D.-T.; Baeyens, A. Potentiation of the abscopal effect by modulated electro-hyperthermia in locally advanced cervical cancer patients. Front. Oncol. 2020, 10, 376. [CrossRef]

83. Chi, M.-S.; Mehta, M.P.; Yang, K.-L.; Lai, H.-C.; Lin, Y.-C.; Ko, H.-L.; Wang, Y.-S.; Liao, K.-W.; Chi, K.-H. Putative abscopal effect in three patients treated by combined radiotherapy and modulated electrohyperthermia. Front. Oncol. 2020, 10, 254. [CrossRef]

84. Wust, P.; Stein, U.; Ghadjar, P. Non-thermal membrane effects of electromagnetic fields and therapeutic applications in oncology. Int. J. Hyperth. 2021, 38, 715–731. [CrossRef]

85. Wust, P.; Kortüm, B.; Strauss, U.; Nadobny, J.; Zschaeck, S.; Beck, M.; Stein, U.; Ghadjar, P. Non-thermal effects of radiofrequency electromagnetic fields. Sci. Rep. 2020, 10, 13488. [CrossRef]

86. Yang, K.-L.; Huang, C.-C.; Chi, M.-S.; Chiang, H.-C.; Wang, Y.-S.; Hsia, C.-C.; Andocs, G.; Wang, H.-E.; Chi, K.-H. In vitro comparison of conventional hyperthermia and modulated electro-hyperthermia. Oncotarget 2016, 7, 84082–84092. [CrossRef] [PubMed]

87. Cha, J.; Jeon, T.-W.; Lee, C.G.; Oh, S.T.; Yang, H.-B.; Choi, K.-J.; Seo, D.; Yun, I.; Baik, I.H.; Park, K.R.; et al. Electro-hyperthermia inhibits glioma tumorigenicity through the induction of E2F1-mediated apoptosis. Int. J. Hyperth. 2015, 31, 784–792. [CrossRef]

88. Andocs, G.; Rehman, M.U.; Zhao, Q.-L.; Tabuchi, Y.; Kanamori, M.; Kondo, T. Comparison of biological effects of modulated electro-hyperthermia and conventional heat treatment in human lymphoma U937 cell. Cell Death Discov. 2016, 2, 16039. [CrossRef] [PubMed]

89. Vancsik, T.; Forika, G.; Balogh, A.; Kiss, E.; Krenacs, T. Modulated electro-hyperthermia induced p53 driven apoptosis and cell cycle arrest additively support doxorubicin chemotherapy of colorectal cancer in vitro. Cancer Med. 2019, 8, 4292–4303. [CrossRef]

90. Forika, G.; Balogh, A.; Vancsik, T.; Zalatnai, A.; Petovari, G.; Benyo, Z.; Krenacs, T. Modulated electro-hyperthermia resolves radioresistance of Panc1 pancreas adenocarcinoma and promotes DNA damage and apoptosis in vitro. Int. J. Mol. Sci. 2020, 21, 5100. [CrossRef] [PubMed]

91. Wust, P.; Veltsista, P.D.; Oberacker, E.; Yavvari, P.; Walther, W.; Bengtsson, O.; Sterner-Kock, A.; Weinhart, M.; Heyd, F.; Grabowski, P.; et al. Radiofrequency electromagnetic fields cause non-temperature-induced physical and biological effects in cancer cells. Cancers 2022, 14, 5349. [CrossRef]

92. Portoro, I.; Danics, L.; Veres, D. Increased efficacy in treatment of glioma by a new modulated electro-hyperthermia (mEHT) protocol. Oncothermia J. 2018, 24, 344–356.

93. Aas, A.T.; Brun, A.; Blennow, C.; Stromblad, S.; Salford, L.G. The RG2 rat glioma model. J. Neurooncol. 1995, 23, 175–183. [CrossRef]

94. Danics, L.; Schvarcz, C.A.; Viana, P.; Vancsik, T.; Krenács, T.; Benyó, Z.; Kaucsár, T.; Hamar, P. Exhaustion of protective heat shock response induces significant tumor damage by apoptosis after modulated electro-hyperthermia treatment of triple negative breast cancer isografts in mice. Cancers 2020, 12, 2581. [CrossRef]

95. Minnaar, C.A.; Szasz, A. Forcing the antitumor effects of HSPs using a modulated electric field. Cells 2022, 11, 1838. [CrossRef] [PubMed]

96. Szasz, O. Local Treatment with Systemic Effect: Abscopal Outcome. In Challenges and Solutions of Oncological Hyperthermia; Szasz, A., Ed.; Cambridge Scholars: Cambridge, UK, 2020; Chapter 11; pp. 192–205.

97. Reinhold, H.S.; van den Berg-Blok, A. The influence of a heat pulse on the thermally induced damage to tumour microcirculation. Eur. J. Cancer Clin. Oncol. 1983, 19, 221–225. [CrossRef] [PubMed]

98. Tisa, T.A.; Nisha, Z.A.; Kiber, M.A. Design of an Enhanced Temperature Control System for Neonatal Incubator. Bangladesh J. Med. Phys. 2013, 5, 53–61. [CrossRef]

99. Lu, C.H.; Chen, W.T.; Hsieh, C.H.; Kuo, Y.Y.; Chao, C.Y. Thermal cycling-hyperthermia in combination with polyphenols, epigallocatechin gallate and chlorogenic acid, exerts synergistic anticancer effect against human pancreatic cancer PANC-1 cells. PLoS ONE 2019, 14, e0217676. [CrossRef] [PubMed]

100. Kim, K.S.; Hernandez, D.; Lee, S.Y. Time-multiplexed two-channel capacitive radiofrequency hyperthermia with nanoparticle mediation. Biomed. Eng. Online 2015, 14, 95. [CrossRef] [PubMed]

101. Yaghmazadeh, O. Pulsed high-power radio frequency energy can cause non-thermal harmful effects on the brain. arXiv 2023, arXiv:2309.03479v1. [CrossRef] [PubMed] [PubMed Central]

102. Li, C.-Y.; Lin, S.-M.; Wan, Y.-Y. Prediction of Temperature Field and Thermal Damage of Multilayer Skin Tissues Subjected to Time-Varying Laser Heating and Fluid Cooling by a Semianalytical Method. Math. Probl. Eng. 2020, 2020, 5074280. [CrossRef]

103. Chung, M.-K.; Güler, A.D.; Caterina, M.J. Biphasic currents evoked by chemical or thermal activation of the heat-gated ion channel. J. Biol. Chem. 2005, 280, 15928–15941. [CrossRef] [PubMed]

104. Ding, G.R.; Li, K.C.; Wang, X.W.; Zhou, Y.C.; Qiu, L.B.; Tan, J.; Xu, S.L.; Guo, G.Z. Effect of electromagnetic pulse exposure on brain micro vascular permeability in rats. Biomed. Environ. Sci. 2009, 22, 265–268. [CrossRef]

105. Wang, Q. The study of dose-response relationship of pulsed electromagnetic radiation on rat blood-brain-barrier. Chin. J. Dis. Control Prev. 2003, 7, 401–404.

106. Li, K.; Zhang, K.; Xu, S.; Wang, X.; Zhou, Y.; Zhou, Y.; Gao, P.; Lin, J.; Ding, G.; Guo, G. EMP-induced BBB-disruption enhances drug delivery to glioma and increases treatment efficacy in rats. Bioelectromagnetics 2018, 39, 60–67. [CrossRef] [PubMed]

107. Wang, S.; Song, Z.; Yuan, Y.; Guo, G.; Kang, J. Effects of pulse parameters on the temperature distribution of a human head exposed to the electromagnetic pulse. Sci Rep. 2021, 11, 22938. [CrossRef] [PubMed] [PubMed Central]

108. Sorrell, R.G.; Muhlenfeld, J.; Moffett, J.; Stevens, G.; Kesten, S. Evaluation of pulsed electromagnetic field therapy for the treatment of chronic postoperative pain following lumbar surgery: A pilot, double-blind, randomized, sham-controlled clinical trial. J. Pain Res. 2018, 11, 1209–1222. [CrossRef] [PubMed]

109. Lisi, A.J.; Scheinowitz, M.; Saporito, R.; Onorato, A.A. Pulsed Electromagnetic Field Therapy Device for Non-Specific Low Back Pain: A Pilot Randomized Controlled Trial. Pain Ther. 2019, 8, 133–140. [CrossRef] [PubMed]

110. Guo, S.; Sersa, G.; Heller, R. Editorial: Pulsed electric field based technologies for oncology applications. Front. Oncol. 2023, 13, 1183900. [CrossRef] [PubMed] [PubMed Central]

111. Nuccitelli, R. Application of Pulsed Electric Fields to Cancer Therapy. Bioelectricity 2019, 1, 30–34. [CrossRef] [PubMed] [PubMed Central]

112. Cao, T.L.; Le, T.A.; Hadadian, Y.; Yoon, J. Theoretical Analysis for Using Pulsed Heating Power in Magnetic Hyperthermia Therapy of Breast Cancer. Int. J. Mol. Sci. 2021, 22, 8895. [CrossRef] [PubMed] [PubMed Central]

113. Mir, L.M.; Belehradek, M.; Domenge, C.; Orlowski, S.; Poddevin, B.; Belehradek, J., Jr.; Schwaab, G.; Luboinski, B.; Paoletti, C. Electrochemotherapy, a new antitumor treatment: First clinical trial. Comptes Rendus L'academie Des Sci. Ser. III 1991, 313, 613–618.

114. Galvano- or Electrochemical Tumor Therapy (ECT). Available online: https://www.klinik-st-georg.de/en/klinik-st-georg/stgeorge-hospital/therapies/galvano-or-electrochemical-tumor-therapy-ect/ (accessed on 15 February 2024).

115. Campana, L.G.; Daud, A.; Lancellotti, F.; Arroyo, J.P.; Davalos, R.V.; Di Prata, C.; Gehl, J. Pulsed Electric Fields in Oncology: A Snapshot of Current Clinical Practices and Research Directions from the 4th World Congress of Electroporation. Cancers 2023, 15, 3340. [CrossRef]

116. Preta, G. New Insights Into Targeting Membrane Lipids for Cancer Therapy. Front. Cell Dev. Biol. 2020, 8, 571237. [CrossRef]

117. Robinson, V.S.; Garner, A.L.; Loveless, A.M.; Neculaes, V.B. Calculated plasma membrane voltage induced by applying electric pulses using capacitive coupling. Biomed. Phys. Eng. Express 2017, 3, 025016. [CrossRef]

Preclinical Verification of Modulated Electro-Hyperthermia

PART I. – In Vitro Research

Andras Szasz

Department of Biotechnics, Hungarian University of Agriculture and Life Sciences, 2100 Gödöllő, Hungary

Email: biotech@gek.szie.hu

Citation

Szasz, A. (2024) Preclinical Verification of Modulated Electro-Hyperthermia – Part I. – In vitro research

Oncothermia Journal 38, August 2026., 71-112.
https://oncotherm.com/SzaszA_2024_Preclinical_verification_of_mEHT-Part_I

Abstract

Modulated electro-hyperthermia (mEHT) targets tissue's natural electric and thermal heterogeneities to heat the cancer cells selectively. The applied 13.56 MHz radiofrequency (RF) is a carrier of the low-frequency modulation. The high-frequency part was chosen to select the malignant lesion using the specialties of the tumor: the higher conductivity and dielectric constant of the tumor than its host. The electric field selects the tumor, and the low-frequency amplitude modulation polarizes and excites the transmembrane proteins of the malignant cells. The dominant absorption of the energy by the microscopic clusters of the membrane rafts acts like nanoparticle heating. Exciting the membrane produces various apoptotic signals. The processes were modeled using silico and phantom experiments, which proved the concept. The preclinical verification was made in vitro and in vivo, and in the end, clinical proofs validated the method. Our objective is to follow all the development steps from the laboratory to the clinics in a trilogy of articles. This present is the first part, which deals with in silico, phantom, and in vitro research.

Keywords

Modulated Electro-Hyperthermia, mEHT, In Silico Calculations, Phantom Measurement, In Vitro Experiments, Thermal Effects, Nonthermal Processes, Apoptosis

1. Introduction

Cancer therapies have rapidly developed in the last decades. All classical treatments like chemotherapy (ChT), radiotherapy (RT), and surgery (Op) went through intense variation. The new, highly effective drugs and the personalized medication renewed the ChT. The emerging immuno-oncology (IO) introduced a new concept of cancer elimination with the help of the body's regulative capabilities instead of cytotoxic drugs. The tomotherapy and the ion-beam therapies made a breakthrough in RT, while in surgery, the high-preciosity, remotely operated surgery devices and new laparoscopic solutions represent vital developments. Hyperthermia also had numerous new developments and improved technical realizations, but its medical recognition remained behind the conventional treatments. Conventional oncological hyperthermia intends to heat the tumor as much as possible. However, bioelectromagnetics and immunology are game changers in oncological hyperthermia, far beyond the task of simple heating. The hyperthermia process had changed. The method thermally induces various processes governed by bioelectrodynamics. The thermal effect is a part of the energy that heats and appears in the temperature increase. Another energy part excites electric and chemical processes that are well-organized in space and time, choosing the optimal cell death to eliminate the malignancy. Cell destruction does not depend only on temperature, it could be guided by nonthermal processes, knowing that the living structures are more chemical than thermal "machines." Oncological hyperthermia is a method to kill malignant cells by absorbing energy characterized by a specific absorption rate (SAR). The SAR acts synergistically with thermal and nonthermal effects. The critical part of energy absorption is how the thermal effects ensure optimal conditions for the nonthermal molecular processes. Optimal oncologic hyperthermia sensitizes certain complementary methods like radio (RT) and chemotherapies (ChT). In hyperthermic effects, in

addition to the thermal impact, we consider the nonthermal processes, which cannot be produced thermally alone but use thermal conditions to optimize the triggered reactions.

Thermal homeostasis, a fascinating process that regulates the body's temperature compared to a set point in the hypothalamus, is at the heart of our research. It seeks to restore the baseline condition with a nonlinear regulation, including improving electrolyte transport in the heated area and intensifying various physiological mechanisms supporting its forceful control. Living organisms are not thermal 'machinery' but rather chemical entities. The thermal effects are conditional, and the ignited reactions are chemical, with their reaction rate being sharply temperature-dependent. Interestingly, nonthermal changes can be electromagnetically promoted, adding another layer of complexity to our study.

The increasing target's temperature promotes the nonthermal "chemical machinery" [1] [2]. These effects must be used in synergy, which is realized by the well-chosen modulated radiofrequency (RF) electromagnetic effect in the mEHT technique [3]. The thermal and nonthermal effects form a synergy (Figure 1) and determine the actual processes together. The thermal component provides the appropriate temperature of the tumor microenvironment (TME) by heating the membrane rafts [4]. Another general thermal action affects the extracellular matrix (ECM) and a part of the TME. This acts mechanically and molecularly [5], accompanying the thermal absorption of transmembrane protein clusters.

The incorporation of energy happens at clusters of transmembrane proteins [6], [7] [8]. The nonthermal component excites the membrane receptors of the cells. The well-chosen radiofrequency electric current can deliver energy for molecular excitations involving various ionic and molecular interactions [9]. The process only has a moderate thermal effect and excites the molecules or structures that fit the applied resonant conditions.

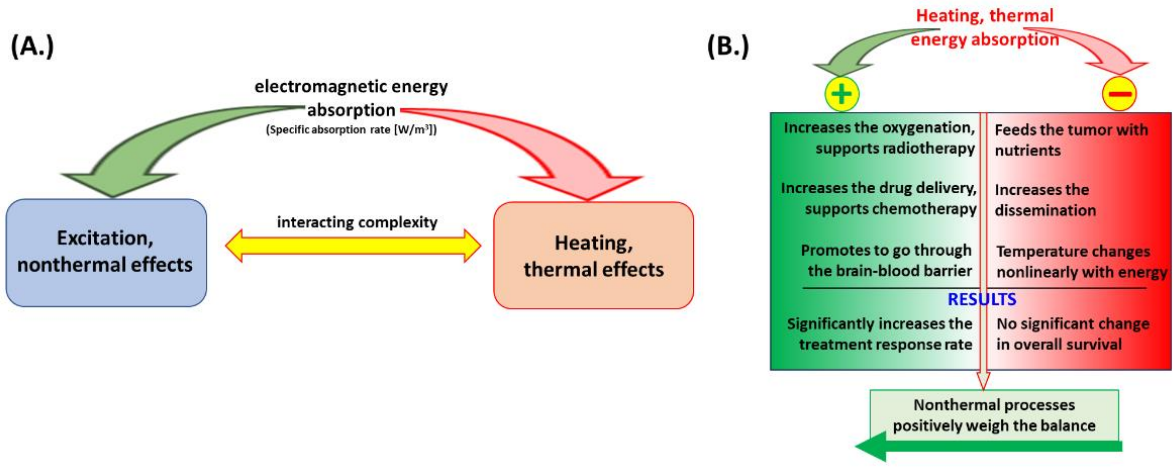

Figure 1. The synergy of the thermal and nonthermal effects. (A.) The division of the electrodynamic energy to thermal and nonthermal components and its complex cooperation. (B.) The thermal energy absorption balances between the pro and antitumoral processes. The nonthermal component tilts the balance towards antitumoral effects.

Researchers in conventional oncological hyperthermia usually share the opinion of the editorial comment of the European Journal of Cancer in 2001: the biological effects are impressive, but physically, the heat delivery is problematic. The famous formulation blames physics: "The biology

is with us, the physics are against us" [10]. Later, it was slightly modified, blaming the physiology against the well-defined hyperthermic goal, the high temperature [11]. Recently, the opinion of blaming was questioned [12]. This paper aims to present the preclinical data of a novel hyperthermia method called modulated electro-hyperthermia (mEHT), which directly presents the biophysical and physiological support in the hyperthermic elimination of malignancy. This article presents the preclinical data of a novel hyperthermic method, modulated electro-hyperthermia (mEHT), which directly demonstrates the hyperthermic destructiveness of malignant tumors with intensive support for the biophysical and physiological processes.

2. Method

The modulated electro-hyperthermia (mEHT) electric field. It is a kind of hyperthermia that targets tissue's natural electric and thermal heterogeneities and, with these particular properties, identifies and destroys cancer cells with definite carrier frequency and its optimally chosen modulation [2] [3]. The applied 13.56 MHz radiofrequency (RF) is a high-frequency carrier of low-frequency modulation [1]. The high-frequency part was chosen to select the malignant lesion using the specialties of the tumor: the higher conductivity and dielectric constant of the tumorous cancer than its host. The frequencies are chosen for the optimal use of the frequency dependence of natural heterogeneities [3] [4]. The electric field selects the tumor, and the low-frequency amplitude modulation polarizes and excites the transmembrane proteins of the malignant cells. The primary guidance of mEHT is biophysical using updated bioelectromagnetic considerations. The intensive proliferation of tumors is accompanied by a high metabolic rate, which produces extensive ionic density and higher electrolyte content in the tumor microenvironment (TME). Consequently, the tumor has high electric conductivity, which could guide the applied radiofrequency current to flow through it. Furthermore, the current may differentiate the autonomic malignant cells from the networked healthy counterparts in the heterogenic tumor mass. These selection facilities allow a heterogeneous, targeted effect instead of the intention of the overall isothermal heating of the tumor mass [13]. The essential step is the energy absorption of the transmembrane proteins in cancer cells and triggering intracellular signals driving immunogenic cell death, a special kind of apoptosis [14]. The carrier frequency modulation supports choosing the appropriate intracellular signal pathways [15] [16]. Time-fractal modulation endorses the selection of malignant cells [6], heating them locally to the hyperthermia temperature to induce cellular changes in the targeted cells by thermal and nonthermal mechanisms [1]; Figure 2 The thermal component of the absorption heats the selected membrane rafts, which is the source of the temperature of the tumor, as is standard in heterogenic seeds or nanoparticle heating processes. In contrast, the nonthermal processes excite signal pathways for programmed cell death [17]. The principle of the nonionizing radiation used by mEHT is very similar to the principle of ionizing radiation (radiotherapy, RT). The RT isodose actively concentrates on DNA damage using homogeneous radiation to produce heterogeneous (nanorange) effects to induce apoptosis. The mEHT is also a radiation isodose but nonionizing in the RF range and focuses in nano range on transmembrane proteins exciting apoptotic signals.

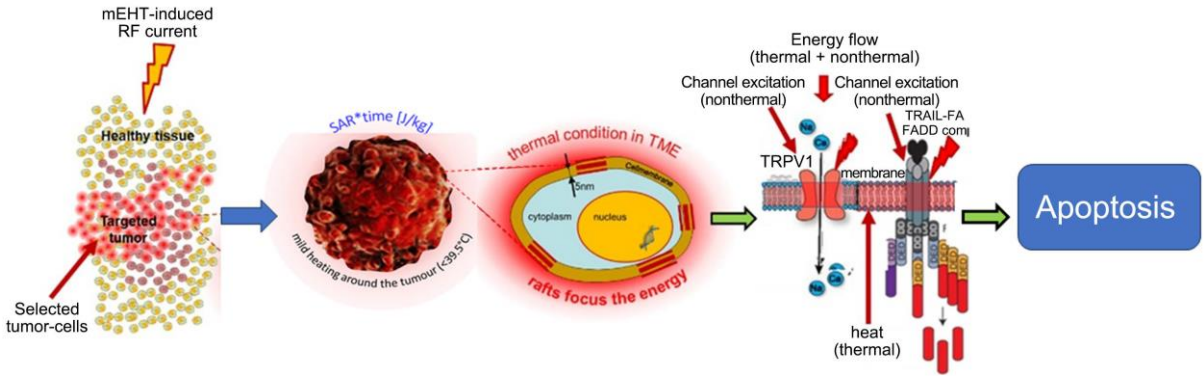

Figure 2. The transmembrane proteins of malignant cells absorb the energy in thermal and nonthermal forms. The nonthermal effect gives the primary drive for the apoptotic signal pathway (see below in the results).

The technical realization of the mEHT uses numerous biophysical concerns [13] [18] [19]:

1) The radiofrequency (RF) carrier frequency is 13.56 MHz. It is a freely applicable ISM band [20], so it does not need shielding.

2) The energy is capacitively coupled but avoids isothermal heating; it does not use the plane-wave method. The capacitively coupled electric field has precise impedance matching, mimicking the contact electrode conditions [21]. The precise impedance matching produces negligible reflected power (~1 W) and behaves like galvanic contact with the skin.

3) The method automatically selects the cancer cells, considering the well-measurable biophysical differences between the malignant and healthy tissues [22].

4) The maximum adequate output power of mEHT is limited to 250 W, less than for isothermal heating, but high enough to select and excite the membrane rafts of the malignant cells [1], and sensitize them to the radio [23] [24] and chemotherapies [25] [26] in clinical applications.

5) The modulation spectrum is a low-frequency time-fractal [27], described by fractal physiology [28] [29], which agrees with the homeostatic molecular temporal balance [15]. mEHT extensively uses the modulation technique to identify fractal structures in space and time (dynamics) [15]. It helps the temporal arrangement of the homeostatic regulation on the molecular level.

6) The membrane rectifies (demodulates) the signal [30] [31], which acts in the low-frequency range.

7) The correct impedance matching provides an appropriate electric field that ensures the current density (j).

8) The modulated j -current density actively produces both the thermal and nonthermal effects.

9) The patient is interactively connected to the electric circuit, like a discrete element of an RF circuit. This solution allows the patient to be controlled in real-time because the treated tumor is actively sensed and targeted as part of the tuned electric circuit [32].

10) The excited transmembrane ion channels function like RF rectifiers and low-pass filters [33].

Preclinical research is a long, multistep investigation process. It starts with the concept, proven in silico research and verified by phantom measurements. Phantoms lack more complexity than living organisms. This model verifies only the thermal effects. The research continues with in vitro experiments, which miss the physiological regulation processes we could model in the next step in vivo . All models give new knowledge, which appears as feedback for the previous research steps, which continues until the data show enough accuracy for the proof of the concept, the advantages and disadvantages, and safety to start the clinical phase Figure 3.

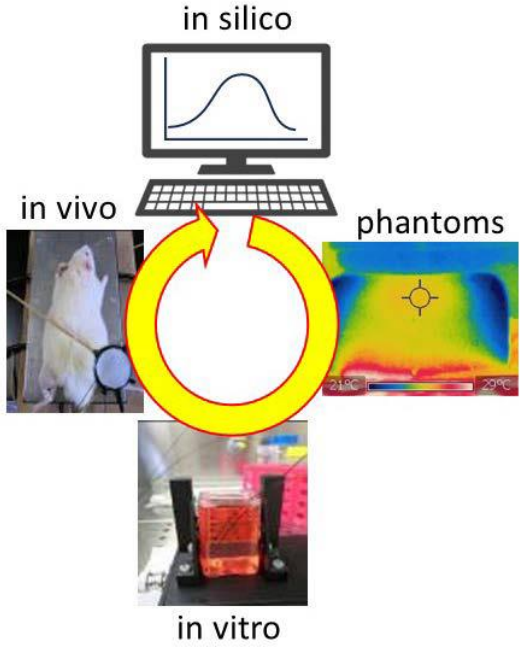

Figure 3. The preclinical methods have intensive feedback from in silico to in vivo through phantoms and in vitro experiments until all information is harmonized.

The in silico calculations are primarily based on bioelectromagnetic and thermal modeling of the living tissues, applying the commercial, highly specialized software (Computer Simulation Technology (CST), Darmstadt, Germany), and the various solutions of the Pennes bioheat equation [34]. The first period with growing temperature was calculated, which is too early to consider the conventional term in the equation, considering that the physiological reactions have a considerable time lag. However, in some cases, the convection term was considered using the linear approach.

In further research, when long-time heating is considered, the new approach [35] could be considered. The phantom measurements used tissue-equivalent materials or meat tissues, mimicking the actual thermal situation in living objects. The phantom models describe the thermal effects, but due to the essence of the phantom construction, those cannot follow nonthermal effects.

The in vitro and in vivo research are more complex. These methods have a lot in common, but the physiological regulation in vivo shows the temporal development of the synergy of thermal and nonthermal effects during energy absorption. The feedback mechanisms differentiate the temporal progress in the two kinds of experiments. The thermal processes have a complex nonlinear interaction with the homeostatic regulation, which tries to keep thermal homeostasis. The hypothalamus receives the thermal signal (primarily from TRP receptors) and acts to reduce the temperature. The principal effects are the blood flow with vasodilation and the sweating trying to cool with the evaporating process. The thermal regulation balances the incoming energy, which nonlinearly fluctuates in equilibrium Figure 4. incoming energy [36]. The fluctuation has various physiological components, including the opposition sensory mechanisms [37] and the various relaxation times of the different processes. The primary relaxation times could be measured with NMR [38], and the complex processes can be calculated using multiple physiological measurements [39] [40].

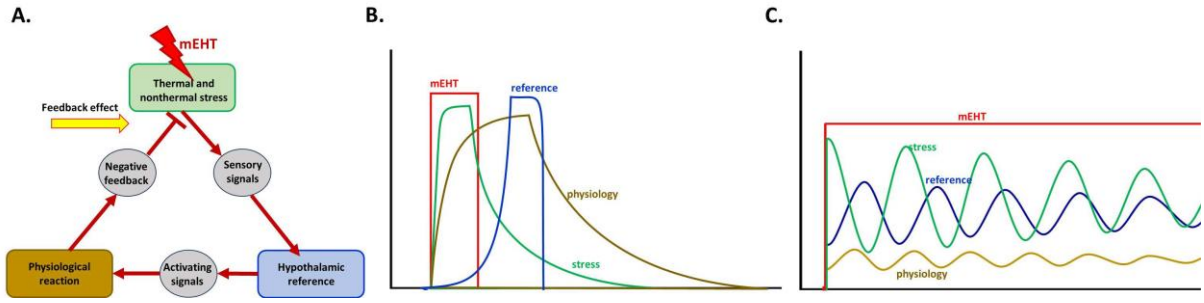

Figure 4. Effect of timing in homeostatic control. (A.) The feedback mechanism of regulation. (B.) The developments of the various signals. (C.) The signal modification during the mEHT process.

The in vitro cellular mechanisms have a short chemical reaction (1 s) timescale while its molecular developments take a long time (> 1 h). This feedback synergizes with in vivo development, and the observed signal is 1/f noise [41] [42]. The in vivo experiments are fundamentally different from the human clinical observations, but the allometry could help to emphasize the similarities [43]-[45].

The limitation of all such in silico calculations is the extensive complexity of living organisms. The homeostatic control includes multiple negative feedback regulations, which can be followed only in a simplified mathematical approach.

3. In Silico Considerations

The most important in silico publications and their results are shown in Table 1. The apoptotic signal by the mEHT excited membrane receptors and the apoptosis by the single or double-strand breaking of DNA by ionizing radiation are similar in their molecular selection principle. Nevertheless, despite conceptional similarities, the two methods have an essential difference: the nonionizing electromagnetic processes have massive thermal effects as the basis of hyperthermia; on the contrary, the thermal component is minimal in ionizing radiation, and it is primarily an unwanted side effect of radiotherapy. The final goal is shared: destroy the tumor cells with well-chosen molecular effects.

Table 1. In silico considerations in preclinical research.

Idea, considerations	Method	Findings	Conclusion	Ref.
The temperature development is stochastic.	Modified Pennes equation.	Temperature develops by Weibull distribution.	Dynamic, nonlinear development of temperature.	[46]
The correct dosing of hyperthermia needs chemical considerations.	Chemical transitions with multiple Arrhenius fit.	The correct dose needs transition-state theory (Eyring).	The presently applied CEM43Tx dose has to be modified.	[47]
Electromagnetic resonances in oncotherapies.	Self-organizing considerations of homeostasis.	Stochastic resonance describes the enzymatic and collective processes well.	The optimal synergy of thermal and nonthermal components needs modulation.	[9]
The membrane rafts robustly absorb energy.	Electromagnetic description of the rafts and their environment.	The membrane rafts have a highly tremendous specific absorption rate.	Membrane rafts are selectively heated, and their temperature is exceptionally high.	[4]
The energy absorption of the extracellular matrix makes special conditions.	Thermodynamical considerations with Onsager's theorem.	The temperature gradient is enormously high on membranes, increasing the intracellular pressure and diffusion conditions.	The tissues have nonuniform temperature development, and the heterogeneity determines the hyperthermia effects.	[5]
Study the dosing and depth effect.	Impedance matching coupling.	Impedance matching extends the penetration depth.	The coupling technique of the electromagnetic field is an essential factor in the treatment's success.	[48]
Critical analysis of the available literature on nonthermal effects.	Biophysical and electrophysical model for nonthermal membrane effects.	Transmembrane ion channels rectify and low pass filtering. Resonances cause membrane depolarization.	Exists nonthermal antiproliferative effects of mEHT. It may improve future treatments in oncology.	[33]
Clarifies how the amplitude modulation interacts with thermal effects.	Bioheat transfer equation for tumor model.	Low-frequency amplitude modulation increases extracellular absorption.	The mEHT energy absorption has only subtle thermal and mostly nonthermal effects.	[49]
How the modulation affects the glycolysis.	Pennes equation with stochastic solution.	The modulated electric field affects the chemical reaction rate similarly to the temperature.	The modulation of the electric field is directly connected to thermal effects.	[50]
Time fractal modulation as a factor of the self-organized homeostatic synchrony.	Fluctuations and stochastic resonance in biosystems.	1/f noise production.	Environmental noises synchronize the stochastic processes, but the system has noiseless internal signal communications.	[15]
How does the time-fractal amplitude modulation destroy the cancer cells?	Thermal and nonthermal synergy with homeostatic feedback.	The time-fractal amplitude modulation could destroy the cells out of the healthy cellular network.	The modulation of the RF-carrier frequency, with the homeostatic 1/f signal, selectively targets the malignant cells.	[15]
Clarify the role of the heat shock proteins.	Study the conditions of HSP development.	The HSP's Intra or extracellular (or membrane) location determines their actions.	The immunogenic actions depend on the HSP info delivery in the extracellular matrix.	[51]

Study of immunogenic effects of mEHT.	Immunogenic cell death and damage-associated molecular pattern.	The mEHT may induce immunogenic effects by innate and adaptive immune processes.	Tumor-specific immune reaction products abscopal effect.	[14]
Bioelectromagnetism of angiogenesis.	The electric field induces polarization and current.	The mesenchymal ↔ epithelial transition depends on the electric field.	The appropriate electric field may influence the mesenchymal ↔ epithelial transition.	[52]
Angiogenesis has allometry.	Allometric scaling on a self-organized basis.	Allometric relation exists between tumor mass and cell death.	The inflammatory feedback could explain some unsuccessful tumor treatments.	[45]
Comparison of capacitively coupled methods.	Comparison of plane wave and impedance matching capacitive coupling.	The impedance matching has better performance than the plane wave coupling.	Self-selection is a good approach that could have immunogenic effects.	[21]
Model simulation of applicators for preclinical experiments of mEHT.	Temperature and SAR calculation for small electrodes (Ø10mm) developed for in-vivo murine models.	The SAR is strongly inhomogeneous. The different tumor growth stages have different temperature and SAR profiles.	The SAR is extreme in heterogenic places. The model verifies the nonthermal effects.	[53]

The nonthermal effect in mEHT involves "when, under the influence of a field, the system changes its properties in a way that cannot be achieved by heating" [54], like feeding cannot be replaced with the same heating energy. The nonthermal component excites the membrane receptors of the cells [2]. The thermal and nonthermal (electric) effects have similar Arrhenius-like exponential reaction rates [50]. The well-chosen electric current can deliver energy for molecular excitations involving various ionic and molecular interactions [46]. The process has a conditional thermal effect and excites the molecules or structures that fit the applied resonant conditions [9]. Two essential effects are considered for selection: thermal absorption and nonthermal excitation. The thermal component provides the appropriate temperature of the TME by heating the membrane rafts [4] Figure 5. which are nano-range clusters, widely vary by size 10 - 100 nm [55]; 25 - 700 nm [56]; 100 - 200 nm [57]. The rafts trigger intracellular signal pathways and determine cellular processes [58]. The temperature of these nano-units increases by the square of their radius [59]. The thermal process of mEHT heats the TME and the rafts, which serve for thermal and nonthermal processes. The RF current flows through the tumor and heats the extracellular electrolytes. Due to the high ionic concentration, the TME absorbs more energy than the ECM in more distant regions. The energy analysis of the heating differences explains how this effect contributes to cell-killing mechanisms [5].

Another general thermal action affects the extracellular matrix (ECM) and a part of the TME. This acts mechanically and molecularly [5], accompanying the thermal absorption of transmembrane protein clusters. The point selection shows of ~1 MW/kg absorbing possibility in 100 µm sphere [12] [49]. The rafts absorb an average. $\sim 350 \frac{\mathrm{kW}}{\mathrm{kg}}$ [5], which fits the interval of nanoscopic heating 100 - 500 kW/kg [60]. The selected rafts' temperature is over the tissue's thermal averaging. The ECM also absorbs energy from RF current. The TME is especially heated due to the locally high ionic concentration and dielectric permittivity. This thermal process induces a temperature gradient

between the TME and the cytosol through the membrane. The energy analysis reveals how the gradient contributes to cell-killing mechanisms [5].

Figure 5. The particular nano effects in the cell membrane calculated by Computer Simulation Technology (CST) [4]. The point at touching two cells has concentrated energy absorption $(\sim 2 \cdot 10^8 \frac{\mathrm{W}}{\mathrm{m}^3})$, while the cluster of transmembrane proteins (membrane rafts) absorbs more than double $(\sim 5 \cdot 10^8 \frac{\mathrm{W}}{\mathrm{m}^3})$ power, which promotes apoptosis by igniting appropriate signal pathways and gradually heating the entire cell and the tumor.

The thermal processes provide optimal conditions by increasing the reaction rate of the chemical reactions ignited by the nonthermal effects [46]. Due to its enormously high fixed polarization, the cell membrane rectifies the periodically changing electric field (≈107 V/m) Figure 6(A). [61]. The applied electric power dominantly functions nonthermally [49]. Silico models could approach the best carrier frequency chosen, 13.56 MHz, in the overlapping region of β and δ frequency dispersion, [33], using membrane charging, orientation of transmembrane proteins, dipolar mechanisms, and tumor selection. The chosen modulation was taken from the $\alpha\alpha$ dispersion guiding the electrochemical effects and active membrane processes, including the excitation of transmembrane proteins [3] [15], Figure 6(B). The applied modulated RF triggers apoptotic pathways [53], and the nonthermal antiproliferative membrane effects induce ion fluxes (especially of Ca2+) and/or resonances causing membrane depolarization [33].

Nonthermal activity makes structural changes that affect the intracellular polymerization of cytoskeleton filaments [62] [63]. The fluctuations are also essential in the electromagnetic interaction, showing thermal and electric noise limitation in the TME-connected membrane [64] [65]. The molecular models concentrate on the membrane effects, showing the thermal and nonthermal results. The same heat conditions force the same processes in the cytosol ER and other cellular organelles. The heat-sensitive transient receptor potential vanilloid receptor (TRPV) also senses the same temperature for action. The mEHT causes the excess ionic concentration [7], which increases the influx of Ca^{2+} ions from the ECM to the cytosol. The high iCa2+ promotes apoptosis in the mitochondria- dependent intrinsic signal pathway [66].

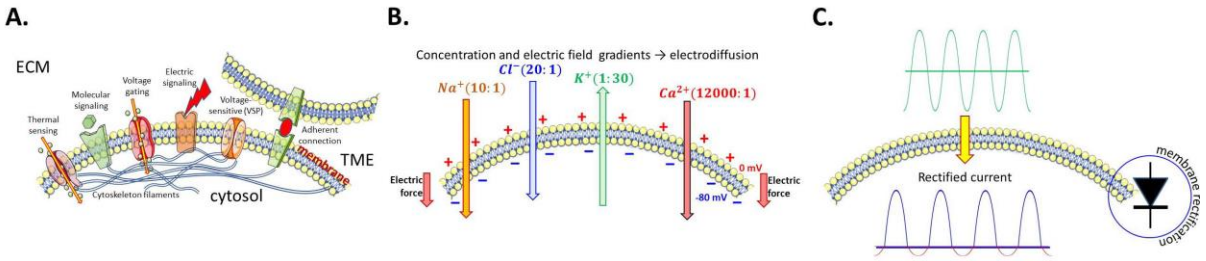

Figure 6. Nonthermal membrane processes. (A.) The various ion channels are sensitive to different ignitions, including thermal and non-thermal effects. (B.) The ion gradients and the field gradient make electrodiffusion, working differently on the various ions (only the most common ionic exchanges are shown). The membrane controls the ion flows similarly to the transistor effect. (C.) The membrane rectifies the electric field, working like a diode.

A remarkable feature is that the thermal and nonthermal effects have similar electrical mechanisms with modulation [50], harmonizing the complex interaction phenomena of the electric field. The nonthermal activity causes structural changes affecting the intracellular polymerization of filaments [2]. The fluctuations also have an essential role in the electromagnetic interaction, showing thermal and electric noise limitation in the TME-connected membrane [64] [65].

4. Phantom Measurements

Various phantom systems were checked for the thermal effect of mEHT. The publications of phantom research are summarized in Table 2.

Table 2. Phantom measurements in preclinical research.

Material	Method	Result	Conclusion	Ref.
Agar phantom (6 kg, 24 × 24 × 8.5 cm).	mEHT, Ø30 cm applicator, 150 W, 30 min, infrared thermometry.	> 3.5˚C temperature increase, absorbed ~24.5 W/kg, with 74% efficacy, bulk absorbs in a cone shape, at the bottom 50%.	The phantom shows high efficacy of bulk heating with satisfactory penetration depth.	[67] [68]
Egg-white in distilled water, cylindrical tank, Ø10 cm, height 25 cm.	mEHT temperature measurement in water and egg white, 75 W, 15 min.	Significant temperature difference, egg white has a 5-times increase, which agrees with the simulation.	The heating selection in the distilled water + egg white heterogenic arrangement is proven.	[69]
Chopped porcine meat (mixed muscle), cylindrical tank, Ø10 cm, height 25cm.	mEHT, temperature measurement in depth by 5 cm, 75 W, 1 h, Ø10 cm applicator.	The temperature rises from 23˚C to 44˚C on the top and to 40˚C at the bottom after 1 h. The temperature decreases linearly with the depth.	The heating efficacy and the reached temperature were appropriately high, as expected in clinical applications.	[69]
Chopped porcine meat (mixed muscle), cylindrical tank, Ø10 cm, height 31 cm.	mEHT, temperature measurement in depth by 5 cm, 100 W, 1 h, Ø10 cm applicator.	The temperature rises from 27˚C to 55˚C on the top and 45˚C on the bottom. There was a hump of temperature in 10 cm depth.	The heating efficacy is high, and the method could reach high temperatures.	[70]

Egg white, pork liver, and red caviar in distilled water.	mEHT, protein denaturalization, and coagulation measurement in the samples. Ø20 cm applicator.	The liver showed inside denaturalization, egg white coagulated, and caviar was cooked inside, while the water temperature increased only ~3˚C.	The selection of energy absorption is proven in these phantom arrangements.	[70]
Chopped pork muscle + fat meat phantom, 6.6 - 7.2 kg in Ø20 cm and 20 cm high plastic cylinder. The impedance of the sample was 23.9 + i76.8 Ω.	mEHT 150 W, 1 h (~540 kJ), thermally isolated setup, Ø20 cm applicator.	Temperature rises from 22.5˚C to 38˚C (ΔT~15.5˚C) at the top and 35.5˚C (ΔT~13˚C) at the bottom.	The temperature growth shows appropriate conditions in this model for clinical use.	[71]
Chopped pork muscle + fat meat phantom, covered with paper soaked in saline, mimicking the patient's sweating.	mEHT 50, 100, 150 W, 1 h, thermally isolated setup, Ø20 cm applicator.	The shape of the temperature rise changes. The maxima of ΔT are 2˚C at 500 s, 8˚C at 150s, and 15.5˚C at 1600 s for 50, 100, and 150 W power, respectively.	The patient's perspiration robustly raises the surface temperature in this phantom model and could reach thermal toxicity in the skin.	[71]
Pocrine ribs with skin, muscle, and connective tissue. The liver is placed in the middle of the phantom, forming a "sandwich" arrangement.	mEHT Ø20 cm applicator, 100 W, 15 - 26 min. The ready phantom was ~10 cm thick. A metallic implant (hyp replacement) was also tried inside the "sandwich".	The temperature rises at 26 minutes on the skin, at 16.6˚C - 17.3˚C, ribs 9.5˚C - 14.3˚C, liver surface 7.9˚C - 8.5˚C, and liver inside 6.2˚C - 6.6˚C. Metallic implant 9.5˚C.	The rise in the temperature of the liver in the phantom was enough for clinical requirements. The skin, however, would have thermal toxicity. (No blood circulation.)	[72]
Porcine liver using arterial hepatica to model blood perfusion.	mEHT Ø20 cm applicator, 100 W, 60 min. 0.03, 0.06, and 0.32 L/min/kg perfusions were modeled.	Temperature growth was ~1.2˚C by 5 min in all samples but stabilized at 38.2˚C, 40.1˚C, and 43.2˚C in 0.32, 0.06, and 0.03 L/min/kg perfusion, respectively.	The mEHT method looks satisfactory for heating tissues with blood perfusion. Thermal toxicity in the skin is less probable.	[72]
Multilayer "sandwich" structure of pork with layers of skin, adipose tissue, muscle, liver, and adipose tissue skin in Ø20 cm and 20 cm high plastic cylinder.	mEHT, Ø20 cm applicator, 100 W, 1.5 h.	The maximum temperature was reached after 65 minutes, at 32.5˚C in healthy and 37˚C in tumorous liver.	The mEHT may select between the phantom structure's healthy and tumorous liver tissues.	[67]
Spherical model for necrotic tumor. Outside deionized water, inside egg white and 0.9% NaCl saline is embedded in the egg white to model the necrosis.	mEHT, Ø20 cm applicator, 100 W, 20 min. The experiment was done on the water mattress of the treatment bed of the EHY2000+ device.	From 23˚C, the maximal temperatures are 53˚C for egg white, 43.5˚C for saline, 34.5˚C for deionized water around, and 28˚C for the treatment bed underneath.	The selection was shown with this multilayer spherical model.	[73]

The conventional thermal impact is measured with an agar phantom [68]. The phantom had a 6 kg weight (24 × 24 × 8.5 cm size) treated with 150 W for 30 min, treated with an EHY2000+ device using a 30 cm diameter applicator Figure 7. The measurement with infrared thermography shows only the surface temperature at 22˚C room temperature, which is considerably lower than in the bulk material. The observed shape of the heat distribution was a truncated cone, and the temperature was increased by ~4˚C, in good linear approximation (R2 = 0.9691).

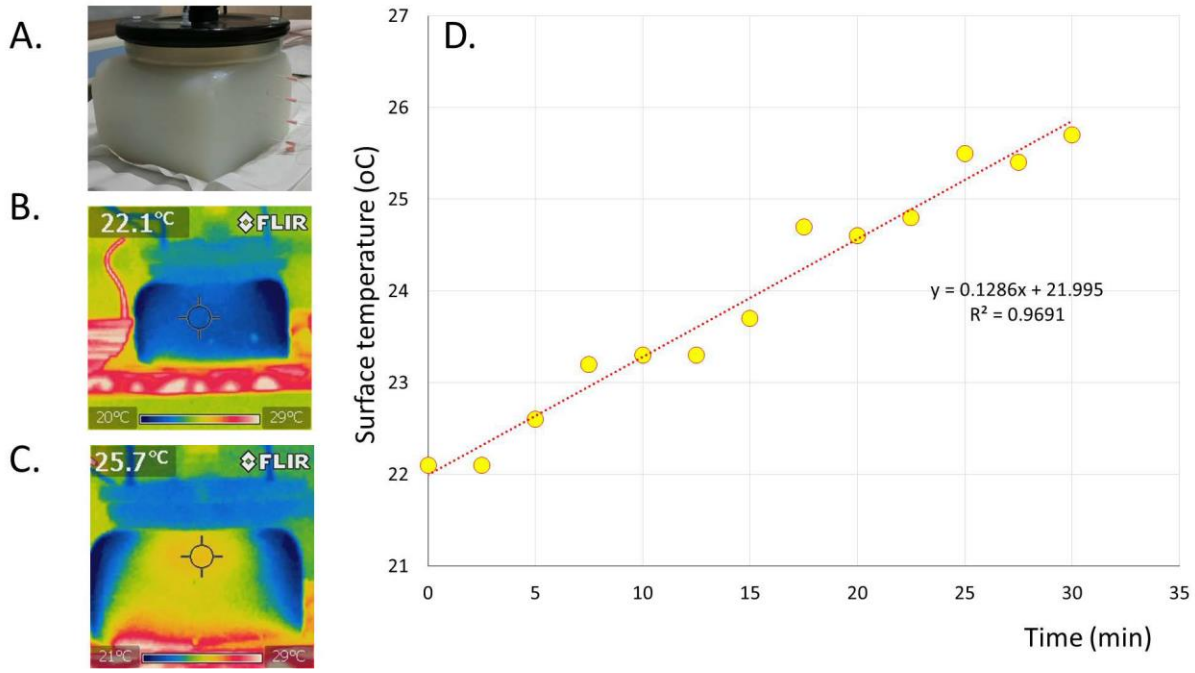

Figure 7. The agar phantom measurement. (A.) The temperature distribution is measured by thermometry. (B.) Linear dependence of the surface temperature from the time.

For more realistic experiments, chopped port meat (a muscle and fat mixture) was placed in a long cylindrical plastic holder. Three different setups were measured at other times (Figure 8). The dynamic linear temperature development is clearly shown in all experiments [69]-[71].

Phantoms were used to study the method's energy focus. Various actual tissues (pieces of liver, egg white, caviar) were placed in distilled water in the cylindrical holder [74]. A more realistic phantom was developed with a liver embedded in pork ribs (Figure 9 [72]. The temperature measurement of various phantom parts proved the satisfactory temperature increase. The same model was used for a larger metallic implant in the treating volume. The inserted hip joint was not heated extremely, proving the safety of the implants in the targeted volume. The effect of blood flow was also modeled with this experimental setup, pumping room-temperature electrolytes into the arteria hepatica. Without blood perfusion, the temperature changes rapidly, while higher perfusions moderate the temperature change and reach the thermal balance sooner.

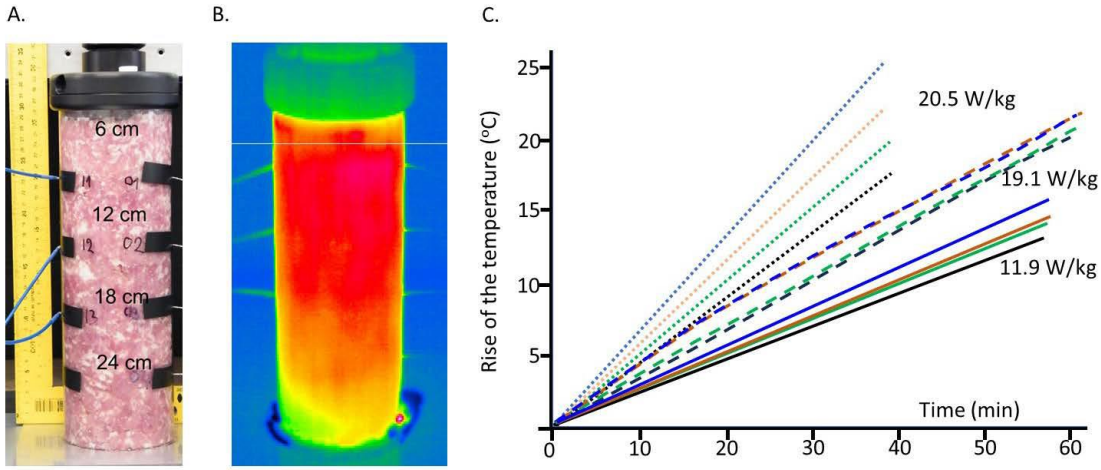

Figure 8. The Cylindric chopped meat phantom experiments. (A.) Meat phantom setup from [69]. (B.) The infrared thermography of the phantom after 40 min treatment. (C.) The various phantom experiments showed a linear temperature development, in which the slope depends on the setup. The experiment with SAR = 20.5 W/kg was made in a cylinder 31 cm in length and 10 cm in diameter, and 100 W power (40 min) was used with a 10 cm diameter applicator [70]. The experiment with SAR = 19.1 W/kg was done in a cylinder 30 cm in length and 10 cm in diameter, and 75 W (60 min) power was used with a 10 cm diameter applicator [69]. The experiment with SAR = 11.9 W/kg was done in a cylinder 20 cm in length and 20 cm in diameter, and 150 W (60 min) power was used with a 20 cm diameter applicator [71]. The results correspond well with the in silico simulations [69].

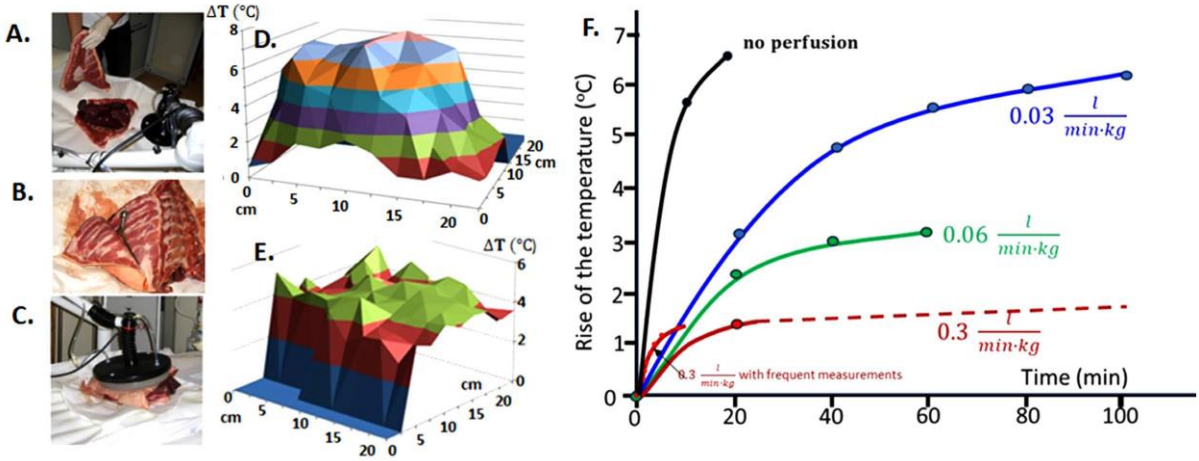

Figure 9. The pork rib phantom experiment (100 W). (A.) Pork liver "embedded" in the pork rib. (B.) A metallic hip replacement placer in the rib of pork. The most significant temperature of the inserted metallic implant after 1 h treatment was 9.5˚C. (C.) The treatment of the "sandwich" structures with the EHY2000 device. (D.) The temperature rises in the subcutis layer at 20 min 100W. The most considerable temperature in the skin after 1 h treatment ranges from 16.6˚C - 17.3˚C. (E.) The temperature rises in the embedded liver after 20 min 100 W. The most significant temperature in the liver after 1 h treatment ranges from 6.2˚C - 8.5˚C. (F.) The phantom simulation of the blood perfusion with the liver phantom forcing room-temperature electrolytes through the arteria hepatica. The measured discrete points (20-minute intervals) are connected to guide the eye. The large perfusion case was measured at a higher frequency (1 min intervals) at the start of the temperature rise, showing a more precise quasi-isothermal start.

The phantom measurements describe the processes only partly. They have no dynamic feedback. Primarily, the physiologically regulated blood perfusion is missing. In the last experiment (Figure 9), the perfusion was modeled, but no feedback regulation was possible.

5. In Vitro Measurements

Modulated electro-hyperthermia (mEHT) was studied in vitro. The mEHT is a hyperthermia, which targets tissue's natural electric and thermal heterogeneities [74]. It recognizes the cancer cells selectively and destroys them [19]. The electric field selects the tumor, and the low-frequency amplitude modulation polarizes and excites the transmembrane proteins of the malignant cells [16]. The dominant absorption of the energy by the microscopic clusters of the membrane rafts

acts like nanoparticle heating [4]. Exciting the membrane produces various apoptotic signals. The in vitro experiment had a glass cuvette with distilled water, and the condenser applicators were tightly attached to the cuvette walls. The investigated cell suspension was placed in a polyethylene plastic bag and immersed in the water Figure 10. The LabEHY (Oncotherm, Budaors, Hungary) provided a well-controlled amplitude-modulated radiofrequency (RF) signal with a 13.56 MHz frequency. The temperature was controlled with specialized thermometers immune to RF radiation. The experimental conditions are discussed in detail in every referred article.

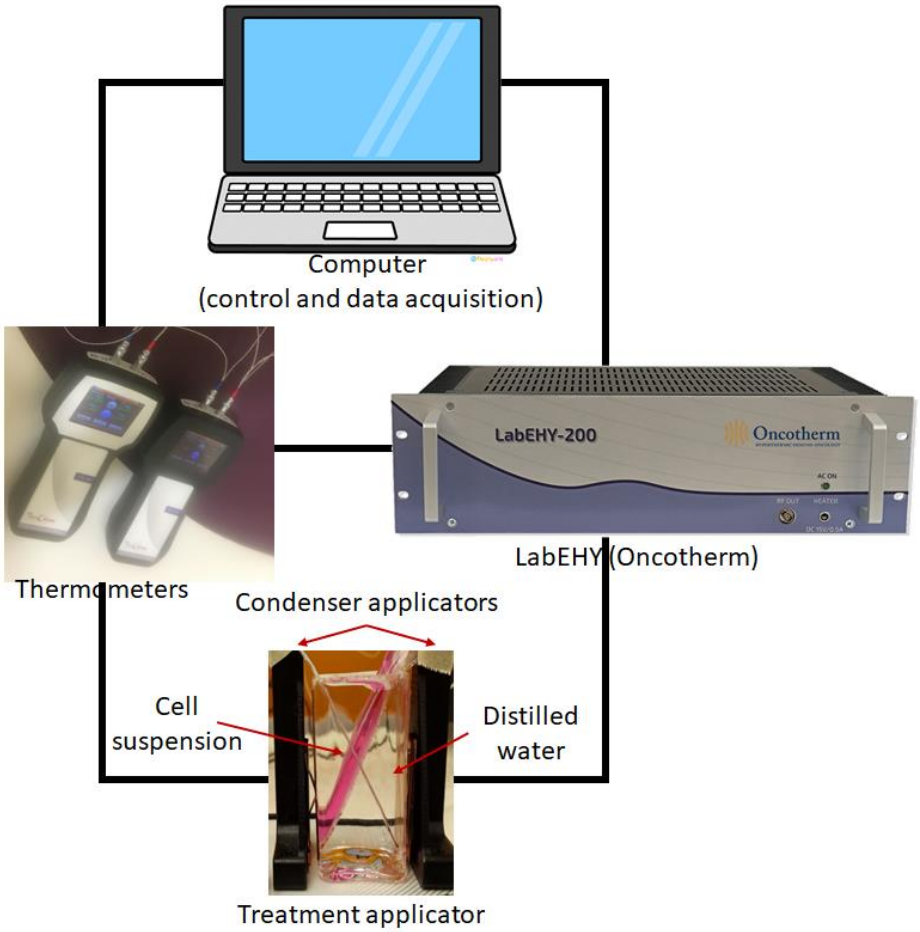

Figure 10. The experimental setup of the in -vitro application.

The in vitro research covers multiple cell lines and various methods to evaluate the results. The most frequent methods are Western blot, immunohistochemistry, flow cytometry, MTT assay, TUNEL, and clonogenic assay. The various results are shown in Table 3.

Table 3. In vitro preclinical research.

Tumor cells	Method	Result	Conclusion	Ref.
mEHT treated coculture of human fibroblast and, HCK and HaCat, A431cells.	The same treatment was given to the fibroblast together with cell variants with different proliferation forces.	The mEHT treatment did destroy the malignant A431 cells, but the healthy and nonmalignant cells remained unchanged.	The mEHT treatment is selective for malignant A431 cells *in vitro*.	[75]

mEHT treated Huh7 and HepG2 cell lines.	mEHT (3x), 42˚C, 60 min, Clonogenic analysis, Western blot, RNA sequencing.	Significant apoptosis by an increase of tumor suppressor SEPT4 with the restoration of p21.	Tumor suppressor SEPT4 mediates the massive apoptosis in HCC cells.	[76]
mEHT treated HepG2 cell line.	mEHT 42˚C, 30min. Comparison of cHT and wHT at 42˚C. Measured with Annexin V positive cells, SubG1 ratio, Western blot.	mEHT had significantly higher apoptosis than other methods. wHT produced a high apoptotic rate as mEHT (42˚C) at 45.5˚C. mEHT significantly increased the caspase 3, 8, 9, and the extracellular HSP70. Calreticulin and E-cadherin also increased by mEHT.	mEHT causes significantly higher apoptosis than other methods by the selective energy deposit.	[77]
MCF7, WiDr and U87MG cell-lines treated with mEHT.	mEHT 42˚C, 30 min. cHT and wHT at 42˚C. Measured with Annexin V positive cells.	The apoptotic rate was significantly higher than wHT and cHT at the same 42˚C temperature	The heterogeneous mEHT is superior to homogeneous heating intentions.	[77]
CT26 murine colorectal cancer cell line treated with mEHT.	mEHT 42˚C, 30 min, 8 - 9 W comparison with wHT same temperature and time. Annexin V/PI, flow cytometry, Western blot, ELISA	Significantly higher apoptosis with mEHT than in wHT at the same temperature. HSP70 was released from the cells. mEHT induced a greater HSP response than wHT did.	mEHT is a significantly better apoptosis inducer than homogeneous wHT heating.	[78]
OVCAR-3, SK-OV-3, HeLa and SNU-17 cells treated with mEHT.	Apoptotic markers such as cleaved are measured. FACS and Western Blot were used.	Significant apoptosis was measured in all cell lines. p-P38, c-Cas-3, and PARP were increased.	mEHT treatment is sufficient for the degradation of tumor cell lines.	[79]
CT26 murine colorectal cancer cell line treated with mEHT.	mEHT 42˚C, 30 min, 8 - 9 W reacted injected DC. MHCII, CD80, and CD11c DC surface markers are measured with FACS analysis for matured and immature DC cells.	mEHT changed the DC surface markers in both the matured and unmatured cells. The fluorescent intensity of MHSII and CD80 was significantly higher in mature DC than in immature counterparts.	mEHT changes the DC surface markers in both DC states but is significantly higher in mature states.	[78]
Aggressive and radioresistant 9L rat gliosarcoma and MCF-7 and MDCK cell lines treated with mEHT.	Clonogenic assay for mEHT treated 9L cell line combined with megavolt radiation: propidium iodide staining, 10 MV, 5 Gy.	mEHT selectively attacked the L9 cells, but those were shortly repaired. The proliferation arrested cancerous MCF-7, but the non-cancerous MDCK remained unchanged. mEHT and the RT synergetically induced cell death, reducing normalized survival.	Combining mEHT with megavolt irradiation could cause cell death for the radioresistant L9 cells.	[80]
Panc1, a KRAS and TP53 mutant, radioresistant pancreas ductal adenocarcinoma cell line treated with mEHT.	mEHT 20 - 25 W 5min until 42˚C, keep with 7 - 8 W for 60 min. Cell viability, apoptosis by Annexin V/PI, immunohistochemistry, flow cytometry, clonogenic assay, and Western blot were applied.	mEHT made significant apoptosis; mono and combined treatments affected the tumor progenitor/stem cell populations. Accumulation of γH2AX indicates DNA double-strand breaks and upregulation of the cyclin-dependent kinase inhibitor $p21^{waf1}$.	mEHT treatment can contribute to tumor growth inhibition and apoptosis induction and resolve radioresistance of Panc1 cells.	[81]

Panc1 and Capan1 cell line, ALDH+ cancer stem cell (CSC) fraction.	mEHT 60 min + 2 Gy radiation (137 Cs source) (RT), Annexin V/7-AAD staining, immunohistochemistry and flow cytometry were applied.	mEHT + RT combined therapy caused significantly more apoptotic cell death in both cell lines than the single modalities alone. The CSC fraction was reduced by mEHT involvement, but RT did not change it.	The leading factor of mEHT application alone or combined is the induction of γH2AX and significant reduction of CSC.	[81]
HT29 and SW480 human colon cancer cell lines were treated with mEHT.	mEHT and wHT are compared with proliferation and clonogenicity.	mEHT significantly reduced the proliferation and clonogenicity in both cell lines compared to wHT.	mEHT creates significant nonthermal effects in addition to the thermal.	[61]
CT26 mice colorectal cancer cell line + reservatol (Res) and nanosized curcumin (Cur) combined with mEHT.	mEHT and wHT comparison, 42C 30 min, 10-12 W, Annexin V-FITC, Western blot, Immunofluorescent analysis FACS.	Cell viability decreased by Res and Cur. Cell-cycle arrest by Res + Cur, Apoptosis, and immunogenic cell death were detected, and CRT development was significantly higher when mEHT was combined with Cur + Res.	The complementary treatment of mEHT with Cur and Res shows promising potential for clinical applications against malignancies.	[82]
C26 mouse colorectal cancer cell line + doxorubicin (Dox) treated by mEHT.	mEHT 42˚C, 60 min (2x), 1 µmol/L Dox. immunohistochemistry and qPCR, as well as time-course follow-up, were applied.	mEHT with Dox made significant CRT and HSP70 development, reduced antiapoptotic and increased proapoptotic molecules with $p21^{waf1}$.	mEHT activates both caspase-dependent apoptosis and $p21^{waf1}$-mediated growth arrest pathways by the p53 protein.	[83]
Mouse colorectal adenocarcinoma C26 Double tumor where only one is treated with mEHT.	mEHT 42˚C, 30 min (2x) and 60 min (2x). Measured cellular morphology, apoptosis, immunochemistry, Western blot, flow cytometry.	Significant cell damage compared to the untreated tumor, significant CRT and HSP70 development, inactivation of pRAF, and activation of pERK1/2.	mEHT causes significant apoptosis and DAMPs, so it can potentially induce immunogenic cell death.	[84]
A549 cell line treated with mEHT.	mEHT and wHT comparison in heating phases (25˚C→37˚C, 37˚C -42˚C) and in thermal equilibrium (42˚C 30 min, 60 min) The power pulsing was also studied.	It is proven that mEHT produces a significantly higher apoptosis rate than wHT. The main apoptotic phase is connected to the heating process's growing temperature (dT/dt).	The time derivative of temperature is the primary addition to apoptosis with mEHT. It may be used for the pulsed strategy of the mEHT treatment.	[85]
U87-MG and A172 cells treated by mEHT.	mEHT (42˚C, 60 min) three times every 2nd day tested for growth inhibition using MTT colorimetric, FACS, and microscopic analysis.	The growth inhibitory effects were observed. The colony formation was significantly suppressed, and apoptosis was induced in both cell lines. Gene expression of RNA 34 commonly deregulated genes is identified.	mEHT induced the inhibition of cell proliferation and clonogenicity, as well as significantly promoting apoptosis.	[86]
U937 cell line treated with mEHT.	mEHT, 42˚C, 30 min. Flow cytometry, Western blot, microarray gene expression, comparison with wHT, gene map, IPA.	Different heat treatments have various responses. mEHT induced significant apoptotic cell death, while wHT had significantly less. mEHT upregulates a whole cluster of genes. The Fas, c-Jun N-terminal kinases (JNK), and ERK signaling pathways were dominant to induce apoptotic cell death in mEHT, whereas the cell-protective mechanisms dominated in the case of conventional heating.	We measured the different responses of wHT and mEHT heating. mEHT activates death-related signal pathways, which wHT does not.	[87]

U937 cell line treated with mEHT.	Compare mEHT to wHT in 39˚C - 46˚C interval for apoptosis, measured by flow cytometry Annexin V/PI.	The apoptotic rate for mEHT at 40˚C was similar to that of wHT at 44˚C. However, the high difference remained for 41˚C at mEHT measurements.	The mEHT makes the apoptotic rate equivalent to wHT at 4˚C lower temperature, assuming that the membrane rafts have such an exceptionally high temperature.	[88]
HepG2, A549, U87MG, and CT26 cell lines and liposomal Dox uptake were treated with mEHT.	mEHT 42˚C, 30 min, 10 - 12 W (3x). Flow cytometry and immunofluorescence measured the Dox release. Substrate assay and Westre blot were used for the study.	mEHT alone suppressed cell viability, and together with liposomal Dox, its drop was significant. The drug release was the highest, with mEHT 42˚C. Uptake of Dox with mEHT was higher than with wHT.	The mEHT-induced particle uptake was by macropinocytosis. Dox + mEHT arrests the proliferation. mEHT-enhanced uptake of Dox may amplify the therapeutic effect.	[89]
HepG2 and various shapes and sizes of gold nanoparticles were treated with mEHT.	mEHT 15 W, 10 min. Sphere-like, urchin-like, and rod-like gold nanoparticles. Measured relative cell viability and apoptosis rate.	The mEHT effect was suppressed by the addition of gold nanoparticles. The heat generation with gold nanoparticles was negligible.	The nanoparticle addition worsens the cell-killing. The incoming energy is shared between the membrane rafts and nanoparticles.	[90]
HT29, SW480, SW620, LoVo, and HCT116 cell lines treated with mEHT.	Modulated (mEHT) and unmodulated (EHT) treatments were compared. Mechanical, thermal, and electric parameters were measured. A comparison with wHT was also done.	Temperature was significantly higher in wHT than in mEHT and EHT, but the apoptosis was substantially higher in mEHT and EHT. The Young moduli differences at 41˚C could vary the resonance frequencies.	Resonance frequencies can be approximated from electricity data (Young moduli), showing agreement with the treatment data.	[53]
mEHT for 4T1 and 4T07 cell lines.	mEHT 42˚C, 30min temperature rise is 2.3˚C/min. Histopathology, RT-PCR, mass spectrometry, and nanostring analysis were done.	One of the most upregulated genes/proteins was the mouse C4 complement C4b. C4b mRNA was measurable by qPCR from *in vitro* 4T1 cell culture.	mEHT treatment in monotherapy induced a significant upregulation of C4b mRNA 2 h after treatment. HSP70 and C4b relative expressions are proportional to each other.	[91]
SCCVII and SAS cell lines.	Comparison of mEHT and wHT in combination with RT. Flow cytometry, clonogenic assay, survival time.	Apoptosis and autophagy are significantly increased with combined RT + mEHT treatment and the thermal component increases the effect.	The increased apoptosis and survival time indicate the excellence of the mEHT + RT treatment.	[92]
A549 and NCI-H1299 lung cancer cell lines.	Measurement of radiosensitivity change by addition of mEHT to RT.	Measured α and β values of the linear-quadratic equations of cell survival curves show more than doubling the sensitivity.	The mEHT addition to RT significantly increases the cell sensitivity to radiation.	[93]

The cellular selection was shown in coculture experiments, [75] [94]. Co-culture with normal human skin fibroblasts as a model of a squamous carcinoma growing within connective tissue cells (100.000/ml) were exposed to mEHT, incubated for 24 h at 37˚C, fixed, and stained with crystal violet. The healthy human keratinocytes (HCK) were unaffected by the mEHT treatment, while the highly proliferating but non-malignant (HaCat) cells had a low distortion rate among the unaffected healthy fibroblasts, and the aggressively malignant A431 cells in the co-culture with healthy fibroblasts show a highly selective distortion of malignant cells, while the fibroblasts were not hurt Figure 11.

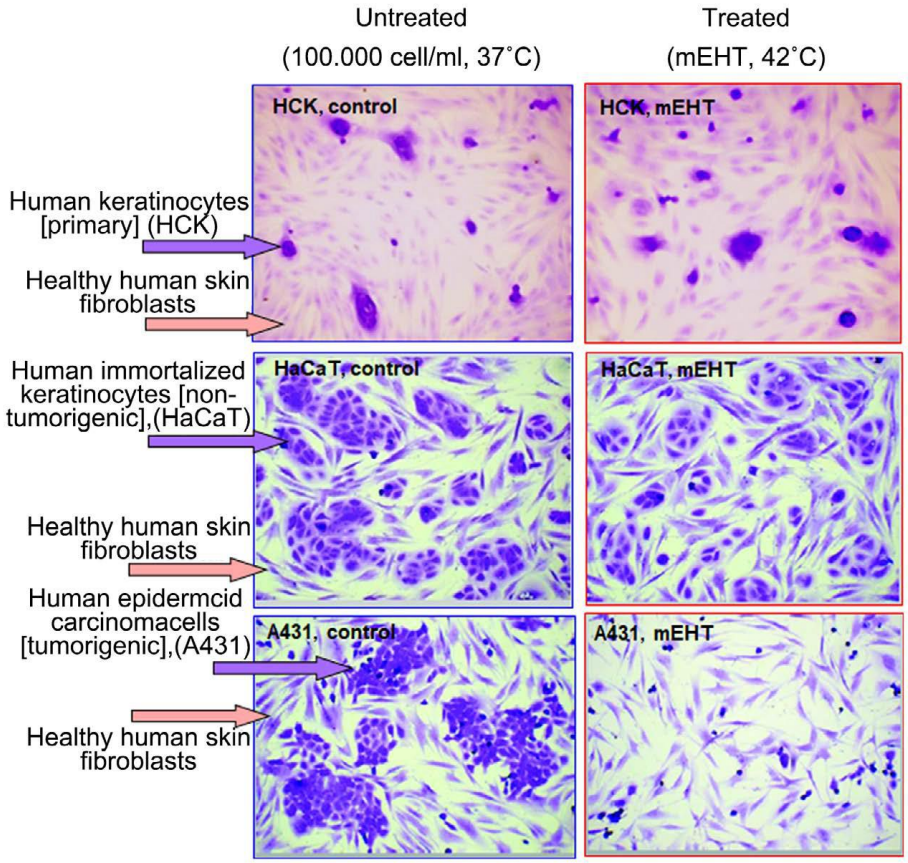

Figure 11. Demonstration of the cellular selection of mEHT treatment (42˚C, 30 min) in co-culture of human fibroblasts and healthy, proliferating but not tumor genetic and aggressively malignant keratinocytes compared to the untreated control.

The thermal effects could be calibrated by in vitro experiments. The reference calibration uses the U937 human lymphoma cell line [87] [88], and the HT29 and A431 [13] cell lines. The effect has given a possibility to make a reference calibration of mEHT compared to wHT on HepG2 cells shown at ~5˚C [77], while in the U937 cell line [88], it shows a > 3˚C shift to the advantage of mEHT over wHT (Figure 12). It is supposed that the difference indicates a 3 + ˚C higher temperature of rafts than of the TME. The gain of tumor destruction at 42˚C is ≈ 4.9 fold. Measurements show the mEHT induces apoptosis targeting the rafts, they have a higher temperature than the average medium indicates, and the temperature of the selected cells (T_{cell}) is well over the average ($T_{cell} >> T_{mEHT}$).

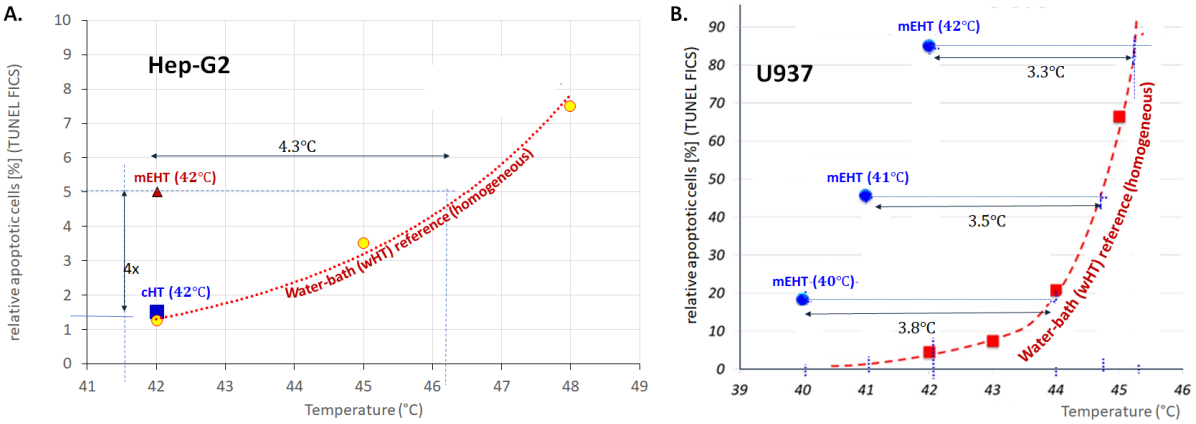

Figure 12. The calibration of the thermal factor by homogeneous conventional wHT. (A.) The wHT calibrates the apoptosis of HepG2 cells by thermal effect (temperature only). The measured mEHT causes effective apoptosis at 42˚C. According to the calibration, this corresponds to the 47˚C in the calibration curve with the same HepG2 cell line [77]. (B.) Another calibration measurement with the U937 cell line. The mEHT shows a > 3˚C temperature difference in apoptotic efficacy at all measured points [88].

Maintaining the temperature compensates for the energy losses, so it needs less dose. The unchanged temperature with lower current density produces significantly less apoptosis as the active heating period raises the temperature [85]; Figure 13. In this way, the apoptotic cellular degradation could be used for dosing during the active heating period. The experiment reveals that the applied power plays a decisive role in the apoptotic processes.

The absorbed power has thermal and nonthermal effects, which we may divide by the high power application but remove the absorbed thermal component by cooling the system. So, the large electric current density (j) makes the nonthermal action effective. Measurements on the U937 cell line prove this concept [95]. The concentration of apoptotic cells grows linearly with the current density j of mEHT; Figure 14. The standard mEHT treatment was performed at 41˚C, with a standard current of 2.8A, as shown in Figure 12(B). The current was increased to 3.8A and 4.5A, while intensive cooling suppressed the temperature of the target to 36˚C. The control is a sham experiment that fits a linear line with larger-than-standard currents. The heat effect of the standard treatment could be approximated from this experiment, which is under 10% of apoptotic cells, as shown in Figure 12(B). wHT treatment. Approximately 36% higher current (1.36 times more current) as standard at 41˚C needs to have the same apoptosis in the cooled sample to 36˚C. This gives a value of ~37% of the absorbed energy being nonthermal. Further, 18.5% more current causes 33% more apoptosis nonthermally. The nonthermal impact on HT29 and SW480 human colorectal cancer cell lines shows a significant change in the ionic fluxes. Also, the mEHT nonthermal effect has doubled the antiproliferative and anticlonogenic activity compared to the purely thermal wHT at the same 42˚C temperature [61].

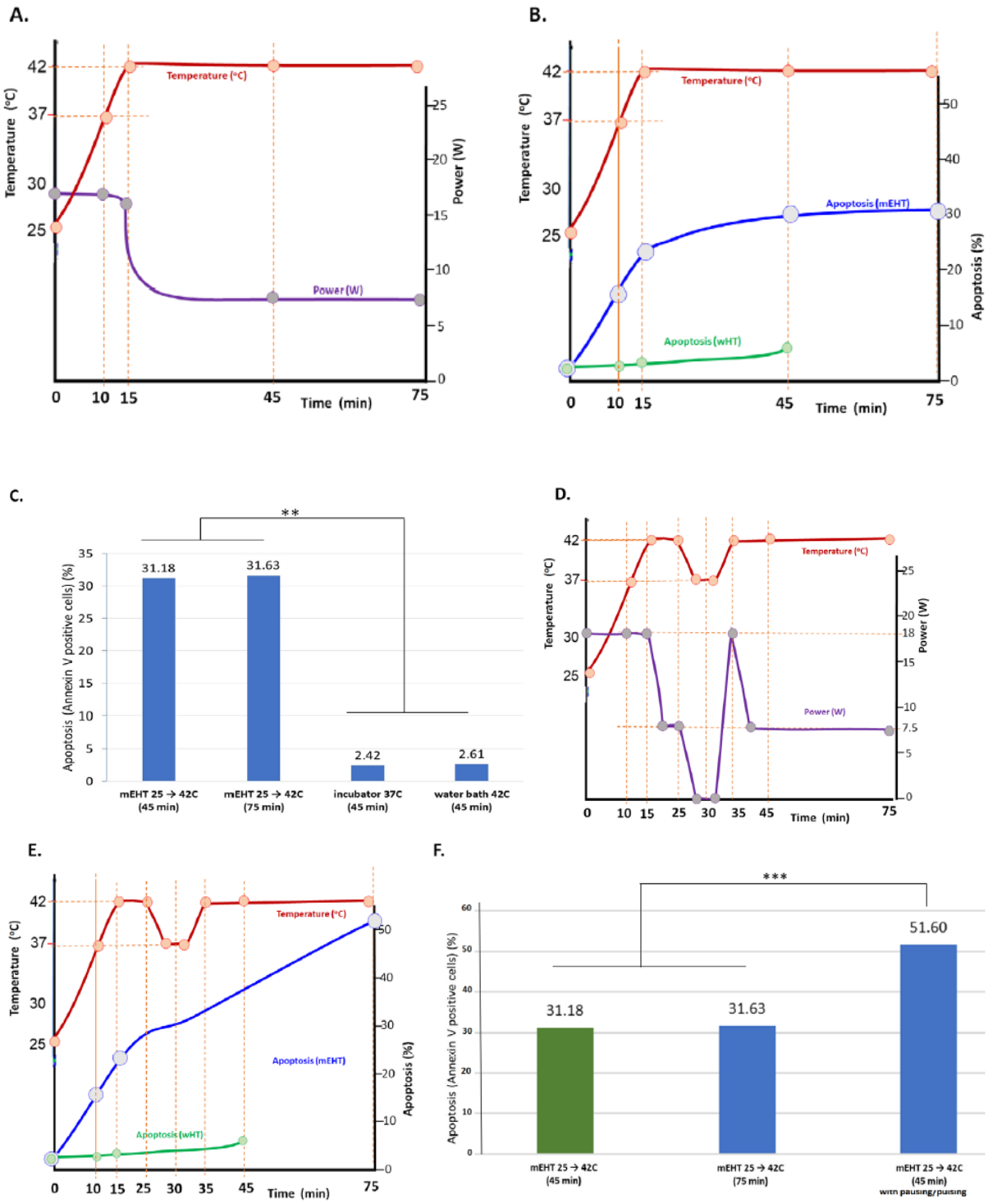

Figure 13. The effect of heating and maintaining the temperature on apoptosis [85]. At the same temperature, the mEHT had significantly more apoptotic cells than the wHT. (A.) The temperature develops over time and with applied power. (B.) The apoptosis saturated when the temperature became constant during the treatment's maintenance period. The apoptosis rate by mEHT is much higher than that of wHT. The slope of temperature rise and the corresponding more extensive power causes most of the apoptotic processes. (C.) The apoptotic cell death is significantly higher with mEHT than with wHT or incubator. (D.) The thermal equilibrium was interrupted by a cooling to 37°C by a power pulsing. (E.) The apoptosis drastically increased by the power pulse. (F.) The pulsed mEHT provides a very significant increase in apoptosis.

The percentage of the apoptosis induced by mEHT grows by increasing current density, which participates in both fundamental processes of this method: in the thermal and nonthermal action components. The thermal effects ensure the conditions for optimal nonterminal (excitation) processes and the rates of chemical reactions (mostly enzymatic assistance) afterward. The current density j appears as an ultimate dose of mEHT, as shown in Figure 14. We may regard the current density as a dose of the treatment, having the same role in mEHT as the ionizing isodose in RT. The qualitative dose equivalence of mEHT with RT defines the harmonizing basis of cellular degradation in two different lung can cer cell lines, A549 and NCI-H1299 [93]. The thermal radiosensitivity parameters were approached by the standard linear-quadratic model. The RT (2 - 8 Gy) + mEHT (42˚C, 30 min) increased the linear factor (α) of A549 and NCI-H1299 cell lines from 0.23 Gy to 0.53 Gy and from 0.24 Gy to 0.51 Gy, respectively, which shows the doubling of radiosensitivity with mEHT addition [93].

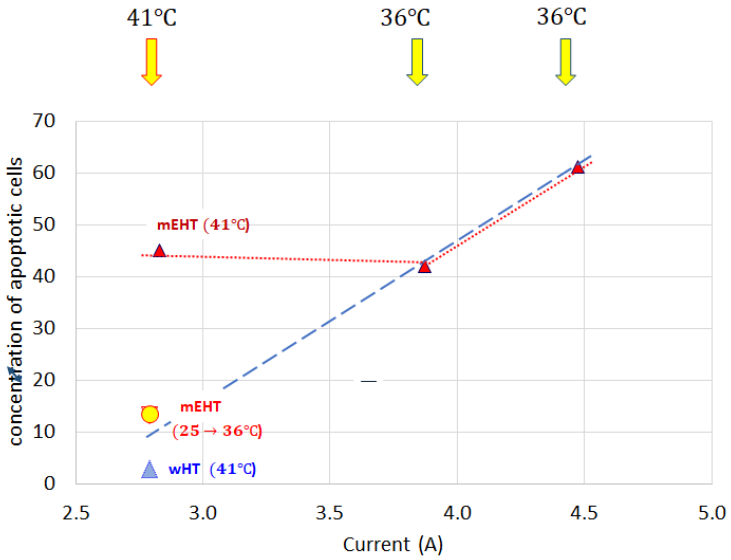

Figure 14. The apoptosis increases with the increase of current density [95]. The higher current density was reached by intensive cooling of the sample, keeping the medium at 36˚C, while the standard treatment was at 41˚C. (A red dotted line connects the measured data points to guide the eye.) The measured control apoptosis at 36˚C fits a line with the cooled higher current on the same 36˚C temperature. The apoptosis produced by wHT is less than the 36˚C control of mEHT. (The values fit to Figure 12(B))

The gold nanoparticles (NPs) are frequently chosen for selective nanoparticle heating with a 13.56 MHz electric field [96]. This selective energy absorption provides a pure thermal effect for NPs, those thermally absorb the energy and heat their environment. Gold NP suspension was added to increase the thermal impact of mEHT [90]. NPs addition significantly reduced the apoptosis of the HepG2 cell line compared to the mEHT stand-alone treatment (Figure 15). The energy-sharing between the membrane rafts and the NPs probably causes this contradictory effect. The phenomenon supports the proof of the nonthermal energy absorption selection by mEHT. Further noteworthy information is that the intracellular NP addition has significantly more apoptosis inhibition, which depends on the disturbance of the apoptotic signal pathways in the cell.

Comparison of the modulated (mEHT) with the unmodulated (EHT) treatments heating the same experiment setup with 10W power gives further clues of the nonthermal impact of mEHT [53] Figure

16. The power deposition of the medium without cells is significantly lower than in the cancer cell treatments, probably due to the cells' selective and intensive energy absorption. 1 million cells were in 1ml (approximately 0.1% of the volume), and the power deposition increased by ~20%, showing the method's high cellular selectivity. The EHT absorbed significantly more rate (~5%) than the mEHT. The rate difference could be due to the nonthermal processes, which use energy but do not increase the temperature. Consequently, we may approximate the nonthermal energy consumption of 5% of the incident power.

Apoptosis changed significantly in all cell lines compared to wHT, but the mEHT differed significantly only in the HT29 cell line in this experiment. The timing of apoptosis measurement is critical because this process requires a longer time. The measurements were done in vitro a short time after treatment when only early apoptosis could be detected.

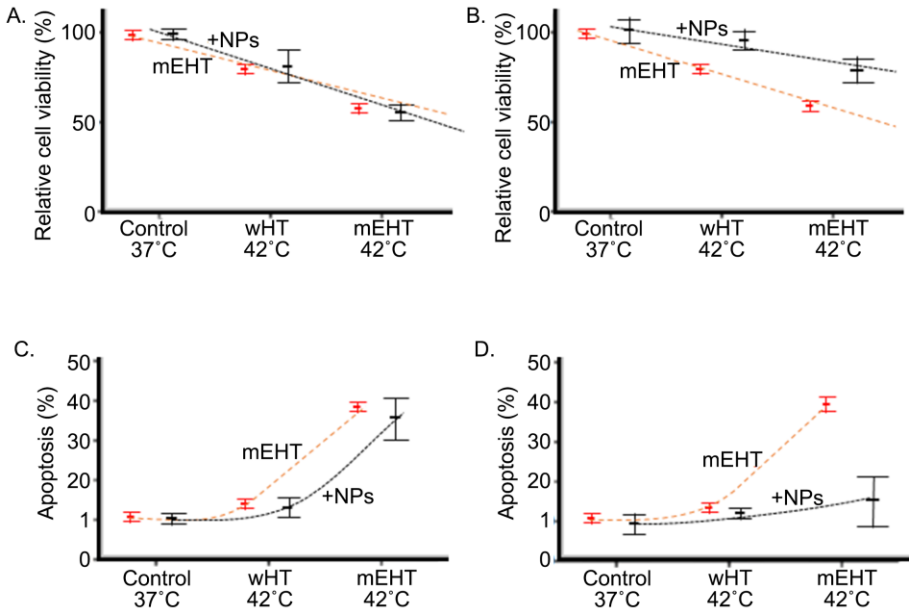

Figure 15. The effect of gold nanoparticles on the wHT and mEHT results at the same 42°C temperature in the HepG2 cell line [90]. The red markers are mEHT stand-alone, and the black ones are the various shapes of NPs. The red dashed and black dotted lines guide the eye, respectively. (A.) The relative cellular viability was measured by MTT assay with extracellular NPs. (B.) The relative cellular viability was measured by MTT assay with intracellular NPs. (C.) The relative apoptosis with extracellular NPs. (D.) The relative apoptosis with intracellular NPs.

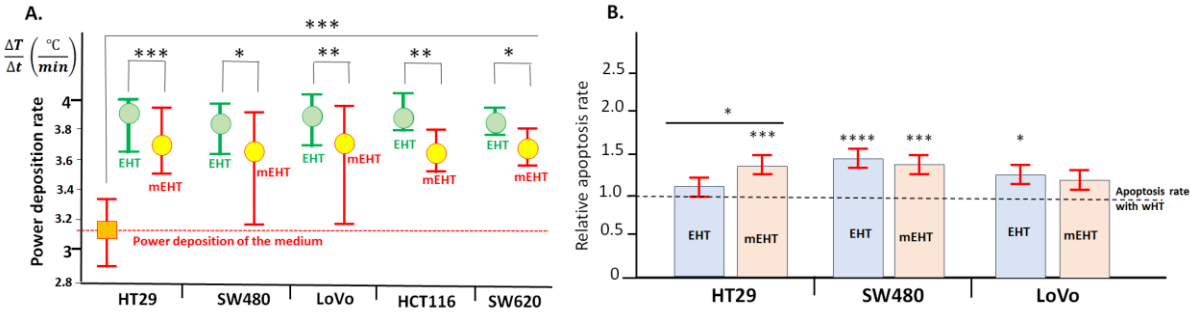

Figure 16. Effect of modulation in vitro for various colorectal cell lines [53]. (A.) The power deposition rate (temperature time derivative) supports the selection and the nonthermal effects.

(B.) the relative apoptotic rate to the control is > 1 in all cell lines. The differences between modulated and nonmodulated treatments are significant only in the HT29 cell line.

The apoptotic rate is significantly higher by mEHT than that caused by wHT. It is a notable observation that the cell distortion does not change significantly between 24 h and 48 h posttreatment measurements, so the direct cell distortion is finished 24 h after the treatment, and the processes turn to such molecular changes, which appear later in the system. Consequently, the standardized experimental protocol used 24 h after treatment investigation with 42°C, 30 min treatment conditions. The comparison of mEHT to wHT and to plane-wave fitted, non-modulated capacitive hyperthermia (cHT) at the same temperature shows significant differences in the cell cycle control after 24 h of the hyperthermia treatments in the HepG2 cell line [77]. Different cell lines showed the dominance of apoptosis of mEHT in comparison with wHT at the same standard treatment conditions Figure 17. mEHT applications focus on induced apoptosis [97] [98].

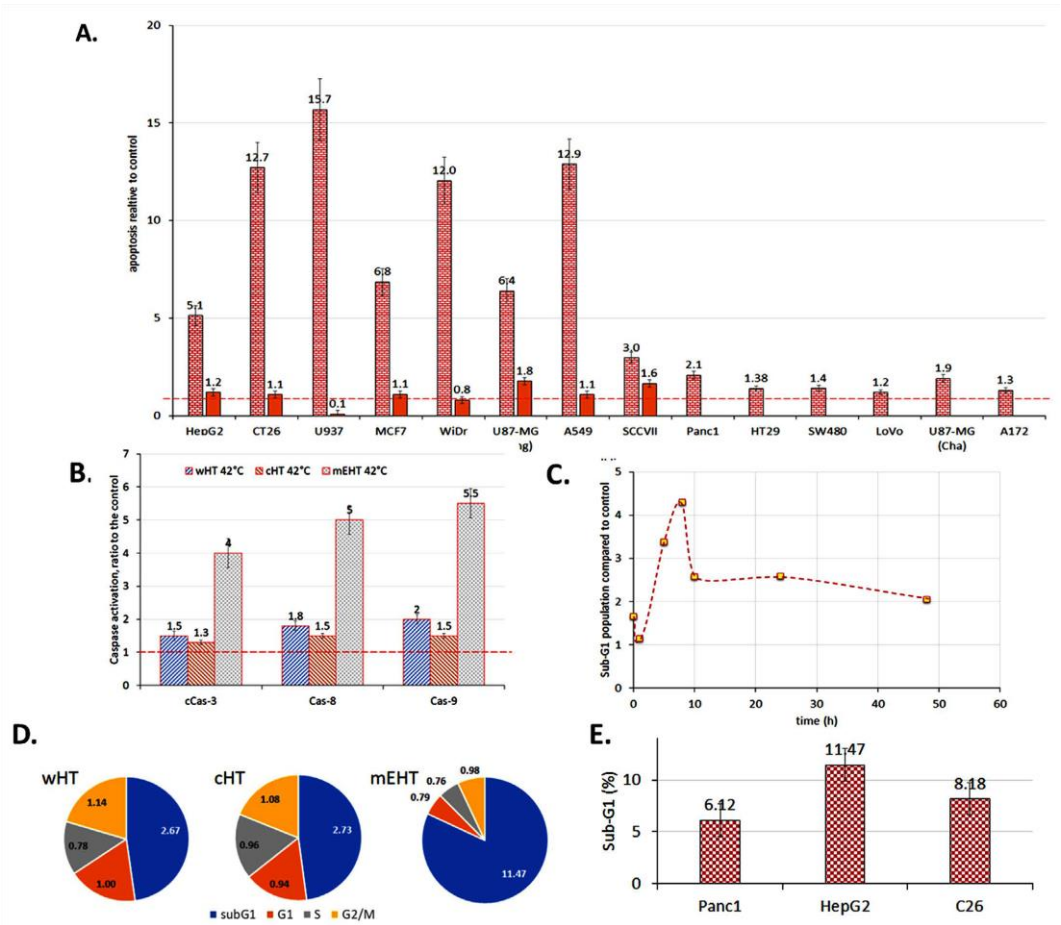

Figure 17. The cell death of various cell lines. (A.) Apoptosis (relative to the control) comparison of wHT and mEHT using the same experimental conditions 42°C 30 min. The results on cell lines were published: HepG2 [77], CT26 [78], U937 [87], MCF7 [77], WiDr [77], U87-MG (Yang) [77], A549 [85], SCCVII [92], Panc1 [81], HT29 [53], SW480 [53], LoVo [53], U87-MG (Cha) [86], A172 [86]. (B.) The cleaved Caspase-3 (cCas-3), the Caspase-8 (Cas-8), and Caspase-9 (Cas-9) show the external and internal pathways of apoptosis and appeared significantly more than in wHT or cHT hyperthermia methods [77]. (C.) The Sub-G1 cell population by time peaks at 8 h where the DNA fragmentation happens in the OVCAR cell line. [79] (D.) The sub-G1 apoptotic character in the cell

cycle is dominant for mEHT treatment [77]. (D.) Comparison of SubG1 measurements Panc1 [81], HepG2 [77], C26 [83]. (E.)

The stand-alone mEHT treatments demonstrate the capability of the method. The experiment proves the superiority of mEHT and presents similarities between wHT and cHT, both of which are devoted to homogeneous mass-heating, while mEHT has heterogeneous selective action. The mEHT method causes caspase-dependent paths through Cas8 (extrinsic way) and Cas9 (mitochondrial, intrinsic way) [77] [99] and independent [100] [101] apoptosis. The detailed molecular investigation shows the apoptosis in mEHT processes Figure 18. Apoptosis regulation-related gene expression at the mRNA level, such as XIAP, BCL-2, and BCL-XL, is suppressed compared to the control. In contrast, the proapoptotic ones (PUMA, BAX, BAK-1) increase, and both groups return to baseline at 9-24 h. A notable factor at the protein level is the arrest of the XIAP effect to block the main path of caspase-dependent apoptosis by the secretion of SMAC/Diabolo [102] and Septin4 [76]. The p21 cyclin- dependent kinase inhibitor also increased compared to the control (Figure 18(C)), and it could promote or inhibit apoptosis. Noteworthy, the p21 could be a primary mediator of the p53 cell cycle arrest; its presence expresses the wild p53 tumor-suppressor, which also had been increased in the mEHT process (Figure 18(D)).

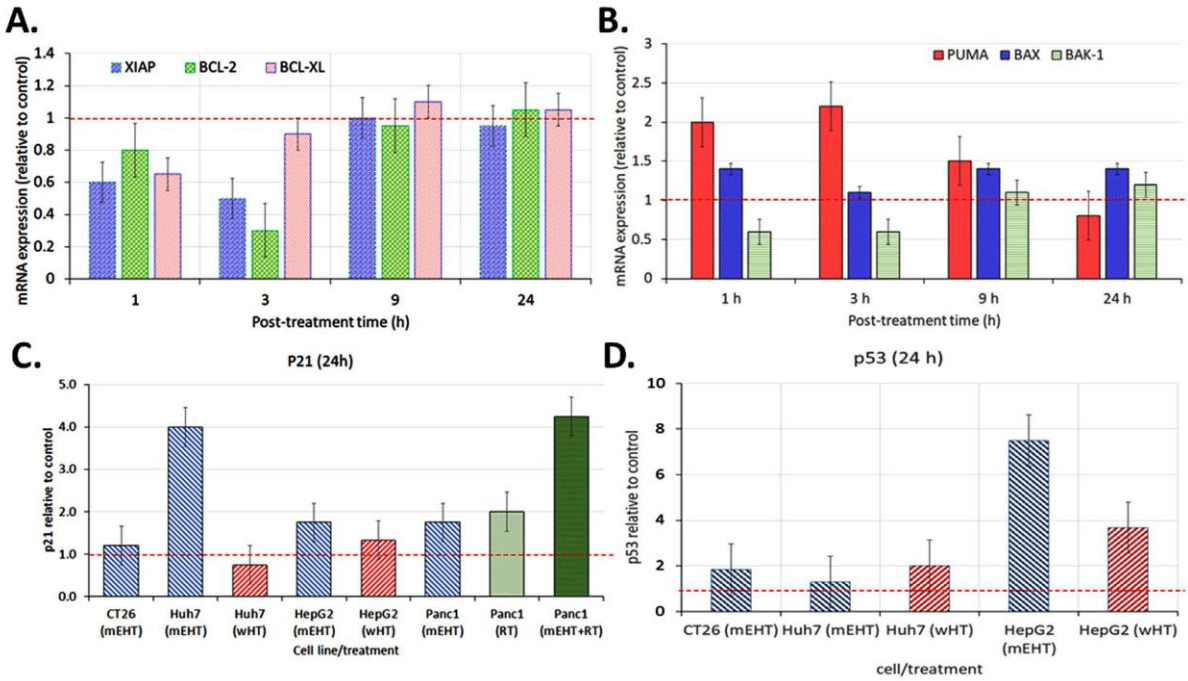

Figure 18. Anti and proapoptotic factors. (A.) Antiapoptotic gene expressions by time development [83]. (B.) Proapoptotic gene expressions by time development [83]. (C.) p21 expression at 24 h posttreatment for different cell lines: CT26 [83], Huh7 [76], HepG2 [76], Panc1 [81]. The wHT, RT, and RT + mEHT experiments are also shown for comparison. (D.) p53 expression at 24 h posttreatment for different cell lines CT26 [83], Huh7 [76], HepG2 [76]. The wHT experiments are also shown for comparison.

The in vitro preclinical complementary treatments also show the superiority of mEHT with add-in complementary applications. mEHT in combination with radiotherapy (RT) significantly improved the apoptotic ratio compared with wHT combined with RT [92] (Figure 19(A)). There was also a substantial increase in autophagy with the mEHT combinations Figure 19(B). Autophagy can act as

a defense mechanism to prevent apoptosis by self-cleaning or recycling the process of reusing cellular components. The mEHT-increased temperature raises the apoptosis/autophagy ratio, which proves that autophagy does not block the apoptotic processes, and excessive autophagy also leads to cell death. (Figure 19(C)). Cell cycle arrest of malignant cells has been demonstrated in the aggressively radioresistant cell line (L9), which mEHT + RT could resensitize [80], and also in complementary mEHT + RT treatment of radio-resistive Panc1 cell line [81] (Figure 19(D)). Caspase-involved extrinsic and intrinsic apoptotic signal pathways accompany the resensitizing [81] [92], (Figure 19(E)). The apoptosis in the function of the phosphorylated H2AX (γH2AX) serves as a marker of DNA damage, and repair shows peculiarity in the radioresistant Panc1 cell line. The mEHT with the same γH2AX RT causes more apoptosis than RT, indicating the possibility of different apoptotic pathways. Still, RT damages the DNA strands; mEHT affects apoptotic pathways of the cell, having fewer DNA breaks in the process but more apoptotic outcomes because this death form does not depend on the DNA repair enzymes. Furthermore, the combined mEHT + RT treatment has a significantly higher γH2AX, indicating aggressive DNA damage in the apoptotic process. Although the apoptosis was not increased, this observation suggests rapid DNA restoration by repairing enzyme activities due to the temperature-risen reaction rate in the Panc1 radio-resistive cell line (Figure 19(F)). Noteworthy, mEHT also destroys the tumor stem cells in pancreatic adenoma-carcinoma cell lines (Panc1 and Capan) [97], as well as dramatically reduced cancer stem cells (CD133+) population in glioma cell lines (U87-MG and A172) after mEHT treatment [86].

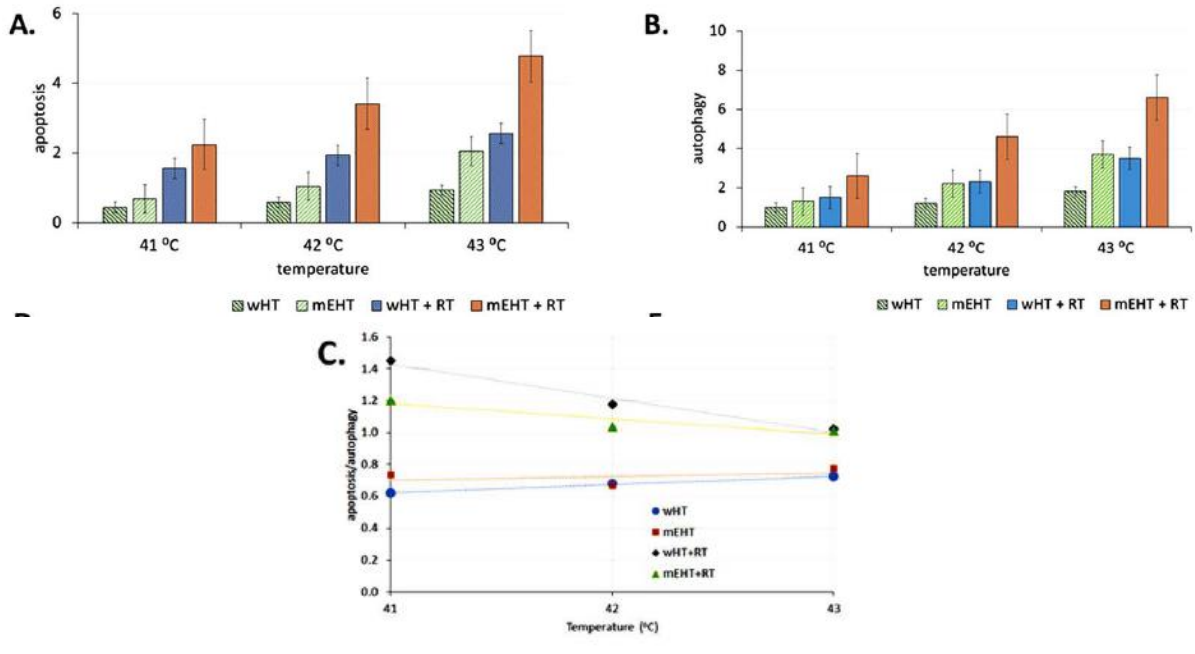

D.

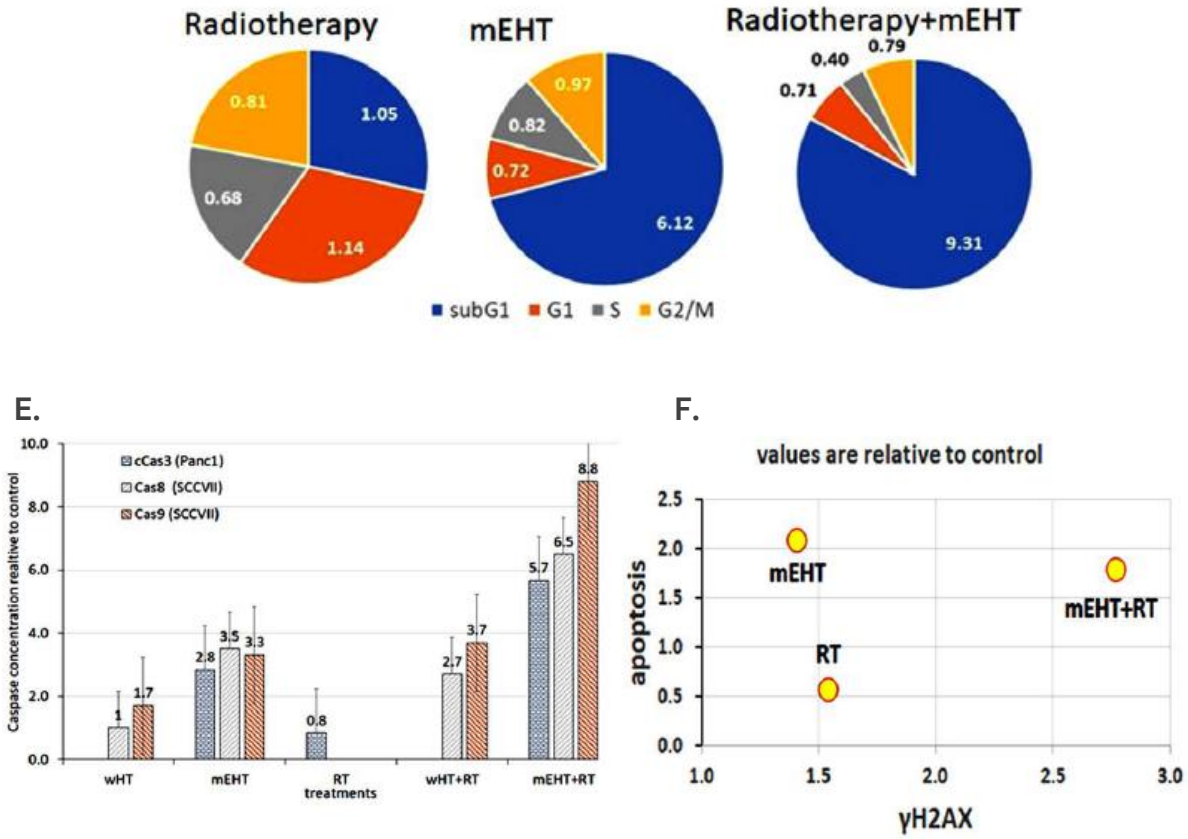

Figure 19. Various experiments of RT + mEHT combined therapy. (A.) Apoptosis in different temperatures with various treatments [92]. (B.) Autophagy in different temperatures with the various treatments [92]. (C.) Apoptosis and autophagy ratio. (D.) Effect on cell cycle of the therapies [81]. (E.) Caspase concentration relative to control Panc1 cell line [81], SCCVII cell line [92]. (F.) apoptosis dependence on γH2AX expressions [81].

Complementary applications with chemotherapy also have advantages observed in vitro. The mEHT highly promotes the intake of liposomal doxorubicin (Lipodox), together with an effective decrease of cellular viability in mEHT + Lipodox combined therapy in various cell lines (Figure 20(A) [89]. The doxorubicin damages DNA and interferes with DNA replication. MEHT improves the release of doxorubicin compared to the same temperature wHT treatment Figure 20(B). Effective cell cycle arrest was observed in the C26 cell line in a combined mEHT + Lipodox combination [83] Figure 20(C), but mEHT dominates the apoptosis indicated by subG1 quantity.

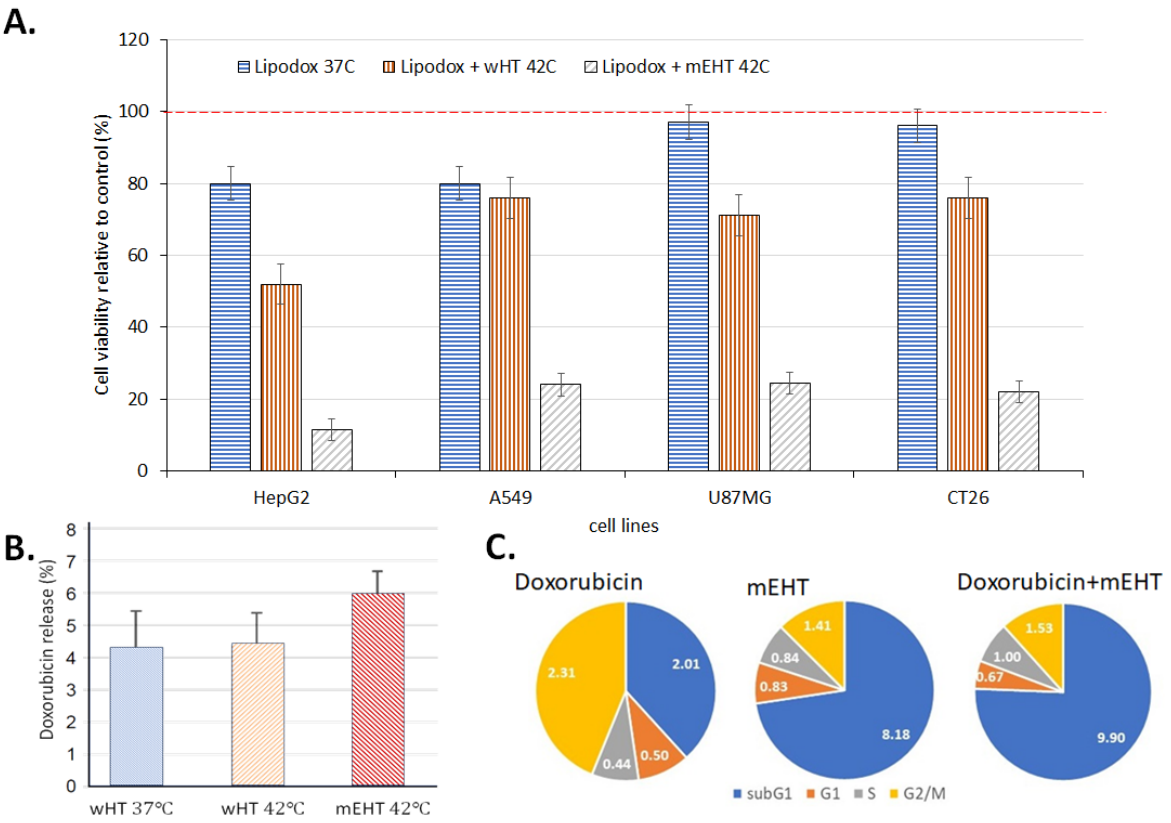

Figure 20. Complementary application of mEHT with liposomal doxorubicin (Lipodox). (A.) Cell viability for different cell lines [89]. The addition of mEHT significantly improved all cases. (B.) The doxorubicin release of Lipodox in a medium heated by wHT and mEHT [89]. (C.) The cell cycle changes by mEHT application [83].

Electrical stimuli increase the penetration of drugs like doxorubicin, and the nonthermal processes could bypass the multidrug resistance [103] in vitro. Further proof supports the theoretically established molecular models concentrating on the synergic thermal and nonthermal membrane effects. One obvious process of the thermal and nonthermal processes is loading the system with various stresses, inducing systemic and cellular reactions.

The addition of the nonthermal effect to the conventional thermal one significantly modifies the gene expression of the U937 cell line in comparison to wHT and mEHT samples [87] Figure 21. The strong upregulations are in the stress protein genes and their connected processes.

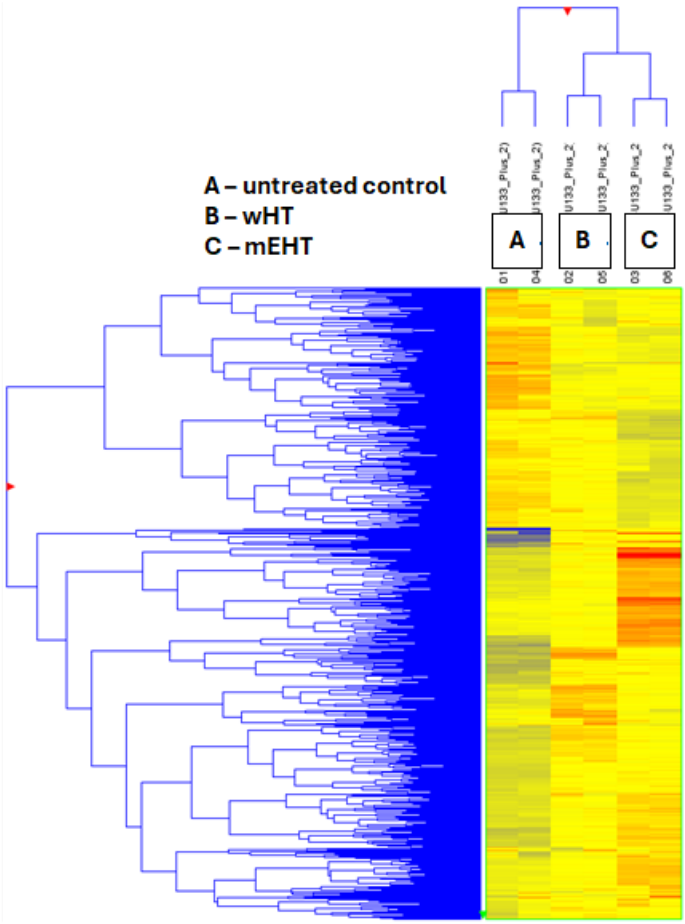

Figure 21. Gene comparison of the control, wHT, and mEHT-treated cell lines. The significant differences show the impact of the nonthermal effects.

The system develops stress- (or heat-shock) proteins (HSPs). HSPs are molecular chaperones playing a role in protein maturation or degradation. HSPs can refold and repair the stress-damaged unfolded proteins or inhibit their denaturation in response to stress. The function of HSPs is not limited to the protection on a cellular basis. They have a role in protecting multicellular structures and may even participate in systemic processes in the organism. Their intracellular chaperoning maintains the balance between the intracellular proteins. HSPs regulate apoptosis and protect the cells from mechanical, chemical, thermal, or electromagnetic stressors. However, it has multifaceted behavior as most actors in the complex living system could promote or inhibit inflammation, tumoral growth, and immune processes. The gene chip heat map and ingenuity pathway analysis (IPA) on the U937 human lymphoma cell line (Figure 22 [87]) revealed some activated stress responses differentiating wHT and mEHT processes. Notably, the cytoprotective functions of the thermal impact (wHT) show strong activation of HSP70, HSP90, and BAG3 genes. The cytoprotective action of HSPs and proliferation promoter BAG3 could play a role in the resistance to heat therapy and support the further development of tumors. The activated HSPs arrest apoptosis by interfering with caspase activation, directly inhibiting apoptosis and indirectly blocking tumor distortion. The effect of mEHT is different. There is no such massive upregulation of HSPs as in wHT, and the BAG3 is downre gulated, allowing the apoptotic processes. According to the HSP protein measurements, the HSPs linearly develop after the heat treatment for days, demonstrating the intensive continuous processes after the treatment. The slope of HSP development grows approximately twofold higher with mEHT than with wHT at the same

temperature, indicating the difference in the posttreatment processes caused by the pure thermal and synergic thermal nonthermal impact.

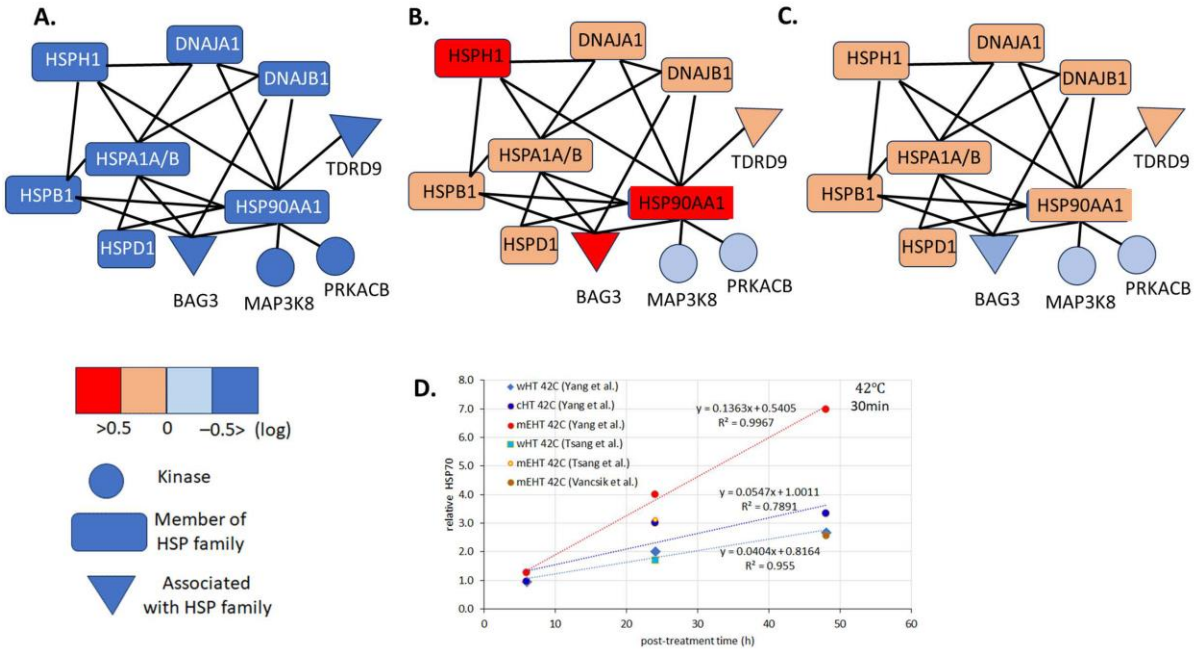

Figure 22. The IPA analysis of gene chip heat map [87]. A specific cytoprotective gene network (heat shock proteins, HSPs) was activated in the case of wHT treatment but not in mEHT-treated samples. (A.) Unheated control, (B.) wHT result. (C.) mEHT result. (D.) Increase of HSPs by posttreatment time [77] [83].

The metabolic profiles of the targeted malignant cells have elevated glycolysis [104]. The efficacy of mEHT may correlate with the tumor metabolic profile by the targeted selection [105]. Different molecules majorly involved in the mEHT processes were measured as having a key influence on the cancer cells' fate by mEHT Figure 23. The reactive oxygen species (ROS) are more than doubled compared to the same temperature wHT and cHT [77] Figure 23(A). The calreticulin (CRT) is also significantly increased by mEHT Figure 23(B). Despite the simple thermal effect (wHT and cHT treatments) not showing such improvement. Noteworthy is that the plane wave capacitive coupling (cHT) method works like wHT in ROS level and CRT, which shows its thermal dominance in homogenous thermal heating, while on the contrary, selecting nonthermal processes massively increases the ROS and CRT products. This proves the nonthermal effects of mEHT on the U937 cell line well. The mRNA changes for inflammatory chemokines CXCL9,10,11 and matrix metalloproteinase (MMP-2) in A2058 melanoma cell lines [108] Figure 23(C), Figure 23(D). also supports the advantages of mEHT. The chemokines bind to a specific receptor called CXCR3 on immune cells, particularly T cells, attracting them to the tumor site and potentially promoting an immune response against the cancer. However, suppressing CXCL9, 10 while increasing CXCL11 could support tumor progress. The increase in MMP-2 signifies a growth in the activity of an enzyme that breaks down components of the extracellular matrix (ECM), a double-edged sword that promotes or blocks promote or block cancer growth. The mEHT lowers the mitochondrial membrane potential in approximately a quarter of malignant cells. At the same time, the wHT (only thermal process, changes only a tiny fraction of cells Figure 23(E), which could be connected to

the increased ROS level and promotes the cytochrome c (Cyt-c) secretion, a point of nonreturn of apoptosis, may compensate well for the opposite effect of inflammatory cytokines and MMP-2. The decreased membrane potential of mitochondria [87] well supports the mitochondria-associated apoptotic process. The mEHT induces the Ca2+ influx with the assistance of E2F1 [86], which regulates the HSPs without heat shock [106], supporting the possible factors of the nonthermal effect of applied electric current. The five-fold increase in the Ca2+ positive cells relative to the same temperature wHT Figure 23(F). strongly supports the high impact of nonthermal processes. The Ca2+ acts as a second messenger inside cells. Depending on its concentration and location within the cell, it triggers various cellular responses. Its massive and sustained influx can contribute to cell death and promote apoptosis in the mitochondria-dependent intrinsic signal pathways. The wHT represented thermal impact also forces the increase of the Ca^{2+} ion concentration in the cell, but mainly from the internal sources, processes in the cytosol ER and other cellular organelles, and some influx by the heat-sensitive transient receptor potential vanilloid receptor (TRPV), which also senses the same temperature for action.

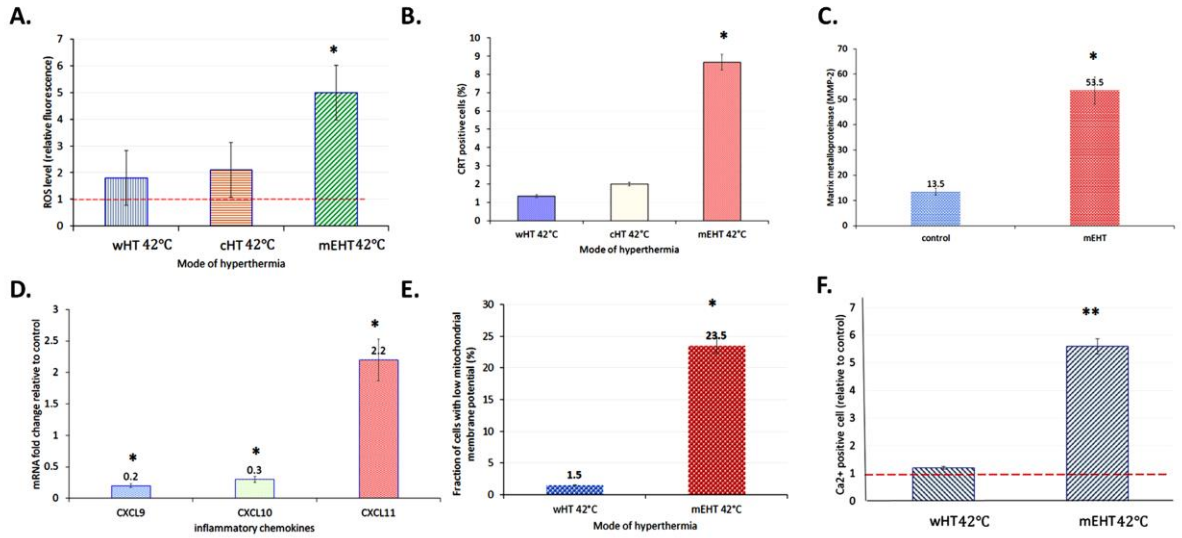

Figure 23. Involvement of various molecules is measured 24 h posttreatment of mEHT. (A.) ROS level, HepG2 cell line [77]. (B.) Development of inflammatory chemokines A2058 cell line [108]. (C.) MMP-2 development A2058 cell line [108]. (D.) The calreticulin expression HepG2 cell line [77]. (E.) The fraction of cells with lowered mitochondrial membrane potential U937 cell line [87]. (F.) The mEHT significantly triggers the Ca2+ influx, while only thermal processes make minor changes, U937 cell line [87].

The only thermal effects (wHT) induce only a minor influx, but the synergy of thermal and nonthermal processes massively causes a significant Ca2+ influx to malignant cells. The temperature affected the internal. Ca2+ release can not be the origin of such considerable ion concentration because the temperature did not change. Noteworthy nonthermal effects cause the reconstruction of the intercellular E-cadherin/$\beta\beta$-catenin connection, allowing the regular networking of the cells [77] [75] [107] which may be a factor in the inhibition of the proliferative activity of the tumor.

Detailed molecular analysis of the U937 cell line with western blot (WB) [87], [95] shows the FAS starting external apoptotic path through cCas-8, which signal had pointed expression

enhancement from 1 h to 3 h after mEHT treatment. In contrast, the wHT-treated cell line did not show a similar effect. The FAS, p-JNK N-terminal kinases (JNK), and p-ERK signaling pathways dominate the apoptotic pathway, also developing markedly for 1 h to 3 h posttreatment in mEHT but not in wHT, well demonstrating the synergic nonthermal component to the pure thermal delivery by wHT. The ingenuity pathway study shows these remarkable differences in Figure 24. The significant difference between the only thermal wHT and a nonthermal addition with mEHT also determines these results. Contrary to the temperatures in both heating methods being the same, the observed difference in pathway activations is likely primarily due to the electric field effects [87]. The IPA demonstrated a specific gene network containing cell death-related genes, such as EGR1, JUN, and CDKN1A.

The expression levels of these genes were elevated only in the cells treated with mEHT. However, complex networking must explain how various double-faced molecular actions can become proapoptotic activity. The CDKN1A gene (coding p21 protein), a critical cell cycle regulator, plays a critical role in cell cycle control and DNA repair. It is a crucial tumor suppressor gene and has a central role in that part of IPA (Figure 24(C)). Its high upregulation is observed only in the mEHT process despite the same thermal effect in wHT treatment.

The further remarkably upregulated genes, the EGR1, JUN, TNF, and SMAD, all have multifaceted behavior. The importance of the extracellular processes is that the ERK gene (extracellular signal-regulated gene) is highly expressed and activates CDKN1A, TNF, JUN, EGR1 IER3, and MAFF (Figure 24(F)), which are actively upregulated in death-related genes (Figure 24(C)). With their multifaceted behavior, the main processes that could actively help the tumor death are various. TNF can directly kill cancer cells but also may promote tumor metastasis. TNF superfamily contains the TRIAL receptors, which are excited by nonthermal mEHT impact [17], [14].

Despite its complex role, TNF may be an immunostimulant for certain cancers. The ERK (Extracellular signal-regulated Kinase) is another player with a double-edged sword role in cancer. When the ERK pathway is abnormally activated, it can lead to uncontrolled cell growth. Still, the very high levels of ERK activity can also trigger cell death or senescence, potentially acting as a tumor suppressor. In some cancers, EGR-1 acts as a tumor suppressor, but it may have the opposite effect, promoting tumor growth. JUN protein also plays a complex role in cancer, with the potential to both promote and suppress tumors depending on the context. Its overexpression can contribute to uncontrolled cell growth but can also have antitumor activity; it might trigger cell death (apoptosis).

The IPA-involved SKIL, IER3, MAFF, SMAD, and HBEGF molecules are also a double-edged sword. Still, commonly, they may promote extracellular rearrangements, which may help the metastases or cell apoptosis. The mEHT turns these complex processes to the positive side, assisting the apoptosis and tumor degradation.

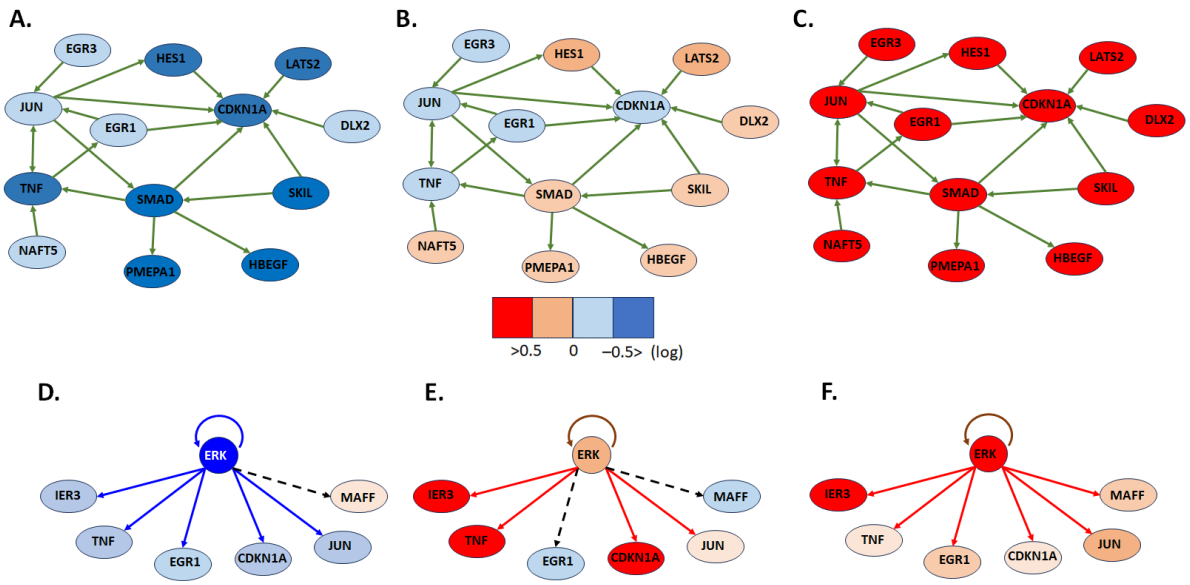

Figure 24. The gene maps and IPA analysis show significant differences in the gene regulation between wHT and mEHT-treated U937 cell lines at the same 42°C [87]. (The edge (form) lebels of molecules are not shown.) (A.) and (D.) controls are 37°C (B.) and (E.) the wHT and (C.) and (F.) the mEHT results. Both maps show the upregulation of the CDKN1A and ERK pathways from wHT to mEHT.

Another investigation [86] reveals the number of mRNA transcripts up- or down-regulated in U87-MG or A172 cells after mEHT treatment. The majority of the extra up and downregulated genes differ by U87-MG and A172 cell lines, but 19 and 15 up and down-regulation overlapped, respectively [86].

6. Conclusion

The thermal and nonthermal differences clearly appear in the comparative studies of only thermal water bath hyperthermia (wHT), and electrothermal (mEHT) experiments, shown in Figures 12-24. The advantage of the combined thermal and nonthermal treatment is proven. The thermal conditional basis works similarly to ionizing radiation combination, when combined with the nonthermal electric field. The in vitro experiments (Figure 25) verified the in silico calculations and the proofs of the concept using phantoms of modulated electro-hyperthermia. The robust apoptosis of the malignant cells is shown on very different cell lines, such as mEHT, which is significantly far ahead of the pure thermal effects of water bath treatment. These observations significantly impact nonthermal processes and may open new ways to evaluate the effect of hyperthermia with nonionizing radiations. In this frame, ionizing radiation (radiotherapy, RT) and nonionizing hyperthermic oncology could be united, considering the molecular effects of RT on DNA strands, in principle is the same nano-selection as the mEHT impacts on the nanoscopic localization transmembrane proteins. While the RT is focused on the break of chemical bonds, and the thermal effects have only a tiny portion of the energy absorption, in nonionizing hyperthermia, the thermal effects boost the nonthermal molecular actions.

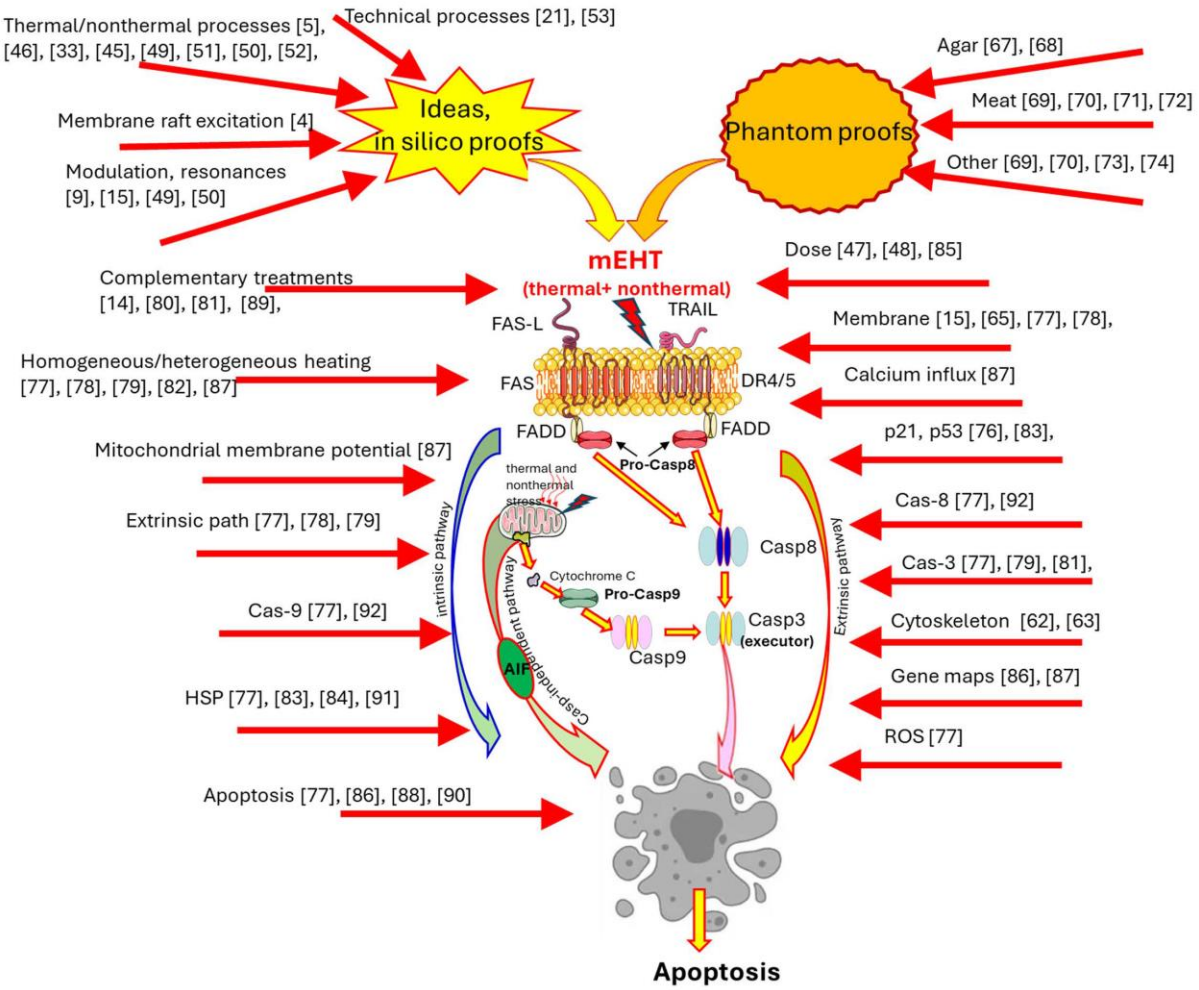

Figure 25. The structure of publications is discussed in this paper.

The following parts of this series will show the in vivo preclinical results, which strongly verify the above conclusion, and the clinical studies finally validate the mEHT concept.

Acknowledgments

I am thankful to the listed authors for their diligent research.

Fund

This research received external funding from the Hungarian Government, grant number GINOP_PLUSZ_2.1.1-21-2022-00058.

Conflicts of Interest

The author declares no conflicts of interest regarding the publication of this paper.

References

[1] Szasz, A. (2019) Thermal and Nonthermal Effects of Radiofrequency on Living State and Applications as an Adjuvant with Radiation Therapy. Journal of Radiation and Cancer Research, 10, 1-17. https://doi.org/10.4103/jrcr.jrcr_25_18

[2] Szasz, A.M., Lorant, G., Szasz, A. and Szigeti, G. (2023) The Immunogenic Connection of Thermal and Nonthermal Molecular Effects in Modulated Electro-Hyperthermia. Open Journal of Biophysics, 13, 103-142. https://doi.org/10.4236/ojbiphy.2023.134007

[3] Szasz, A. (2022) Heterogeneous Heat Absorption Is Complementary to Radiotherapy. Cancers , 14, Article 901. https://doi.org/10.3390/cancers14040901

[4] Papp, E., Vancsik, T., Kiss, E. and Szasz, O. (2017) Energy Absorption by the Membrane Rafts in the Modulated Electro-Hyperthermia (mEHT). Open Journal of Biophysics, 7, 216-229. https://doi.org/10.4236/ojbiphy.2017.74016

[5] Szasz, A., Vincze, G., Szasz, O. and Szasz, N. (2003) An Energy Analysis of Extracellular Hyperthermia. Electromagnetic Biology and Medicine , 22, 103-115. https://doi.org/10.1081/jbc-120024620

[6] Szasz, O. (2014) Oncothermia—Nano-Heating Paradigm. Journal of Cancer Science & Therapy, 6, 117-121. https://doi.org/10.4172/1948-5956.1000259

[7] Vincze, G., Szigeti, G.P., Andocs, G. and Szasz, A. (2015) Nanoheating without Artificial Nanoparticles. Biology and Medicine , 7, Article 249.

[8] Szasz, A. (2013) Electromagnetic Effects in Nanoscale Range. In: Shimizu, T. and Kondo, T., Eds., Cellular Response to Physical Stress and Therapeutic Applications , Nova Science Publishers, Inc., 55-81.

[9] Szasz, A. (2021) Therapeutic Basis of Electromagnetic Resonances and Signal-Modulation. Open Journal of Biophysics, 11, 314-350. https://doi.org/10.4236/ojbiphy.2021.113011

[10] Nielsen, O.S., Horsman, M. and Overgaard, J. (2001) A Future for Hyperthermia in Cancer Treatment? European Journal of Cancer , 37, 1587-1589. https://doi.org/10.1016/s0959-8049(01)00193-9

[11] Osinsky, S., Ganul, V., Protsyk, V., Knyazeva, O., Pivnjuk, V., Olijnichenko, G. and Olijnichenko, P. (2004) Local and Regional Hyperthermia in Combined Treatment of Malignant Tumors: 20 Years Experience in Ukraine. The Kadota Fund International Forum 2004, Awaji, 15-18 June 2004.

[12] Wust, P., Nadobny, J., Zschaeck, S. and Ghadjar, P. (2020) Physics of Hyperthermia— Is Physics Really against Us? In: Szasz, A., Ed., Challenges and Solutions of Oncological Hyperthermia , Cambridge Scholars, 346-376. https://www.cambridgescholars.com/product/978-1-5275-4817-6

[13] Ferenczy, G.L. and Szasz, A. (2020) Technical Challenges and Proposals in Oncological Hyperthermia. In: Szasz, A., Ed., Challenges and Solutions of Oncological Hyperthermia , Cambridge Scholars, 72-90. https://www.cambridgescholars.com/product/978-1-5275-4817-6

[14] Lee, S. and Szasz, A. (2022) Immunogenic Effect of Modulated Electro-Hyperthermia (mEHT) in Solid Tumors. In: Rezaei, N., Ed., Interdisciplinary Cancer Research, Springer International Publishing, 1-28. https://doi.org/10.1007/16833_2022_74

[15] Szasz, A. and Szasz, O. (2020) Time-Fractal Modulation of Modulated Electro- Hyperthermia (mEHT). In: Szasz, A., Ed., Challenges and Solutions of Oncological Hyperthermia , Cambridge Scholars, 377-415. https://www.cambridgescholars.com/product/978-1-5275-4817-6

[16] Szasz, A. (2022) Time-Fractal Modulation—Possible Modulation Effects in Human Therapy. Open Journal of Biophysics , 12, 38-87. https://doi.org/10.4236/ojbiphy.2022.121003

[17] Krenacs, T., Meggyeshazi, N., Forika, G., Kiss, E., Hamar, P., Szekely, T., et al . (2020) Modulated Electro-Hyperthermia-Induced Tumor Damage Mechanisms Revealed in Cancer Models. International Journal of Molecular Sciences , 21, Article 6270. https://doi.org/10.3390/ijms21176270

[18] Szasz, A. (2015) Bioelectromagnetic Paradigm of Cancer Treatment Oncothermia. In: Rosch, P.J., Ed., Bioelectromagnetic and Subtle Energy Medicine , CRC Press, 323-336.

[19] Szasz, O. (2019) Bioelectromagnetic Paradigm of Cancer Treatment—Modulated Electro-Hyperthermia (mEHT). Open Journal of Biophysics , 9, 98-109. https://doi.org/10.4236/ojbiphy.2019.92008

[20] RECOMMENDATION ITU-R SM.1056-1. Limitation of Radiation from Industrial, Scientific and Medical (ISM) Equipment. https://www.itu.int/dms_pubrec/itu-r/rec/sm/R-REC-SM.1056-1-200704-I!!PDF-E.pdf

[21] Szasz, A. (2021) The Capacitive Coupling Modalities for Oncological Hyperthermia. Open Journal of Biophysics , 11, 252-313. https://doi.org/10.4236/ojbiphy.2021.113010

[22] Szasz, O., Szasz, M.A., Minnaar, C. and Szasz, A. (2017) Heating Preciosity—Trends in Modern Oncological Hyperthermia. Open Journal of Biophysics , 7, 116-144. https://doi.org/10.4236/ojbiphy.2017.73010

[23] Yeo, S. (2015) Definitive Radiotherapy with Concurrent Oncothermia for Stage IIIB Non-Small-Cell Lung Cancer: A Case Report. Experimental and Therapeutic Medicine, 10, 769-772. https://doi.org/10.3892/etm.2015.2567

[24] Chi, M., Mehta, M.P., Yang, K., Lai, H., Lin, Y., Ko, H., et al . (2020) Putative Abscopal Effect in Three Patients Treated by Combined Radiotherapy and Modulated Electrohyperthermia. Frontiers in Oncology, 10, Article 254. https://doi.org/10.3389/fonc.2020.00254

[25] Fiorentini, G., Sarti, D., Mambrini, A., Hammarberg Ferri, I., Bonucci, M., Sciacca, P.G., et al . (2023) Hyperthermia Combined with Chemotherapy vs Chemotherapy in Patients with Advanced Pancreatic Cancer: A Multicenter Retrospective Observational Comparative Study. World Journal of Clinical Oncology , 14, 215-226. https://doi.org/10.5306/wjco.v14.i6.215

[26] Lee, S.Y., Lee, D.H. and Cho, D. (2023) Modulated Electrohyperthermia in Locally Advanced Cervical Cancer: Results of an Observational Study of 95 Patients. Medicine , 102, e32727. https://doi.org/10.1097/md.0000000000032727

[27] Oncotherm Kft (2006) Hyperthermia Device for the Selective Treatment and Monitoring of Surface Tissue. EP 2174689 A1 (Europe).

[28] Deering, W. and West, B.J. (1992) Fractal Physiology. IEEE Engineering in Medicine and Biology Magazine , 11, 40-46. https://doi.org/10.1109/51.139035

[29] Bassingthwaighte, J.B., Leibovitch, L.S. and West, B.J. (1994) Fractal Physiology. Oxford University Press. https://doi.org/10.1007/978-1-4614-7572-9

[30] Astumian, R.D., Weaver, J.C. and Adair, R.K. (1995) Rectification and Signal Averaging of Weak Electric Fields by Biological Cells. Proceedings of the National Academy of Sciences , 92, 3740-3743. https://doi.org/10.1073/pnas.92.9.3740

[31] Sabah, N.H. (2000) Rectification in Biological Membranes. IEEE Engineering in Medicine and Biology Magazine , 19, 106-113. https://doi.org/10.1109/51.816251

[32] Granted Patents: CN 104640601 B, China (2016); EP 2888003 A1, Europe (2016); 10-1714280, South Korea (2017); 6127142, Japan (2017); 2626899, Russia (2017); US9,937,357 B2, USA (2018).

[33] Wust, P., Stein, U. and Ghadjar, P. (2021) Non-Thermal Membrane Effects of Electromagnetic Fields and Therapeutic Applications in Oncology. International Journal of Hyperthermia , 38, 715-731. https://doi.org/10.1080/02656736.2021.1914354

[34] Wissler, E.H. (1998) Pennes' 1948 Paper Revisited. Journal of Applied Physiology , 85, 35-41. https://doi.org/10.1152/jappl.1998.85.1.35

[35] Ostadhossein, R. and Hoseinzadeh, S. (2022) The Solution of Pennes' Bio-Heat Equation with a Convection Term and Nonlinear Specific Heat Capacity Using Adomian Decomposition. Journal of Thermal Analysis and Calorimetry , 147, 12739-12747. https://doi.org/10.1007/s10973-022-11445-x

[36] Cloutier, M. and Wang, E. (2011) Dynamic Modeling and Analysis of Cancer Cellular Network Motifs. Integrative Biology, 3, 724-732. https://doi.org/10.1039/c0ib00145g

[37] Hernandez-Nunez, L., Chen, A., Budelli, G., Berck, M.E., Richter, V., Rist, A., et al . (2021) Synchronous and Opponent Thermosensors Use Flexible Cross-Inhibition to Orchestrate Thermal Homeostasis. Science Advances , 7, eabg6707. https://doi.org/10.1126/sciadv.abg6707

[38] Mathur-De Vre, R. (1984) Biomedical Implications of the Relaxation Behaviour of Water Related to NMR Imaging. The British Journal of Radiology , 57, 955-976. https://doi.org/10.1259/0007-1285-57-683-955

[39] Benson, H. (1983) The Relaxation Response: Its Subjective and Objective Historical Precedents and Physiology. Trends in Neurosciences , 6, 281-284. https://doi.org/10.1016/0166-2236(83)90120-0

[40] Li, X., Sun, S., Yao, J. and Sun, Z. (2020) Using Relaxation Time to Characterize Biological Effects of Different Mutagens. Scientific Reports , 10, Article No. 13941. https://doi.org/10.1038/s41598-020-70600-2

[41] West, B.J. (1990) Fractal Physiology and Chaos in Medicine. World Scientific. https://doi.org/10.1142/1025

[42] Musha, T. and Sawada, Y. (1994) Physics of the Living State. IOS Press.

[43] Herman, A.B., Savage, V.M. and West, G.B. (2011) A Quantitative Theory of Solid Tumor Growth, Metabolic Rate and Vascularization. PLOS ONE, 6, e22973. https://doi.org/10.1371/journal.pone.0022973

[44] West, G.B., Brown, J.H. and Enquist, B.J. (2004) Growth Models Based on First Principles or Phenomenology? Functional Ecology , 18, 188-196. https://doi.org/10.1111/j.0269-8463.2004.00857.x

[45] Szasz, O., Vincze, G., Szigeti, G.P., Benyo, Z. and Szasz, A. (2018) An Allometric Approach of Tumor-Angiogenesis. Medical Hypotheses , 116, 74-78. https://doi.org/10.1016/j.mehy.2018.03.015

[46] Szasz, O. and Szasz, A. (2021) Approaching Complexity: Hyperthermia Dose and Its Possible Measurement in Oncology. Open Journal of Biophysics , 11, 68-132. https://doi.org/10.4236/ojbiphy.2021.111002

[47] Lee, S., Szigeti, G. and Szasz, A. (2018) Oncological Hyperthermia: The Correct Dosing in Clinical Applications. International Journal of Oncology , 54, 627-643. https://doi.org/10.3892/ijo.2018.4645

[48] Szasz, O., Szigeti, G.P., Vancsik, T. and Szasz, A. (2018) Hyperthermia Dosing and Depth of Effect. Open Journal of Biophysics , 8, 31-48. https://doi.org/10.4236/ojbiphy.2018.81004

[49] Wust, P., Ghadjar, P., Nadobny, J., Beck, M., Kaul, D., Winter, L., et al . (2019) Physical Analysis of Temperature-Dependent Effects of Amplitude-Modulated Electromagnetic Hyperthermia. International Journal of Hyperthermia , 36, 1245-1253. https://doi.org/10.1080/02656736.2019.1692376

[50] Vincze, G. and Szasz, A. (2018) Similarities of Modulation by Temperature and by Electric Field. Open Journal of Biophysics , 8, 95-103. https://doi.org/10.4236/ojbiphy.2018.83008

[51] Minnaar, C.A. and Szasz, A. (2022) Forcing the Antitumor Effects of HSPs Using a Modulated Electric Field. Cells , 11, Article 1838. https://doi.org/10.3390/cells11111838

[52] Szasz, O., Szigeti, G.P., Szasz, A. and Benyo, Z. (2018) Role of Electrical Forces in Angiogenesis. Open Journal of Biophysics , 8, 49-67. https://doi.org/10.4236/ojbiphy.2018.82005

[53] Wust, P., Veltsista, P.D., Oberacker, E., Yavvari, P., Walther, W., Bengtsson, O., et al . (2022) Radiofrequency Electromagnetic Fields Cause Non-Temperature-Induced Physical and Biological Effects in Cancer Cells. Cancers , 14, Article 5349. https://doi.org/10.3390/cancers14215349

[54] Mills, R.E. (1982) Frohlich's Nonthermal Excitations in Biological Systems. Physics Letters A , 91, 91-94. https://doi.org/10.1016/0375-9601(82)90274-2

[55] Gramse, G., Dols-Perez, A., Edwards, M.A., Fumagalli, L. and Gomila, G. (2013) Nanoscale Measurement of the Dielectric Constant of Supported Lipid Bilayers in Aqueous Solutions with Electrostatic Force Microscopy. Biophysical Journal , 104, 1257-1262. https://doi.org/10.1016/j.bpj.2013.02.011

[56] Dharia, S. (2011) Spatially and Temporally Resolving Radio-Frequency Changes in Effective Cell Membrane Capacitance. PhD Theses, University of Utah.

[57] Pike, L.J. (2003) Lipid Rafts: Bringing Order to Chaos. Journal of Lipid Research, 44, 655-667. https://doi.org/10.1194/jlr.r200021-jlr200

[58] Horvath, I., Multhoff, G., Sonnleitner, A. and Vigh, L. (2008) Membrane-Associated Stress Proteins: More than Simply Chaperones. Biochimica et Biophysica Acta (BBA)-Biomembranes , 1778, 1653-1664. https://doi.org/10.1016/j.bbamem.2008.02.012

[59] Govorov, A.O. and Richardson, H.H. (2007) Generating Heat with Metal Nanopar ticles. Nano Today , 2, 30-38. https://doi.org/10.1016/s1748-0132(07)70017-8

[60] Dutz, S. and Hergt, R. (2013) Magnetic Nanoparticle Heating and Heat Transfer on a Microscale: Basic Principles, Realities and Physical Limitations of Hyperthermia for Tumour Therapy. International Journal of Hyperthermia , 29, 790-800. https://doi.org/10.3109/02656736.2013.822993

[61] Wust, P., Kortum, B., Strauss, U., Nadobny, J., Zschaeck, S., Beck, M., et al . (2020) Non-Thermal Effects of Radiofrequency Electromagnetic Fields. Scientific Reports , 10, Article No. 13488. https://doi.org/10.1038/s41598-020-69561-3

[62] Vincze, G. and Sziget, G.P. (2016) Reorganization of the Cytoskeleton. Journal of Advances in Biology, 9, 1872-1882.

[63] Vincze, G. and Szasz, A. (2015) Reorganization of Actin Filaments and Microtubules by Outside Electric Field. Journal of Advances in Biology, 8, 1514-1518.

[64] Vincze, G., Szasz, N. and Szasz, A. (2004) On the Thermal Noise Limit of Cellular Membranes. Bioelectromagnetics , 26, 28-35. https://doi.org/10.1002/bem.20051

[65] Vincze, G. (2015) Effect of Cellular Membrane Resistivity Inhomogeneity on the Thermal Noise-Limit. Journal of Advances in Physics , 11, 3171-3183. https://doi.org/10.24297/jap.v11i3.6859

[66] Guo, J., Lao, Y. and Chang, D.C. (2009) Calcium and Apoptosis. In: Lajtha, A. and Mikoshiba, K., Eds., Handbook of Neurochemistry and Molecular Neurobiology , Springer, 597-622. https://doi.org/10.1007/978-0-387-30370-3_33

[67] Szasz, A. (2017) Oncothermia Is a Kind of Hyperthermia. Hot Topics: Temperature, Dose, Selectivity. Oncothermia Journal , 20, 105-120.

[68] Chi, K.-H. and Wang, Y.-S. (2017) Private Communication. Department of Radiation Therapy & Oncology Shin Kong Wu Ho-Su Memorial Hospital Taipei University and Molecular Medicine and Biochemical Engineering, National Chiao Tung University, Hsinchu, Taiwan Region.

[69] Hossain, M.T., Prasad, B., Park, K.S., Lee, H.J., Ha, Y.H., Lee, S.K., et al . (2016) Simulation and Experimental Evaluation of Selective Heating Characteristics of 13.56 MHz Radiofrequency Hyperthermia in Phantom Models. International Journal of Precision Engineering and Manufacturing , 17, 253-256. https://doi.org/10.1007/s12541-016-0033-9

[70] Nagy, G., Meggyeshazi, N. and Szasz, O. (2013) Deep Temperature Measurements in Oncothermia Processes. Conference Papers in Medicine , 2013, Article 685264. https://doi.org/10.1155/2013/685264

[71] Orczy-Timko, B. (2020) Phantom Measurements with the EHY-2030 Device. In: Szasz, A., Ed., Challenges and Solutions of Oncological Hyperthermia , Cambridge Scholars, 416-428.

[72] Herzog, A. (2008) Messung der Temperaturverteilung am Modell der nicht perfundierten Schweineleber bei lokaler Hyperthermie mit Kurzwellen mit 13,56 MHz. Forum Hyperthermie, 1/10, 30-34.

[73] Szigeti, G.P., Szas, A.M. and Szasz, O. (2020) Oncothermia Is a Kind of Oncological Hyper-Thermia—A Review. Oncothermia Journal , Special Edition, 8-48.

[74] Szasz, A. (2023) Memristor Hypothesis in Malignant Charge Distribution. Open Journal of Biophysics , 13, 51-92.

[75] Andocs, G., Szasz, O. and Szasz, A. (2009) Oncothermia Treatment of Cancer: From the Laboratory to Clinic. Electromagnetic Biology and Medicine , 28, 148-165. https://doi.org/10.1080/15368370902724633

[76] Jeon, T., Yang, H., Lee, C.G., Oh, S.T., Seo, D., Baik, I.H., et al . (2016) Electro- Hyperthermia up-Regulates Tumour Suppressor Septin 4 to Induce Apoptotic Cell Death in Hepatocellular Carcinoma. International Journal of Hyperthermia , 32, 648-656. https://doi.org/10.1080/02656736.2016.1186290

[77] Yang, K., Huang, C., Chi, M., Chiang, H., Wang, Y., Hsia, C., et al . (2016) In vitro Comparison of Conventional Hyperthermia and Modulated Electro-Hyperthermia. Oncotarget , 7, 84082-84092. https://doi.org/10.18632/oncotarget.11444

[78] Tsang, Y., Huang, C., Yang, K., Chi, M., Chiang, H., Wang, Y., et al . (2015) Improving Immunological Tumor Microenvironment Using Electro-Hyperthermia Followed by Dendritic Cell Immunotherapy. BMC Cancer , 15, Article No. 708. https://doi.org/10.1186/s12885-015-1690-2

[79] Yang, W., Han, G.H., Shin, H., Lee, E., Cho, H., Chay, D.B., et al . (2018) Combined Treatment with Modulated Electro-Hyperthermia and an Autophagy Inhibitor Effectively Inhibit Ovarian and Cervical Cancer Growth. International Journal of Hyperthermia , 36, 9-20. https://doi.org/10.1080/02656736.2018.1528390

[80] McDonald, M., Corde, S., Lerch, M., Rosenfeld, A., Jackson, M. and Tehei, M. (2018) First in vitro Evidence of Modulated Electro-Hyperthermia Treatment Performance in Combination with Megavoltage Radiation by Clonogenic Assay. Scientific Reports , 8, Article No. 16608. https://doi.org/10.1038/s41598-018-34712-0

[81] Forika, G., Balogh, A., Vancsik, T., Zalatnai, A., Petovari, G., Benyo, Z., et al . (2020) Modulated Electro-Hyperthermia Resolves Radioresistance of Panc1 Pancreas Adenocarcinoma and Promotes DNA Damage and Apoptosis in vitro. International

Journal of Molecular Sciences , 21, Article 5100.

https://doi.org/10.3390/ijms21145100

[82] Kuo, I., Lee, J., Wang, Y., Chiang, H., Huang, C., Hsieh, P., et al . (2020) Potential Enhancement of Host Immunity and Anti-Tumor Efficacy of Nanoscale Curcumin and Resveratrol in Colorectal Cancers by Modulated Electro-Hyperthermia. BMC Cancer , 20, Article No. 603. https://doi.org/10.1186/s12885-020-07072-0

[83] Vancsik, T., Forika, G., Balogh, A., Kiss, E. and Krenacs, T. (2019) Modulated Electro- Hyperthermia Induced P53 Driven Apoptosis and Cell Cycle Arrest Additively Support Doxorubicin Chemotherapy of Colorectal Cancer in vitro. Cancer Medicine , 8, 4292-4303. https://doi.org/10.1002/cam4.2330

[84] Kiss, E., Vancsik, T., Forika, G., Hamar, P. and Krenacs, T. (2017) Testing Modulated Electro-Hyperthermia Using C26 Colorectal Carcinoma Cell Line in vitro. Oncothermia Journal , 20, 217-227.

[85] Kao, P.H., Chen, C., Tsang, Y., Lin, C., Chiang, H., Huang, C., et al . (2020) Relationship between Energy Dosage and Apoptotic Cell Death by Modulated Electro- Hyperthermia. Scientific Reports, 10, Article No. 8936. https://doi.org/10.1038/s41598-020-65823-2

[86] Cha, J., Jeon, T., Lee, C.G., Oh, S.T., Yang, H., Choi, K., et al . (2015) Electro- Hyperthermia Inhibits Glioma Tumorigenicity through the Induction of E2F1-Mediated Apoptosis. International Journal of Hyperthermia , 31, 784-792. https://doi.org/10.3109/02656736.2015.1069411

[87] Andocs, G., Rehman, M.U., Zhao, Q., Tabuchi, Y., Kanamori, M. and Kondo, T. (2016) Comparison of Biological Effects of Modulated Electro-Hyperthermia and Conventional Heat Treatment in Human Lymphoma U937 Cells. Cell Death Discovery, 2, Article No. 16039. https://doi.org/10.1038/cddiscovery.2016.39

[88] Andocs, G., Rehman, M.U. and Zhao, Q. (2015) Nanoheating without Artificial Nanoparticles Part II. Experimental Support of the Nanoheating Concept of the Modulated Electro-Hyperthermia Method, Using U937 Cell Suspension Model. Biology and Medicine , 7, 1-9.

[89] Tsang, Y., Chi, K., Huang, C., Chi, M., Chiang, H., Yang, K., et al . (2019) Modulated Electro-Hyperthermia-Enhanced Liposomal Drug Uptake by Cancer Cells. International Journal of Nanomedicine , 14, 1269-1279. https://doi.org/10.2147/ijn.s188791

[90] Chen, C., Chen, C., Li, J., Chen, Y., Wang, C., Wang, Y., et al . (2019) Presence of Gold Nanoparticles in Cells Associated with the Cell-Killing Effect of Modulated Electro-Hyperthermia. ACS Applied Bio Materials , 2, 3573-3581. https://doi.org/10.1021/acsabm.9b00453

[91] Schvarcz, C.A., Danics, L., Krenacs, T., Viana, P., Beres, R., Vancsik, T., et al . (2021) Modulated Electro-Hyperthermia Induces a Prominent Local Stress Response and Growth Inhibition in Mouse Breast Cancer Isografts. Cancers , 13, Article 1744. https://doi.org/10.3390/cancers13071744

[92] Matsumoto, Y., Hayshi, J., Sekino, Y., Fukumitsu, N., Saito, T., Ishikawa, H. and Sakurai, H. (2018) Radiosensitization Effect of Novel Cancer Therapy, mEHT. Toward Overcoming Treatment Resistance. Oncothermia Journal , 25, 68-84.

[93] Prasad, B., Kim, S., Cho, W., Kim, J.K., Kim, Y.A., Kim, S., et al . (2019) Quantitative Estimation of the Equivalent Radiation Dose Escalation Using Radiofrequency Hyperthermia in Mouse Xenograft Models of Human Lung Cancer. Scientific Reports, 9, Article No. 3942. https://doi.org/10.1038/s41598-019-40595-6

[94] Brunner, G. (2006) Zellulare Hyperthermie-Effekte in vitro in einem Progressionsmodell des Plattenepithelkarzinoms. Klinik Hornheide , Munster University , Germany, Hyperthermia Symposium, Cologne, 22-23 September 2006.

[95] Andocs, G., Rehman, M.U., Zhao, Q., Tabuchi, Y., Kanamori, M. and Kondo, T. (2016) Comparison of Biological Effects of Modulated Electro-Hyperthermia and Conventional Heat Treatment in Human Lymphoma U937 Cells. Cell Death Discovery , 2, Article No. 16039. https://doi.org/10.1038/cddiscovery.2016.39

[96] Gannon, C.J., Patra, C.R., Bhattacharya, R., Mukherjee, P. and Curley, S.A. (2008) Intracellular Gold Nanoparticles Enhance Non-Invasive Radiofrequency Thermal Destruction of Human Gastrointestinal Cancer Cells. Journal of Nanobiotechnology, 6, Article No. 2. https://doi.org/10.1186/1477-3155-6-2

[97] Forika, G., Balogh, A. and Vancsik, T. (2019) Elevated Apoptosis and Tumor Stem Cell Destruction in a Radioresistant Pancreatic Adenocarcinoma Cell Line When Radiotherapy Is Combined with Modulated Electrohyperthermia. Oncothermia Journal , 26, 90-98.

[98] Meggyeshazi, N., Andocs, G. and Krenacs, T. (2012) Modulated Electro-Hyperthermia Induced Programmed Cell Death in HT29 Colorectal Carcinoma Xenograft. Virchows Archiv, 461, S131-S132.

[99] Danics, L., Schvarcz, C.A., Viana, P., Vancsik, T., Krenacs, T., Benyo, Z., et al . (2020) Exhaustion of Protective Heat Shock Response Induces Significant Tumor Damage by Apoptosis after Modulated Electro-Hyperthermia Treatment of Triple Negative Breast Cancer Isografts in Mice. Cancers , 12, Article 2581. https://doi.org/10.3390/cancers12092581

[100] Meggyeshazi, N., Andocs, G., Spisak, S., et al . (2013) Modulated Electrohyperthermia Causes Caspase Independent Programmed Cell Death in HT29 Colon Cancer Xenografts. Virchows Archiv , 463, 329.

[101] Meggyeshazi, N., Andocs, G., Balogh, L., Balla, P., Kiszner, G., Teleki, I., et al . (2014) DNA Fragmentation and Caspase-Independent Programmed Cell Death by Modulated Electrohyperthermia. Strahlentherapie und Onkologie , 190, 815-822. https://doi.org/10.1007/s00066-014-0617-1

[102] Meggyeshazi, N., Andocs, G., Spisak, S. and Krenacs, T. (2013) Early Changes in Mrna and Protein Expression Related to Cancer Treatment by Modulated Electrohyperthermia. Conference Papers in Medicine , 2013, Article 249563. https://doi.org/10.1155/2013/249563

[103] Janigro, D., Perju, C., Fazio, V., Hallene, K., Dini, G., Agarwal, M.K., et al . (2006) Alternating Current Electrical Stimulation Enhanced Chemotherapy: A Novel Strategy to Bypass Multidrug Resistance in Tumor Cells. BMC Cancer , 6, Article No. 72. https://doi.org/10.1186/1471-2407-6-72

[104] Krenacs, T. and Benyo, Z. (2017) Tumor Specific Stress and Immune Response Induced by Modulated Electrohyperthermia in Relation to Tumor Metabolic Profiles. Oncothermia Journal , 20, 264-272.

[105] Forika, G., Vancsik, T., Kiss, E., Hujber, Z., Sebestyen, A., Krencz, I., et al . (2017) The Efficiency of Modulated Electro-Hyperthermia May Correlate with the Tumor Metabolic Profiles. Oncothermia Journal , 20, 228-235.

[106] Li, J., Chauve, L., Phelps, G., Brielmann, R.M. and Morimoto, R.I. (2016) E2F Coregulates an Essential HSF Developmental Program that Is Distinct from the Heat-Shock Response. Genes & Development , 30, 2062-2075. https://doi.org/10.1101/gad.283317.116

[107] Szasz, A., Szasz, N. and Szasz, O. (2010) Oncothermia: Principles and Practices. Springer Science. https://doi.org/10.1007/978-90-481-9498-8

[108] Vancsik, T., Mathe, D., Horvath, I., Varallyaly, A.A., Benedek, A., Bergmann, R., et al . (2021) Modulated Electro-Hyperthermia Facilitates NK-Cell Infiltration and Growth Arrest of Human A2058 Melanoma in a Xenograft Model. Frontiers in Oncology , 11, Article 590764. https://doi.org/10.3389/fonc.2021.590764

Preclinical Verification of Modulated Electro-Hyperthermia

PART II. – In Vivo Research

Andras Szasz

Department of Biotechnics, Hungarian University of Agriculture and Life Sciences, 2100 Gödöllő, Hungary

Email: biotech@gek.szie.hu

Citation

Szasz, A. (2024) Preclinical Verification of Modulated Electro-Hyperthermia – Part II. – In vivo research

Oncothermia Journal 38, August 2026., 113-149.
https://oncotherm.com/SzaszA_2024_Preclinical_verification_of_mEHT-Part_II

Abstract

The treatments of malignant diseases nowadays are rapidly developing. One of the groups of novel therapies applies electromagnetic fields to destroy the malignant lesions. The thermal (heating) and nonthermal (polarization, molecular excitations) processes are combined in novel methods. The non-ionizing energy absorption from the electric field may produce substantial heat, increasing the targeted lesion's temperature and inducing hyperthermic effects. The modulated electro-hyperthermia (mEHT) uses thermal conditions to optimize and accelerate the chemical reactions induced by the nonthermal excitation of the electric field. The mEHT cooperates with the body's homeostatic control and harmonizes the mutual efforts to destroy the malignancy. Our objective is to show in vivo proof of the combined complementary electromagnetic impact on various tumors produced by mEHT. Furthermore, we present evidence of the increasing efficacy of the complementary application of mEHT with conventional treatments.

Keywords

mEHT, Cancer Treatment, Thermal, Nonthermal, Electric, In Vivo, Tumor Destruction

1. Introduction

Cancer therapies have rapidly developed in the last decades [1]. All classical treatments like chemotherapy (ChT), radiotherapy (RT), and surgery (Op) went through intense development. The new highly effective pharma products, the personalized and targeted approaches, the complex, versatile protocols, and the precise pointing of malignant lesions increased the success rate of the conventional treatment.

New therapies focus on extending patient survival with an acceptable quality of life. Despite the robust development, the estimated 2+ million new cases in 2024 [2] derail the optimistic and encouraging outlook for cancer care. Intensive efforts in drug development drive the progress of cancer therapies. Another challenge, however, is the present oncotherapies have severe adverse effects and toxicity, which limits their applications. There are 95% of the new cancer drugs applied in clinical studies have no approval because of their high toxicity [3]. Nonionizing electromagnetic therapies group different approaches without chemical toxicity. Like radiotherapy (ionizing radiation), electromagnetic energy absorption could cause thermal toxicity (burns), which differs from other adverse effects. This toxicity does not develop comorbidities. Avoiding its side effects or treating the accidentally appearing one is relatively easy. The electromagnetic impact on chosen reactions could increase the efficacy and decrease the toxicity of the complementary applied therapy [4]-[6]. The selection of malignancy by biophysical effects looks optional [7] [8], and the thermal effects of the nonionizing could accelerate the excited chemical reactions (but chemically active) electromagnetic radiation [9]. These advantages support electromagnetic energy absorption as a helpful therapy, both standalone and in complementary applications.

The chemically active nonthermal electromagnetic effects are calculated and verified in vitro cell culture experiments [10]. The synergy of thermal and nonthermal effects had been measured in

vitro but the selectivity considering intensive physiological feedback can be studied only in vivo. The present part of the series aims to show the in vivo research and review its results.

2. Method

The modulated electro-hyperthermia (mEHT) technical solution is classical capacitive coupling with radiofrequency (RF) application at 13.56 MHz. A plan-parallel condenser provides the energy to the experimental animal between the electrodes, which are asymmetric [11].

The mEHT is a hyperthermia method, which, in addition to the thermal energy absorption, uses nonthermal, electric field-dependent molecular excitations, increasing the tumor-destruction facility of the energy [7]. mEHT targets the electric and thermal differences between the malignant and healthy tissues and the micro heterogeneities at the tumor microenvironment (TME) [9]. The electric field selects the highly proliferative tumors by their high electric conductivity, and the low-frequency amplitude modulation active in polarization and molecular excitations of transmembrane proteins of the malignant cells [5] [6]. Various apoptotic signals are excited by external electric field impact. The frequencies are optimized for the best performance [5] [8]. The electric field selects the tumor, and the low-frequency amplitude modulation polarizes and excites the transmembrane proteins of the malignant cells. The primary guidance of mEHT is biophysical using updated bioelectromagnetic considerations. The selective targeting modifies the conventional hyperthermia which intends to heat the entire mass of the tuor iso-thermally. The heterogeneous heating uses the thermal effects on the targeted molecules to accelerate the signal transduction which is triggered by the nonthermal impact [12]. The transmembrane molecular targeting of nonionizing radiation by a modulated electric field is like the ionizing radiation (radiotherapy, RT), which targets also molecular components in the strand of DNA.

The devices for in vivo use were the LabEHT100 and LabEHY200 (Oncotherm, Budaors, Hungary). The animal lies on the rectangular-shaped 6 × 12 cm size grounded electrode. To prevent the mice from cooling, the temperature of the counter electrode was controlled; it was kept at 37°C during the treatment. The round-shaped opposing electrode (applicator) is above the animal, is 18 mm in size, and can be adjusted with a flexible holder to the necessary position above the treated tumor. A bolus with distilled water ensures optimal electromagnetic coupling. The applicator is cooled with circulating water. The allometric scaling estimates the speed of mice physiology (including the heartbeats) to be seven times quicker than that of humans. Due to the rapid physiological feedback, an ultrafast tuning system makes the prompt automatic adjustment of animal reactions possible. The temperature intratumoral, skin, and rectal measured, and the electric tuning status with the forwarded and reflected powers are also registered in real-time. The sampling frequency is 60/min. The temperature was controlled with specialized thermometers immune to RF radiation. The experimental conditions are discussed in detail in every referred article.

The animals are anesthetized during the treatment. The experimental setup is shown in Figure 1.

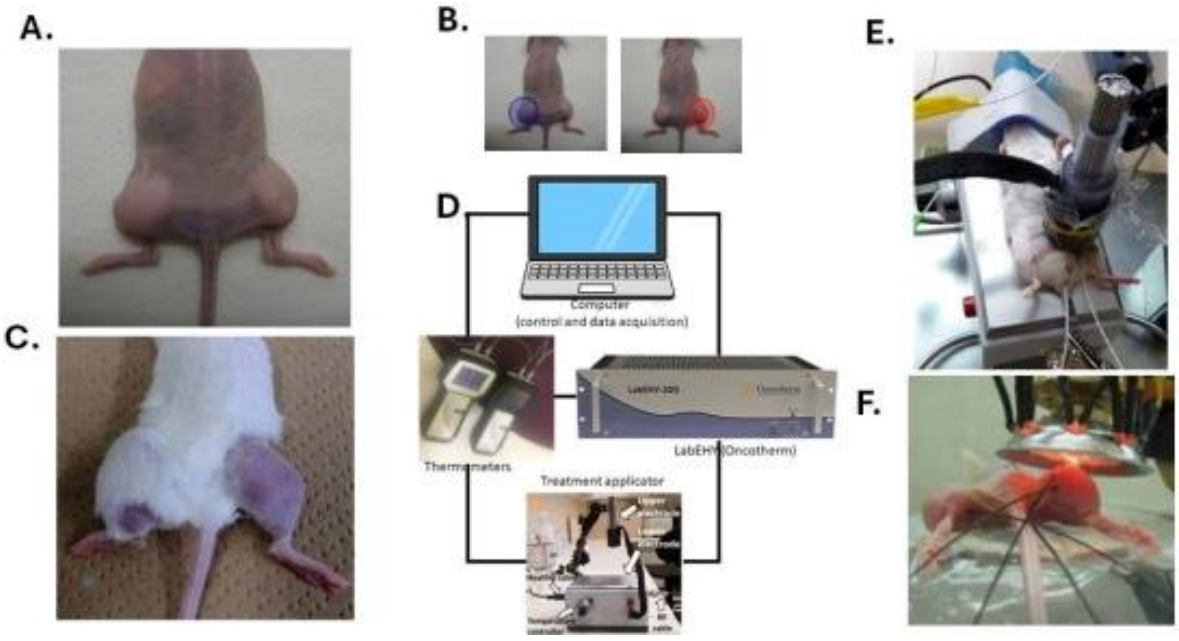

Figure 1. Experimental setup of the in vivo experiments. Some experimental animals had their own untreated control tumor in a symmetrical position, usually in the left and right femoral regions.

(A.) In the immunocompromised (nude) mice, the two tumors are supposed to be independent.
(B.) Only one tumor is treated (always the right side) with mEHT; the other is used for comparison. In immunocompromised nude mice, the untreated tumor is regarded as a control.
(C.) In immunocompetent mice, we expect immune reactions. The two tumors distantly inoculated tumors are connected, making it possible to measure the abscopal effect in distant locations.
(D.) The measuring setup.
(E.) mEHT treatment of a mouse.
(F.) Infrared hyperthermia (iHT) treatment.

Numerous cancer-bearing companion animals (dogs and cats) were successfully treated with mEHT [13]. These treatments better approach human tumorous cases because they have larger body weights than rodents. The larger body mass shifts the physiological timing to longer scales, better approaching human conditions. The naturally developed, not inoculated tumors also allow these treatments to be closer to human studies.

The technical details of the treatment are described elsewhere [14]-[17]. The treatment conditions mostly follow a standard protocol of 42°C in the tumor for 30 min. The time from the inoculation of the tumor cells to the first mEHT treatment depends on the tumor size, which is approximately 2 g when the experimental process starts. In some experiments, Matrigel is used to control growth. The applied power varies by the animals and their tumors, ranging from 1 W to 8 W. The treated tumors were studied using various methods. The tumor in its 3D form was studied with size (caliper and ultrasound) and its activity (bioluminescence signals). The excised ex vivo tumors were characterized by their size/weight. The tumors are usually cut in half; one is frozen, formalin-fixed, and embedded in paraffin for further investigation. The frozen samples are helpful for genetic and protein analysis and Western blot, FACS, PCR, the paraffin-embedded samples for morphological

studies, multiple immunohistochemistry, and signal pathway analyses; the most frequent processes with then excised samples are shown in Figure 2.

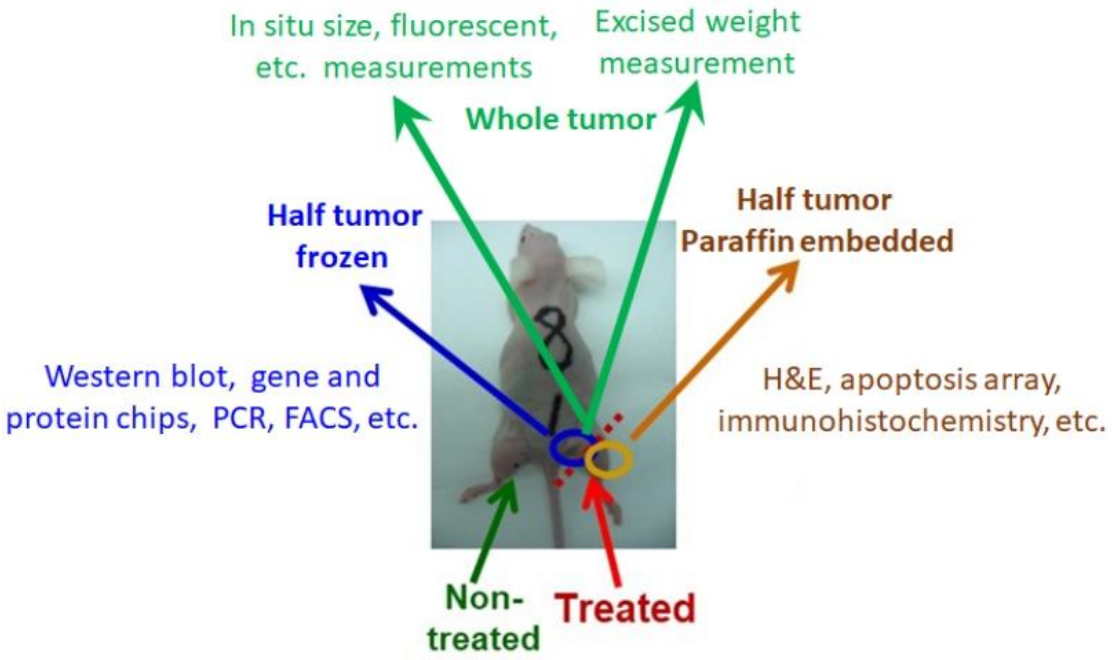

Figure 2. In immunocompromised mice, the primary measurement categories of the treated tumor are as follows: the whole tumor is measured in situ, while the excised (ex vi-vo) tumors, after measuring their weight, are halved, serving different measurements.

The results are compared to sham mEHT treatment, infrared hyperthermia, or distant, untreated tumors in the same animal.

3. In Vivo Measurements

The publications on in vivo measurements are collected in **Table 1.**

Table 1. In vivo preclinical research.

Tumor cells	Method	Result	Conclusion	Ref.
FSaII was inoculated into the femoral region of the C3H mice and treated with mEHT and RT.	mEHT 41°C, 10 + 30 min, 2 - 3 W, plus irradiation 15 Gy (1.3 Gy/min). Studied the tumor growth, apoptosis, and HIF-1α, VEGF, and CA-9 were measured.	The tumor growth was inhibited, and the apoptosis rate increased with the combined treatment. Furthermore, it reduced the RT, increased hypoxia, and increased blood perfusion.	The combined treatment enhances the anti-tumor effect of high-dose irradiation and minimizes the side effects of the RT.	[18]

RG2 [D74] glioma cell line was inoculated into the parietal lobe of syngeneic Fischer 344 rats, treated with pulsed mEHT.	MRI was measured on the 8th and 15th days after inoculations. Four groups of animals were compared using sham, mEHT stand-alone, mEHT + TMZ, and the pulsed mEHT in a time-course protocol.	The pulsed mEHT was superior to all other treatment groups.	The pulsed mEHT looks like a further novel development of the conventional mEHT method.	[19]
4T1 was inoculated into BALB/c mice, isograft, and treated with mEHT.	mEHT 42˚C, 5 + 30 min, (skin 39.5˚C, body 37.8˚C.) Apoptosis was measured with multiple other characteristics of change in time course.	HSP70 was significantly induced by mEHT, with a maximum of 12 h after treatment. The cell destruction and cC3 have their maximum at 24 h, and the viability is significantly decreased. 5 mEHT treatment significantly suppressed the Ki67 proliferation marker.	The massive HSP70 development exhausts the cells and plays a major role in losing cell protection against stress, consequently promoting cellular destruction.	[20]
Huh-7 and HepG2 cell lines xenograft in nude mice treated with mEHT.	mEHT 42˚C, 5 + 30 min, (skin 39.5˚C, body 37.8˚C) caliper ruler monitored.	mEHT significantly inhibited the growth of human HCC xenografts in nude mice.	On the 19th day, the control tumor was double that of the mEHT-treated one.	[21]
U87-MG and A172 human glioma cells inoculated into BALB/c nude mice xenograft.	mEHT 42˚C, 30 min, 3 W (3x), time course study. RNA sequencing a caliper ruler was used.	Inhibited tumor growth, significant apoptotic rate, reduced cell migration.	Increased p53 and E2F1, reduced PARP1 in mRNA level, suppressed CD133+ cancer stem cells.	[22]
HT29 human metastatic colorectal xenograft model. BALB/c nude mice.	mEHT 42˚C, 30 min, 4 W, time-course study with Immunohistochemistry, Western blot, TUNEL assay.	Significant apoptosis of the malignant cells, DNA fragmentation, AIF mediated apoptotic pathway.	Caspase-independent apoptosis, with mitochondrial permeabilization and DNA fragmentation.	[23]
HT29 xenograft model, BALB/c nude mice treated with mEHT.	mEHT 42˚C, 30 min, 4 W, time-course study with Immuno-histochemistry, microarray, apoptosis array,	Measured damage-associated molecular pattern (HSP70, CRT, HMGB1 and HSP90).	mEHT induces a spatiotemporal sequence of DAMP signals HT29 cancer, and it can be a potential local inducer of immunogenic cell death.	[24]
HT29 xenograft model. MEHT treated BALB/c nude mice.	mEHT 42˚C, 30 min, 4 W, time-course study with Immunohistochemistry, apoptosis analysis.	mEHT caused selective tumor destruction, and upregulation of TRAIL-R2 and FAS was observed.	mEHT caused massive caspase-independent cell death.	[25]

C26 allografts of immunocompetent (BALB/c) mice plus immunostimulant MTE.	mEHT 42˚C, 30 min, 1 - 3 W, Immunohistochemistry, TUNEL assay apoptosis analysis, comparison of the treated and nontreated tumors of the same mouse. Extra immune stimulant (MTE) is applied.	The damage-associated molecular pattern was measured (CRT, HSP70, HMGB1). Ki67 was suppressed. Dendritic cells were matured, and antigen-presenting showed tumor-specific killer T-cells and their invasion into the tumor.	The mice with immune stimulants had an abscopal effect, showing the same development in the untreated tumor as in the treated one. ICD formed tumor-specific immune reactions.	[26]
CT26 allografts of immunocompetent (BALB/c) mice plus dendritic cell immunostimulant.	mEHT 42˚C, 30 min, DC cells inoculated intratumorally to the femoral area, cytotoxic T lymphocyte assay, ELISPOT, Immunohistochemistry.	Significant HSP70 release was measured in comparison to wHT with the same temperature. The DC-combined mEHT inhibited cell growth, and the substantial appearance in CD45+, F4/80, and Eosinophil leukocytes were measured.	mEHT can create a favorable tumor microenvironment for an immunological chain reaction. Rechallenging the same tumor was ineffective. The DC-combined mEHT worked as an antitumor-vaccination.	[27]
A2058 human melanoma cell line and NK cell immunotherapy combined with mEHT.	mEHT 42˚C, 30 min, NK cells or IL-2 independent NK-92MI injected subcutaneously to right and left femoral region. Only the right side was treated.	Intensive hsp70 expression followed by significant upregulation of cC3 and p53. NK cell accumulation was in the treated tumor but not in the untreated side. Upregulation of CXCL11 and MMP2 was observed.	mEHT ultimately leads to completely eradicating melanoma and appears to be a good combination with NK immunotherapy.	[28]
CT26/BALB/c mice tumor model mEHT with Cur and Res combined treatment.	mEHT 42˚C, 30 min, 10 - 12 W, tumor growth, and immune cell infiltration were measured together with cell viability, apoptosis, Western blot, and immunohistochemistry comparison with wHT.	mEHT with Cur and Res combination inhibited the growth of CT26 cancer by inducing apoptosis and HSP70 expression of tumor cells while recruiting CD3+ T-cells and F4/80+ macrophages.	Cur and Res combined with mEHT synergistically increased HSP release and immune response, showing enhanced anti-tumor efficacy.	[29]
B16F10 allograft cells inoculated to female C57Bl/6 mice (offspring of C57Bl/6 colonies) in the right inguinal area.	mEHT 42˚C, 30 min, measured tumor-size, HSP70, PUMA, γH2AX, DAMP signaling was measured.	Upregulation of cytoplasmic and cell membrane HSP70 Increased PUMA and AIF1 and rise of cC3 without significant apoptosis. But, γH2AX indicated DNA double-strand breaks, which upregulated p53 protein and downstream p21waf1 and p27kip. mEHT promoted the release of DAMP; it reduced MHC-I levels in tumor cells.	mEHT-related tumor shrinkage was primarily mediated by p53, upregulating the cyclin-dependent kinase inhibitors. Reduced cytotoxic T-cell response was observed despite increased DAMP signaling. Decreased tumor antigen and MHC-I levels suggest that NK cells and macrophages were the major contributors to tumor eradication.	[30]

FSaIIcells inoculated subcutaneously in the femoral region of C3H mice. mEHT plus 15 Gy RT, with Mef, was applied.	mEHT 41˚C, 30 min, metformin was intraperitoneal, 150 mg/kg. HIF-1*a*, VEGF, PD-L1, and TUNEL apoptosis were measured.	Irradiation markedly increased the expression of HIF-1 *a*, VEGF, PD-L1, and mEHT, which was reduced by the mEHT combined treatment and enhanced the suppression of tumor growth.	The increased tumor response to 15 Gy irradiation by mEHT and Mef alone or in combination was due, in part, to the abrogation of the radiation-induced upregulation of HIF-1*a* and its downstream targets VEGF and PD-L1.	[31]
A549 and NCI-H1299 cell-line BALB/c nude mice heterotopic xenograft treated with mEHT.	The linear-quadratic (LQ) model was used for an equivalent radiation dose of mEHT, 42˚C, 30 min.	mEHT + RT arrested the tumor growth, significantly increased the apoptosis.	The thermal enhancement of mEHT was determined, and the estimated equivalent radiation was calculated.	[32]
A549 and NCI-H1299 cell line BALB/c nude mice heterotopic xenograft treated with mEHT.	mEHT 42˚C, SAR = 250 W/kg, CEM43 dose calculated and compared to the measurements.	The tumor has > 3C higher temperature than the surrounding muscles, with good agreement with the numerical calculations. The tumor has > 4 times larger CEM43 than the surrounding.	The experiments proved the selection of the energy absorption, which is automatically well-localized on the tumor, and the host has less heating.	[33]
CT26 allografts of immunocompetent (BALB/c) mice plus liposomal Dox.	mEHT 42˚C, 30 min, tumor in femoral region, 10 mg/kg liposomal Dox. The effect was compared with wHT.	mEHT enhanced the liposomal Dox uptake. The combined treatment arrests the tumor growth. The effects were significantly higher than in wHT cases.	mEHT stimulated the activity of receptors and enzymes of cancer cells. Consequently, the uptake of Dox significantly increased after mEHT and effectively enhanced the drug's therapeutic effect.	[34]
The liver of a healthy pig was mEHT treated.	mEHT 150 W, 60 min, 540 kJ, anesthetized female pig 49.5 kg Immediate maximal, or step-up heating.	Shallow intrahepatic temperature > 42˚C, deep intrahepatic temperature > 41˚C, skin temperature < 41˚C, rectal temperature < 39˚C	The measurements show a definite increase in the temperature of the liver of a living, anesthetized pig treated with mEHT.	[35]
Companion animals with mEHT are dedicated for veterinarian use.	VetEHY system treated dogs and cats. Step-up heating, < 35 W. Spontaneously occurring tumors.	All treated cases have shown remarkable improvement, tumor shrink, and better animal movability.	mEHT is a powerful veterinarian tool for companion animals and valuable for comparative clinical oncology.	[13]
mEHT was applied with a high Vitamin C dose for the C26 murine model.	Vit.C 2g/kg dose, mEHT 42˚C, 30 min.	A histopathological study was made *ex vivo* 24 hours after treatment. Vit.C had no effect as monotherapy. The combined treatment had high fluctuations. The tumor distribution was the same in both tumors of the animal.	The study does not allow a definite conclusion, but a sign of the possible abscopal effect was observed.	[36]
mEHT was used for the HT29 xenograft mouse model on female NMRI nu/nu mice.	mEHT 1 W, 5 + 30 min. < 40˚C, Bioluminescent method was used. Matching electric parameters were measured.	mEHT had significantly less dT/dt than EHT. However, the skin temperature and depth were slightly higher in mEHT. The matching impedances differ between the EHT and mEHT.	The study demonstrates the non-temperature-dependent anticancer effects of mEHT, shows the role of modulation, and promises more effective cancer therapy.	[37]

HT29 metastatic xenograft model. BALB/c nude mice treated with mEHT.	mEHT 42˚C, 30 min, 4 W, time-course study. TUNEL apoptosis analysis.	mEHT caused a selective tumor destruction, and upregulation of TRAIL-R2, FAS, FADD, SMACK/Diabolo, HTRA2/Omi HSP60 and HSP70 were measured.	mEHT treatment upregulates a range of proteins related to apoptosis induction and heat shock response within 24 hours post-treatment.	[38]
Human squamous cell lung cancer cell-line BALB/c nude mice heterotopic xenograft treated with mEHT.	mEHT 42˚C, 30 min, power < 2.5 W. Local temperature sensors: intratumoral, host tissue, rectal measurement. Conductivity and dielectric constant were also measured.	Tumor temperature 42˚C, muscle host 34˚C, rectum 30˚C, and the treatment bed 28˚C. The calculated simulation corresponds well with the measurements.	The measured temperature mapping and the thermal dose agree well with the numerical calculation.	[39]
mEHT for HT29 xenograft model. The irHT and mEHT at 42˚C, and mEHT at 38˚C, were compared.	mEHT and iHTwas 42˚C, 60 min (32 V/m field), and additional mEHT 38˚C. Micromorphological analysis 24 h after treatment.	The dead cell ratio was significantly higher with mEHT compared to other groups. Notably, the mEHT 38˚C, also did substantially better tumor destruction than the iHT on 42C.	A strong synergy of thermal and nonthermal components is shown, proving the importance of the nonthermal effects.	[40]
Effect of repeated mEHT treatment in 4T07 TNBC. 4T07 cells were inoculated orthotopically in female BALB/c mice.	mEHT 42˚C, 30 min, skin temperature just over the tumor 40˚C (3 W) The repeated treatments were studied by tumor size, cC3, HSP70, immune profile (CD3+, CTLA4, PD-1, PD-L1), p21, and Ki67.	The five-treatment repetition shows a significant positive change in all measured parameters in 4T07 TNBC.	Repeated treatment improves the effect of mEHT and is well applicable for TNBC tumors, suggesting positive clinical performance.	[41]
mEHT for B16F10 melanoma pulmonary metastases. Repeated treatment of lung.	mEHT 30 min, 42˚C (lung) 40˚C (pharyngeal) and 38.5˚C (rectal temperatures). Measured immunohistochemistry, flow cytometry, and apoptotic and necrotic cell death. 6 times repeated treatment.	mEHT induced significant anti-tumor effects and the downregulation of Ki67 expression, as well as made significant DNA double-strand breaks, significantly increased CD3+, CD8+ T-lymphocytes, and F4/80+CD11b+ macrophage density in the whole lung.	mEHT inhibits tumor growth and spontaneous proliferation of B16F10 melanoma in a mouse pulmonary metastasis model. mEHT is a complementary therapeutic option to chemo- and/or radiotherapy. The massive infiltration of tumors by CD3+ and CD8+ T-lymphocytes and by F4/80 CD11b-positive macrophages indicates the ability of mEHT to mobilize the immune response in treated animals.	[42]
mEHT for therapy-resistant TNBC model with 4T1 and 4T07 cell lines inoculated orthotopically into female BALB/c mice.	mEHT (5x) 42˚C, 30 min, skin temperature 40˚C. Measured properties: morphology, HSP70, Ki67, gene expression.	mEHT significantly inhibited tumor growth and diminished Ki67. It produced several stress-related factors. mEHT treatment induced innate immune-response reactions, among others, in the tumor. Thirteen stress-related genes were observed to be significantly upregulated.	mEHT has effective antitumor effects in the highly aggressive and rapidly growing 4T1/4T07 TNBC, even in monotherapy. The exhaustion of protective mechanisms diminished cancer proliferation and active caspase-mediated apoptotic tumor cell death.	[43]
SAS tumor.	Comparison of mEHT and mEHT + RT. Tumor size, survival time, and apoptotic signals were measured.	The survival time significantly increased with combined RT + mEHT treatment, and the tumor growth was inhibited.	The increased apoptosis and survival time indicate the excellence of the mEHT + RT treatment.	[44]

C3H/He mice inoculated with SCCVII to the left femoral and in the chest region. Dendritic cell immune stimulation was applied.	mEHT 42°C 30 min, Flow cytometry, immunohistochemistry, CD3+, CD4+ and CD8+ immune-cell detection.	The CD8+ and S100 were more strongly expressed in the DC plus mEHT treatment group than in control or stand-alone therapies, although Foxp3 expression was much higher in the control group.	A significant abscopal effect was measured between the treated femoral and untreated chest regions of the mice. The local treatment also became a whole-body immune attack on the metastatic lesions.	[45]
BxPC-3 human pancreatic adenocarcinoma xenograft.	mEHT treatment compared to control the tumor size is measured and compared to sham (10-10 mice).	The tumor sizes were significantly reduced, and mEHT inhibits the growth.	The mEHT significantly responds to mice in the resistive, aggressive pancreatic tumor.	[14]
4T1 cells were orthotopically injected into Balb/C mice.	Variants of liposomal doxorubicin were compared, and the release of the drug and the mechanism of the cell distortion were measured.	The mEHT treatment significantly promoted the release of the drug in the locally treated volume, the highest rate was with LTLD.	The mEHT treatment helps target the tumor with liposomal doxorubicin.	[46]
A549 xenograft injected into the flank of Balb/C mice.	RT + mEHT expression profile of nuclear receptors NR4A3 and KLF11.	That NR4A3 and KLF11 are critical for increasing the efficacy of radiotherapy combined with mEHT.	The study identified the molecular mechanism to sensitize lung cancer to RT + mEHT.	[47]
OVCAR-3, SNU-17, PDTX-19 cell lines treated with mEHT.	Tumor volume was studied in the time course. Cell number and Western blot were compared for mEHT and wHT 24 and 48 h after treatment.	The superiority of mEHT is observed in all cases; the difference between mEHT and wHT increases over time. The addition of 3-methyladenine (3-MA) increased the effects.	mEHT induced the death of ovarian and cervical cancer cells through apoptosis, and its anticancer effect was enhanced by inhibiting mEHT-induced autophagy.	[48]
9L glioma tumor allograft.	Tumor tissue oxygenation level was measured using an O2-sensitive electrode system. Standard 42°C 30 min mEHT.	Oxygen level was significantly higher (almost double) in the treated tumor than before.	mEHT substantially increases the oxygen level in tumors in 9 L gliomas in rats.	[49]
Companion animals (dogs and cats) with tumors) treated with mEHT.	Natural tumors of dogs were treated after failure of conventional (surgery and chemotherapy) treatments.	Significant shrinking of tumors (even lung metastasis) was achieved together with improved quality of life of the animals.	The mEHT is a valuable tool for veterinary oncology and gives stable information for human clinical applications.	[13]

Most treatments were made on rodents. However, the thermal efficacy was measured in vivo on a healthy female pig (49.5 kg) liver, which is a model of a deep-seated, highly blood-perfunded organ [35]. The tumor focus was unavailable without the tumor in the liver, but the focus on the liver in the large-sized experimental animal was proven. The temperature dynamically grew in the liver mass while its surrounding temperature was behind (Figure 3). The results show that mEHT can thermally impact the liver without raising the skin temperature; no surface overheating was observed, and the skin and the fatty tissue remained in a safe heating regime. Anesthesia influences temperature development in a short time. The physiological control actively regulates thermal homeostasis, having isothermal heating in the liver, while in a deep anesthetic state, the regulation is slower and less effective. The step-up heating condition in deep anesthesia allows for weaker physiologic reactions, making thermal regulation (Figure 3(C)).

The temperature development was measured in various experimental setups [50]. The typical temperature measurements in mice and dogs show good deep heating focus (Figure 4) Noteworthy is the temperature in the lung (Figure 4(D)), which is well distinguishable high despite the cooling by the animal's breathing Figure 4(D). The power started high, but keeping the temperature enough was a fraction of the initial value because keeping the temperature only replaces the "lost" heat caused by the environmental conditions. Various treatment setups and tumor sizes influence temperature development, and the starting power is decided for the initial slope of the temperature plot.

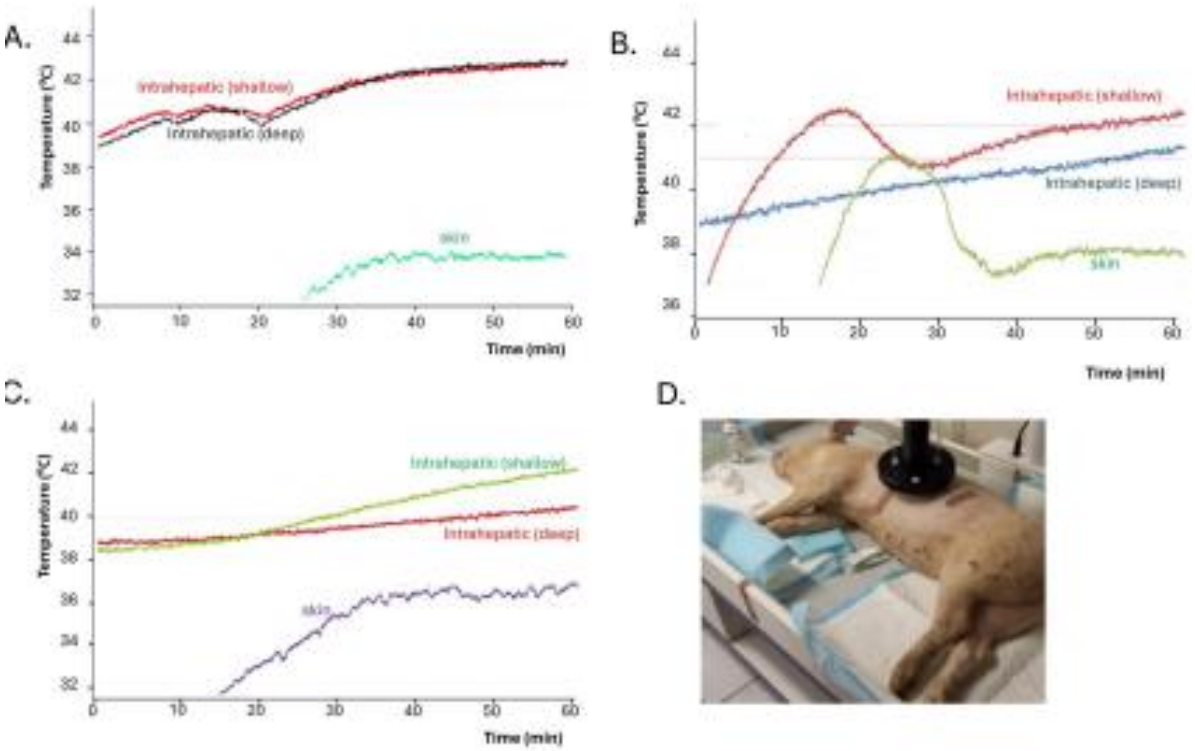

Figure 3. Temperature measurement in the liver of a healthy pig (42˚C, 60 min, 150 W max.) (A.) The permanent 150 W power treatment was started 10 min after anesthesia. (B.) The permanent 150 W power treatment was started 30 min after anesthesia. (C.) Step-up heating treatment from 60 W to 150 W. (D.) The anesthetized animal during the treatment.

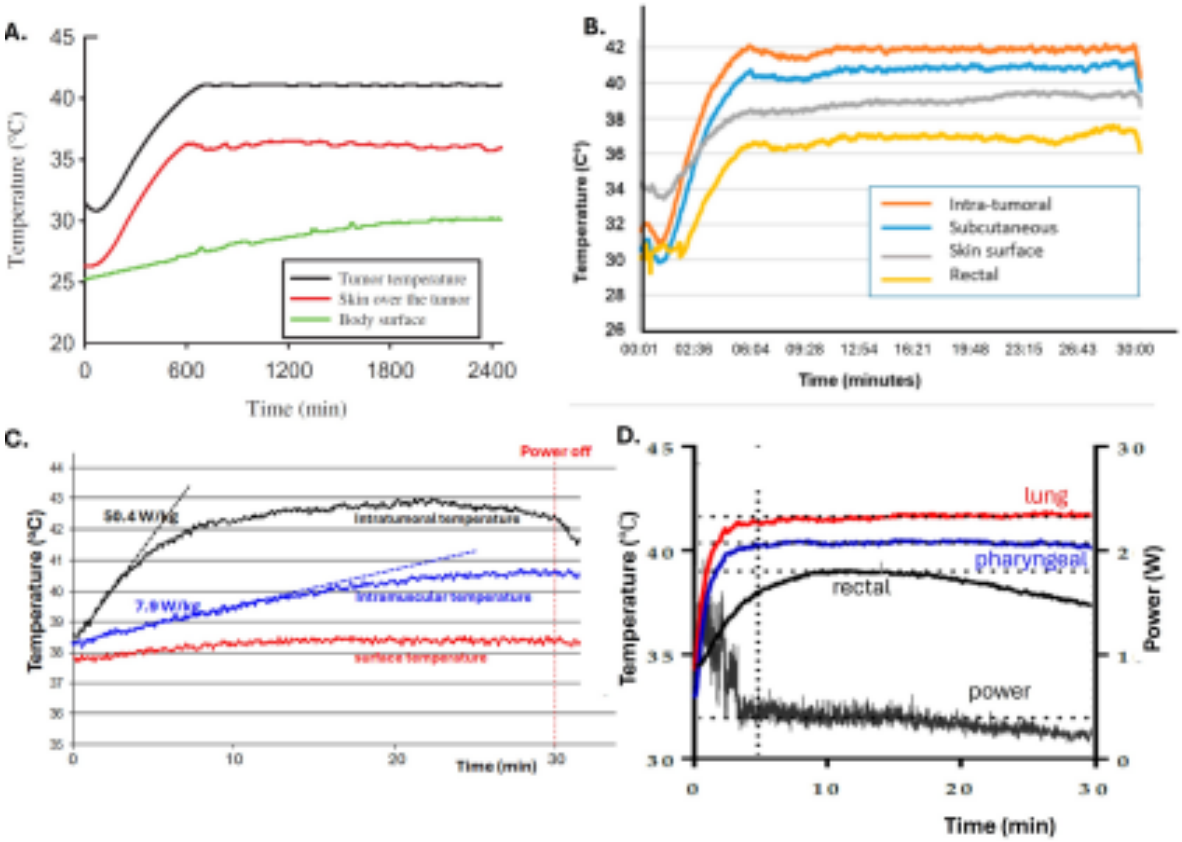

Figure 4. Typical temperature measurements (A.) FSall fibrosarcoma [18], (B.) B16F10 melanoma [30], (C.) Recurrent epithelial cell carcinoma of the lower neck region of a bull-terrier [50], (D.) B16F10 pulmonary melanoma metastasis [42].

The intratumoral temperature is usually fixed in the protocol for 42℃,(30 min treatment time), but the extratumoral temperatures vary by the animal, the tumor, and the environment Figure 5.

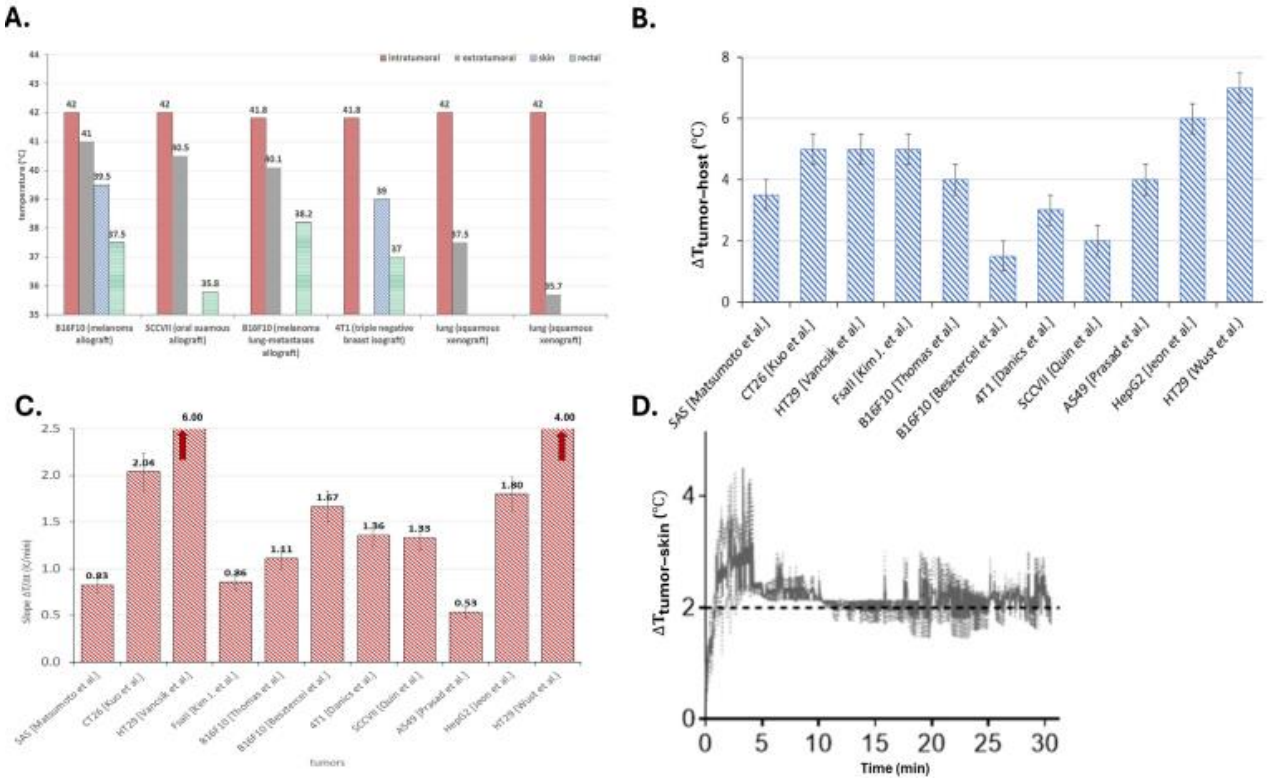

Figure 5. The thermal conditions of the various experiments. (A.) The temperature values are in different sensor locations: B1610 [30], SCCVII [45], B1610 metastasis [42], 4T1 [20], and lung squamous [33] [39]. (B.) The temperature difference between the tumor core and its surroundings: SAS [44], CT26 [29], HT29 [26], FSall [18], B16F10 metastasis [42], B16F10 [30], 4T1 [20], SCCVII [45], A549 [32], HepG2 [21], HT29 [37]. (C.) The time derivative of the temperature measures the dynamics of the temperature growth. (SAS [44], CT26 [29], HT29 [26], FSall [18], B16F10 metastasis [42], B16F10 [30], 4T1 [20], SCCVII [45], A549 [32], HepG2 [21], HT29 [37].) (D.) The skin temperature was 3°C lower than the intratumoral, but with thermal homeostasis, it stabilized on 2°C difference [20].

The thermal component of mEHT heats the target. When the power adjusted step-up for a longer time (~1000 s) from 1.5 W to 2.5 W, the steady temperature growths proportionally reaching 42°C in the tumor and ~33°C in nearby tissues after 1000 s, when the power is downregulated to 2 W [33]. This high difference between the tumor and host temperatures is caused by the cooperative changes with thermal homeostasis and relatively high cooling, which requires 2 W power to keep the temperature constant. These special conditions were used for temperature mapping in a murine model, which agrees well with the simulations. In humans, the efficacy of mild temperature hyperthermia was studied in cervical cancer, which increases the peritumoral temperature to 38.5°C, with proper blood flow for the complementary treatments [51]. The synergy of thermal and nonthermal processes induced by mEHT destroys the tumor, Figure 6.

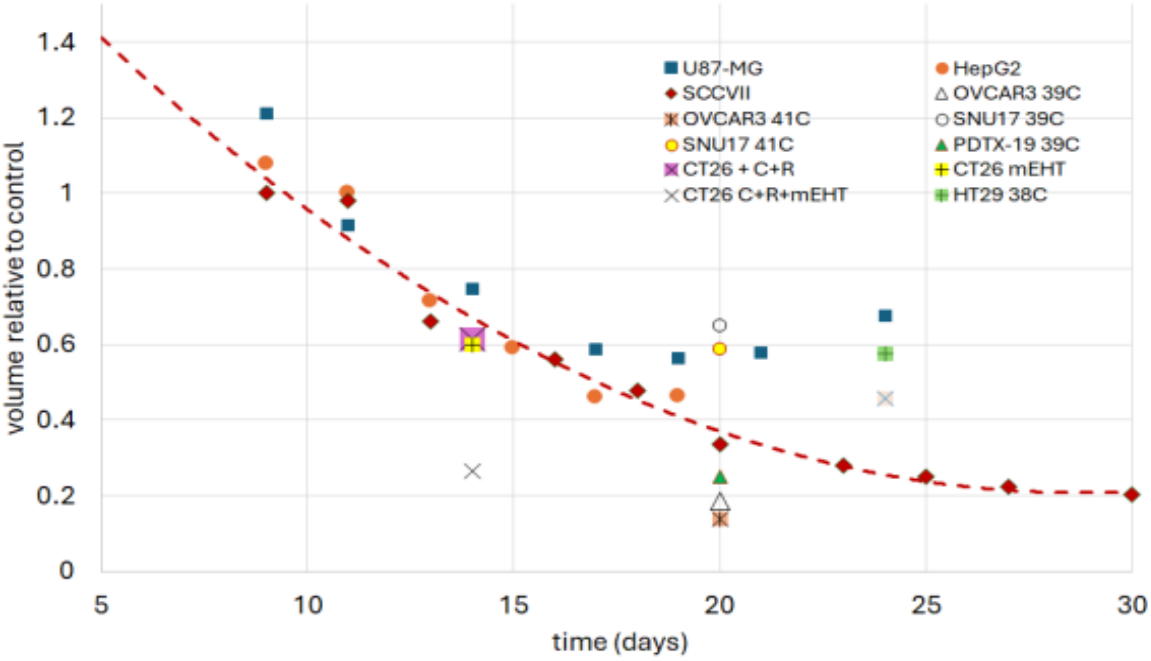

Figure 6. The tumor volume relative to control was measured in various tumors in different publications. (U87-MG [22], SCCVII [45], HepG2 [21], OVCAR [48], SNU17 [48], PDTX-19 [48], CT26 [29], HT29 [40].)

The tumor inhibition by oncothermia on human pancreatic adenocarcinoma cell line (BxPC-3) in female CD-1 mice (10-10 animals are involved). On Day 72, mice were sacrificed, and their tumors were excised and weighed. A significant difference was observed in the total weight of excised tumors between the control and treated groups. In summary, there were a total of ten treatment doses administered to each mouse (six doses in cycle 1 and four doses in cycle 2) using oncothermia [14], Figure 7. The mice responded well to the treatments, and no adverse side effects were observed. The treatment does not change the average body weight of mice. The tumor growth inhibition was 66% after the second cycle ($p < 0.0005$) measured on excised tumor weights.

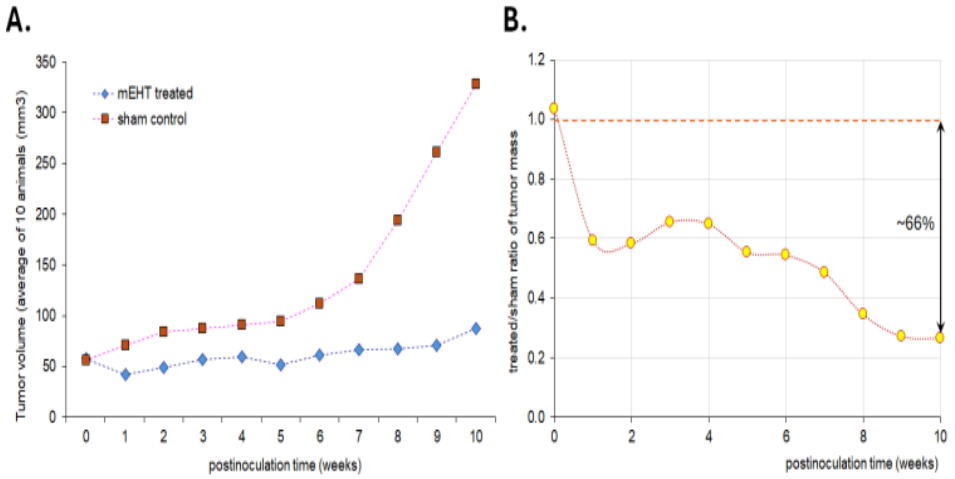

Figure 7. The pancreatic adenocarcinoma (BxPC-3) xenograft experiment [14]. (A.) The tumor volume of the treated and sham control is from the inoculation of the cancer cells. (B.) The ratio of mEHT to sham shows significant growth inhibition.

It is noteworthy that the suppression of the tumor volume may be observed at temperatures as low as 39˚C. Figure 8, measured in gynecological (ovary and cervix) tumor models. The tumor volume was significantly below the control in all cases.

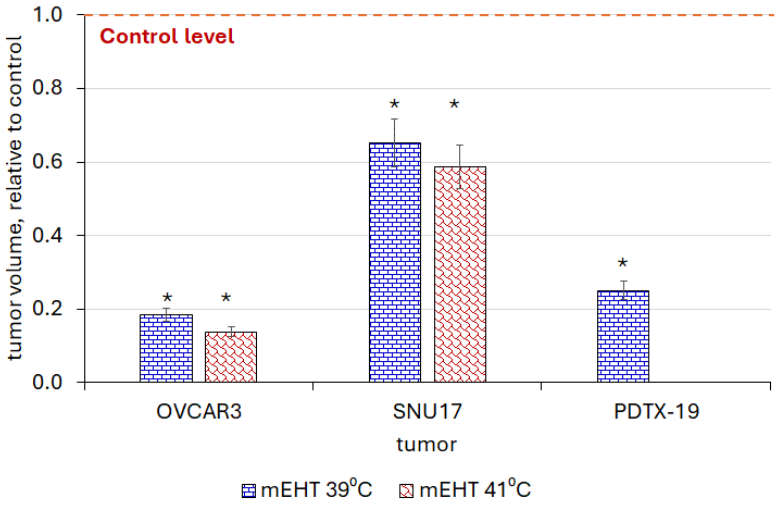

Figure 8. Temperature as low as 39˚C significantly suppresses the volume of ovarian (OVCAR-3) and uterus cervical (SNU-17, PDTX-19) tumors compared to the control in the athymic nude mice model. A 2C temperature increase reduces the tumor volume by 25% and 10% in OVCAR-3 and SNU-17 tumors, respectively [48]. The reference control is shown with a dotted line at 1.

Obtaining information about the synergy of thermal and nonthermal effects needs infrared heating [40] instead of the inapplicable water bath, which was in vitro a plausible pure thermal reference. The nonthermal addition to the thermal basis (42˚C) increased the dead tumor part ≈ 4.3 times larger than the only thermal effect in HT29 colorectal carcinoma [40], **Figure 9.** It is noteworthy to check that the nonthermal component, the difference between the mEHT treatment and control, both at 38˚C, shows a missing value to the mEHT 42˚C results are about the same as those of the measured thermal effect alone.

Apoptotic cell death dominates tumor cell destruction with intensive development of apoptotic bodies, **Figure 10.** The volume of apoptosis depends on the treatment time and rapidly grows by the posttreatment time of the mEHT. The tumor destruction ratio (TDR, %) differs between the treated and distant, nontreated tumors. Notably, the dead area in the nontreated tumor decreases over time, while the treated tumor increases it. The ratio of the dead areas became constant from 48 h to 72 h, making the distant tumors' interaction probable over time. In the early stages, the mitochondrial changes (decrease of membrane potential and opening transition pores); in the late stages, the caspase activation nucleus karyopycnosis, loss of cell membrane integrity, and DNA fragmentation occur.

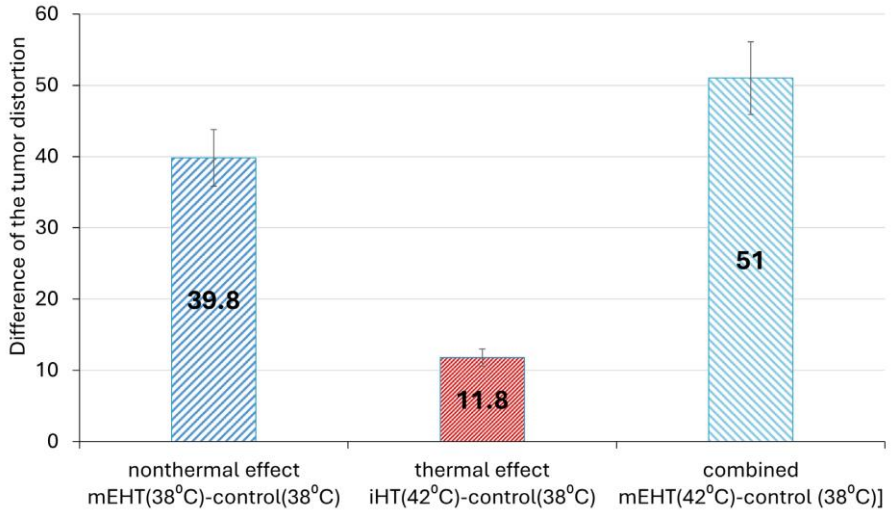

Figure 9. The comparison of thermal (infrared heating, iHT) and combined thermal and nonthermal (mEHT) effects relative to control [40]. The mEHT was done in temperatures of 38°C and 42°C, the sham control at 38°C and the iHT at 42°C. The comparison of sham and iHT shows the pure thermal effects and the mEHT (38°C to sham the pure nonthermal. The sum of thermal and nonthermal components gives the combined effects, which was measured with mEHT at 42°C, indeed.

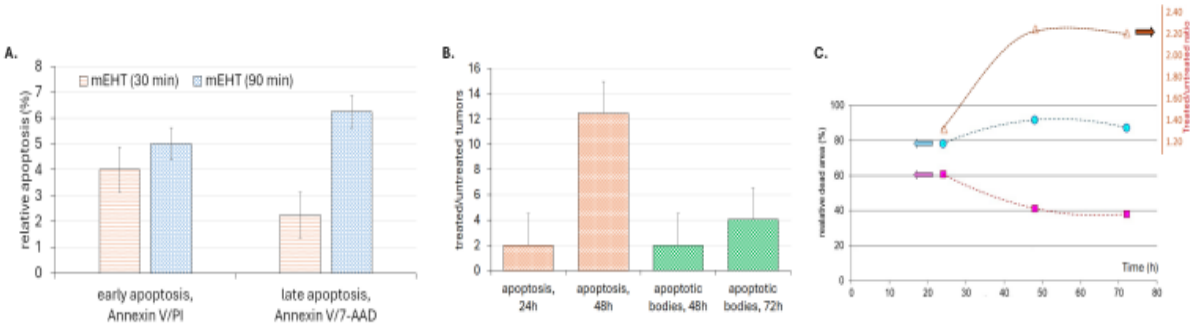

Figure 10. The apoptotic ratio of treated tumors. (A.) Early and late apoptosis (measured with Annexin V/PI and Annexin V/7-AAD, respectively) in B16F10 lung metastasis of melanoma in mice registered 24 h after treatment [42]. (B.) Late apoptosis and apoptotic bodies 24 h and 48 h after treatment of HT29 xenograft in mice [52]. The ratio of the treated and non-treated tumors in the same animals is shown. (C.) The development of the dead area (%) is treated and nontreated tumors on the same mouse [52]. The ratio of the percentages is shown in the secondary axis. The lines are guiding for the eye.

The stress-induced antiapoptotic chaperones HSP70 and HSP90 are exhausted in the cytosol [20] and turn proapoptotic by relocating to the membrane and expressing in the tumor microenvironment (TME). The internal HSPs (iHSPs) exhaustion is connected to the subsequent cell destruction **(Figure 11)**. The shifts in the time course points of different tumor entities could be only the effect of the discrete point measurements (**Figure 11(A)**). The iHSP90 has its maximum much earlier than the iHSP70 **(Figure 11(B)**), and TDR follows the iHSP expressions in their baseline return [20] **(Figure 11(C)**). The identical dynamism of the destruction and cCas-3 shows the dominance of the caspase-dependent apoptotic pathways in 4T1 tumors [20]. Notably, the significant development of chaperoning iHSPs was a few hours posttreatment, indicating that the combined stress of the mEHT treatment excited intracellular processes, which induced the chaperone activity.

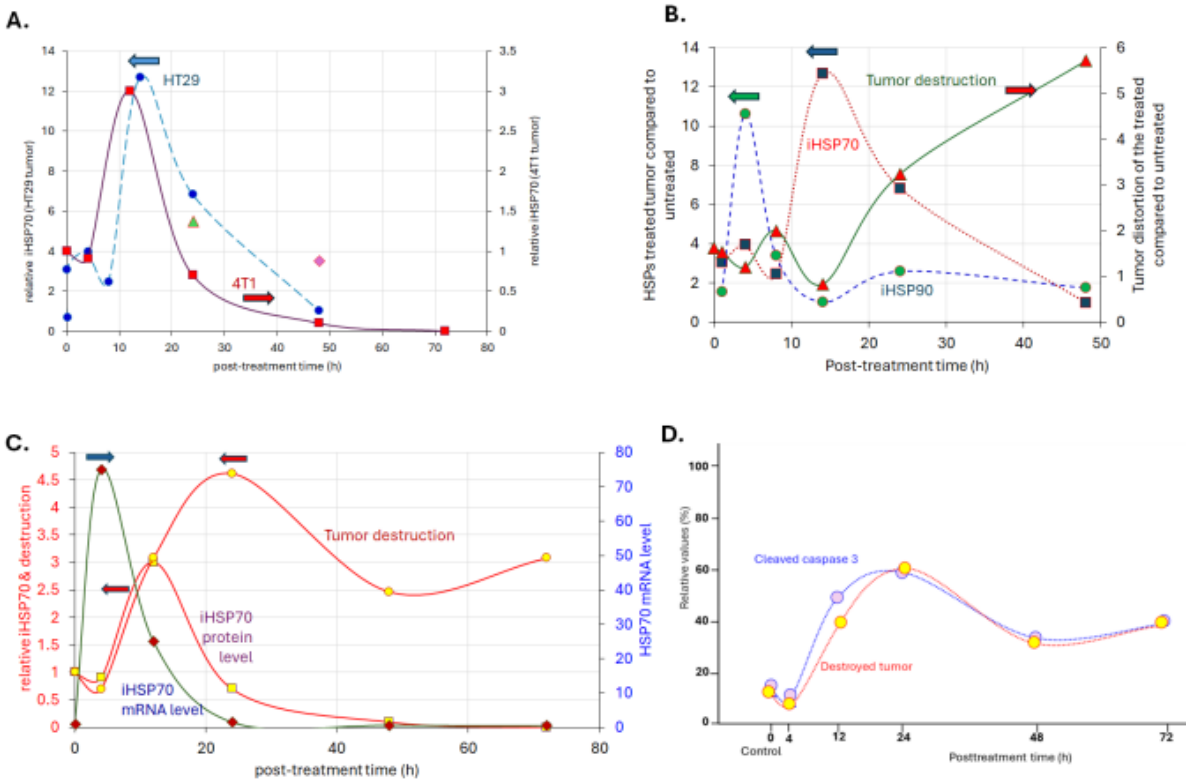

Figure 11. The HSP chaperons and the cell destruction by time-course experiments. (A.) iHSP70 development in HT29 [24] and 4T1 [20] tumors. Other measurements in single time point 24 h (4T1 tumors, ▲, [43]), and 48 h (B16F10 tumors, ♦, [30]) are also shown. (B.) The progressing dynamism of iHSP70 and iHSP90 with cellular distraction [23] [24]. (C.) The iHSP development in mRNA and protein levels was followed by the destruction of the 4T1 tumor [20]. (D.) the cCas-3 and the tumor-destruction dynamisms are identical [20].

The gene study 4 h post-mEHT (42˚C, 30 min) treatment of HT29 tumor xenograft showed significant differences between the wHT and mEHT at the same 42˚C temperature, and both significantly altered from the sham control [24] **(Figure 12)**. The mEHT mostly upregulates the expression of iHSPs at the mRNA level. The HSPA1A, HSPA6, and HSPA8 genes encode various HSP70 family members (proteins 1A, 6, and 8, respectively). The HSPD1 and HSPH1 genes encode HSP60 and HSP105 chaperons, respectively. The death receptor D6 (TNFRSF21) is upregulated, and the surface receptor activator of osteoclasts, RANK (TNFRSF11), as well as Calpain 1 and 9, which support the cell autonomy and defecting the cytoskeleton, are downregulated. The BAG gene encodes the cochaperone of HSP70, and the EGR1 gene encodes a transcription factor protein, which is involved in multiple upregulated apoptotic processes. In general, we conclude from the gene map analysis that the mEHT strongly supports the apoptosis of the selected tumor cells and destroys the tumor “softly”. Nonnecrotic destruction helps liberate undeformed intracellular information from the dying cell, which could trigger antitumoral immune processes. Some other gene mapping [21] [22] [43] strongly support the above observations in vivo, which was also seen in vitro [53]. The gene map shows a distinct difference in the gene regulations between the homogeneous wHT and inhomogeneous mEHT treatment sat the same 42˚C temperature. Injection of NR4A3 or KLF11 siRNA into mouse A549 lung xenograft tumors knock down the effectiveness of RT and its combined application with mEHT [47], revealing some aspects of the mechanism of sensitization of A459 tumors for RT and mEHT in xenograft experiments.

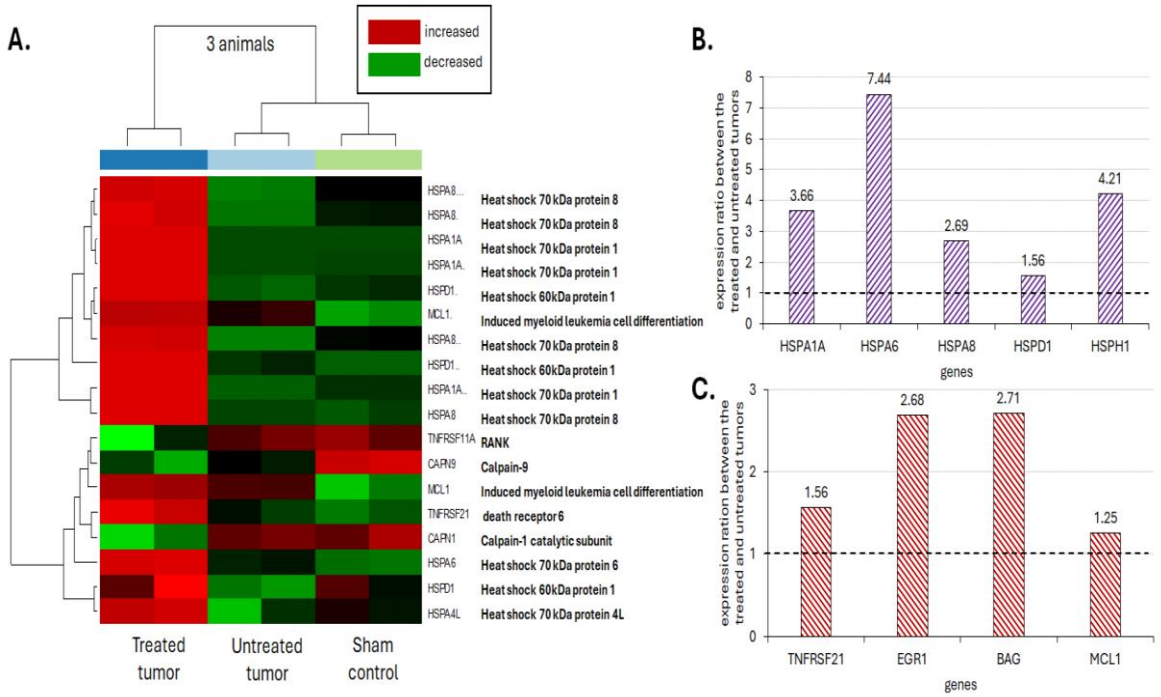

Figure 12. The mRNA gene chip results from some primary players of the mEHT effect. (Affymetrix 3′ IVT Express Kit (Affymetrix, Santa Clara, CA, USA). Samples were hybridized on HGU133 Plus2.0 arrays [24]. Pooled samples from 3 animals. (A.) The massive upregulation of iHSPs and death receptor D6 together with the proapoptotic MCL1. (B.) The values of the up regulation of iHSP genes. (C.) Some other up regulated genes help the apoptotic processes.

The protein expression (Proteome Profiler Human Apoptosis Kit) of HT29 tumor in xenograft experiments, 8 h, 14 h, and 24 h after mEHT treatment (42°C, 30 min) shows many proteins, including pro and anti-apoptotic sets. 8 h posttreatment, the transmembrane excitation of the extrinsic pathway shows an increase of TRAILR2/DR5 and FAS-FADD complex and enhanced expression of antiapoptotic proteins, which activity drastically reduced at 14 h and further at 24 h posttreatment observations. The catalase protein remains active after 24 h, which probably regulates ROS production to the level necessary for proper apoptosis to avoid necrosis. All other proteins remain under the reference level after 24 h posttreatment of HT29 xenograft measurement **(Figure 13)** [52].

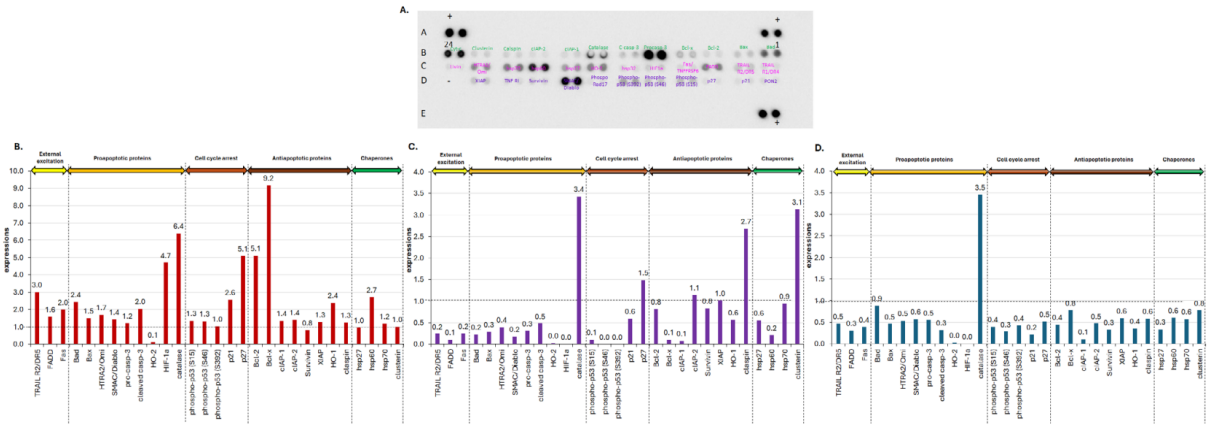

Figure 13. Relative expressions of proteins play a majority role in apoptotic processes [52]. The baseline is shown with dashed lines at 1. (A.) The matrix of the Proteome profiler human apoptosis kit array. (B.) 8 h after mEHT treatment. (C.) 14 h after mEHT treatment. (D.) 24 h after mEHT treatment.

The cyclin-dependent kinase (CDK) inhibitors p21 and p27 are highly activated in the first 6 h after mEHT treatment and assist apoptosis by acting at different stages of the cell cycle as checkpoint controllers under the regulation of the p53 tumor-suppressor protein. The p27 CDK remains activated at 14 h posttreatment, preventing premature DNA synthesis. When the cell encounters stress like DNA damage, p53 becomes activated and plays a critical role in deciding cell fate. It can trigger cell cycle arrest to allow for DNA repair or initiate apoptosis (programmed cell death) if the damage is too severe. The activated p53 may trigger apoptosis by initiating proapoptotic genes and inhibiting antiapoptotic genes. The base form is the unphosphorylated p53 protein, which has modifications by the phosphate group (PO4) bonded to serine (S) amino acids at positions 15, 46, or 392, modifying its regulatory mechanisms. Phospho-p53 (S15) increases the p53 protein stability and enhances the ability to bind to DNA and activate its target genes. The phospho-p53 (S46) promotes apoptosis, and the phospho-p53 (S392) is involved in transcriptional activation and potentially modulates its role in cell death pathways independent of transcription. The mEHT treatment significantly increases the expression of p53, p21, and p27 proteins in various tumors of treated mice, while the wHT effect is moderate, **Figure 14.**

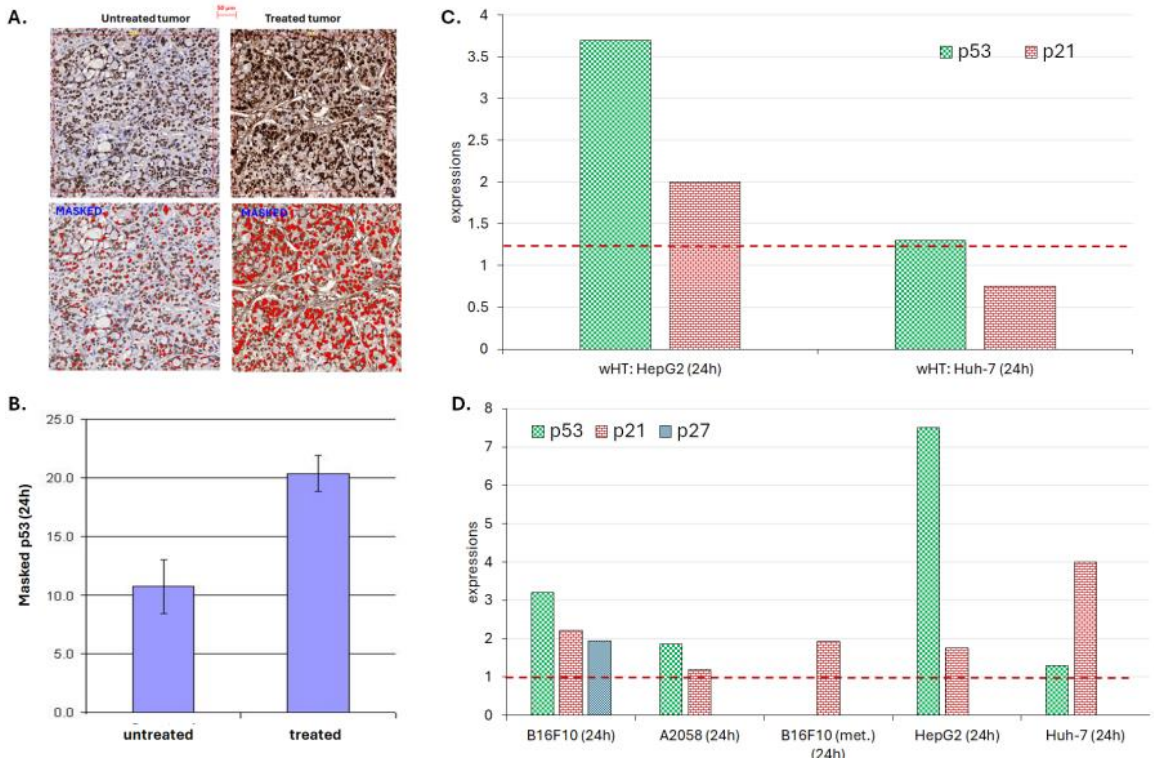

Figure 14. The expression of p53, p21, and p23 proteins in various tumor types. (A.) Immunohistochemical pattern of p53 protein 24 h after treatment on HT29 xenograft [54]. (B.) The masked p53 was significantly higher in the treated tumor than the untreated one in the same animal [54]. (C.) Development of p53 and p23 proteins 24 h after wHT[21]. (D.) Expressions of p53, p21, p27 proteins in various tumors 24 h after the mEHT treatment. (B16F10 [30], A2058 [28], B16F10 metastasis [42], HepG2 [21], Huh-7 [21]).

The mEHT extrinsically excites pathways for apoptosis [4] [55]. The extrinsic signal starts in the TRAIL death receptor with FADD and FAS complexes [38]. The TRAIL signaling, as usual in complex systems, has a dual effect, being pro-or antitumoral, depending on the TME conditions [56]. The membrane fluidity increases due to thermal effects [57]. Investigating the thermal and nonthermal complexity of apoptosis shows that the mEHT excites numerous apoptotic pathways in the cell, **Figure** 15. The optimally modulated carrier signal directs the TRAIL to be proapoptotic. Massive apoptosis is noted with mEHT treatments, likely following the caspase-dependent extrinsic signal pathway with Caspase-8 (Cas8). The path may split towards the Cas3 followed by apoptosis (Cas8 Cas3 apoptosis → →), or to mitochondria by signal transfer of BID protein. Mitochondria may ignite the intrinsic signals for apoptosis [20]. The intrinsic path has two options: it could be caspase-dependent (through Cas9), involving apoptosis-inducing factor (AIF) [23] [58]. AIF is usually located in the mitochondrial intermembrane space, but it is translocated to the nucleus, generating chromatin condensation and DNA degradation, providing an additional signal pathway for apoptosis. This process has the potential to affect untreated tumors as well. A notable factor is the arrest of the XIAP effect to block the main path of caspase-dependent apoptosis by the secretion of SMAC/Diabolo [38] and Septin4 [21]. The ignited nonthermal chemical processes are massively gained by the thermal conditions, producing a complex network resulting in apoptosis.

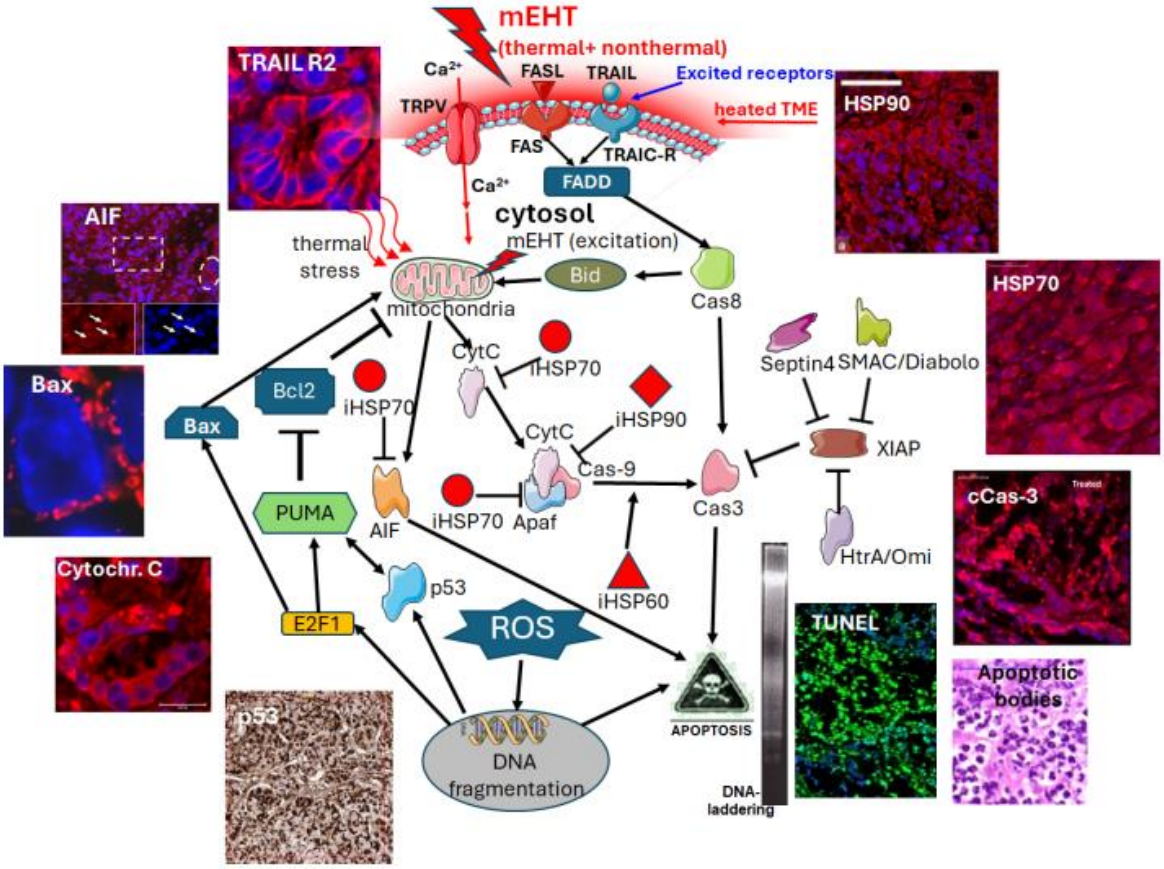

Figure 15. The mEHT excited apoptotic pathways. Some immunohistochemical results are shown around [23] [24] [52]. The main apoptotic pathways, without detailed molecular involvements. Multiple pathways may cause apoptosis after the mixture of thermal and nonthermal energy absorption. The protective mechanisms of intracellular HSPs exhausted, and the network of multiple possible pathways executes the apoptotic process.

Thermal stress strongly supports the intrinsic apoptotic pathway through BAX and cytochrome c (point of no return), finishing the apoptosis through the cleaved Cas3 (cCas3) path. DNA fragmentation drives tumor-cell degradation [59]. The induced stress by mEHT upregulates the tumor suppressor p53 protein, one of the key cell-cycle regulation and DNA repair players. The p53 "master switch" drives the DNA fragmentation and the appearance of apoptotic bodies.

Noteworthy that mEHT also destroys the tumor stem cells in the U87-MG and A172 human glioma cells inoculated into BALB/c nude mice xenograft [22].

The appropriately chosen modulation may trigger resonant excitations of the transmembrane proteins, excite the TRAIL R2 (DR5) death receptor, and activate the apoptotic pathway. Despite the increased expression of iHSPs, the mEHT inhibits tumor growth and supports apoptotic processes [25]. The expression of HSP70s has its maximum at around 12 h posttreatment. The extremely large complex thermal and non-thermal stresses exhaust the HSP protective response [20]. The intracellularly overproduced antiapoptotic HSPs relocate to the cell membrane or are released to the TME. The exhausted HSPs cannot block the apoptotic process [20]. Another antiapoptotic protein, the XIAP, is arrested by Septin-4 [21], SMAC/Diabolo, and HTRA-2 proteins in HT29 xenograft treated with mEHT 42°C 30 min. [52]. The development of the primary components was measured by immunohistochemistry of resected tumors of the sacrificed animals, **Figure 16.**

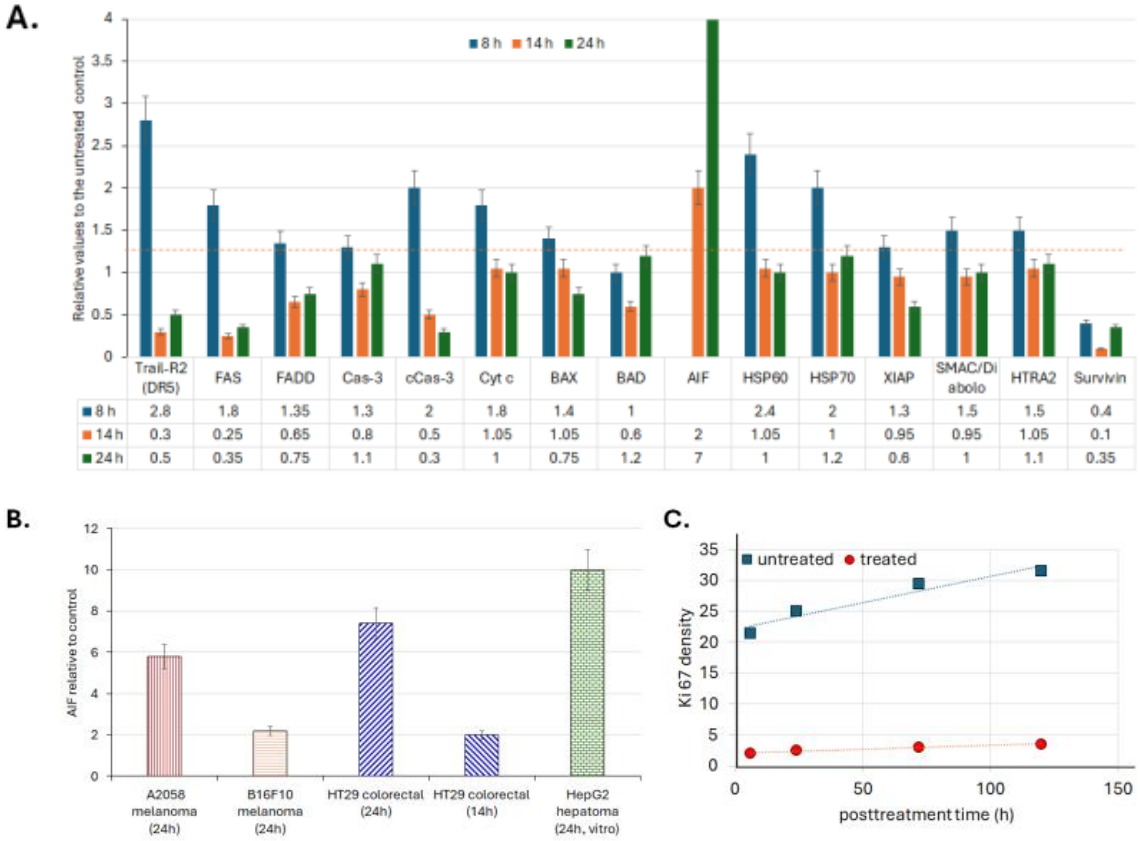

Figure 16. Mayor molecules are involved in the mEHT-induced apoptotic process. (A.) The development is shown 8 h, 14 h, and 24 h after treatment in HT29 xenograft [52]. (B.)

The caspase-independent AIF pathway in A2058 [28], B16F10 [30], HT29 [23], and HepG2 (in vitro [60]) tumors. The Ki67proliferation marker protein, expressed in the nuclear membrane only in the dividing cells, is strongly suppressed (about one order of magnitudes) by mEHT in rat glioma (L9) [49].

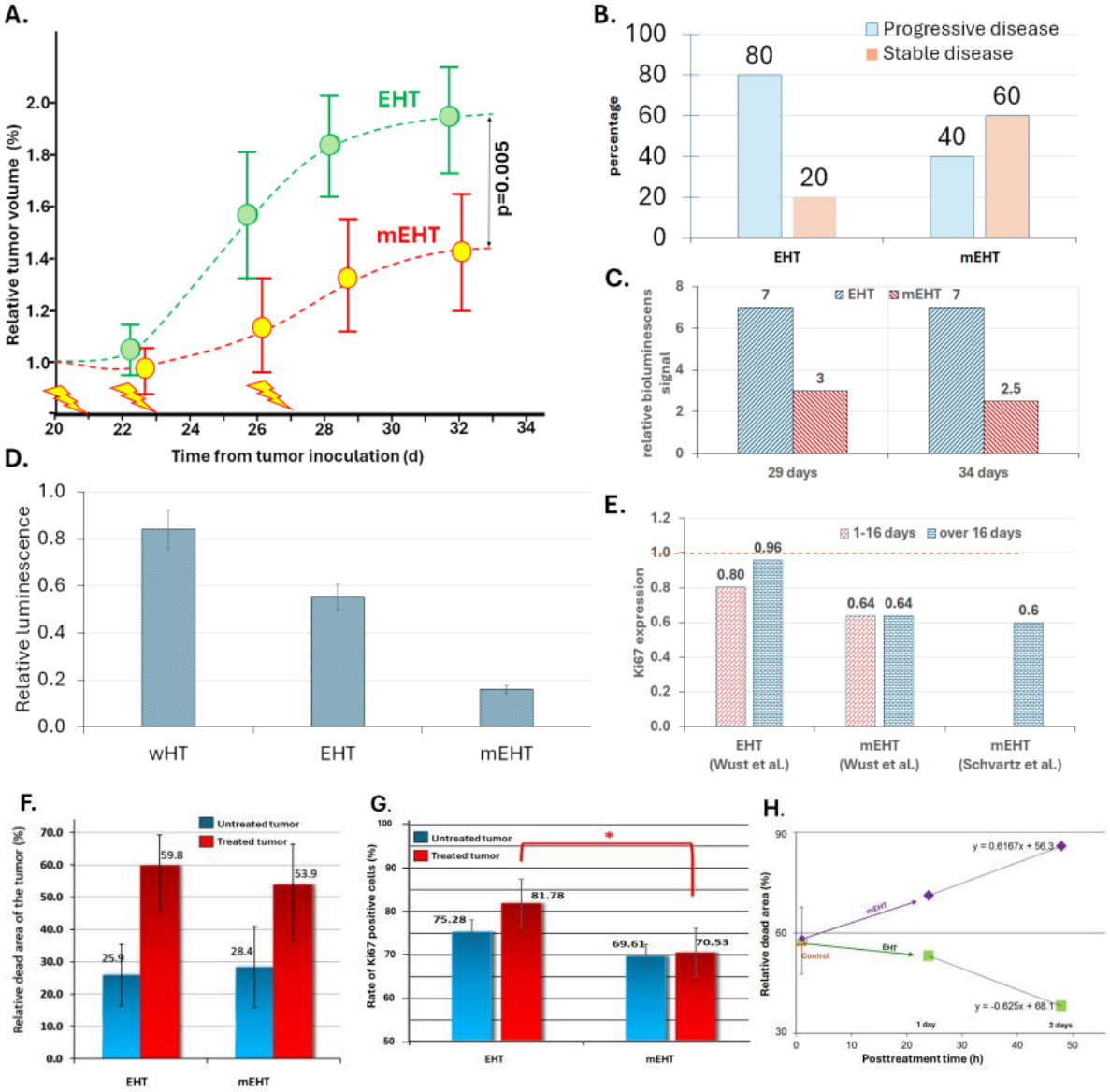

Figure 17. Effect of modulation in mEHT treatment [37]. (A.) Changes in relative tumor volume after inoculation of HT29 tumor. After 5 days of the last (3rd) treatment, the difference became significant between tumor distraction by EHT and mEHT. (B.) The development of the diseases also favors modulated treatment. (C.) Between the 29th and 34th days, the dereference is stabilized. Compared to wHT, the unmodulated EHT has the advantage of tumor growth measured by the non-invasive bioluminescent method. (E.) The Ki67 proliferation marker is significantly suppressed in mEHT compared to EHT, which is proven by 4T1 tumors [43], too. (F.) The modulation effect in mice with double-distant C26 colorectal tumors inoculated in the two femoral regions. The right side was treated while the left was regarded as a control [65]. (G.) The Ki67 proliferation marker significantly decreases with the treatment in both (treated and untreated) tumors of the same mouse [65]. However, the modulation has no significant difference from the unmodulated one in C26 tumors. (H.) The relative dead area in the middle cross-sections of the isolated tumor was taken from both sides after treatment on only one side. The

difference became obvious by the elapsed time: the treated tumor shrank further, increasing the dead area, while the untreated grew in HT29 tumors [66].

The amplitude modulation of the carrier frequency signal (13.56 MHz) increases the effective value of the electric field of mEHT. It supports the cytoskeleton's polymerization and the reorganization of the cytoskeletal network. Cytoskeletal polymerization has a significant effect on cancer cells, which inhibits cellular plasticity and cell migration. The 1/f fractal noise modulation introduces a huge amplitude increase at the carrier frequency, increasing its selective excitation facility. The noise modulation approach is like the harmonizing method [61], whose application is emerging in physiology [62]. The modulation may promote the execution of the enzymatic processes [63], modifying the transition between the initial and final states of molecules [64]. The applied modulation orchestrates the spatiotemporal order of the exported molecules to the TME and may trigger resonant excitations of the transmembrane proteins and extrinsically excite signal pathways for apoptosis. The benefits of modulation appear compared to the unmodulated (EHT) treatments (**Figure 17**). [37] Modulation experiments with the mice having two distant tumors in their femoral regions also show the advantage of the modulation [65] [66], **Figure 17(F), Figure 17(G), Figure 17(H).** The pulsing modulation pattern further improves tumor destruction [19],

Figure 18. The pulsed signal significantly increases apoptosis (suppresses the Ki67 proliferating marker), decreases the growth rate, and develops fewer antiproliferative iHSP70 chaperones.

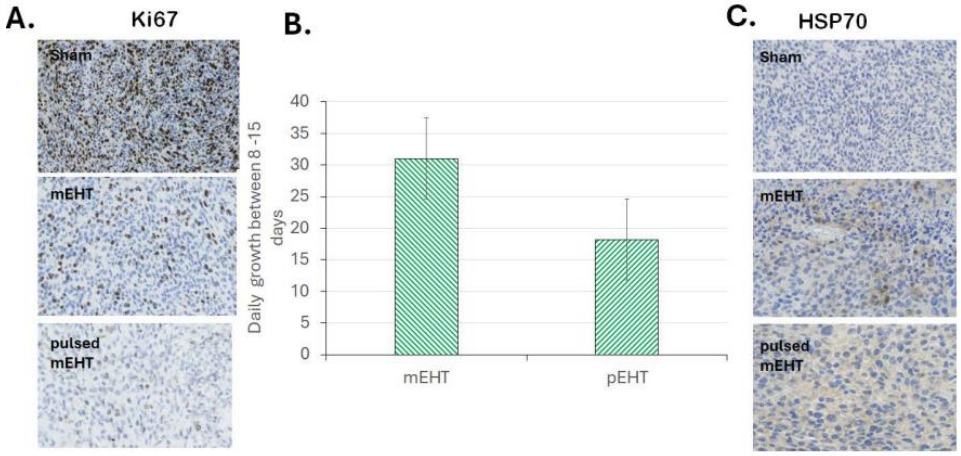

Figure 18. Effect of pulsed modulation measured in RG2 (D74) glioma is Fisher rats [19]. (A.) Ki67 proliferation marker. (B.) The growth of the tumor between 8 - 15 days. (C.) Development of the iHSP70 in different treatments.

The thermal component of mEHT acts in synergy with the electric excitation, affecting the repair of DNA. The induced upregulation of cyclin-dependent kinase inhibitor protein (1 21waf p) and the reduced Ki67 proliferation marker correlates with the expression of the γ H AX 2 , which is a sensitive molecular marker of DNA damage, **Figure 19.** When p27 was unsuccessful in inhibiting premature DNA synthesis, the double-strand break (DSB) in DNA (shown by the γ H AX 2) leads to apoptosis in mEHT-treated tumors [30] [42]. mEHT activates DSB production.

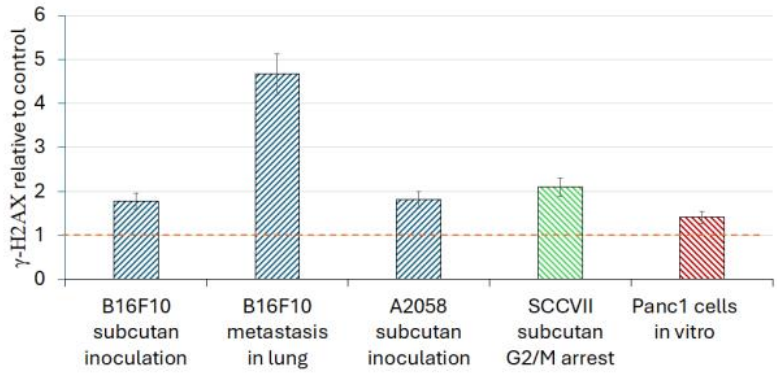

Figure 19. The relative expression of the γ H AX 2 in various tumors developed by inoculation of cancer cell lines. The reference level is 1, indicated by a dashed line. (Subcutaneous B16F10 [30], metastatic B16F10 [42], subcutaneous A2058 [28], subcutaneous SCCVII [45], and Panc1 (*in vitro*) [67]).

DNA damage by DSB could be promoted with an ionization beam of RT in complementary applications with mEHT. The TDR with RT + mEHT combination shows a significant decrease. The tumor volume increase is inhibited more in combined treatment than in standalone treatments, and survival decreases most rapidly in combined therapy of mice [44], Figure 20. The only thermal treatment with RT (RT + wHT) does not show the same inhibition of tumor growth as the RT + mEHT does.

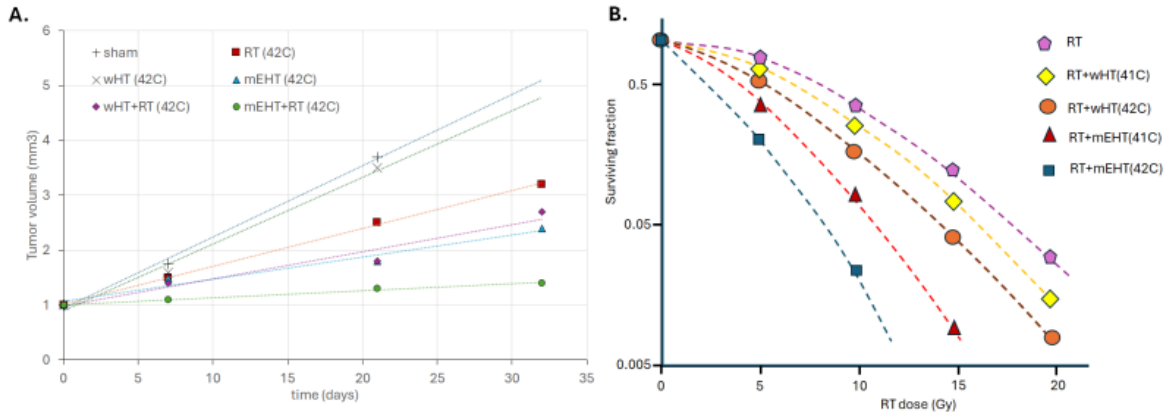

Figure 20. Growth inhibition with complementary RT + mEHT treatment combination for mice having tumors by inoculated SAS cancer cells. (A.) The RT + mEHT combination slows the growth of tumor volume. The tumor volume practically did not change in 32 days after treatment, while RT alone or its combination with wHT had 2+ times higher growth rate. (B.) The surviving fraction of various treatment modalities shows the superiority of RT + mEHT.

The equivalent dose for apoptosis was determined [32] in **Figure 21** for tumors of A549 and NCI-H1299 cells in BALB/c nude mice in a xenograft experiment. The amount of apoptosis was the same with RT and mEHT on tumors by inoculated A549 cells five days posttreatment (mEHT standard before RT (42˚C, 30 min)/session, RT standard 5 Gy/fraction, daily 2 times). The equivalent dose calculation used the in vitro determination of linear-quadratic equations from cell survival curves at standard RT + mEHT treatment: $\alpha_{A549} = 0.5318$, $\alpha_{NCI-H1299} = 0.5141$, and $\beta_{A549} = 0.0283$, $\beta_{NCI-H1299} = 0.0163$.

The α value in vivo linearly depends on the temperature with a slope 0.005 $\frac{1}{Gy \cdot ^{\circ}C}$ starting from α = 0.056 at 40.5°C. The apoptosis relative to the control did not show differences between the standard RT and mEHT treatments, but their combined treatment showed ~20+% more apoptosis than the addition of the two independently obtained values (**Figure 21(A)**), which supports that the combination is not additive but synergetic. The mEHT equivalent changes by temperature, starting with 20 Gy at 37°C and almost doubling to 42°C (**Figure 21(B)**).

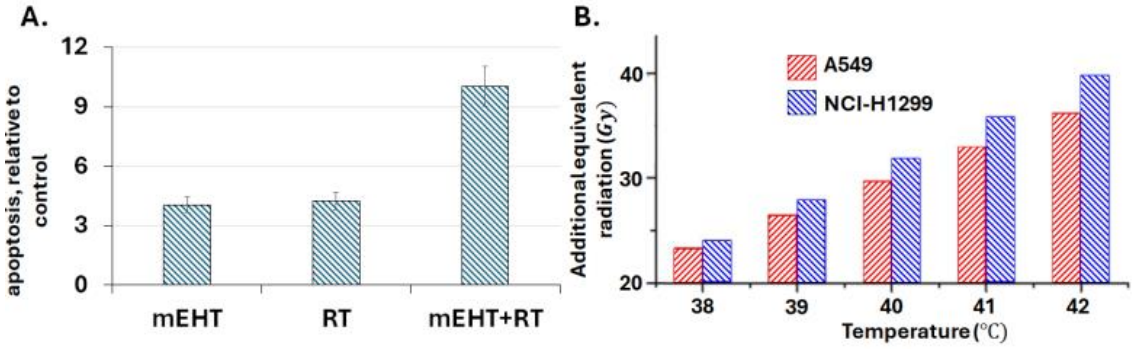

Figure 21. The equivalent dose determination [32]. (A.) Apoptosis measurement compared to the control. (B.) The equivalent radiation dose to addition to 20 Gy at 37°C baseline.

The measurements of oxygenation (p O2) before and right after the mEHT treatment showed a 78% increase in the p O2 value on the treated side compared to untreated in Fisher rats with inoculated L9 glioma cell line in double tumors [68]. This increase supports the complementary therapy with RT. The mEHT generally increases blood flow in tumors, as shown in cervix tumors [51], and the higher blood flow increases oxygenation. On the contrary, the RT decreases blood flow due to damaged vessels, consequently increasing hypoxia in addition to hypoxic tumors. Hypoxia activates the hypoxia-inducible factor-1α (HIF 1- α) and the homeostatic regulation induces vascular endothelial growth factor (VEGF) to revascularization and could promote tumor recurrence. HIF-1α can interact with the tumor suppressor protein p53, potentially leading to increased p53 activity and downstream pro-apoptotic signalling. While RT (15 Gy) alone upregulated the HIF-1$\alpha\alpha$ mEHT with 41°C, 30 min treatment suppressed it together with the VEGF in FSalltumors of C3H mice [18]. The mEHT promoted the apoptosis of tumor cells and suppressed the tumor growth rate, **Figure 22.**

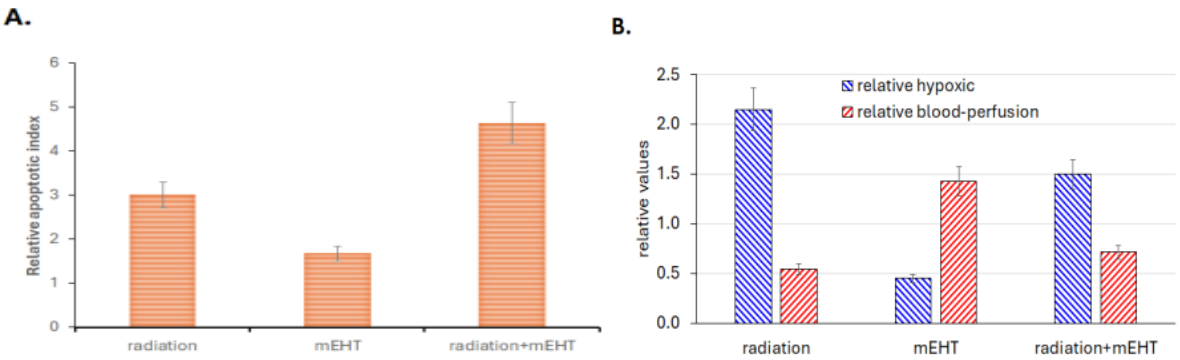

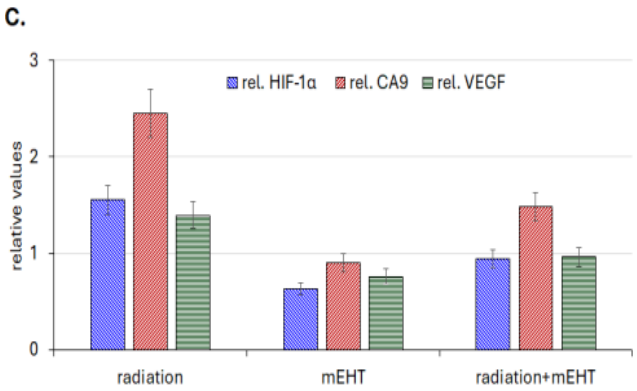

Figure 22. The synergy of RT (15 Gy) and mEHT (41°C, 30 min) combined application [18]. (A.) Apoptosis, relative to control. (B.) Relative hypoxia and blood perfusion in the targeted tumor. (C.) The relative HIF-1α, CA9 (Carbonic anhydrase IX, CA9, having a significant role in tumor acidification) and VEGF.

Electrical stimuli increase the penetration of drugs like doxorubicin [69] in vivo, and the application of electromagnetic fields has been shown clinically to increase the sensitivity of cells to the effects of chemotherapies such as paclitaxel and doxorubicin [70] [71]. The complementary application of mEHT with chemotherapy improves the cellular destruction of the targeted tumors. The therapeutic effect of thermosensitive liposomal encapsulated doxorubicin (LTLD) was studied in BALB/c mice with tumors inoculated with 4T1 triple-negative breast cancer (TNBC) [46]. The variants of administered doxorubicin (free doxorubicin, (DOX); PEGylated liposomal DOX, (PLD); and LTLD) were compared by their DOX accumulation in tumors after mEHT. The TDR increased significantly by mEHT treatment and further grew by DOX, PLD, and LTLD in that order. The LTLD practically destroyed the complete tumor measured 24 h after the 3rd mEHT treatment. The tumor destruction was massively apoptotic through the cCas-3 signal pathway, which was measured linearly with TDR. The apoptotic process was also indicated by the significant decrease of the Ki67 proliferation marker on the nuclear membrane of the dividing cells [46], **Figure 23(A).** The LTLD success shows the importance of the thermal effects for thermosensitive liposomes. In another model, murine colon carcinoma-inoculated CT26 cells were measured and treated with only thermal (wHT) and complex thermal and nonthermal (mEHT) effects [34]. While the thermal effects are effective, its synergy with nonthermal processes in mEHT doubles the release of doxorubicin. The mEHT significantly enhanced the uptake of liposome-encapsulated doxorubicin in BALB/c mice. Noteworthy that the liposomal envelope did not release the doxorubicin in the extracellular matrix but was directly liberated in the cytosol of tumor cells, **Figure 23(B)**. In consequence, the tumor growth was significantly suppressed by mEHT, indicating the efficacy of the nonthermal component of the energy absorption. The effect of the thermal factor was earlier also proven by wHT treatment at 39°C - 40°C [72].

Other complementary applications with pharma products also show the advantage of the mEHT. The metformin increases the efficacy of mEHT (41°C) +RT (15 Gy) complementary application in FSall fibrosarcoma in C3H mice. The apoptotic index and cCas-3 grow parallel with the metformin administration, showing the caspase-dependent apoptotic pathway in this tumor [31]. The metformin suppresses the expression of HIF-1α, VEGF and PD-L1, increasing the efficacy of the standalone treatments, **Figure 24.**

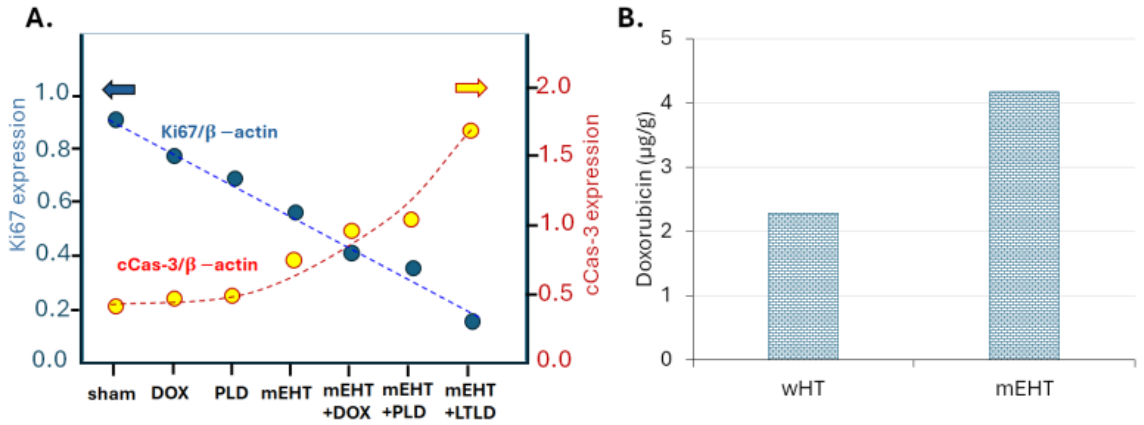

Figure 23. Application of mEHT for liposomal doxorubicin preparations [34] [46]. (A.) The development of cCas-3 and decreased Ki67 were shown with different treatments of 4T1 TNBC tumors in mice. The TDR develops proportionally with cCas-3 [46]. (B.) The release of doxorubicin in the tumor by wHT and mEHT [34]

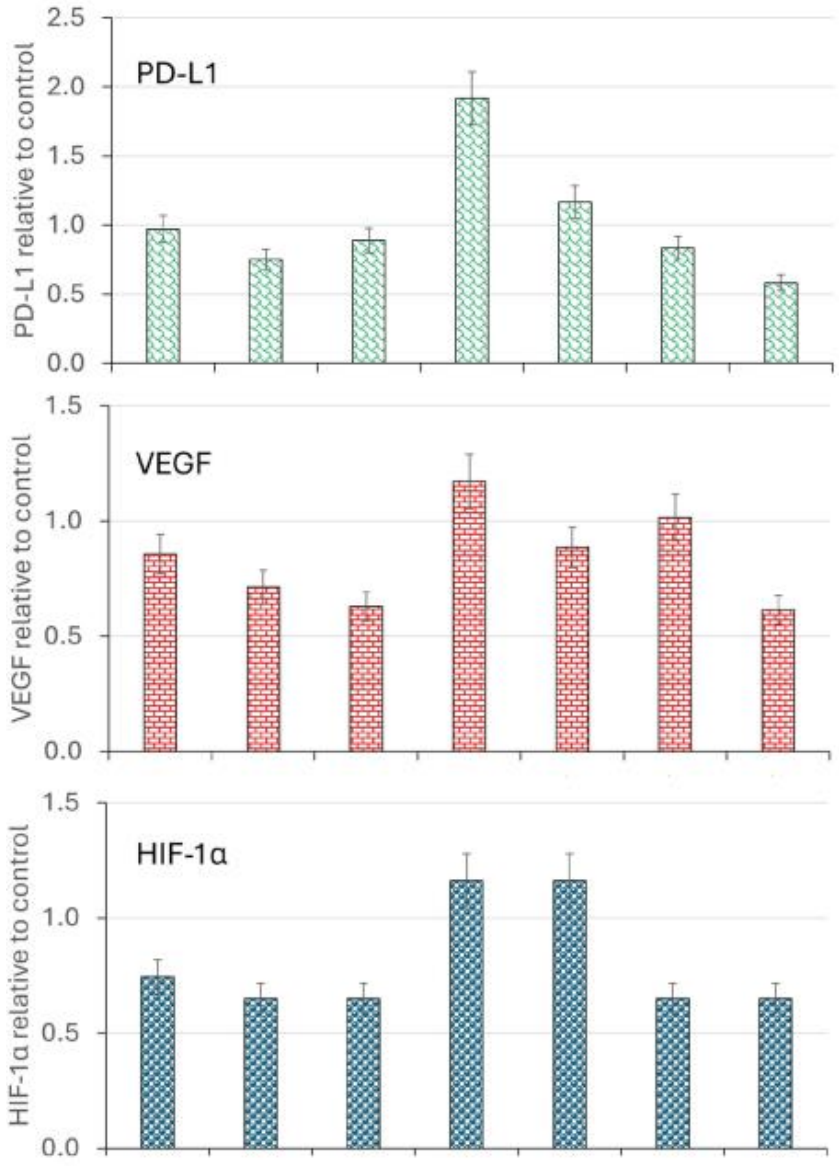

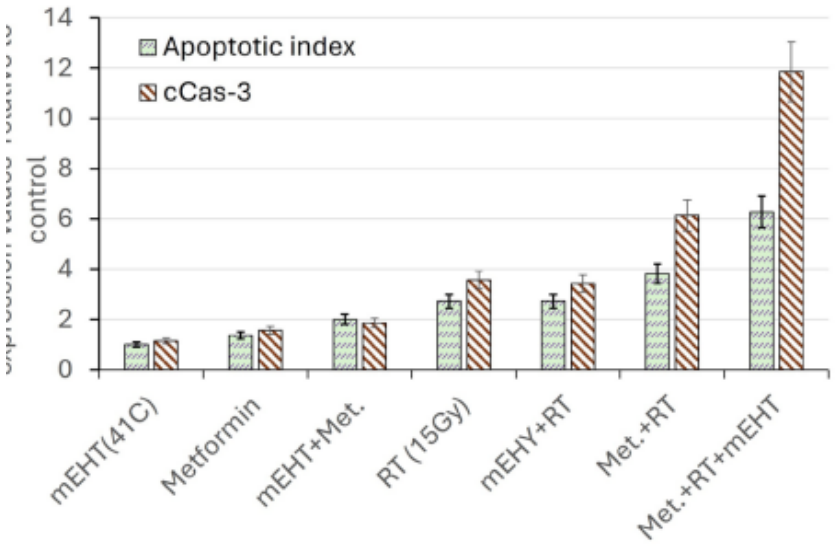

Figure 24. Complementary application of mEHT with Metformin medication. The results are from the 5th day after treatment [31].

Curcumin and resveratrol, effective antioxidants and immune activators were added as medications during the mEHT treatment period of inoculated CT26 cells forming allograft tumors in BALB/c mice. The added medication significantly induced cell cycle arrest and apoptosis of CT26 cells, significantly decreasing the weights of the excised tumors from the euthanized animals [29], **Figure 25.** The mEHT significantly elevated the serum concentrations of curcumin and resveratrol. The combination induced HSP70 expression while recruiting CD3+ T-cells and F4/80+ macrophages [29].

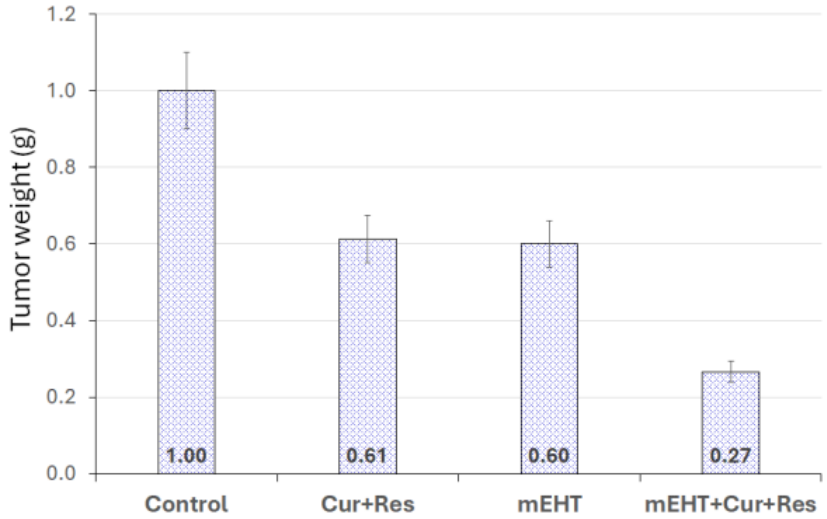

Figure 25. Effect of curcumin and resveratrol on tumor weight excised from the euthanized animals.

Preclinical animal experiments on dogs and cats have a notable advantage because the tumors are naturally developed, not inoculated to the animal. The mEHT treatments of dogs show successful tumor degradation proven by various diagnostic methods, including imaging controls [13]. The treatments of dogs showed significant shrinking of tumors and considerable improvement in the quality of life of the animals [13]. These preclinical treatments, together with the validation of the

method, help to optimize the technical solutions of mEHT because the body size of the animal is much larger than that of the rodents, and some of those approach human size, **Figure 26.** Consequently, these studies can be transferred directly to human clinical applications to develop more precise treatment systems for clinical oncology.

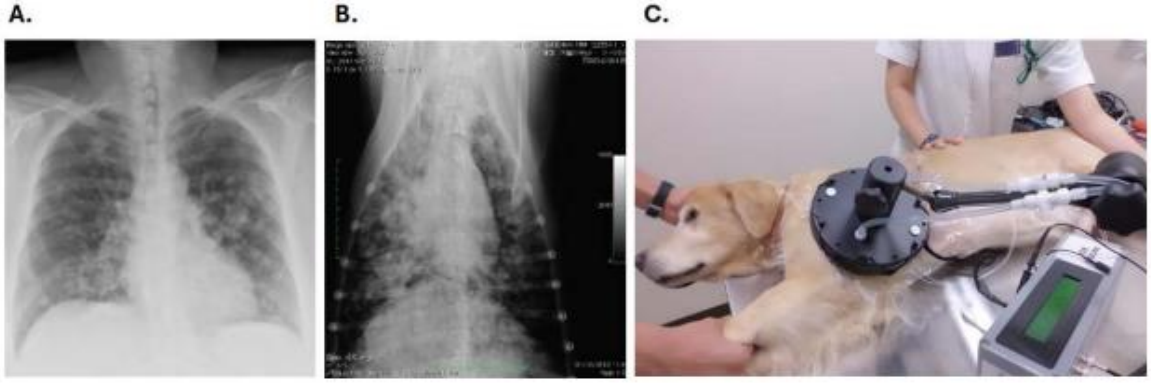

Figure 26. The similarity of the clinical imaging of humans and companion animals. (A.) Pulmonary metastases from recurrent melanoma in a human patient (image courtesy of Dr. DG. Borgeson), (B.) The same lung metastasis of melanoma in a Labrador dog [13]. (C.) mEHT treatment of a dog having pulmonary melanoma metastasis.

Numerous successful veterinary cases were observed [73]. Many cases were treated with mEHT after first or second-line unsuccessful surgery and/or chemotherapy, **Figure 27.**

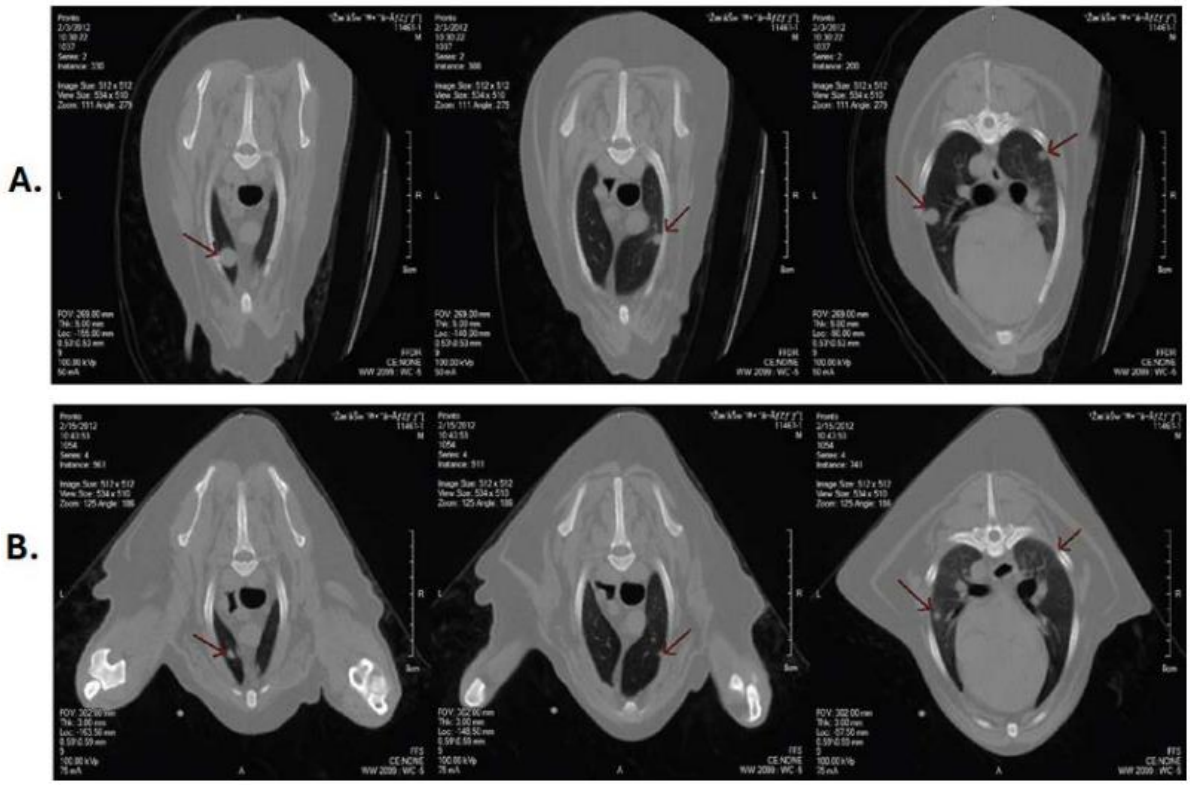

Figure 27. X-ray image of the lung metastasis of melanoma of an 8-year-old male Cocker spaniel. (A.) The images after unsuccessful chemotherapy, before mEHT treatment. The metastatic lesions are pointed by arrows. (B.) The same image after treatment. A significant decrease in the size of the lesions is observed, and some of those completely disappeared.

4. Conclusions

The in vitro experiments in the previous part of the series about mEHT results had shown clear pieces of evidence of how the nonthermal electric field, compared to the only thermal treatment (wHT) sinergetically improved the cell destruction [10]. The primary message from the preclinical experiments in vivo is that electromagnetic energy absorption has thermal and nonthermal effects appearing synergistically in the mEHT. The strong synergy appears in many comparisons

- The only thermal (iHT) and mEHT treatments declared strong synergy **(Figure 9).** [40]
- The observed massive appearance of extracellular HSP70 (eHSP70) 72 h post treatment is a strong addition to the thermally developed intracellular iHSP70 induced by hyperthermia **(Figure 11).**
- The mRNA gene chip results show the characteristic gene up and down regulation differences when the non-thermal effect is active **(Figure 12).**
- The marked p53 and p21 appear when the non-thermal component is added in **Figure 14.**
- The effect of modulation in mEHT shows significant changes when the non-thermal addition was given **(Figure 17).**[37]
- The pulsing treatment (which decreases the thermal but increases the non-thermal absorptions), increases the cell destruction **(Figure 18).**
- The complementary applications of mEHT with the conventional methods (RT and ChT) also show the advantages of the mEHT.

The well-chosen modulated radiofrequency (RF) signal may trigger resonant excitations of the transmembrane proteins, which triggers extrinsic apoptotic signals. The focused thermal factor generates hyperthermic conditions. The increased temperature provides an appropriate situation for the nonthermal electric field exciting processes by optimizing the chemical reaction rates and enzymatic reactions. The direct thermal and nonthermal effects complete each other, making a complex synergy of mEHT actions, **Figure 28.**

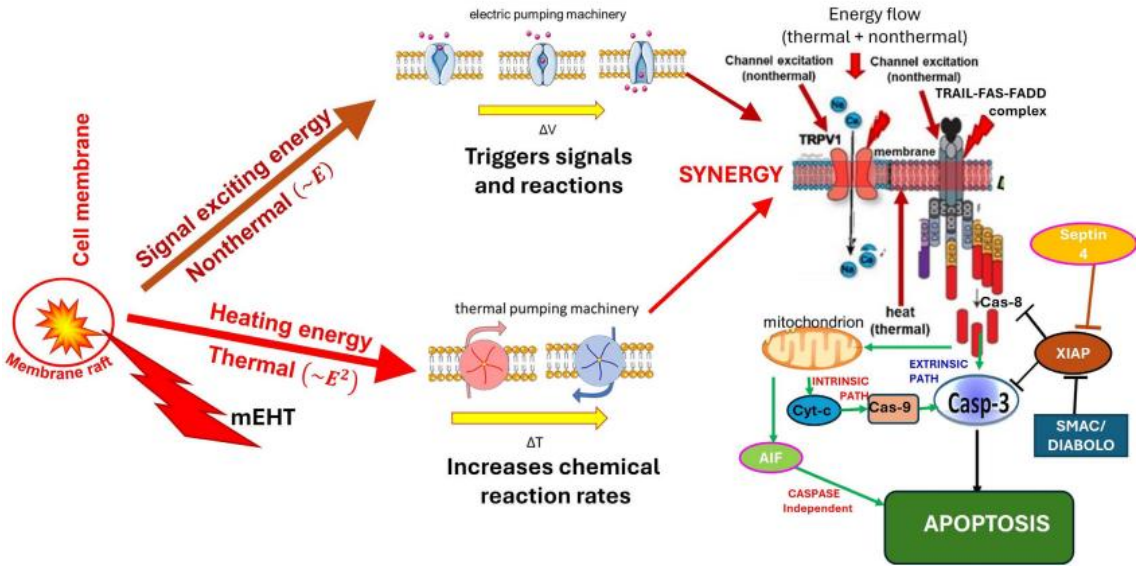

Figure 28. The measured thermal and nonthermal effects of mEHT. The thermal effect has an Arrhenius character, while the nonthermal effects are quantum-mechanical, promoting the enzymatic processes through a transitional state. The thermal conditions optimize and accelerate the non-thermal processes.

The *in vivo* experiments reinforce the previous in vitro observations [10], and the physiologic conditions make further support which drives the expectations from the clinical applications. The in vitro and in vivo proofs verify the usefulness of the mEHT making promises to a significant step forward in human oncology.

Acknowledgements

I am thankful to the listed authors for their diligent research.

Fund

This research received external funding from the Hungarian Government, grant number GINOP_PLUSZ_2.1.1-21-2022-00058

Conflicts of Interest

The author declares no conflicts of interest regarding the publication of this paper.

References

[1] Escargueil, A. (2023) Feature Reviews in Cancer Therapy. https://www.mdpi.com/journal/cancers/special_issues/reviews_cancer_therapy

[2] Siegel, R.L., Giaquinto, A.N. and Jemal, A. (2024) Cancer Statistics, 2024. CA: A Cancer Journal for Clinicians, 74, 12-49. https://doi.org/10.3322/caac.21820

[3] Pancholi, N.J. (2924) Experts Forecast 2024, Part 4: Cutting-Edge Tech for Oncology Drug Discovery, Cancer Research Catalyst. https://www.aacr.org/blog/2024/01/31/experts-forecast-2024-part-4-cutting-edge-te ch-for-oncology-drug-discovery/

[4] Szasz, A. (2021) Therapeutic Basis of Electromagnetic Resonances and SignalModulation. Open Journal of Biophysics, 11, 314-350. https://doi.org/10.4236/ojbiphy.2021.113011

[5] Szasz, A. (2022) Time-Fractal Modulation—Possible Modulation Effects in Human Therapy. Open Journal of Biophysics, 12, 38-87. https://doi.org/10.4236/ojbiphy.2022.121003

[6] Szasz, A. and Szasz, O. (2020) Time-Fractal Modulation of Modulated ElectroHyperthermia (MEHT). In: Szasz, A., Ed., Book Challenges and Solutions of Oncological Hyperthermia, Cambridge Scholars, 377-415.

[7] Szasz, O. and Szasz, A. (2016) Nanothermia: A Heterogenic Heating Approach. Journal of Cancer Research and Therapeutics, 12, 1132-1137. https://doi.org/10.4103/0973-1482.197568

[8] Szasz, O. (2019) Bioelectromagnetic Paradigm of Cancer Treatment—Modulated Electro-Hyperthermia (MEHT). Open Journal of Biophysics, 9, 98-109. https://doi.org/10.4236/ojbiphy.2019.92008

[9] Szasz, A. (2022) Heterogeneous Heat Absorption Is Complementary to Radiotherapy. Cancers, 14, Article 901. https://doi.org/10.3390/cancers14040901

[10] Szasz, A. (2024) Preclinical Verification of Modulated Electro-Hyperthermia. Part I. in Vitro Research. International Journal of Clinical Medicine.

[11] Bini, M., Ignesti, A., Millanta, L., et al. (1985) An Unbalanced Electric Applicator for RF Hyperthermia. IEEE Transactions on Biomedical Engineering, 32, 638-641. https://doi.org/10.1109/TBME.1985.325596

[12] Krenacs, T., Meggyeshazi, N., Forika, G., et al. (2020) Modulated Electro-Hyperthermia-Induced Tumor Damage Mechanisms Revealed in Cancer Models. International Journal of Molecular Sciences, 21, Article 6270. https://doi.org/10.3390/ijms21176270

[13] Andocs, G., Osaki, T., Tsuka, T., Imagawa, T., et al. (2013) Oncothermia Research at Preclinical Level. Hindawi Publishing Corporation Conference Papers in Medicine, 2013, Article ID: 272467. http://Www.Hindawi.Com/Archive/2013/272467/

[14] Szasz, A., Szasz, N. and Szasz, O. (2010) Oncothermia—Principles and Practices. Springer Science. https://link.springer.com/book/10.1007/978-90-481-9498-8

[15] Szasz, A., Szasz, O. and Szasz, N. (2006) Physical Background and Technical Realization of Hyperthermia. In: Baronzio, G.F. and Hager, E.D., Eds., Hyperthermia in Cancer Treatment: A Primer, Springer, 27-59. https://doi.org/10.1007/978-0-387-33441-7_3

[16] Szasz, A. (2015) Bioelectromagnetic Paradigm of Cancer Treatment Oncothermia. In: Rosch, P.J., Ed., Bioelectromagnetic and Subtle Energy Medicine, CRC Press and Taylor & Francis Group, 323-336.

[17] Szasz, A. (2014) Oncothermia: Complex Therapy by EM and Fractal Physiology. 2014 XXXIth URSI General Assembly and Scientific Symposium, Beijing, 16-23 August 2014.

[18] Kim, W., Kim, M.S., Kim, H.J., et al. (2017) Role of HIF-1α in Response of Tumors to a Combination of Hyperthermia and Radiation in vivo. International Journal of Hyperthermia, 34, 276-283. https://doi.org/10.1080/02656736.2017.1335440

[19] Portoro, I., Danics, L. and Veres, D. (2018) Increased Efficacy in Treatment of Glioma by a New Modulated Electro-Hyperthermia (MEHT) Protocol. Oncothermia Journal, 24, 344-356.

[20] Danics, L., Schvarcz, C.S., Viana, P., et al. (2020) Exhaustion of Protective Heat Shock Response Induces Significant Tumor Damage by Apoptosis after Modulated Electro-Hyperthermia Treatment of Triple Negative Breast Cancer Isografts in Mice. Cancers, 12, Article 2581. https://pubmed.ncbi.nlm.nih.gov/32927720/

[21] Jeon, T.-W., Yang, H., Lee, C.G., O, S.T., et al. (2016) Electro-Hyperthermia Up-Regulates Tumour Suppressor Septin 4 to Induce Apoptotic Cell Death in He- patocellular Carcinoma. International Journal of Hypertension, 7, 1-9. https://doi.org/10.1080/02656736.2016.1186290

[22] Cha, J., Jeon, T.-W., Lee, C.-G., et al. (2015) Electro-Hyperthermia Inhibits Glioma Tumorigenicity Through the Induction of E2F1-Mediated Apoptosis. International Journal of Hyperthermia, 31, 784-792. https://doi.org/10.3109/02656736.2015.1069411

[23] Meggyeshazi, N., Andocs, G., Balogh, L., et al. (2014) DNA Fragmentation and Caspase-Independent Programmed Cell Death by Modulated Electrohyperthermia. Strahlentherapie und Onkologie, 190, 815-822. https://doi.org/10.1007/s00066-014-0617-1

[24] Andocs, G., Meggyeshazi, N., Balogh, L., et al. (2014) Upregulation of Heat Shock Proteins and the Promotion of Damage-Associated Molecular Pattern Signals in a Colorectal Cancer Model by Modulated Electrohyperthermia. Cell Stress and Cha- perones, 20, 37-46. https://doi.org/10.1007/s12192-014-0523-6

[25] Meggyeshazi, N., Andocs, G. and Krenacs, T. (2013) Programmed Cell Death In- duced by Modulated Electro-Hyperthermia. Hindawi Publishing Corporation Con- ference Papers in Medicine, 2013, Article ID: 187835.

[26] Vancsik, T., Kovago, C.S., Kiss, E., et al. (2018) Modulated Electro-Hyperthermia Induced Loco-Regional and Systemic Tumor Destruction in Colorectal Cancer Al- lografts. Journal of Cancer, 9, 41-53. https://doi.org/10.7150/jca.21520

[27] Tsang, Y.-W., Huang, C.-C., Yang, K.-L., et al. (2015) Improving Immunological Tumor Microenvironment Using Electro-Hyperthermia Followed by Dendritic Cell Immunotherapy. BMC Cancer, 15, Article 708. http://Www.Ncbi.Nlm.Nih.Gov/Pubmed/26472466

[28] Vancsik, T., Mathe, D., Horvath, I., et al. (2021) Modulated Electro-Hyperthermia Facilitates NK-Cell Infiltration and Growth Arrest of Human A2058 Melanoma in a Xenograft Model. Frontiers in Oncology, 11, Article 590764. https://www.frontiersin.org/articles/10.3389/fonc.2021.590764/full

[29] Kuo, I.-M., Lee, J.-J., Wang, Y.-S., et al. (2020) Potential Enhancement of Host Immunity and Anti-Tumor Efficacy of Nanoscale Curcumin and Resveratrol in Colorectal Cancers by Modulated Electro-Hyperthermia. BMC Cancer, 20, Article 603. https://pubmed.ncbi.nlm.nih.gov/32600429/

[30] Besztercei, B., Vancsik, T., Benedek, A., et al. (2019) Stress-Induced, P53-Mediated Tumor Growth Inhibition of Melanoma by Modulated Electrohyperthermia in Mouse Models Without Major Immunogenic Effects. International Journal of Mo- lecular Sciences, 20, Article 4019. https://Www.Mdpi.Com/1422-0067/20/16/4019

[31] Kim, H., Kim, D., Kim, W., et al. (2022) The Efficacy of Radiation Is Enhanced by Metformin and Hyperthermia Alone or Combined against FSall Fibrosarcoma in C3H Mice. Radiation Research, 198, 190-199. https://doi.org/10.1667/RADE-21-00231.1

[32] Prasad, B., Kim, S., Cho, W., et al. (2019) Quantitative Estimation of the Equivalent Radiation Dose Escalation Using Radiofrequency Hyperthermia in Mouse Xeno- graft Models of Human Lung Cancer. Nature, 9, Article 3942. https://www.nature.com/articles/s41598-019-40595-6

[33] Kim, J.-K., Prasad, B. and Kim, S. (2017) Temperature Mapping and Thermal Dose Calculation in Combined Radiation Therapy and 13.56 MHz Radiofrequency Hyperthermia for Tumor Treatment. Optical Methods for Tumor Treatment and Detection: Mechanisms and Techniques in Photodynamic Therapy XXVI, San Francisco, 28-29 January 2017, Article ID: 1004718. http://spie.org/publications/proceedings/paper/10.1117/12.2253163?origin_id=x431 8

[34] Tsang, Y.-W., Chi, K.-H., Huang, C.-C., Chi, M.-S., et al. (2019) Modulated Elec- tro-Hyperthermia-Enhanced Liposomal Drug Uptake by Cancer Cells. International Journal of Nanomedicine, 14, 1269-1579. https://doi.org/10.2147/IJN.S188791

[35] Balogh, L., Polyak, A., Postenyi, Z., et al. (2016) Temperature Increase Induced by Modulated Electrohyperthermia (Oncothermia®) in the Anesthetized Pig Liver. Journal of Cancer Research and Therapeutics, 12, 1153-1159. https://doi.org/10.4103/0973-1482.197561

[36] Kovago, C.S., Meggyeshazi, N., Andocs, G. and Szasz, A. (2013) Report of the Pi- lot-Study Done for the Proposed Investigation on the Possible Synergic Effect Be- tween High Dose Ascorbic Acid

Application and Oncothermia Treatment. Hindawi Publishing Corporation Conference Papers in Medicine, 2013, Article ID: 386913.

[37] Wust, P., Veltsista, P.D., Oberacker, E., Yavvari, P., Walther, W., Bengtsson, O., et al. (2022) Radiofrequency Electromagnetic Fields Cause Non-Temperature-Induced Physical and Biological Effects in Cancer Cells. Cancers, 14, Article 5349. https://Www.Mdpi.Com/2072-6694/14/21/5349

[38] Meggyeshazi, N., Andocs, G., Spisak, S., et al. (2013) Early Changes in MRNA and Protein Expression Related to Cancer Treatment by Modulated Elec- tro-Hyperthermia. Hindawi Publishing Corporation Conference Papers in Medi- cine, 2013, Article ID: 249563.

[39] Prasad, B., Kim, S., Cho, W., et al. (2018) Effect of Tumor Properties on Energy Absorption, Temperature Mapping, and Thermal Dose in 13,56-MHz Radiofre- quency Hyperthermia. Journal of Thermal Biology, 74, 281-289. https://doi.org/10.1016/j.jtherbio.2018.04.007

[40] Andocs, G., Renner, H., Balogh, L., Fonyad, L., Jakab, C. and Szasz, A. (2009) Strong Synergy of Heat and Modulated Electro—Magnetic Field in Tumor Cell Killing, Study of HT29 Xenograft Tumors in a Nude Mice Model. Strahlentherapie Und Onkologie, 185, 120-126. https://doi.org/10.1007/s00066-009-1903-1

[41] Danics, L., Schvarcz, C.S. and Zolcsak, Z. (2018) Modulated Electro Hyperthermia Inhibits Tumor Progression in a Triple Negative Mouse Breast Cancer Model. Oncothermia Journal, 24, 442-454.

[42] Thomas, M.B., Major, E., Benedek, A., Horváth, I., Máthé, D., Bergmann, R., et al. (2020) Suppression of Metastatic Melanoma Growth in Lung by Modulated Electro-Hyperthermia Monitored by a Minimally Invasive Heat Stress Testing Approach in Mice. Cancers, 12, Article 3872. Https://Pubmed.Ncbi.Nlm.Nih.Gov/33371498/

[43] Schvarcz, C.S.A., Danics, L., Krenacs, T., Viana, P., Beres, R., et al. (2021) Modulated Electro-Hyperthermia Induces a Prominent Local Stress Response and Growth Inhibition in Mouse Breast Cancer Isografts. Cancers, 13, Article 1744. https://Pubmed.Ncbi.Nlm.Nih.Gov/33917524/

[44] Matsumoto, Y., Hayshi, J., Sekino, Y., Fukumitsu, N., Saito, T., Ishikawa, H. and Sakurai, H. (2018) Radio-Sensitization Effect of Novel Cancer Therapy, Oncother- mia ~ Toward Overcoming Treatment Resistance. 2018 Annual Conference of Jap- anese Hyperthermia Society, Fukui, 26-28 March 2018.

[45] Qin, W., Akutsu, Y., Andocs, G., et al. (2014) Modulated Electro-Hyperthermia Enhances Dendritic Cell Therapy Through an Abscopal Effect in Mice. Oncology Reports, 32, 2373-2379. https://doi.org/10.3892/or.2014.3500

[46] Aloss, K., Bokhari, S.M.Z., Leroy Viana, P.H., Giunashvili, N., Schvarcz, C.A., SzénáSi, G., et al. (2024) Modulated Electro-Hyperthermia Accelerates Tumor Delivery and Improves Anticancer Activity of Doxorubicin Encapsulated in Lyso-Thermosensitive Liposomes in 4T1-Tumor-Bearing Mice. International Journal of Molecular Sciences, 25, Article 3101. https://doi.org/10.3390/ijms25063101

[47] Son, B., Jeon, J., Lee, S., et al. (2019) Radiotherapy in Combination with Hyper- thermia Suppresses Lung Cancer Progression via Increased NR4A3 and KLF11 Ex- pression. International Journal of Radiation Biology, 95, 1696-1707. https://doi.org/10.1080/09553002.2019.1665213

[48] Yang, W., Gwan, H.H., Shin, H.-Y., et al. (2018) Combined Treatment with Mod- ulated Electro-Hyperthermia and an Autophagy Inhibitor Effectively Inhibit Ova- rian and Cervical Cancer Growth. International Journal of Hyperthermia, 36, 9-20. https://doi.org/10.1080/02656736.2018.1528390

[49] Andocs, G., Okamoto, Y., Kawamotot., Osaki, T., Tsuka, T., Imagawa, T., Minami, S., Balogh, L., Meggyeshazi, N. and Szasz, O. (2013) Oncothermia Basic Research at in Vivo Level. The First Results in Japan. Hindawi Publishing Corporation Confe- rence Papers in Medicine, 2013, Article ID: 197328.

[50] Szasz, O. (2011) Temperature Measurements during Oncothermia (Collection of Temperature Measurements in Loco Regional Hyperthermia). Oncothermia Journal, 4, 62-86.

[51] Lee, S.-Y., Kim, J.-H., Han, Y.-H., et al. (2018) The Effect of Modulated Electro- Hyperthermia on Temperature and Blood Flow in Human Cervical Carcinoma. International Journal of Hyperthermia, 34, 953-960. https://doi.org/10.1080/02656736.2018.1423709

[52] Meggyeshazi, N. (2015) Studies on Modulated Electrohyperthermia Induced Tumor Cell Death in a Colorectal Carcinoma Model. Ph.D Thesis, Semmelweis University. https://repo.lib.semmelweis.hu/bitstream/handle/123456789/3956/meggyeshazinora.e.pdf?sequence=4

[53] Andocs, G., Rehman, M.U., Zhao, Q.-L., Tabuchi, Y., Kanamori, M. and Kondo, T. (2016) Comparison of Biological Effects of Modulated Electro-Hyperthermia and Conventional Heat Treatment in Human Lymphoma U937 Cell. Cell Death Dis- covery (Nature Publishing Group), 2, Article 16039. https://www.nature.com/articles/cddiscovery201639

[54] Andocs, G. (2010) Revealing the Mechanism of Action of Modulated Electrothermia Experimentally in Animal Model (HT29 Colorectal Xenograft Study). Annual Meeting of Society for Thermal Medicine, Florida, 23-26 April, 2010.

[55] Szasz, A. (2022) Time-Fractal in Living Objects. Open Journal of Biophysics, 12, 1-26. https://doi.org/10.4236/ojbiphy.2022.121001

[56] de Loof, M., de Jong, S. and Kruyt, F.A.E. (2019) Multiple Interactions Between Cancer Cells and the Tumor Microenvironment Modulate TRAIL Signaling: Implications for TRAIL Receptor Targeted Therapy. Frontiers in Immunology, 10, Article 1530. https://doi.org/10.3389/fimmu.2019.01530

[57] de Andrade Mello, P., Bian, S., Savio, L.E.B., et al. (2017) Hyperthermia and Associated Changes in Membrane Fluidity Potentiate P2X7 Activation to Promote Tumor Cell Death. Oncotarget, 8, 67254-67268. https://doi.org/10.18632/oncotarget.18595

[58] Meggyeshazi, N., Andocs, G., Spisak, S., et al. (2013) Modulated Electrohyperthermia Causes Caspase Independent Programmed Cell Death in HT29 Colon Cancer Xenografts. Virchows Archiv, 463, Article 329.

[59] Meggyeshazi, N., Andocs, G., Balogh, L. and Krenacs, T. (2011) DNA Fragmentation- Driven Tumor Cell Degradation Induced by Modulated Electro-Hyperthermia. Virchows Archiv, 459, S204-S205.

[60] Yang, K.-L., Huang, C.-C., Chi, M.-S., Chiang, H.-C., Wang, Y.-S., Andocs, G., et al. (2016) In Vitro Comparison of Conventional Hyperthermia and Modulated Elec- tro-Hyperthermia. Oncotarget, 7, 84082-84092. Http://Www.Ncbi.Nlm.Nih.Gov/Pubmed/27556507

[61] Springer, M. and Paulsson, J (2006) Harmonies From Noise. Nature, 439, 27-28. https://doi.org/10.1038/439027a

[62] West, J.B. (2013) Fractal Physiology and Chaos in Medicine. World Scientific. https://doi.org/10.1142/8577

[63] Astumian, R.D. and Chock, P.B. (1989) Effects of Oscillations and Energy-Driven Fluctuations on the Dynamics of Enzyme Catalysis and Free-Energy Transduction. Physical Review A, 39, 6416-6435. https://doi.org/10.1103/PhysRevA.39.6416

[64] O'Neill, D.P., Peng, T., Stiegler, P., Mayrhauser, U., Koestenbauer, S., Tscheliessnigg, K., et al. (2011) A Three-State Mathematical Model of Hyperthermic Cell Death. Annals of Biomedical Engineering, 39, 570-579. https://doi.org/10.1007/s10439-010-0177-1

[65] Kiss, E., Andocs, G., Meggyeshazi, N., Vancsik, T., Kovago, C.S., Papp, E. and Kre- nacs, T. (2015) The Role of Modulation in Modulated Electro-Hyperthermia (MEHT). 36th Conference of International Clinical Hyperthermia Society (ICHS), Bad Salzhausen, July 10 2015. https://doi.org/10.1016/j.eujim.2016.08.087

[66] Szasz, O., Andocs, G. and Meggyeshazi, N. (2013) Modulation Effect in Oncother- mia. Hindawi Publishing Corporation Conference Papers in Medicine, 2013, Article ID: 395678.

[67] Forika, G., Balogh, A., Vancsik, T., Zalatnai, A., et al. (2020) Modulated Elec- A. Szasz DOI: 10.4236/ijcm.2024.157020 333 International Journal of Clinical Medicine tro-Hyperthermia Resolves Radioresistance of Panc1 Pancreas Adenocarcinoma and Promotes DNA Damage and Apoptosis in Vitro. International Journal of Mo- lecular Sciences, 21, Article 5100. https://doi.org/10.3390/ijms21145100

[68] Andocs, G., Okamoto, Y., Kawamotot, K., Osaki, T., Tsuka, T., Imagawa, T., Mina- mi, S., Balogh, L., Meggyeshazi, N. and Szasz, O. (2013) Oncothermia Basic Re- search at in vivo Level. The First Results in Japan. Oncothermia Journal, 7, 296-300. https://doi.org/10.1155/2013/197328

[69] Plotnikov, A., Fishman, D., Tichler, T., Korenstein, R. and Keisari, Y. (2004) Low Electric Field Enhanced Chemotherapy Can Cure Mice with CT-26 Colon Carci- noma and Induce Anti-Tumor Immunity. Clinical and Experimental Immunology, 138, 410-416. https://doi.org/10.1111/j.1365-2249.2004.02636.x

[70] Kirson, E.D., Schneiderman, R.S., Dbaly, V., et al. (2009) Chemotherapeutic Treatment Efficacy and Sensitivity Are Increased by Adjuvant Alternating Electric Fields (TTFields). BMC Medical Physics, 9, Article No. 1. https://doi.org/10.1186/1756-6649-9-1

[71] Schneiderman, R.S., Shmueli, E., Kirson, E.D. and Palti, Y. (2010) TTFields Alone and in Combination with Chemotherapeutic Agents Effectively Reduce the Viability of MDR Cell Sub-Lines that Over-Express ABC Transporters. BMC Cancer, 10, Article 229. https://doi.org/10.1186/1471-2407-10-229

[72] Needham, D., Anyarambhatla, G., Kong, G. and Dewhirst, M.W. (2000) A New Temperature-Sensitive Liposome for Use with Mild Hyperthermia: Characteriza- tion and Testing in a Human Tumor Xenograft Model. Cancer Research, 60, 1197-201.

[73] Balogh, L., Andocs, G., Thuroczy, J., Polyak, A., Szasz, O. and Szasz, A. (2009) On- cological and Non-Oncological Applications of Electromagnetic Hyperthermia (Oncothermia) in the Veterinary Clinics—2 Years of Experience. Poster Presenta- tion at 1 International es Oncothermie-Symposium, Köln, 22-23 November 2009.

Abbreviations

CDK	cyclin-dependent kinase
ChT	chemotherapy
DAMP	damage associated molecular pattern
DC	dendritic cell
DNA	deoxyribonucleic acid
HMGB1	high-mobility group protein
HSP	heat-shock protein
ICD	immunogenic cell death mEHT modulated electro-hyperthermia
NK cell	natural killer cell
PCR	polymerase chain reaction
ROS	reactive oxygen species
RT	radiotherapy
Op	surgery
TDR	tumor destruction ratio
TRAIL	tumour-necrosis factor related apoptosis inducing ligand
XIAP	X- linked Inhibitor of apoptosis

Preclinical Verification of Modulated Electro-Hyperthermia

PART III. – Immugenic effects

Andras Szasz

Department of Biotechnics, Hungarian University of Agriculture and Life Sciences, 2100 Gödöllő, Hungary

Email: biotech@gek.szie.hu

Citation

Szasz, A. (2024) Preclinical Verification of Modulated Electro-Hyperthermia – Part III. – In vitro research

Oncothermia Journal 38, August 2026., 150-179.
https://oncotherm.com/SzaszA_2024_Preclinical_verification_of_mEHT-Part_III

Abstract

The modulated electro-hyperthermia (mEHT) method is a unique approach that utilizes all the essential apoptotic pathways through an external radiofrequency (RF) signal. The high-frequency RF is amplitude-modulated and coupled capacitively to the target. The provided energy triggers the death receptors and FAS-FADD complexes in the malignant cells. Multi-pathway apoptosis produces immunogenic cell death (ICD). This ICD provides intracellular information about cancer cells by releasing damage-associated molecular patterns (DAMP), including membrane expression of calreticulin (CRT) and extracellular ATP, HMGB1, and HSP70, executing tumor-specific antigen presentation. The antigen-presenting cells (APCs) play a crucial role in reestablishing immune surveillance and hampering the tumor cells' ability to hide, thereby evading immune attacks. The matured DCs (generally APCs) produce tumor-specific killer and helper T-cells, which have the potential to be active in distant metastases from the treated location. This unique mechanism of action underscores its potential in cancer treatment and extends the local mEHT treatment to the wholebody anticancer therapy with an abscopal effect.

Keywords

mEHT, Cancer, Thermal, Nonthermal, Immunogenic, ICD, DAMP, Tumor-Specific Immune

1. Introduction

Hyperthermia in oncology has its roots in ancient medicine. Heat is regarded as the overall "healer," expecting unspecific effects of the body's natural corrective systems for different symptoms, expecting normalized homeostatic regulation, including immune surveillance.

Hyperthermia is an external disturbance that induces the contra effects of homeostasis, which is the body's natural tendency to maintain a stable internal environment despite changes in external conditions. Thermal homeostatic regulation acts to cool down the stressfully overheated volume. The extreme heat triggers thermal homeostasis to correct the irregularity, extending the therapy task to consider the regulating counteractions.

Hyperthermia must find a way to synergize its cooperation with homeostatic regulation. It must support normal homeostatic processes and avoid provoking physiological regulations like intensive blood perfusion in the target, which may increase the risk of tumor supply and dissemination of malignant cells. The critical components of homeostasis (receptors, neural control, and effectors) must be smoothly tuned to fix the homeostasis at a new, physiologically accepted equilibrium below the thermal limit (42°C in all regions). Focusing on the signaling (social signals) of cells [1] and the pathways of cell communication [2] are the key processes that ensure the harmony of hyperthermia with homeostasis. Oncological hyperthermia faces many technical and medical challenges that are far from a final solution. The complexity of electromagnetic interaction and the physiological feedback mechanisms need extended explanations. Incomplete knowledge of electromagnetic biological and medical processes and the lack of precise measurement of the applied dose hinder the widespread use of hyperthermia in oncology.

Oncological hyperthermia needs to rethink its strategy in the light of immuno-oncology. The strategy to eliminate the tumor must use the well-known military consideration: attack the weakest side of cancer, avert a direct fight with its most potent forces, and stop trying directly to inhibit the most robust property of the malignant development [3]. Cancer's main strength is its proliferation, which makes these cells adaptable and forms the tumor immortal. However, their weakest side is their autonomy, their evading ability of immune surveillance. Cancer cells fight against all healthy and fellow malignant cells, competing for the energy sources to proliferate. The lack of healthy networking creates weak cooperation abilities during malignant development [4]. The weak networking and the "loneliness" behavior make the malignant cells vulnerable. The weak network otherwise helps the proliferative development due to the easy motility and micro and macro metastases forming.

The hyperthermic strategy must be revised to attack the weak side of the malignancy with an alliance of the host system itself. The goal is to provide tumor-specific information to the immune surveillance activity to recognize the malignant cells despite their hidden "identity." The active tumor-specific immune process and the thermally increased enzymatic activity offer a reliable tool to fulfill our final aim of eliminating cancer cells all over the body.

Optimal curative heating helps the natural control to reverse the irregularities caused by cancer and supports the immune processes against the malignant effects. The modulated electro-hyperthermia (mEHT) uses thermal and nonthermal effects synergically, increasing the impact of only heat. The rapidly developed method changed its focus over time [5]. Electromagnetic energy absorption has a double effect: heating for optimal conditions and acting nonthermally to modify the chemical processes [6] [7]. The synergy of these effects supports the homeostatic control with the heterogenic actions: selects the tumor cells and forces energy absorption in microregions of their cell membrane (membrane rafts), heats them high, and excites multiple apoptotic pathways [6] [7], promoting the lost apoptotic surveillance of the homeostasis. Furthermore, the heated microdots (the rafts) heat as secondary heat conduction the cells and the complete tumor, which on this heat transport remains in mild temperature, which does not induce extensive counteraction of the homeostasis. Furthermore, this article aims to present the immunogenic effects that restore the immunosurveillance of the homeostatic control.

The mEHT became a reliable alternative to conventional hyperthermia, concentrating on the molecular and physiological processes directed to immunogenic effects, heading to immuno-oncology [8] [9]

2. Methods

The primary effect of mEHT works in harmony with natural homeostasis. The method uses physiological processes and a modulated radiofrequency (RF) current, which allows the precise targeting and destruction of malignant cells in four steps. These steps involve the use of thermal and electric heterogeneities caused by malignant proliferation. 1) Malignant cells, which are characterized by their high metabolic rate, produce a high ionic concentration in the tumor microenvironment (TME). The amplitude-modulated 13.56 MHz RF current chooses the highly conductive paths of the TME, automatically selecting these tumors. 2) The missing healthy network makes the TME significantly disordered (high dielectric constant), which allows the applied RF to recognize the malignant cell environment. 3) The broken bonds of the network produce multiple

transmembrane proteins and their clusters (rafts). The rafts are good energy absorbers from the RF current [10]. 4) The autonomic cancer cells are unsynchronized, which can be recognized by modulation [11]. The relatively low average temperature accompanies a high thermal effect of mEHT on the transmembrane proteins concentrated primarily in the membrane rafts (**Figure 2**). This solution ensures a high temperature on the membrane of malignant cells, which are selected based on the high concentration of membrane rafts [12]. At the same time, whole tissue temperature is only moderately increased, which increases blood flow sufficiently to support radiation therapy (RT) [13] and drug delivery [14]. However, it does not promote cell dissemination and has no thermal toxicity. In this way, mEHT providessafeand effective hyperthermia (HT).

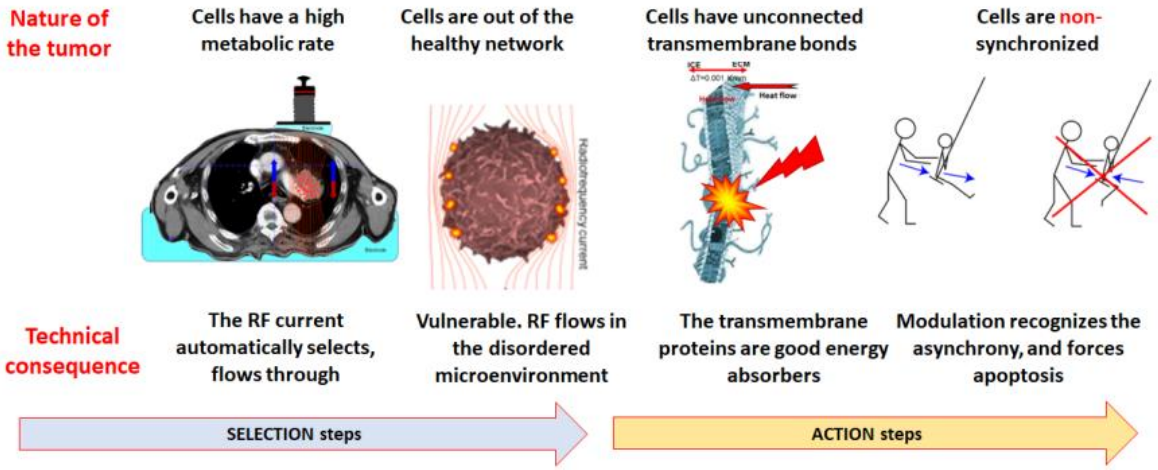

Figure 1. The steps of mEHT: 1) find the tumor with its high metabolic rate, 2) find the cells with their disordered TME, 3) absorb energy and excite transmembrane proteins, 4) Make harmony with homeostatic control.

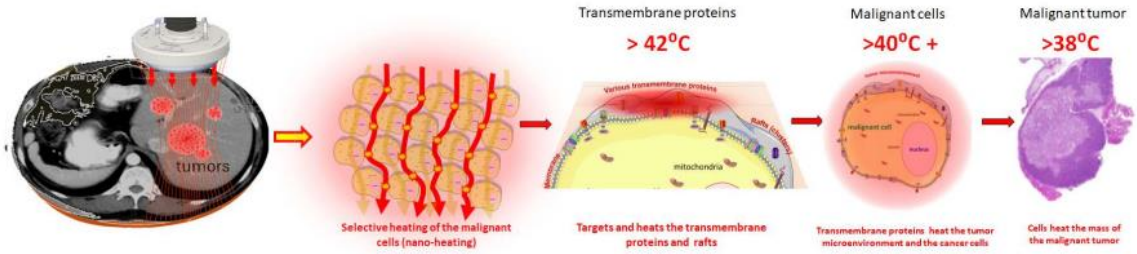

Figure 2. Temperature development with mEHT action: 1) RF current goes through the body part and selects the tumor, as shown in Figure 1. 2) The RF current mostly flows between the cells because of the electric isolation of cell membranes, 3) the membrane rafts absorb energy and are heated up at high temperatures, 4) The heated rafts heat the entire cell with conductive and convective actions, 5) the hot cells heat the entire tumor to mild temperatures.

The mEHT (modulated electro-hyperthermia) technique diverges from the traditional homogeneous (isothermal) heating approach [13], utilizing bioelectromagnetic properties to deliver nonthermal energy, too. This energy stimulates death receptors and other molecules, initiating apoptotic signals within cancer cells [15]. Unlike inflammatory necrosis, which can induce cancer due to the inflammation it causes, mEHT promotes controlled programmed cell death (apoptosis and necroptosis) [6] [7] [16]. This method avoids uncontrolled thermal necrosis, which involves membrane rupture and the release of cellular contents that can harm healthy tissue and trigger

inflammation. Necrosis triggers inflammatory immune reactions, whereas apoptosis allows the immune system to clean up without causing inflammation. Apoptosis is an immunogenic (immune response-inducing) form of cell death, provoking a robust immune response. Immunogenic cell death (ICD) is the pathway that activates the immune system against the dying cells. While apoptosis is a common pathway for ICD, some recent research has identified another immunogenic pathway: necroptosis. Necroptosis is a regulated, programmed form of cell death with some necrotic characteristics.

Effective immunogenic cancer elimination requires tumor-specific information to prepare the immune system for innate and adaptive responses, targeting malignant cells throughout the body via the bloodstream. Antigen-presenting cells (APCs) play a crucial role in this process. Various cells can function as APCs, including professional APCs like dendritic cells (DCs), macrophages, and B cells, as well as nonprofessional APCs like endothelial cells, fibroblasts, and epithelial cells, which can present antigens to T cells under certain conditions. The controlled apoptosis does not randomly destroy the cell membrane, allowing the cell to fragment into apoptotic bodies. This process releases damage-associated molecular patterns (DAMPs), which further signal and prepare the immune system.

Calreticulin (CRT) is expressed in the cell membrane in the set of DAMP molecules. The ER stress response forces the CRT [17], which has an “eat me” signal for phagocytosis [18] [19]. Apoptosis expresses the cell membrane exposure of CRT, while necrosis does not. Necroptotic processes may do it in some peculiar conditions. The CRT-controlled strong Ca2+ influx [20] is a significant factor in apoptosis caused by mEHT [21]. The other member of the DAMP set is the released HMGB1, which represents a “danger signal” [22]. The HMGB1 contributes to immune activation, but contrary, its oxidized form makes the inflammatory responses [23]. Furthermore, the oxidized HMGB1 participates in immune tolerance [24] and may boost the immune checkpoint molecule PD-L1 expression, limiting anticancer immunity [25]. Therefore, the oxidation status of HMGB1 determines the role of HMGB1 in DAMP [26]. The mild thermal process of mEHT favors conditions that do not support oxidization. HMGB1 is a valuable set of DAMP in mEHT processes. Furthermore, ATP is released to the TME as a stress response in the apoptotic phase [27]. The released ATP functions as a “find me” signal [28] and mostly follows an autophagy-dependent pathway [29]. The complex thermal and electric (nonthermal) stress induces heat shock proteins (HSPs) in the cell, functioning as an antiapoptotic chaperon. When the intracellular HSPs (iHSPs) are overloaded in the cell, these start translocation to the malignant cell’s membrane [30], forming membrane HSPs (mHSPs) [31]. The mHSP expression may subsequently alert the innate immune reaction, attracting the NK cells to the mHSP location [32] and trying to eliminate the malignant cell. In the further process, the mHSPs are released extracellularly. Extracellular HSP (eHSP) appears as an “info signal” [33], carries tumor-specific antigen [34], and may build up a tumor immunity [35]. The delivered eHSP peptides can be identified by the innate and adaptive immune systems [36] [37]. In the above set of DAMP molecules (CRT, HMGB1, ATP, and HSP), the eHSPs are crucial components [38]. The spatiotemporal development of DAMP activates APCs to express high levels of MHC class II molecules, essential for presenting antigens to T cells. The mEHT method gently kills tumor cells with programmed cell death, releasing damage-associated molecular patterns (DAMP) [39] and delivering information about malignancy hidden in the intact cancer cell (**Figure 3**)

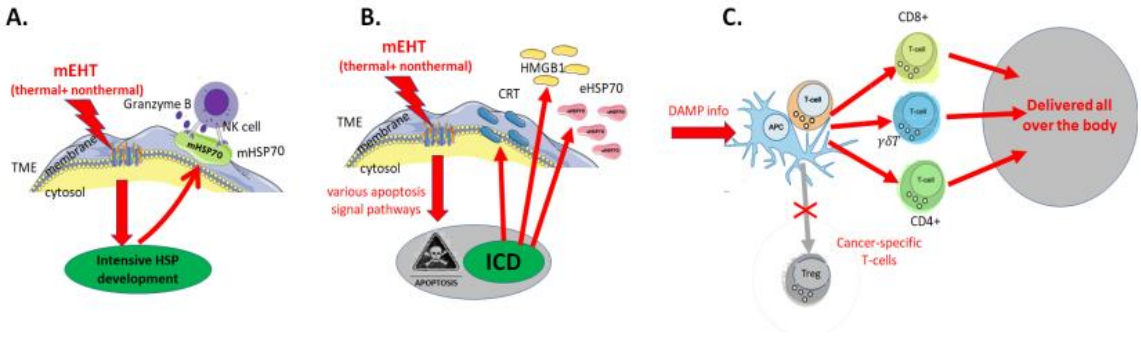

Figure 3. The immunogenic processes. (A.) The broken immune evasion starts with the expression of HSP70 on the membrane, which attracts the NK cells to destroy the cell with released Granzyme B. (B.) The ICD develops DAMP in optimal spatiotemporal order. (C.) The APC cells produce T cells with tumor-specific information to recognize the cancer cells.

Conventional hyperthermia has a relatively high average temperature in the tumor mass (> 40°C) which inactivates the immune cells in the volume [40], and the uncontrolled production of DAMP cannot activate the antigen-presenting APC processes. The mEHT focuses on apoptotic effects hindering the uncontrolled necrotic processes. The "gentle" apoptotic cell death as apoptosis produced by mEHT in moderate average temperature allows obtaining the undeformed spatiotemporal order of the DAMP set of molecules with complete genetic information orchestrating the APC activity for tumor-specific antigen presentation. The relatively mild hyperthermia process keeps the average temperature below 40°C, to ensure the activity of the immune cells, including the APC "professionals". Choosing the model animal for various experimental setups is crucial for immunologic studies. Immunocompetent or deficient (immunocompromised) model animals express different reactions in immune modulatory experiments. Immunocompromised mice were chosen when two independent distant tumors were measured, with the untreated tumor as the control on the same animal. The two distant tumors may be connected in immunocompetent mice and model a distant metastasis. The mEHT method uses an amplitude-modulated 13.56 MHz carrier frequency. The modulation has a special frequency distribution to harmonize with the homeostatic regulation. The experimental device was LabEHY (Oncotherm Kft. Budaors, Hungary). In the earlier parts of this series, we described the *in vitro* [6] and *in vivo* [7] experimental setups.

3. Results

Numerous studies were devoted to investigating the immunogenic effect of mEHT. The immunogenic effects were proven in multiple in vitro and *in vivo* model systems. The leading publications are listed in **Table 1**

Table 1. Leading publications on immunogenic preclinical research with mEHT.

Tumor cells	Method	Result	Conclusion	Ref.
HT29 xenograft model. BALB/c nude mice treated with mEHT.	mEHT 42˚C, 30 min, 4 W, time-course study with Immuno-histochemistry, microarray, apoptosis array.	Measured damage-associated molecular patterns (HSP70, CRT, HMGB1 and HSP90).	mEHT induces a spatiotemporal sequence of DAMP signals HT29 cancer, and it can be a potential local inducer of immunogenic cell death.	[41]
C26 allografts of immunocompetent (BALB/c) mice plus immunostimulant MTE.	mEHT 42˚C, 30 min, 1 - 3 W, Immunohistochemistry, TUNEL assay apoptosis analysis, comparison of the treated and nontreated tumors of the same mouse. Extra immune stimulant (MTE) is applied.	The damage-associated molecular pattern was measured (CRT, HSP70, HMGB1). Ki67 was suppressed. Dendritic cells were matured, and antigen-presenting showed tumor-specific killer T-cells and their invasion into the tumor.	The mice with immune stimulants had an abscopal effect, showing the same development in the untreated tumor as in the treated one. ICD formed tumor-specific immune reactions.	[42]
CT26 allografts of immunocompetent (BALB/c) mice plus dendritic cell immunostimulant.	mEHT 42˚C, 30 min, DC cells inoculated intratumorally to the femoral area, cytotoxic T lymphocyte assay, ELISPOT, Immunohistochemistry.	Significant HSP70 release was measured in comparison to wHT with the same temperature. The DC-combined mEHT inhibited cell growth, and the considerable appearance of CD45+, F4/80, and Eosinophil leukocytes was measured.	mEHT can create a favorable tumor microenvironment for an immunological chain reaction. Rechallenging the same tumor was ineffective. The DC-combined mEHT worked as an antitumor-vaccination.	[43]
A2058 human melanoma cell line and NK cell immunotherapy combined with mEHT.	mEHT 42˚C, 30 min, NK cells or IL-2 independent NK-92MI injected subcutaneously to right and left femoral region. Only the right side was treated.	Intensive hsp70 expression followed by significant upregulation of cC3 and p53. NK cell accumulation was in the treated tumor but not in the untreated side. Upregulation of CXCL11 and MMP2 was observed.	mEHT ultimately lead to the complete eradication of melanoma and appears to be a good combination with NK immunotherapy.	[44]
C3H/He mice inoculated with SCCVII to the left femoral and chest region. Dendritic cell immune stimulation was applied.	mEHT 42˚C, 30 min, Flow cytometry, immunohistochemistry, CD3+, CD4+ and CD8+ immune-cell detection.	The CD8+ and S100 were more strongly expressed in the DC plus mEHT treatment group than in control or stand-alone therapies, although Foxp3 expression was much higher in the control group.	A significant abscopal effect was measured between the treated femoral and untreated chest regions of the mice. The local treatment also became a whole-body immune attack on the metastatic lesions.	[45]
CT26/BALB/c mice tumor model mEHT with Cur and Res combined treatment.	mEHT 42˚C, 30 min, 10 - 12 W, tumor growth, and immune cell infiltration were measured with cell viability, apoptosis, Western blot, and immunohistochemistry comparison with wHT.	mEHT with Cur and Res combination inhibited the growth of CT26 cancer by inducing apoptosis and HSP70 expression of tumor cells while recruiting CD3+ T-cells and F4/80+ macrophages.	Cur and Res combined with mEHT synergistically increased HSP release and immune response, showing enhanced anti-tumor efficacy.	[46]

B16F10 allograft cells inoculated to female C57Bl/6 mice (offspring of C57Bl/6 colonies) in the right inguinal area.	mEHT 42˚C, 30 min, measured tumor-size, HSP70, PUMA, γH2AX, DAMP signaling was measured.	Upregulation of cytoplasmic and cell membrane HSP70 Increased PUMA and AIF1 and rise of cC3 without significant apoptosis. But, γH2AX indicated DNA double-strand breaks, which upregulated p53 protein and downstream p21waf1 and p27kip. mEHT promoted the release of DAMP, it reduced MHC-I levels in tumor cells.	mEHT-related tumor shrinkage was primarily mediated by p53, upregulating the cyclin-dependent kinase inhibitors. Reduced cytotoxic T-cell response was observed despite increased DAMP signaling. Decreased tumor antigen and MHC-I levels suggest that NK cells and macrophages were the major contributors to tumor eradication.	[47]
Effect of repeated mEHT treatment in 4T07 TNBC cells inoculated orthotopically in female BALB/c mice.	mEHT 42˚C, 30 min, skin temperature just over the tumor 40˚C (3 W). The repeated treatments were studied by tumor size, cC3, HSP70, immune profile (CD3+, CTLA4, PD-1, PD-L1), p21, and Ki67.	The five-treatment repetition shows a significant positive change in all measured parameters in 4T07 TNBC.	Repeated treatment improves the effect of mEHT and is well applicable for TNBC tumors, suggesting positive clinical performance.	[48], [49], [50]
BALB/c mice were treated with mEHT, curcumin, and resveratrol in the CT26 allograft model.	mEHT 42˚C, 30 min, dose dependence is measured by proliferation assay, apoptosis, cell viability, Western Blot, FACS, CD3+, F4/80 and HSP70 were measured.	Immunogenic cell death was observed with intensive DAMP at the combined treatment.	Resveratrol and curcumin significantly increased the immunogenic effect of mEHT treatment.	[46]
mEHT treatment studied *in vitro* and *in vivo* with HepG2 cell line.	mEHT (42˚C, 30 min) was used combined with γδT cells 4 h after treatment, and *in vivo* in SCID mice comparing the combined treatment with the standalone therapies.	The mEHT treatment caused γδT ll migration to tumor cells even at 38˚C, where wHT had no effect. *In vivo*, a considerable inhibition of tumor growth was observed.	The γδT cells combined with mEHT significantly destroy tumor cells *in vitro* and *in vivo*.	[51] [52]
mEHT for B16F10 melanoma pulmonary metastases. Repeated treatment of lung.	mEHT 30 min, 42˚C (lung), 40˚C (pharyngeal) and 38.5˚C (rectal temperatures). Measured immunohistochemistry, flow cytometry, and apoptotic and necrotic cell death. 6 times repeated treatment.	mEHT induced significant anti-tumor effects and the downregulation of Ki67 expression, as well as made significant DNA double-strand breaks, significantly increased CD3+, CD8+ T-lymphocytes, and F4/80+CD11b+ macrophage density in the whole lung.	mEHT inhibits tumor growth and spontaneous proliferation of B16F10 melanoma in a mouse pulmonary metastasis model. mEHT is a complementary therapeutic option to chemo- and/or radiotherapy. The massive infiltration of tumors by CD3+ and CD8+ T-lymphocytes and by F4/80 CD11b-positive macrophages indicates the ability of mEHT to mobilize the immune response in treated animals.	[53]

Numerous furtherpublications dealt with the immunogenic effect of modulated electro-hyperthermia and presented its systemic tumor-specific immune effect using only a local treatment [54]-[56]. Thermal and nonthermal effects synergy became a useful complementary tool for radiotherapy, forming dynamic and well-regulated tumor-specific immune reactions following abscopal effects [57] [58]. The abscopal outcome creates a new perspective for the local

treatment, transforming to systemic immune impact on the malignant cells in the entire body, targeting both the micro and macro metastases [59]-[61]. The immunogenic processes may also be gained by oncolytic viral treatment enhancing the immune reactions of the therapy [62] [63].

The developed released HSPs by the stresses of various treatments show the considerable addition of the nonthermal component after 24 h to the standard thermal one *in vitro* measurements [43] [64] (**Figure 4(A)**). Due to the intensive stress with mEHT, the results show considerable HSP release from the tumor cells *in vitro* (Hep-G2 cell line), which makes it possible to transfer the tumor-specific information from the cancer cell. The high iHSP content exhausts the cellular protection, as was shown *in vivo* in 4T1 TNBC isograft experiments [48], and makes it possible to express the membrane and release the molecules to TME. A massive intracellular presence and moderate membrane and extracellular expression were observed in a study of a B16F10 melanoma tumor *in vivo* [47] (**Figure 4(B)**). The eHSP70 proteins appear almost immediately posttreatment in vitro [64], while *in vivo*, it takes more time (2 days) **(Figure 4(C)**) having iHSP70 in the first 48 h period [41]. Due to the suppressed chaperone activity, inhibiting HSP synthesis in the B16F10 melanoma cell line with Quercetin *in vivo* suppresses tumor growth [65]

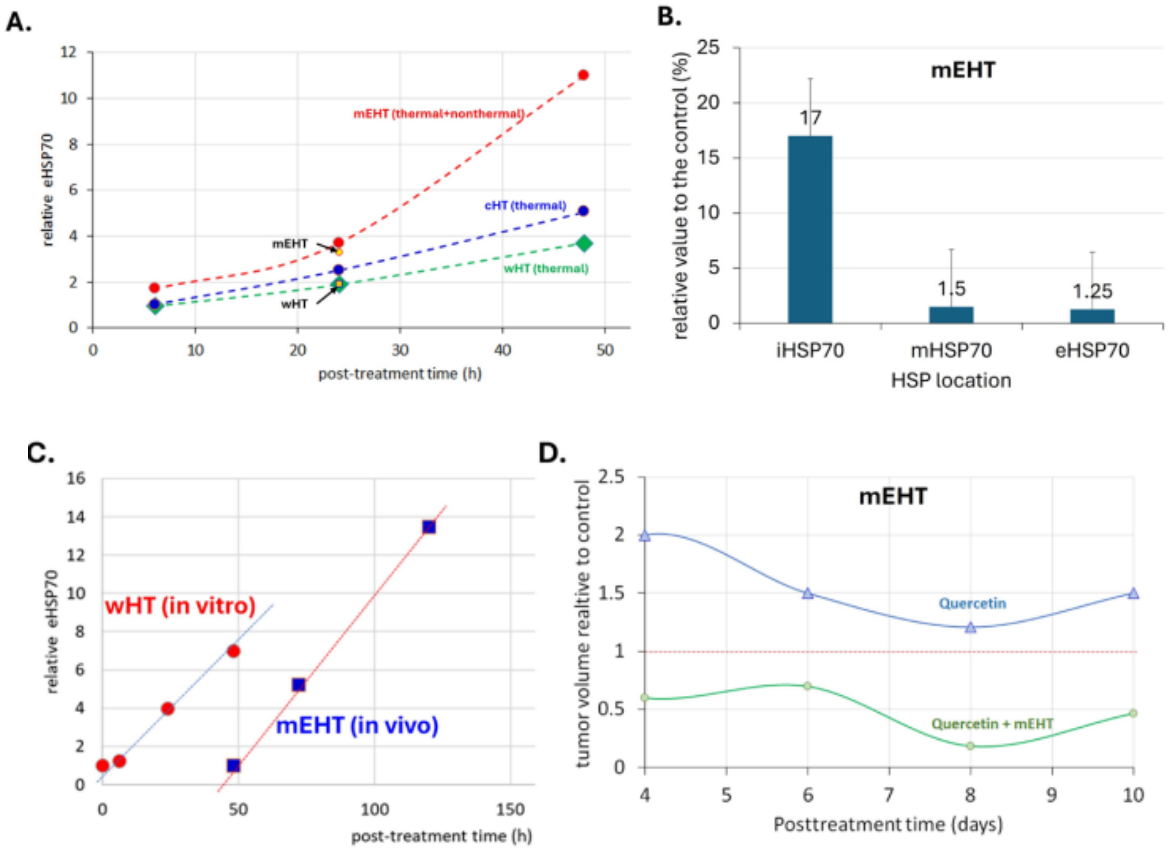

Figure 4. Development of HSP70 by mEHT. (A.) The relative expression of HSP70 in the extracellular matrix [43]. (B.) The relative values of HSP70 proteins in various locations [47]. (C.) The development of the eHSP70 *in vitro* [64] and *in vivo* [41]. The inhibition of iHSP synthesis also inhibits the tumor growth [65]

As we had proved in the previous two parts of the present series [6] [7], the mEHT triggers massive apoptosis. The model animals were BALB/c nu/nu immunocompromised mice with two distant tumor inoculations of the HT-29 human colon cancer cell line. The right tumors were treated, and the left untreated tumors were used as a control (**Figure 5(A)**). The first experiments investigated how independent the distant untreated tumor is from the treated one, observing the tumor growth for a longer time after mEHT treatment. The untreated liaison in the xenograft of immunocompromised mice changes in the standard way, with some necrotic nodules inside. The dead tissue in the treated tumor of the same animal grows over time and develops a leukocyte invasion ring 72 h posttreatment (**Figure 5(B)**). Intensive apoptosis appears in the ring in which cCas3 and late apoptotic detection can follow [66]. Late apoptosis showed the opposite development in treated and untreated tumors [67] (**Figure 5(C)**), the apoptosis continues in the treated and is inhibited in the untreated tumor. The experiments proved that the untreated tumor can be used as a reference in the double tumor model in immunocompromised mice.

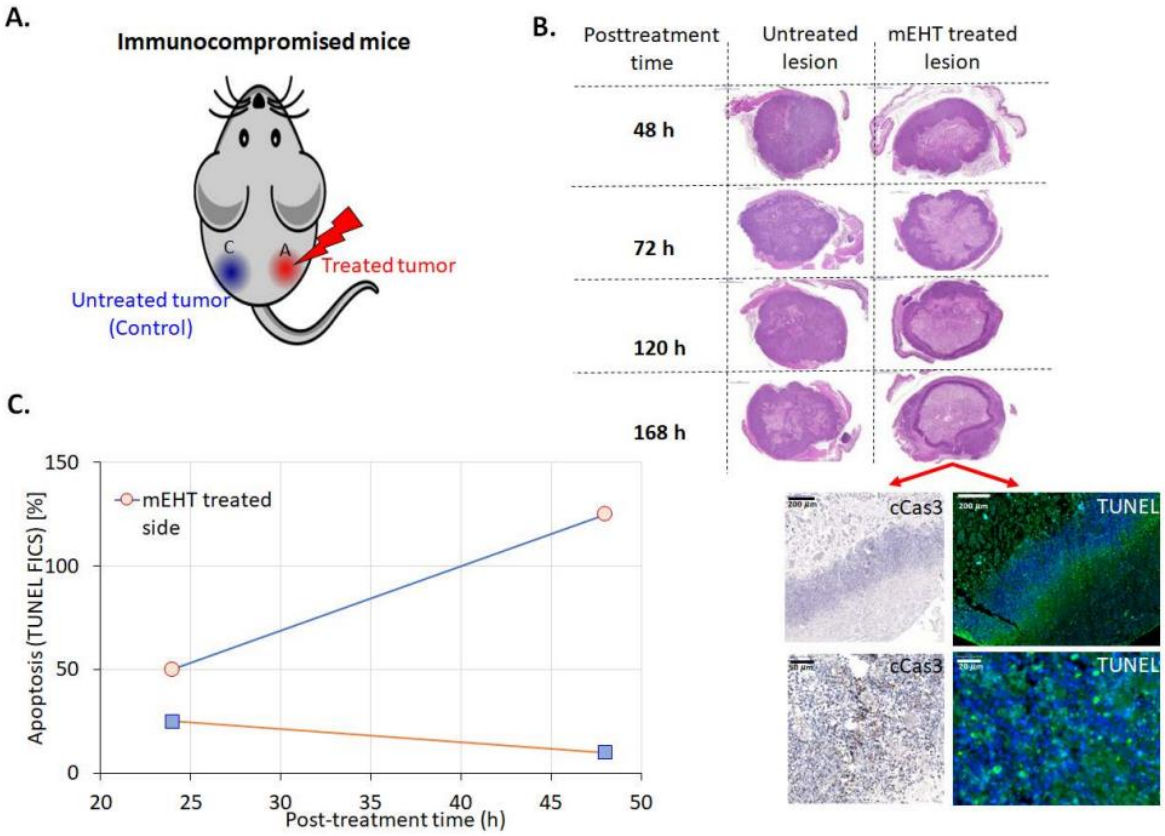

Figure 5. The double tumor connection in immunocompromised mice [66]. (A.) The two tumors in distant sites: "C" is the untreated control tumor, and "A" is the actively treated tumor. (B.) The time development of the treated and untreated tumors. The changes in the "C" site are not significant. (C.) Development of the apoptosis by elapsed time from the mEHT treatment [67]

The development of HSPs in xenograft model HT-29 cancer shows a peculiar feature. The HSP70 has a definite, significant minimum at 48 h, showing a return to the baseline. The HSP90 returned earlier, at 14 h [68] (Figure 6) and was observable intracellularly at 24 h posttreatment and measured extracellularly at 168 h. The immunohistochemical immunofluorescent staining of HSP70 shows a significant expression of these proteins on the cell membrane (mHSP), triggering an innate immune attack by NK cells [32]. The most likely explanation for the double peak of HSP70 is that

the sizeable intracellular concentration could not inhibit the apoptosis, which was executed within two days. After this time, the release of HSP70 to the ECM became dominant, which is well observable with immunohistochemical staining at 72 h timepoint [68]

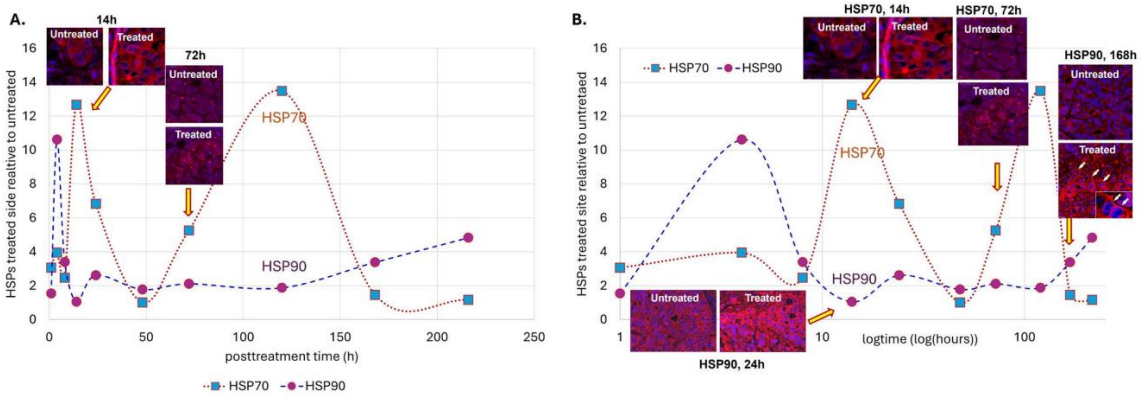

Figure 6. The relative development of HSP70 and HSP90 proteins after the mEHT treatment [68]. (A.) The double peak of HSP70 is probably due to its relocalization from the cytosol. (B.) The same is true for (A.) on a logarithmic scale for a more explicit demonstration of the expression shift of two HSPs.

Both extracellular HSP70 and HSP90 play essential roles in immunogenic processes. These chaperones are intracellularly antiapoptotic and help fold and stabilize proteins within cells. However, the game changes under extreme stress, releasing these HSPs to TME. Because they are proapoptotic, they represent an essential part of the DAMP molecular set. In this way, both proteins activate the immune responses, for example, they can bind to Toll-like receptors (TLRs) or CD91 on dendritic cells and macrophages, activating downstream signaling pathways involved in antigen presentation facilitated by these HSPs. In cancer, extracellular HSP70 and HSP90 released by tumor cells can modulate the TME and influence immune responses against the tumor. Depending on the context, their presence in the TME can induce tumor-specific immune reactions and affect cancer immunotherapy's efficacy. Their multifaceted roles in immunogenic processes act as danger and info signals, modulate immune responses, and influence the interaction between the immune system and cancer.

The immunogenic action of HSP70 and HSP90 shares similarities but also exhibits some differences, particularly in their downstream effects on immune responses. HSP70 and HSP90 can activate innate immune responses by binding to cell membrane receptors on immune cells (mHSP70 and mHSP90). They can interact with receptors like Toll-like receptors (TLRs) and CD91, triggering signaling pathways that lead to the production of pro-inflammatory cytokines and chemokines. However, the specific receptors and signaling pathways activated by mHSP70 and mHSP90 may vary, leading to differences in the magnitude and nature of the immune response. The extracellularly released HSPs (eHSP70 and eHSP90) can enhance antigen presentation by promoting the uptake and processing of antigens by antigen-presenting cells. This can lead to the activation of T cells and the adaptive immune response against tumor cells. However, the mechanisms by which eHSP70 and eHSP90 promote antigen presentation may differ, potentially influencing the quality and specificity of the adaptive immune response. In a short time after treatment, the development of DAMP molecules expresses calreticulin (CRT) 4 h posttreatment with mEHT (**Figure 7**). Notablythe wHT and cHT treatments do not express CRT (*in vitro* Hep-G2

cell experiments, [64]), but mEHT significantly produces these membrane-located molecules both *in vitro* [64], and *in vivo* (HT-29 xenograft experiments [41]) (**Figure 7**). CRT on the membrane (mCRT) marks the cancer cells for recognition and subsequent engulfment by the immune cells, promoting ICD. The mCRT potentially slows tumor growth and aids the natural defense mechanisms against cancer.

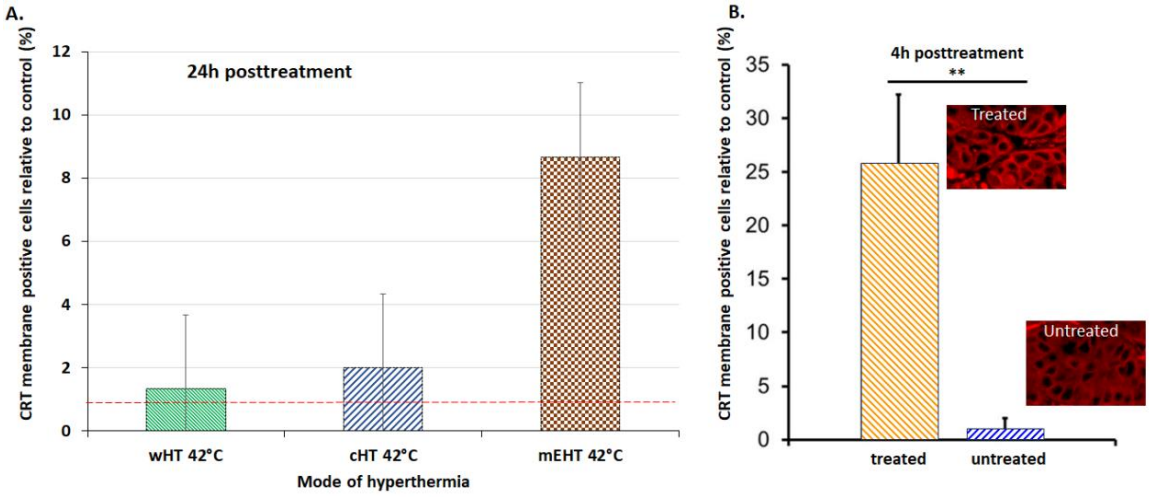

Figure 7. Development of calreticulin after mEHT. A dashed line shows the reference level. (A.) The wHT and cHT have significantly less CRT expression than the mEHT-treated HepG2 cells *in vitro* [64] 24 h after treatment. The relative expression of CRT as early as 4 h after mEHT treatment shows significant differences between the two tumors. The inserts show the membrane localization of CRT in mEHT-treated tumors, while it is not the case in the control [68]

The other immunogenic protein, the HMGB1 in the ICD process is freed from the cytosol, and the cell becomes practically empty from these molecules over 50 h posttreatment in HT29 tumors of immunocompromised mice [41] (**Figure 8**). The distant untreated tumor of the same animal constantly expresses intracellularly HMGB1. The released HSP70 and free ATP appear together with HMGB1, completing the DAMP molecular set in immunocompetent mice with B16F10 melanoma tumors [47].

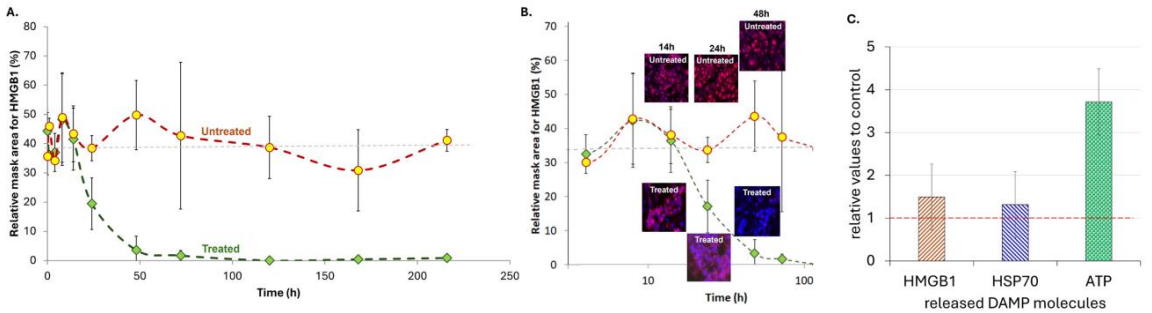

Figure 8. The development of HMGB1 proteins in time course after treatment. A dashed line shows the reference level. (A.) The treated tumor releases the HMGB1 to the extracellular milieu so its expression in the cytosol rapidly decreases, while the control cells keep these proteins [41]. (B.) The logarithmic scale shows that the first 12 h develops parallel in both tumors. The release starts only afterward. (C.) The relative expression of the leading DAMP molecules [47].

The CD3+ T cells play a crucial role in cancer immune defense. CD3+ T cells can recognize cancer cells as foreign or abnormal by recognizing Major Histocompatibility Complex type 1 (MHC I) presentation on the surface of cancer cells. CD3+ cells are T cells that express the CD3 protein on their surface. CD3 is a complex of proteins essential for the signal transduction process in T cells, particularly in activating T cell receptors upon binding to APCs. The CD3+-related cytotoxic T cell-mediated killing is crucial for eliminating cancer cells and controlling tumor growth. The cytokines the CD3+ T cells produce can also exert direct anti-proliferative effects on cancer cells and contribute to their elimination. CD3+ T cells can activate the memory response of adaptive immune surveillance, capable of a rapid and robust immune response upon re-challenging to the same tumor antigens, working like a tumor vaccination, protecting against tumor recurrence. The CD3+ expression does not show deviation until 72 h posttreatment. After a transition period, CD3+ has a maximum at 168 h posttreatment, showing the relatively long time to develop the contribution to the adaptive immune activity, while until 72 h posttreatment, it remains at baseline (**Figure 9**).

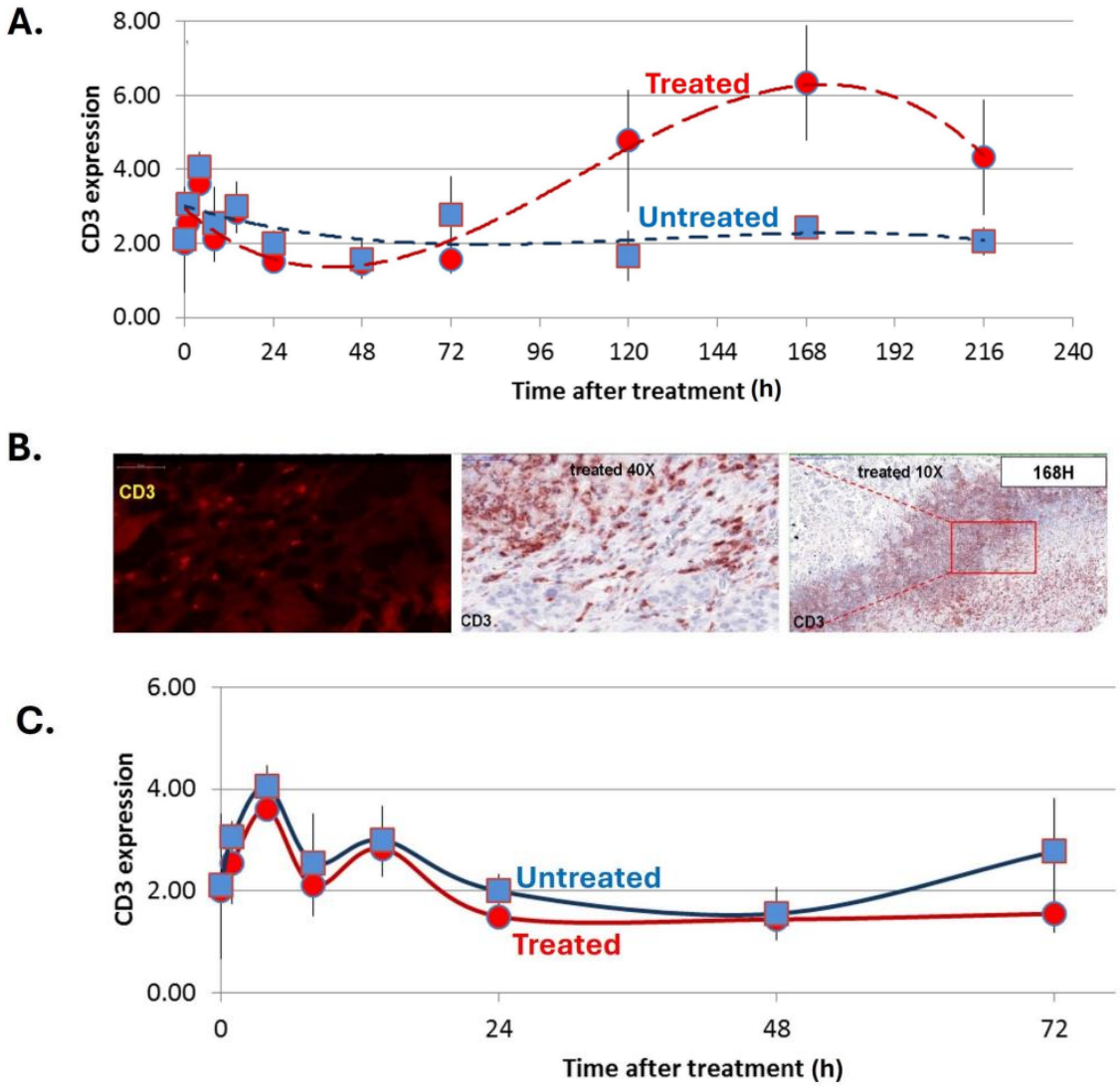

Figure 9. The time course of CD3 expression [68]. (A.) The CD3+ expression significantly develops 72 h after treatment. (B.) The immunohistochemical patterns of CD3+ expression at 168 h after treatment. (C.) The first two days have no deviation of the CD3+ from the control, and it starts being substantially developed after a transition period from 48 h to 72 h.

In a longer timescale after 72 h posttreatment, the neutrophilic activity increase was detected by the development of the enzyme myeloperoxidase (MPO) [68] (**Figure 10**). MPO participates in immune defense and anticancer processes as well. MPO generates reactive oxygen species (ROS), which can induce oxidative stress in cancer cells, leading to DNA damage, lipid peroxidation, and ultimately cell death. The oxidative stress helps in killing cancer cells or making them more susceptible to other treatments like chemotherapy or radiotherapy. MPO can modulate the inflammatory TME by regulating inflammatory mediators and immune cell recruitment, which may contribute to controlling tumor growth and metastasis. MPO has been implicated in regulating immune responses, including activation of T and dendritic cells, facilitating the recognition and elimination of cancer cells, and contributing to anticancer immunity. Like all molecular processes in a complex system, MPO is a double-edged sword, its action is context-dependent. While it may have anticancer effects in specific contexts, it could also promote tumor growth and metastasis under different conditions. The mEHT activates the MPO's anticancer behavior, showing a parallel CD3+ development. CD3+ T cells produce various cytokines, including interferon-gamma (IFN-γ) [52] (**Figure 10(B)**). IFN-γ is primarily produced by activated T cells and NK cells, promoting an anti-tumor immune response to the activation and differentiation of T cells, especially CD8+ cytotoxic T cells and CD4+ T helper 1 (Th1) cells

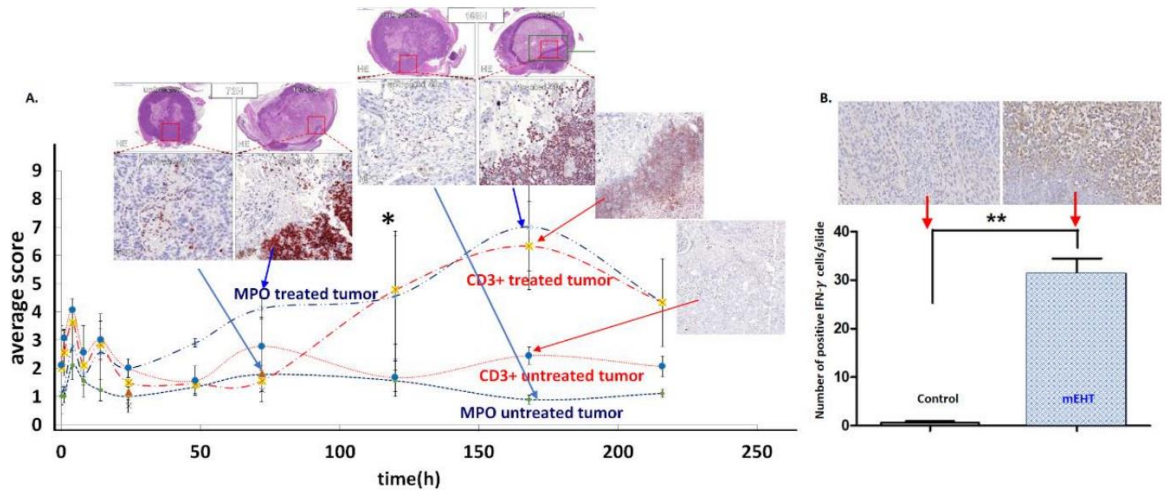

Figure 10. The time course of immune effects. (A.) Development of myeloperoxidase in HT-29 allograft tumor model [68]. (B.) The IFN-γ, compared to the control after mEHT treatment [52]

Melanoma pulmonary metastasis research was conducted with B16F10 injected tumors systemically to the tail vein of female C57BL/6 mice [53] (**Figure 11(A)**). A significant decrease in the metastatic tumor mass was observed in the mEHT-treated tumors compared to the untreated control. The treatment followed a reduced number of pulmonary metastatic nodules accompanied by significant DNA damage (increased γH2AX), downregulation of Ki67 proliferation marker, enhanced immune cell infiltration, and upregulation of p21waf1 expression. The tumor and the whole lung had significantly increased CD3+, CD8+ T-lymphocytes, and F4/80+CD11b+ macrophage density (**Figure 11(B)**), which proves the immunogenic activity of the mEHT treatment.

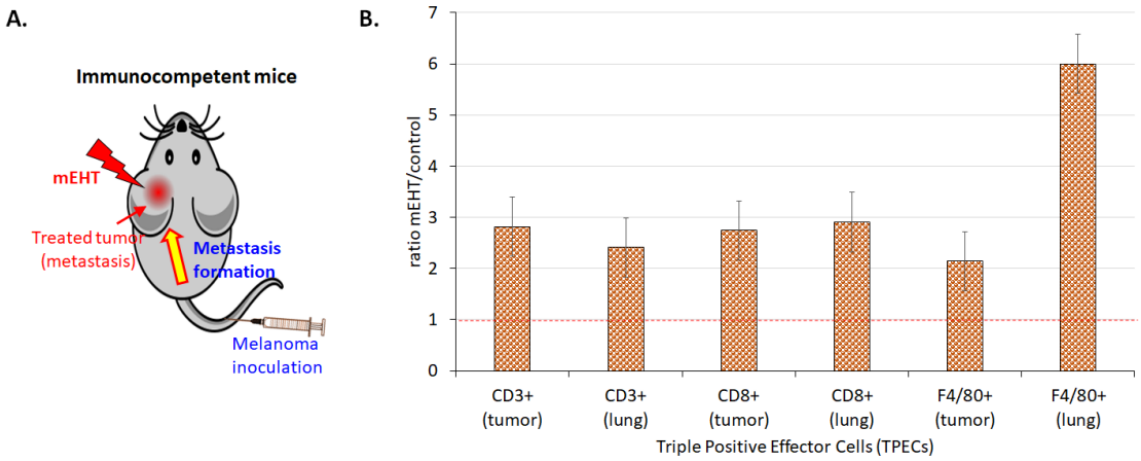

Figure 11. The treatment of lung metastases. (A.) The model. (B.) The gained pulmonary metastasis in immunocompetent mice intensively develops immunogenic cells in the tumor and its vicinity in the healthy tissue of the lung [53]. A dashed line shows the reference level.

Another immune activation with naturopathic remedies (Curcumin and Resveratrol) was applied in an extended study of *ex vivo* (serum from a treated SD rat) for pharmacokinetic research and *in vivo* (allograft BALB/c mice model) for treatment study using CT26 tumor cell subcutaneous inoculation. Curcumin and Resveratrol are natural antioxidants, and both may inhibit the proliferation of some malignant tumors [69] [70]. The mEHT treatment was concomitantly applied with subcutaneously inoculated micro-cumin and micro-resveratrol suspension (curcumin 200 μg and resveratrol 105 μg). For comparison, groups of animals were used as control, and two other groups had Curcumin and Resveratrol or mEHT standalone. The measured immunogenic effect was significant [46] (**Figure 12**).

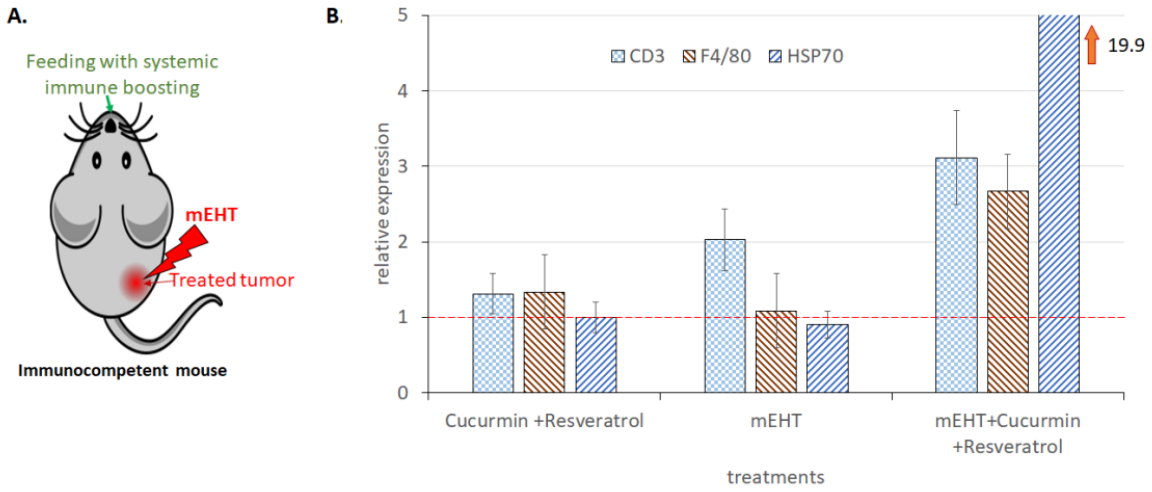

Figure 12. Combined mEHT treatment with curcumin and resveratrol [46]. (A.) The mice were fed curcumin and resveratrol. (B.) The standalone curcumin and resveratrol or mEHT therapies had significantly less DC and macrophage penetration to the tumor than their combined treatment.

The prominent HSP expression is due to the different localizations of this protein not being selected. A dashed line shows the reference level

For checking the attraction of the NK cells by mHSP70 on the membrane of tumor cells produced by mEHT, the tumor infiltration of NK cells was measured and demonstrated the effect [44]. A2058 melanoma cells were inoculated to an immunocompromised xenograft mouse model in both flanks of the animal and mEHT-treated on the right side, while the other was used as control. Substantial NK accumulation happened in the mEHT-treated tumor, while the untreated side did not show changes. Primary human NK or the IL-2 independent NK-92MI cells were distantly injected, far from the tumors, into the research animals after the mEHT treatment. The p53-driven apoptosis was ignited by mEHT monotherapy, supporting the attraction of the distantly injected NK cells. The chemoattractant CXCL11 metalloproteinase MMP2 induced upregulation was observed only in the treated tumor, supporting its growth inhibition and destruction. The destruction was more effective with NK-92MI cell injection than with primary NK, but both NK additions show a higher destruction rate than mEHT alone (**Figure 13**).

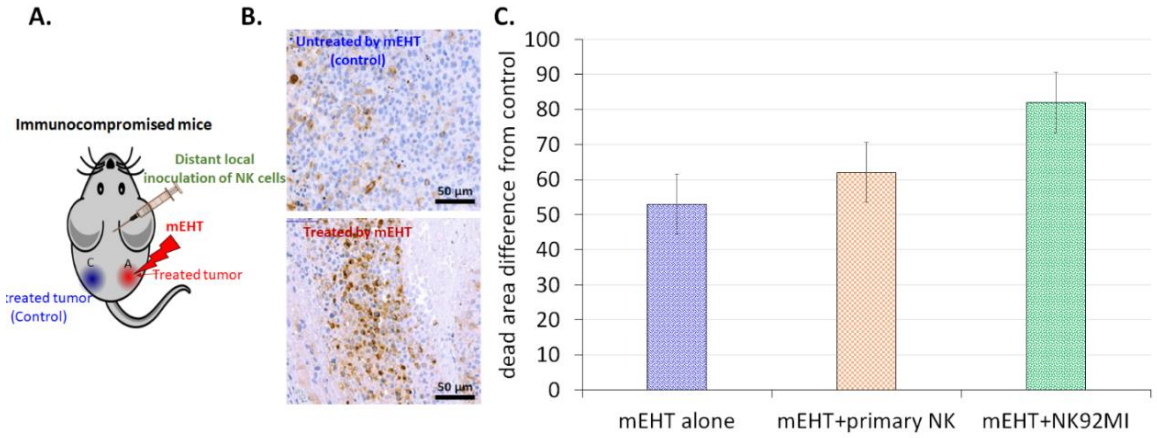

Figure 13. NK cell enrichment by mEHT treatment [44] (A.) In two tumor model experiments, NK cells were injected in a distant location into immunocompromised mice. (B.) The difference between the treated and untreated tumors is shown with immunohistochemical staining. (C.) The effect of NK cells increases the dead tumor area when the mEHT is combined with NK cells.

Another study on inhibiting tumor growth with immune stimulation and mEHT showed the tumor's destructive processes and the effect of immune memory. The immunostimulant was an intratumorally injected DC to the CT26 tumor. Relative to the DC or mEHT alone, the combined therapy significantly inhibited tumor growth [43] [71] (**Figure 14(B)**). The CD45 and F4/80 immunohistochemical studies show a significant elevation of the leucocytes and macrophages in the tumor treated with the combined therapy (**Figure 14(C)**). Notably, the significant increase in the eosinophils in tumors with combined treatment shows the potential role of these cells in immune combat, [72] [73], having substantial changes in the tumor microenvironment which could participate in tumor regression [74], and believed that it is a predictive biomarker for better prognosis [75]. Notably, the rechallenging of the same tumor in mEHT + DC-treated mice was rejected in **Figure 14(D)**, proving the tumor-specific memory of the immune activity of the animal.

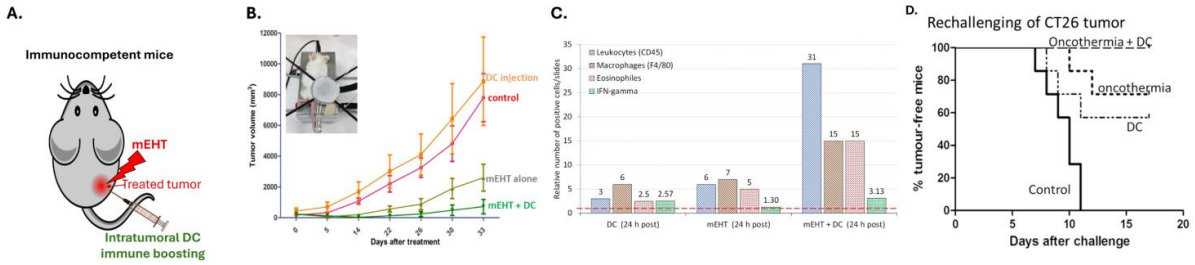

Figure 14. Combined treatment of mEHT with DC intratumoral injection into CT26 allograft *in vivo* model [43]. (A.) The model. (B.) The tumor volume is developed after the various treatments. (The treatment setup is in the insert.) (C.) Relative expression of some immunogenic proteins. A dashed line shows the reference level. (D.) Survival of the animals after rechallenging the tumor.

SCCVII mouse squamous cell carcinoma was inoculated to C3H/He immunocompetent mice in the femoral and chest regions of the animals [45]. This allograft model aims to check the abscopal effect with additional immune stimulation only of the treated tumor. Dendritic cells were injected directly into the femoral tumor three times every other day. The tumor volumes of both locations were measured and found a moderate inhibition of the growth of both tumors. When mEHT was applied to the femoral tumor, the tumor growth inhibition was more prominent and again in both tumors, even though only one was treated. Another group of experimental animals had direct intratumoral DC injection only into the mEHT-treated tumor posttreatment at the 9th, 11th, and 13th days. Tumor volume was measured again in the DC+mEHT treated (femoral location) and nontreated (chest location) tumors. The growth inhibition was drastic in both sites, and the tumor growth was practically arrested (**Figure 15**). The most important immune reactions were measured from the serum together with the tumor volumes. Flow cytometry detected a large expression of CD3+ and CD8+ T cells in the various groups, with the significantly highest value in the DC+mEHT treatment group (**Figure 15(D)**). The optical density measurements confirmed the intensive increase of the CD8+ T cells in combined treatment together with the S100 DC marker protein, which can modulate dendritic cell function and immune responses by promoting the maturation and activation of dendritic cells, enhancing antigen presentation, and influencing the migration of dendritic cells to lymphoid organs. At the same time, the Foxp3 expression was significantly suppressed in the DC + mEHT group of animals, showing the inactivation of Treg cells [45] [76].

The $\gamma\delta T$ cells bridge the innate and adaptive immune responses [77]. The role of $\gamma\delta T$ cells in tumor degradation is multifaceted. $\gamma\delta T$ cells MHC-independently can directly recognize and kill tumor cells, directly exocytosis perforin and granzyme B in the shaped immune synaptic space. They recognize stress-induced molecules on the cell membrane (like mHSP70) [78], and it has excellent support for immunotherapies [79]. Like CD3+ T cells, the $\gamma\delta T$ produces various cytokines such as interferon-gamma (IFN-γ) and tumor necrosis factor-alpha (TNF-α) upon activation. These cytokines have anti-tumor effects by enhancing the activity of other immune cells, such as macrophages and cytotoxic T cells, and inhibiting tumor cell proliferation. $\gamma\delta T$ cells can modulate the activity of different immune cells within the tumor microenvironment [80]. The $\gamma\delta T$ cells injection to NPD-SCID mice having HepG2 hepatocellular tumor [51] [52], the mEHT treatment became more effective than without this injection (**Figure 16(B)**). Notably, the $\gamma\delta T$ cells alone do

not have an antitumoral effect in this model. The *in vitro* experiments show increased tumor degradation with just thermal effect (wHT) at 42°C, but the mEHT-treated HepG2 cell line, together with $\gamma\delta T$ cells, caused notable cell destruction at 38°C, which is further increased in higher 42°C temperature with mEHT (**Figure 16(C)**).

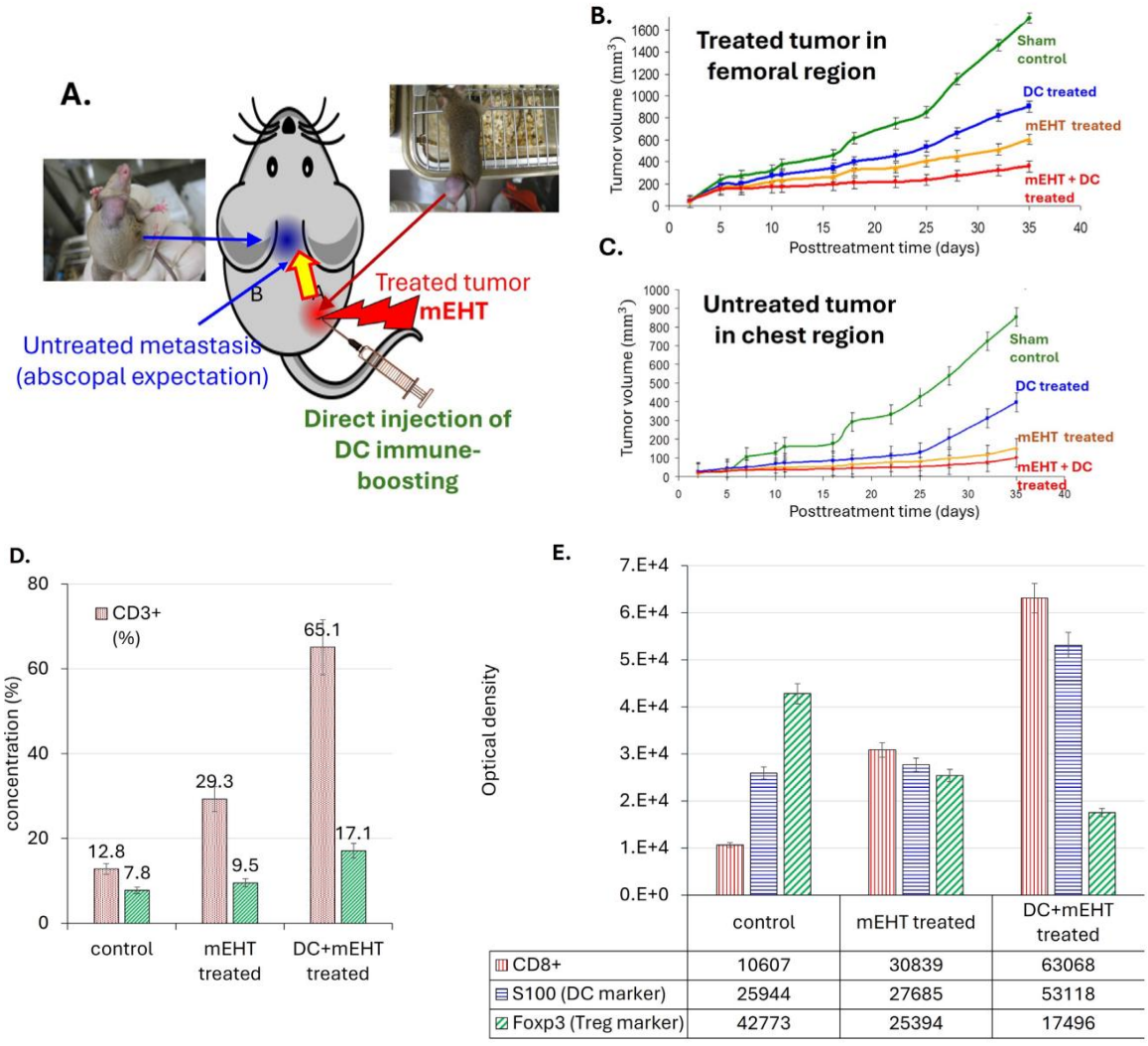

Figure 15. Model of abscopal effect [45]. (A.) The setup of the *in vivo* model shows the distant tumors in the inserts. (B.) The development of the tumor volume after the treatment in the treated (femoral region) SCCVII tumor. (C.) The development of the tumor volume after the treatment was measured in the untreated tumor in a distant location (chest region). (D.) The CD3+ and CD8+ T cells appeared systemically in the mice. The optical density measurement shows the high density of the killer T cells while the protumoral Tregis suppressed.

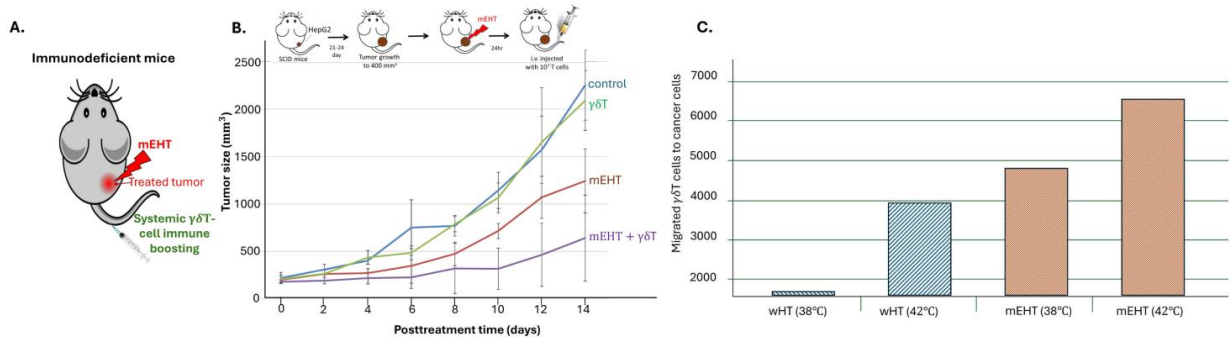

Figure 16. The effect of the $\gamma\delta T$ cells in immunocompetent mice model [51] [52]. (A.) The set-up of the model. (B.) The tumor volume is developed after the different treatments. The protocol is shown in the insert above the graph. (C.) $\gamma\delta T$ migrated to cancer cells. The migration ability of $\gamma\delta T$ cells was measured after mEHT treatment HepG2 cell-line (separated → seeding 24 h → collected 4 h later → measured by flow cytometry).

The new development direction of oncotherapies targets immunogenic effects. mEHT therapy fits this trend and enhances the antitumor immune activity shown in the above results. One of the promising immunotherapies is connected to the inhibition of Programmed Cell Death Protein 1 (PD-1) and Cytotoxic T-lymphocyte-associated protein 4 (CTLA-4). PD-1 on the surface of T cells acts as a brake on the immune system by binding PD-L1 to protein PD-L1 on cancer cells, preventing the T cells from attacking the cancer cells. Anti-PD-1 (aPD-1) therapy allows T cells to attack and destroy cancer cells. CTLA-4 is another protein on the surface of T cells. It is a checkpoint inhibitor, regulating the amplitude of immune responses and hindering the immune system's ability to attack cancer cells. The anti-CTLA-4 (aCTLA-4) therapy reduces the immune evasion of the cancer cells, enabling a more robust immune response against the cancer cells. A study deals with the cooperative activity of these checkpoint inhibitors and mEHT in their complementary application [52]. The complex study compared the stand-alone mEHT, aPD-1, and aCTLA-4 therapies to the control. The therapy protocol for immunocompetent mice has standard mEHT (42°C, 30 min) first and adding aPD1 of aCTLA-4 concomitantly to the tail vein of the mice, and the administration of the checkpoint inhibitors (CPI) was repeated two more times with 3 3-day pauses. (We denote these protocols as aPD1 (=) and aCTLA4 (=)). The action time was also studied using a protocol that administered the checkpoint inhibitors 2 days after mEHT and afterward repeated the CPI two more times with 3 3-day pauses, as was applied in the previous protocol. (We denote these protocols as aPD1 (>) and aCTLA4 (>)). Results show the advantage of mEHT in improving the effect of checkpoint inhibitors (Figure 17). The best results were achieved when aCTLA-4 was applied concomitantly with mEHT (aCTLA4 (=) protocol), with almost half the tumor size at the 16th day posttherapy compared to aCTLA-4 alone. The same difference was observed in aPD-1 therapy, as shown in **Figure 17(C)**.

The systemic immune activity can be measured in the double-tumor mice when the effect of the locally treated tumor on the distant other could be studied.

The first observation of the interaction was measured by injection of lipopolysaccharide (LPS) [81] into mice, triggering primarily the innate immune response of the animal, activating the toll-like receptor 4 (TLR4) signaling pathway and also activating APCs. This immune stimulation developed a distant tumor distortion (abscopal effect), which could be measured 72 h posttreatment (**Figure**

18). Another observation was the immune stimulation with Newcastle Disease Viruses (NDVs) [62] [63], which activates the TRL's signal pathways and creates innate and adaptive immune reactions

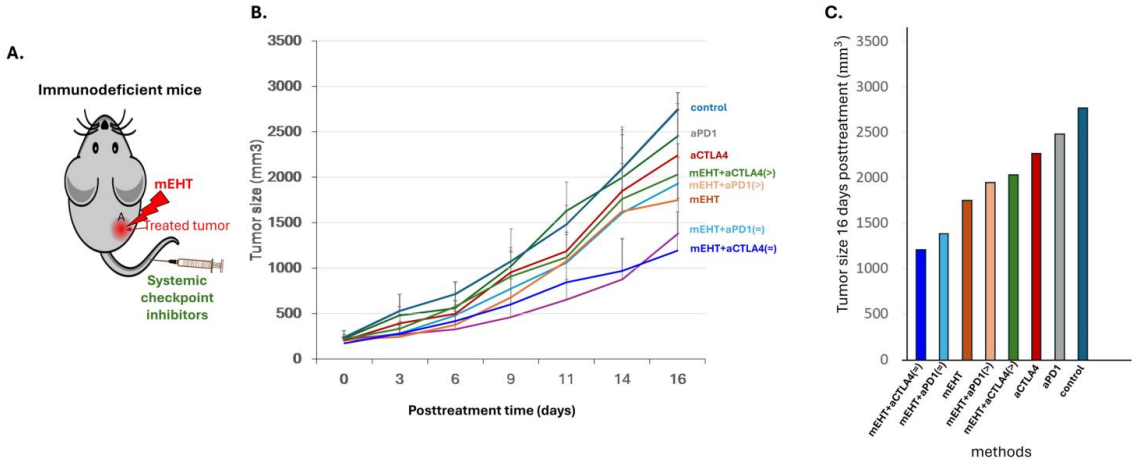

Figure 17. Check point inhibitor study with mEHT support [52]. (A.) The experimental setup NOD-SCID mice, HepG2 tumor. (B.) Growth of the tumor volume by time (days). (C.) Comparison of tumor sizes (mm3) on the 16th day. Significant differences were observed between control and mEHT ($p \cong 0.0006$), control and aPD1 (=) ($p \cong 0.00002$), control and aPD1 (>) ($p \cong 0.002$), control, and aCTLA4 ($p \cong 0.028$), control and aCTLA4 (=) ($p \cong 0.00001$), control and aCTLA4 (>) ($p \cong 0.04$).

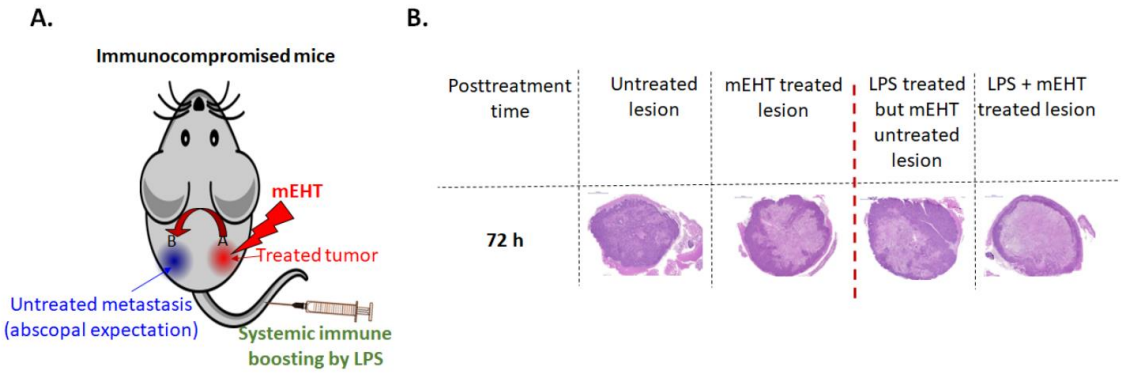

Figure 18. Experiment with lipopolysaccharide (LPS). (A.) The experimental setup. (B.) The treated and untreated tumors were 72 h after treatment.

Learning the results of the LPS experiment, a direct immunostimulant Marsdeniatenacissima (MTE) in BALB/c immune-competent double tumor-bearing mice was injected into the tail vein of the animals (**Figure 19(A)**). For comparison, the mEHT stand-alone therapy was performed first. It was observed the expected phenomena: blocks the proliferation measured with the Ki67 marker [42] and develops a significant amount of DAMP, the eHSP70, CRT, and HMGB1 proteins, which were much less in the untreated tumor (**Figure 19(B)**). The DAMP development was accompanied by significant tumor infiltration by S100 positive antigen-presenting dendritic cells and CD3+ T-cells with only negligible FoxP3 positive regulatory T-cells compared to the distant untreated tumor [42]. When direct immune stimulation with MTE was applied concomitantly with mEHT, tumor destruction was significant in untreated tumors, too. The difference between the two tumors drastically decreased typical DAMP production, and immune reactions also appeared in the distant

untreated tumor. The difference between the treated and untreated tumors is drastically reduced, and the abscopal effect actively destroys the untreated tumor, too. [42] (**Figure 19(B)**)

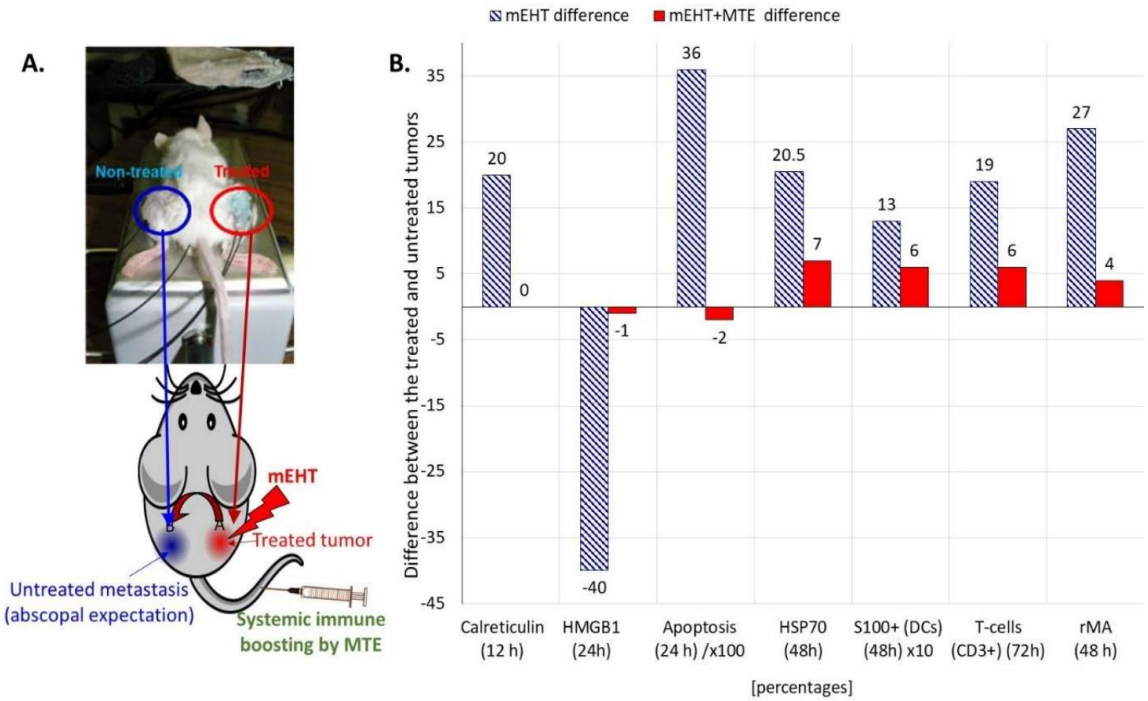

Figure 19. The abscopal research with immunostimulatory MTE in immune-competent mice with C26 murine colorectal adenocarcinoma. (A.) The experimental setup of the double tumor model. (B.) The difference of immunogenic cells of treated and untreated tumors was measured. Without immunostimulatory MTE, the difference was significantly higher in the treated tumor, while when MTE was applied concomitantly with mEHT, the difference was drastically reduced. No significant difference was observed between the treated and untreated tumors.

The immunogenic processes have a definite spatiotemporal order (**Figure 20**) producing the optimally harmonized immune action in the entire body attacking the malignant cells in the treated tumor and distant locations from the treatment site.

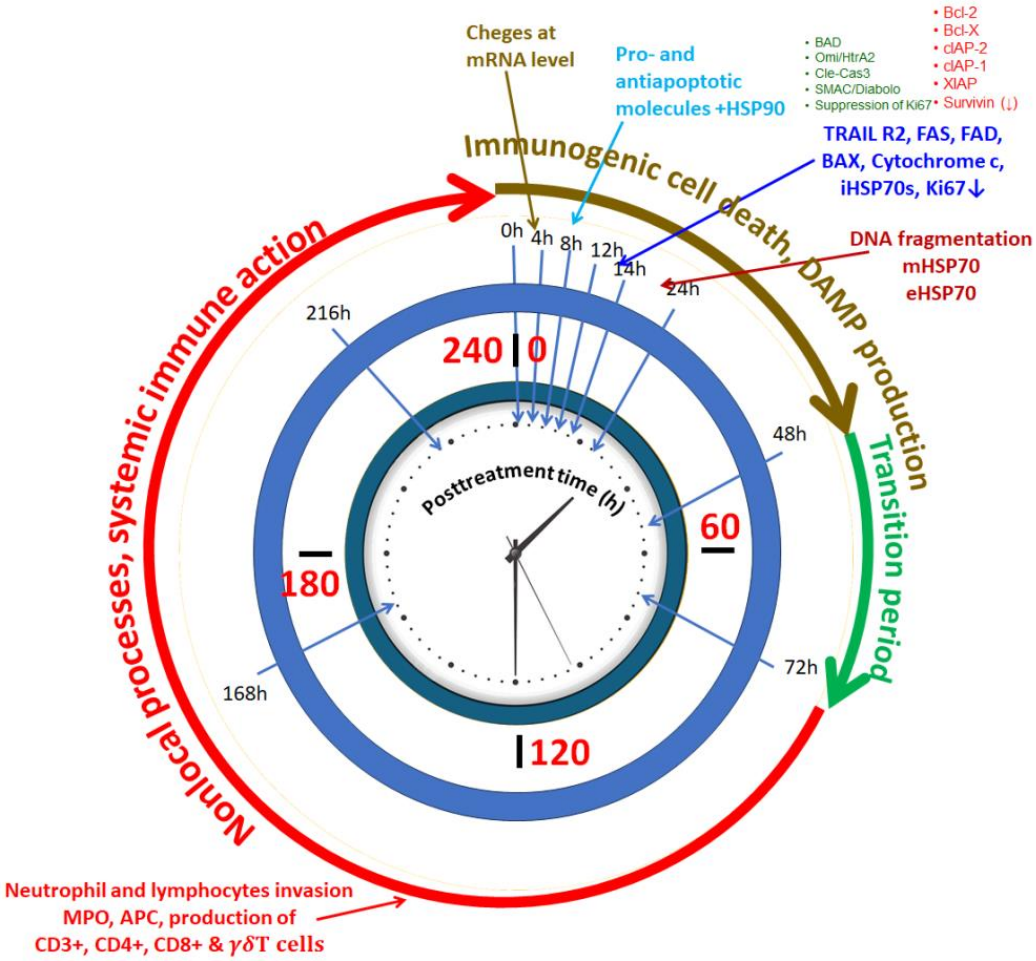

Figure 20. The observed immunogen changes and their timing in the processes induced by mEHT are a synergy of thermal and nonthermal effects.

4. Conclusions

The results described above strongly support the immunogenic activity of mEHT treatment. The ignited and controlled apoptosis releases DAMP, completing ICD. The correctly released DAMP molecules deliver various signals for the nearby antigen-presenting immune cells (like DCs and macrophages), and the APC generates tumor-specific immune activity to attack the malignant cells all over the entire body. The specialties of mEHT in this complex process, which distinguishes it from conventional (thermal alone) hyperthermia, ensure the immunogenic actions:

1) mEHT uses non-thermal effects to ignite immunogenic cell death by exciting some transmembrane proteins.
2) The thermal effect optimizes the nonthermal processes and increases the chemical reaction rates, including the critical enzymatic effects.
3) The expression of the DAMP molecules has a strict spatiotemporal order for optimal ICD processes.

4) The average temperature of the tumor mass remains under 40°C ensure the just-in-time activity of the available immune cells in the TME.

5) The apoptotic process and the mild average temperature do not damage the info delivery from the tumor cells to the TME and APCs.

6) The mEHT transforms the local treatment into a non-local, systemic therapy, avoiding metastatic proliferation and so increasing survival and quality of life.

The mEHT technology renews conventional hyperthermia. The synergy of heating with bioelectromagnetism and its harmony with homeostatic physiology opens possibilities of stable, controlled therapy with survival time and quality of life endpoints. The trends in oncotherapies and hyperthermia oncology show a common direction: the immunogenic goals [82]-[84].

The clinical studies of various medical centers in different countries provide the final validation of these preclinical data [85]-[87].A phase III clinical trial proved the abscopal effect for advanced uterus cervix patients [88] when adding mEHT to systemic conventional radiochemotherapy significantly increased the abscopal effects. The abscopal immunogenic activity of mEHT with a local radiotherapy combination was observed in another clinical study [89]. Altogether, 150+ clinical articles show the advantages of mEHT therapy. The article to summarize the clinical studies is in progress.

Acknowledgments

I am thankful to the listed authors for their diligent research

Fund

This research received external funding from the Hungarian Government, grant number GINOP_PLUSZ_2.1.1-21-2022-00058.

Conflicts of Interest

The author declares no conflicts of interest regarding the publication of this paper.

References

[1] Raff, M.C. (1992) Social Controls on Cell Survival and Cell Death. Nature, 356, 397-400. https://doi.org/10.1038/356397a0

[2] Ferrarelli, L.K. (2014) Focus Issue: Refining the War on Cancer. Science Signaling, 7, eg2. https://doi.org/10.1126/scisignal.2005276

[3] Lineweaver, C.H., Davies, P.C.W. and Vincent, M.D. (2014) Targeting Cancer's Weaknesses (Not Its Strengths): Therapeutic Strategies Suggested by the Atavistic Model. BioEssays, 36, 827-835. https://doi.org/10.1002/bies.201400070

[4] Szasz, A. and Szigeti, G.P. (2024) Exploring Biocomplexity in Cancer: A Comprehensive Review. Open Journal of Biophysics, 14, 154-238. https://doi.org/10.4236/ojbiphy.2024.142009

[5] Lee, S., Fiorentini, G., Szasz, A.M., Szigeti, G., Szasz, A. and Minnaar, C.A. (2020) Quo Vadis Oncological Hyperthermia (2020)? Frontiers in Oncology, 10, Article 1690. https://doi.org/10.3389/fonc.2020.01690

[6] Szasz, A. (2024) Pulsing Addition to Modulated Electro-Hyperthermia. Part I. In vitro Research. International Journal of Clinical Medicine.

[7] Szasz, A. (2024) Pulsing Addition to Modulated Electro-Hyperthermia. Part II. In vivo Research. International Journal of Clinical Medicine

[8] Lee, S. and Szasz, A. (2022) Immunogenic Effect of Modulated Electro-Hyperthermia (mEHT) in Solid Tumors. In: Interdisciplinary Cancer Research, Springer. https://doi.org/10.1007/16833_2022_74

[9] Krenacs, T., Meggyeshazi, N., Forika, G., Kiss, E., Hamar, P., Szekely, T., et al. (2020) Modulated Electro-Hyperthermia-Induced Tumor Damage Mechanisms Revealed in Cancer Models. International Journal of Molecular Sciences, 21, Article 6270. https://doi.org/10.3390/ijms21176270

[10] Papp, E., Vancsik, T., Kiss, E. and Szasz, O. (2017) Energy Absorption by the Membrane Rafts in the Modulated Electro-Hyperthermia (mEHT). Open Journal of Biophysics, 7, 216-229. https://doi.org/10.4236/ojbiphy.2017.74016

[11] Szasz, A. and Szasz, O. (2020) Time-Fractal Modulation of Modulated Electro-Hyperthermia (mEHT). Oncothermia Journal, 24, 318-332.

[12] The Physical Sciences—Oncology Centers Network, Staunton, J.R., et al. (2008) A Physical Sciences Network Characterization of Non-Tumorigenic and Metastatic Cells. Scientific Reports, 3, Article No. 1449.

[13] Szasz, A. (2022) Heterogeneous Heat Absorption Is Complementary to Radiotherapy. Cancers, 14, Article 901. https://doi.org/10.3390/cancers14040901

[14] Lee, S., Kim, J., Han, Y. and Cho, D. (2018) The Effect of Modulated Electro-Hyperthermia on Temperature and Blood Flow in Human Cervical Carcinoma. International Journal of Hyperthermia, 34, 953-960. https://doi.org/10.1080/02656736.2018.1423709

[15] Szasz, O. (2019) Bioelectromagnetic Paradigm of Cancer Treatment—Modulated Electro-Hyperthermia (mEHT). Open Journal of Biophysics, 9, 98-109. https://doi.org/10.4236/ojbiphy.2019.92008

[16] Szasz, O., Andocs, G., Kondo, T., Rehman, M.U., Papp, E., Vancsik, T., et al. (2015) Heating of Membrane Rafts of Cancer-Cells. Journal of Clinical Oncology, 33, e22176. https://doi.org/10.1200/jco.2015.33.15_suppl.e22176

[17] Obeid, M., Tesniere, A., Ghiringhelli, F., Fimia, G.M., Apetoh, L., Perfettini, J., et al. (2006) Calreticulin Exposure Dictates the Immunogenicity of Cancer Cell Death. Nature Medicine, 13, 54-61. https://doi.org/10.1038/nm1523

[18] Kepp, O., Senovilla, L., Galluzzi, L., Panaretakis, T., Schlemmer, F., Madeo, F., et al. (2009) Viral Subversion of Immunogenic Cell Death. Cell Cycle, 8, 860-869. https://doi.org/10.4161/cc.8.6.7939

[19] Krysko, D.V., Ravichandran, K.S. and Vandenabeele, P. (2018) Macrophages Regulate the Clearance of Living Cells by Calreticulin. Nature Communications, 9, Article No. 4644. https://doi.org/10.1038/s41467-018-06807-9

[20] Kwon, M.S., Park, C.S., Choi, K., Park, C., Ahnn, J., Kim, J.I., et al. (2000) Calreticulin Couples Calcium Release and Calcium Influx in Integrin-Mediated Calcium Signaling. Molecular Biology of the Cell, 11, 1433-1443. https://doi.org/10.1091/mbc.11.4.1433

[21] Andocs, G., Rehman, M.U., Zhao, Q., Tabuchi, Y., Kanamori, M. and Kondo, T. (2016) Comparison of Biological Effects of Modulated Electro-Hyperthermia and Conventional Heat Treatment in Human Lymphoma U937 Cells. Cell Death Discovery, 2, Article No. 16039. https://doi.org/10.1038/cddiscovery.2016.39

[22] Klune, J.R., Dhupar, R., Cardinal, J., Billiar, T.R. and Tsung, A. (2008) HMGB1: Endogenous Danger Signaling. Molecular Medicine, 14, 476-484. https://doi.org/10.2119/2008-00034.klune

[23] Kang, R., Chen, R., Zhang, Q., Hou, W., Wu, S., Cao, L., et al. (2014) HMGB1 in Health and Disease. Molecular Aspects of Medicine, 40, 1-116. https://doi.org/10.1016/j.mam.2014.05.001

[24] Kazama, H., Ricci, J., Herndon, J.M., Hoppe, G., Green, D.R. and Ferguson, T.A. (2008) Induction of Immunological Tolerance by Apoptotic Cells Requires Caspase-Dependent Oxidation of High-Mobility Group Box-1 Protein. Immunity, 29, 21-32. https://doi.org/10.1016/j.immuni.2008.05.013

[25] Li, C., Zhang, Y., Cheng, X., Yuan, H., Zhu, S., Liu, J., et al. (2018) PINK1 and PARK2 Suppress Pancreatic Tumorigenesis through Control of Mitochondrial Iron-Mediated Immunometabolism. Developmental Cell, 46, 441-455.e8. https://doi.org/10.1016/j.devcel.2018.07.012

[26] Yu, Y., Tang, D. and Kang, R. (2015) Oxidative Stress-Mediated HMGB1 Biology. Frontiers in Physiology, 6, Article 93. https://doi.org/10.3389/fphys.2015.00093

[27] Galluzzi, L., Buqué, A., Kepp, O., Zitvogel, L. and Kroemer, G. (2016) Immunogenic Cell Death in Cancer and Infectious Disease. Nature Reviews Immunology, 17, 97-111. https://doi.org/10.1038/nri.2016.107

[28] Medina, C.B. and Ravichandran, K.S. (2016) Do Not Let Death Do Us Part: 'Find-Me' Signals in Communication between Dying Cells and the Phagocytes. Cell Death & Differentiation, 23, 979-989. https://doi.org/10.1038/cdd.2016.13

[29] Michaud, M., Martins, I., Sukkurwala, A.Q., Adjemian, S., Ma, Y., Pellegatti, P., et al. (2011) Autophagy-Dependent Anticancer Immune Responses Induced by Chemotherapeutic Agents in Mice. Science, 334, 1573-1577. https://doi.org/10.1126/science.1208347

[30] Vega, V.L., Rodríguez-Silva, M., Frey, T., Gehrmann, M., Diaz, J.C., Steinem, C., et al. (2008) Hsp70 Translocates into the Plasma Membrane after Stress and Is Released into the Extracellular Environment in a Membrane-Associated Form that Activates Macrophages. The Journal of Immunology, 180, 4299-4307. https://doi.org/10.4049/jimmunol.180.6.4299

[31] Shevtsov, M., Balogi, Z., Khachatryan, W., Gao, H., Vígh, L. and Multhoff, G. (2020) Membrane-Associated Heat Shock Proteins in Oncology: From Basic Research to New Theranostic Targets. Cells, 9, Article 1263. https://doi.org/10.3390/cells9051263

[32] Multhoff, G., Botzler, C., Jennen, L., Schmidt, J., Ellwart, J. and Issels, R. (1997) Heat Shock Protein 72 on Tumor Cells: A Recognition Structure for Natural Killer Cells. The Journal of Immunology, 158, 4341-4350. https://doi.org/10.4049/jimmunol.158.9.4341

[33] Kumar, S., Deepak, P., Kumar, S., Kishore, D. and Acharya, A. (2009) Autologous Hsp70 Induces Antigen Specific Th1 Immune Responses in a Murine T-Cell Lymphoma. Immunological Investigations, 38, 449-465. https://doi.org/10.1080/08820130902802673

[34] Calderwood, S.K. and Gong, J. (2016) Heat Shock Proteins Promote Cancer: It's a Protection Racket. Trends in Biochemical Sciences, 41, 311-323. https://doi.org/10.1016/j.tibs.2016.01.003

[35] Albakova, Z., Siam, M.K.S., Sacitharan, P.K., Ziganshin, R.H., Ryazantsev, D.Y. and Sapozhnikov, A.M. (2021) Extracellular Heat Shock Proteins and Cancer: New Perspectives. Translational Oncology, 14, Article ID: 100995. https://doi.org/10.1016/j.tranon.2020.100995

[36] Jolesch, A., Elmer, K., Bendz, H., Issels, R.D. and Noessner, E. (2012) Hsp70, a Messenger from Hyperthermia for the Immune System. European Journal of Cel Biology, 91, 48-52. https://doi.org/10.1016/j.ejcb.2011.02.001

[37] Hickman-Miller, H.D. and Hildebrand, W.H. (2004) The Immune Response under Stress: The Role of HSP-Derived Peptides. Trends in Immunology, 25, 427-433. https://doi.org/10.1016/j.it.2004.05.011

[38] Binder, R.J. (2014) Functions of Heat Shock Proteins in Pathways of the Innate and Adaptive Immune System. The Journal of Immunology, 193, 5765-5771. https://doi.org/10.4049/jimmunol.1401417

[39] Krenacs, T. and Benyo, Z. (2017) Tumor Specific Stress and Immune Response Induced by Modulated Electrohyperthermia in Relation to Tumor Metabolic Profiles. Oncothermia Journal, 20, 264-272.

[40] Beachy, S.H. and Repasky, E.A. (2011) Toward Establishment of Temperature Thresholds for Immunological Impact of Heat Exposure in Humans. International Journal of Hyperthermia, 27, 344-352. https://doi.org/10.3109/02656736.2011.562873

[41] Andocs, G., Meggyeshazi, N., Balogh, L., Spisak, S., Maros, M.E., Balla, P., et al. (2015) Upregulation of Heat Shock Proteins and the Promotion of Damage-Associated Molecular Pattern Signals in a Colorectal Cancer Model by Modulated Electrohyperthermia. Cell Stress and Chaperones, 20, 37-46. https://doi.org/10.1007/s12192-014-0523-6

[42] Vancsik, T., Kovago, C., Kiss, E., Papp, E., Forika, G., Benyo, Z., et al. (2018) Modulated Electro-Hyperthermia Induced Loco-Regional and Systemic Tumor Destruction in Colorectal Cancer Allografts. Journal of Cancer, 9, 41-53. https://doi.org/10.7150/jca.21520

[43] Tsang, Y., Huang, C., Yang, K., Chi, M., Chiang, H., Wang, Y., et al. (2015) Improving Immunological Tumor Microenvironment Using Electro-Hyperthermia Followed by Dendritic Cell Immunotherapy. BMC Cancer, 15, Article No. 708. https://doi.org/10.1186/s12885-015-1690-2

[44] Vancsik, T., Máthé, D., Horváth, I., Várallyaly, A.A., Benedek, A., Bergmann, R., et al. (2021) Modulated Electro-Hyperthermia Facilitates NK-Cell Infiltration and Growth Arrest of Human A2058 Melanoma in a Xenograft Model. Frontiers in Oncology, 11, Article 590764. https://doi.org/10.3389/fonc.2021.590764

[45] Qin, W., Akutsu, Y., Andocs, G., Suganami, A., Hu, X., Yusup, G., et al. (2014) Modulated Electro-Hyperthermia Enhances Dendritic Cell Therapy through an Abscopal Effect in Mice. Oncology Reports, 32, 2373-2379. https://doi.org/10.3892/or.2014.3500

[46] Kuo, I., Lee, J., Wang, Y., Chiang, H., Huang, C., Hsieh, P., et al. (2020) Potential Enhancement of Host Immunity and Anti-Tumor Efficacy of Nanoscale Curcumin and Resveratrol in Colorectal Cancers by Modulated Electro-Hyperthermia. BMC Cancer, 20, Article No. 603. https://doi.org/10.1186/s12885-020-07072-0

[47] Besztercei, B., Vancsik, T., Benedek, A., Major, E., Thomas, M.J., Schvarcz, C.A., et al. (2019) Stress-Induced, P53-Mediated Tumor Growth Inhibition of Melanoma by Modulated Electrohyperthermia in Mouse Models without Major Immunogenic Effects. International Journal of Molecular Sciences, 20, Article 4019. https://doi.org/10.3390/ijms20164019

[48] Danics, L., Schvarcz, C.A., Viana, P., Vancsik, T., Krenács, T., Benyó, Z., et al. (2020) Exhaustion of Protective Heat Shock Response Induces Significant Tumor Damage by Apoptosis After Modulated Electro-Hyperthermia Treatment of Triple Negative Breast Cancer Isografts in Mice. Cancers, 12, Article 2581. https://doi.org/10.3390/cancers12092581

[49] Danics, L. (2021) Antitumor Effects of Modulated Electro-Hyperthermia in 4T1 Triple-Negative Breast Cancer Models. Ph.D. Thesis, Semmelweis University.

[50] Danics, L., Schvarcz, C.S. and Zolcsak, Z. (2018) Modulated Electro Hyperthermia Inhibits Tumor Progression in a Triple Negative Mouse Breast Cancer Model. Oncothermia Journal, 24, 442-454.

[51] Wang, S. and Wang, Y.-S. (2019) Immunotherapy in Combination with Modulated Electro-Hyperthermia. 37th Conference of the International Clinical Hyperthermia Society, Thessaloniki, 19-21 September 2019.

[52] Chi, K.H. (2018) Tumor-Directed Immunotherapy: Combined Radiotherapy and Oncothermia. Oncothermia Journal, 24, 196-235.

[53] Thomas, M.J., Major, E., Benedek, A., Horváth, I., Máthé, D., Bergmann, R., et al. (2020) Suppression of Metastatic Melanoma Growth in Lung by Modulated Electro-Hyperthermia Monitored by a Minimally Invasive Heat Stress Testing Approach in Mice. Cancers, 12, Article 3872. https://doi.org/10.3390/cancers12123872

[54] Szász, A.M., Lóránt, G., Szász, A. and Szigeti, G. (2023) The Immunogenic Connection of Thermal and Nonthermal Molecular Effects in Modulated Electro-hyperthermia. Open Journal of Biophysics, 13, 103-142. https://doi.org/10.4236/ojbiphy.2023.134007

[55] Dank, M., Meggyeshazi, N., Szigeti, G. and Andocs, G. (2016) Immune Effects by Selective Heating of Membrane Rafts of Cancer-Cells. Journal of Clinical Oncology, 34, e14571. https://doi.org/10.1200/jco.2016.34.15_suppl.e14571

[56] Vancsik, T., Kiss, E, Kovago, C.S., Meggyeshazi, N., Forika, G. and Krenacs, T. (2017) Inhibition of Proliferation, Induction of Apoptotic Cell Death and Immune Response by Modulated Electro-Hyperthermia in C26 Colorectal Cancer Allografts. Thermometry Oncothermia Journal, 20, 277-292.

[57] Minnaar, C.A. and Szasz, A. (2022) Forcing the Antitumor Effects of HSPs Using a Modulated Electric Field. Cells, 11, Article 1838. https://doi.org/10.3390/cells11111838

[58] Szasz, A. (2019) Thermal and Nonthermal Effects of Radiofrequency on Living State and Applications as an Adjuvant with Radiation Therapy. Journal of Radiation and Cancer Research, 10, 1-17. https://doi.org/10.4103/jrcr.jrcr_25_18

[59] Szasz, O. (2020) Local Treatment with Systemic Effect: Abscopal Outcome. In: Szasz, A., Ed., Challenges and Solutions of Oncological Hyperthermia, Cambridge Scholars, 192-205.

[60] Szasz, A. (2018) Local Oncothermia Treatment Fights against Systemic Malignancy. Oncothermia Journal, 22, 58-84.

[61] Andocs, G., Meggyeshazi, N., Okamoto, Y., Balogh, L. and Szasz, O. (2013) Bystander Effect of Oncothermia. Conference Papers in Medicine, 2013, Article ID: 953482. https://doi.org/10.1155/2013/953482

[62] Volker, S. (2017) A New Strategy of Cancer Immunotherapy Combining Hyperthermia/oncolytic Virus Pretreatment with Specific Autologous Anti-Tumor Vaccination—A Review. Austin Oncology Case Reports, 2, Article 1006. https://doi.org/10.26420/austinoncolcaserep.1006.2017

[63] Van Gool, S., Makalowski, J. and Feyen, O. (2019) Can We Monitor Immunogenic Cell Death (ICD) Induced with Modulated Electrohyperthermia and Oncolytivc Virus Injections? Oncothermia Journal, 26, 120-125.

[64] Yang, K., Huang, C., Chi, M., Chiang, H., Wang, Y., Hsia, C., et al. (2016) In Vitro Comparison of Conventional Hyperthermia and Modulated Electro-hyperthermia. Oncotarget, 7, 84082-84092. https://doi.org/10.18632/oncotarget.11444

[65] Balogh, A. (2018) mEHT as an Effective Treatment Modality for Melanoma. 36th Annual Conference of the International Clinical Hyperthermia Society (ICHS), Budapest, 28-29 September 2018.

[66] Andocs, G., Meggyeshazi, N., Galfi, P., Balogh, L., Fonyad, L., Muller, L., Szasz, O. and Szasz, A. (2010) Experimental Oncothermia in Nude Mice Xenograft Tumor Models. Oncothermia Journal, 1, 30. https://oncotherm.com/sites/oncotherm/files/2017-07/Experimental_oncothermia_in_nude_mice_xenograft_tumor_models.pdf

[67] Andocs, G., Meggyeshazi, N., Okamoto, Y., Balogh, L., Kovago, C. and Szasz, O. (2013) Oncothermia Treatment Induced Immunogenic Cancer Cell Death. Oncothermia Journal, 9, 28-37. https://oncotherm.com/sites/oncotherm/files/2017-07/Oncothermia_treatment_induced_immunogenic_cancer_cell_death.pdf

[68] Meggyeshazi, N. (2015) Studies on Modulated Electrohyperthermia Induced Tumor Cell Death in a Colorectal Carcinoma Model. Master's Thesis, Semmelweis University. http://repo.lib.semmelweis.hu/handle/123456789/3956

[69] Tomeh, M.A., Hadianamrei, R. and Zhao, X. (2019) A Review of Curcumin and Its Derivatives as Anticancer Agents. International Journal of Molecular Sciences, 20, Article 1033. https://doi.org/10.3390/ijms20051033

[70] Ko, J., Sethi, G., Um, J., Shanmugam, M.K., Arfuso, F., Kumar, A.P., et al. (2017) The Role of Resveratrol in Cancer Therapy. International Journal of Molecular Sciences, 18, Article 2589. https://doi.org/10.3390/ijms18122589

[71] Lukácsi, S., Munkácsy, G. and Győrffy, B. (2024) Harnessing Hyperthermia: Molecular, Cellular, and Immunological Insights for Enhanced Anticancer Therapies. Integrative Cancer Therapies, 23, 1-17. https://doi.org/10.1177/15347354241242094

[72] Simson, L., Ellyard, J.I., Dent, L.A., Matthaei, K.I., Rothenberg, M.E., Foster, P.S., et al. (2007) Regulation of Carcinogenesis by IL-5 and CCL11: A Potential Role for Eosinophils in Tumor Immune Surveillance. The Journal of Immunology, 178, 4222-4229. https://doi.org/10.4049/jimmunol.178.7.4222

[73] Cormier, S.A., Taranova, A.G., Bedient, C., Nguyen, T., Protheroe, C., Pero, R., et al. (2006) Pivotal Advance: Eosinophil Infiltration of Solid Tumors Is an Early and Persistent Inflammatory Host Response. Journal of Leukocyte Biology, 79, 1131-1139. https://doi.org/10.1189/jlb.0106027

[74] Carretero, R., Sektioglu, I.M., Garbi, N., Salgado, O.C., Beckhove, P. and Hämmerling, G.J. (2015) Eosinophils Orchestrate Cancer Rejection by Normalizing Tumor Vessels and Enhancing Infiltration of CD8+ T Cells. Nature Immunology, 16, 609-617. https://doi.org/10.1038/ni.3159

[75] Takeuchi, E., Ogino, H., Kondo, K., Okano, Y., Ichihara, S., Kunishige, M., et al. (2023) An Increased Relative Eosinophil Count as a Predictive Dynamic Biomarker in Non-Small Cell Lung Cancer Patients Treated with Immune Checkpoint Inhibitors. Thoracic Cancer, 15, 248-257. https://doi.org/10.1111/1759-7714.15191

[76] Akutsu, Y., Tamura, Y., Murakami, K., Qin, W., Hu, X., Suganami, A., Suito, H. and Matsubara, H. (2014) Can Modulated Electro-Hyperthermia (mEHT) Elicit Immune Reaction?—From Basic and Clinical Research. Oncothermia Journal, 11, 94.

[77] Holtmeier, W. and Kabelitz, D. (2005) γδT Cells Link Innate and Adaptive Immune Responses. In: Kabelitz, D., Schröder, J.M. and Karger, A.G., Eds., Chemical Immunology and Allergy, KARGER, 151-183. https://doi.org/10.1159/000086659

[78] Zhang, H., Hu, H., Jiang, X., He, H., Cui, L. and He, W. (2005) Membrane HSP70: The Molecule Triggering γδT Cells in the Early Stage of Tumorigenesis. Immunological Investigations, 34, 453-468. https://doi.org/10.1080/08820130500265349

[79] Fisher, J.P., Heuijerjans, J., Yan, M., Gustafsson, K. and Anderson, J. (2014) γδT Cells for Cancer Immunotherapy: A Systematic Review of Clinical Trials. OncoImmunology, 3, e27572. https://doi.org/10.4161/onci.27572

[80] Liu, Y. and Zhang, C. (2020) The Role of Human γδT Cells in Anti-Tumor Immunity and Their Potential for Cancer Immunotherapy. Cells, 9, Article 1206. https://doi.org/10.3390/cells9051206

[81] Roth, J. and Blatteis, C.M. (2014) Mechanisms of Fever Production and Lysis: Lessons from Experimental LPS Fever. Comprehensive Physiology, 4, 1563-1604.

[82] Szasz, A. (2020) Preface. In: Szasz, A., Ed., Challenges and Solutions of Oncological Hyperthermia, Cambridge Scholars, 8-13.

[83] Barich, A.J., Daniilidis, L. and Marangos, M. (2018) Oncothermia and the Paradigm Shift in Integrative Oncology. Oncothermia Journal, 24, 373-404.

[84] Szigeti, G.P., Lee, D.Y. and Hegyi, G. (2017) What Is on the Horizon for Hyperthermic Cancer Therapy? Journal of Traditional Medicine and Clinical Naturopathy, 6, Article ID: 1000217.

[85] Minnaar, C.A., Szigeti, G.P., Szasz, A.M. and Kotzen, J.A. (2022) Review on the Use of Modulated Electro-Hyperthermia as a Stand-Alone Therapy in a Palliative Setting: Potential for Further Research? Journal of Cancer Therapy, 13, 362-377. https://doi.org/10.4236/jct.2022.136032

[86] Szasz, A.M., Minnaar, C.A., Szentmártoni, G., Szigeti, G.P. and Dank, M. (2019) Review of the Clinical Evidences of Modulated Electro-Hyperthermia (mEHT) Method: An Update for the Practicing Oncologist. Frontiers in Oncology, 9, Article 1012. https://doi.org/10.3389/fonc.2019.01012

[87] Lee, S., Lorant, G., Grand, L. and Szasz, A.M. (2023) The Clinical Validation of Modulated Electro-Hyperthermia (mEHT). Cancers, 15, Article 4569. https://doi.org/10.3390/cancers15184569

[88] Minnaar, C.A., Kotzen, J.A., Ayeni, O.A., Vangu, M. and Baeyens, A. (2020) Potentiation of the Abscopal Effect by Modulated Electro-Hyperthermia in Locally Advanced Cervical Cancer Patients. Frontiers in Oncology, 10, Article 376. https://doi.org/10.3389/fonc.2020.00376

[89] Chi, M., Mehta, M.P., Yang, K., Lai, H., Lin, Y., Ko, H., et al. (2020) Putative Abscopal Effect in Three Patients Treated by Combined Radiotherapy and Modulated Electrohyperthermia. Frontiers in Oncology, 10, Article 254. https://doi.org/10.3389/fonc.2020.00254

Abbreviations

APC	antigen presenting cell
ATP	adenosine triphosphate
DAMP	damage associated molecular pattern
DC	dendritic cell
DNA	deoxyribonucleic acid
ECM	extracellular matrix
HMGB1	high-mobility group protein
HSP	heat-shock protein
ICD	immunogenic cell death
mEHT	modulated electro-hyperthermia
NK cell	natural killer cell
ROS	reactive oxygen species
TLR	toll-like receptor

Current understanding of modulated electro-hyperthermia in cancer treatment

Sungmin Kim[1], Jesang Yu[2], Jihun Kang[3], Yunkyung Kim[4], Taek Yong Ko[5]

[1]Department of Radiation Oncology, Dong-A University Hospital, Dong-A University College of Medicine, Busan, Korea

[2]Department of Radiation Oncology, Kosin University Gospel Hospital, Kosin University College of Medicine, Busan, Korea

[3]Department of Family Medicine, Kosin University Gospel Hospital, Kosin University College of Medicine, Busan, Korea

[4]Department of Internal Medicine, Kosin University Gospel Hospital, Kosin University College of Medicine, Busan, Korea

[5]Department of Thoracic and Cardiovascular Surgery, Kosin University Gospel Hospital, Kosin University College of Medicine, Busan, Korea

Citation

Kim, S. et al (2024) Current understanding of modulated electro-hyperthermia in cancer treatment

Oncothermia Journal 38, August 2026., 180-189.
https://oncotherm.com/KimS_2024_Current_understanding_of_mEHT

Traditional hyperthermia involves increasing the temperature at the tumor site above 39°C, including death in cancer cells. Although hyperthermia is an effective cancer treatment, its clinical application has decreased due to potentional complications, including demage to surrounding normal tissue. In recent years, modulated electro-hyperthermia (mEHT) has emerged as an effective and safe treatment modality. mEHT selectively heats tumor cells to 42-43°C, while reducing the average temperature in the treatment are, including the surrounding normal tissue, compared to conventional methods. Additionally, mEHT may be used in combination with systemic chemotherapry and radiation therapy in tumor treatment, providing a synergistic effect to increase efficacy. As chemotherapy and radiation therapy technologies advance, the application of combined mEHT may improve clinical outcomes. In this study, we review and discuss reports on the clinical outcomes of mEHT combined with chemotherapy and/or radiation therapy, which are established anticancer treatments.

Keywords: Hyperthermia; Modulated electro-hyperthermia; Neoplasms; Therapeutics

Introduction

Standard cancer treatment consists of surgery, chemotherapy, and radiation therapy, either alone or in combination [1-3]. Of these, systemic chemotherapy and radiation therapy duration range from several weeks to several months, and takes at least several weeks to confirm the clinical outcomes. If the tumor size increases during follow-up after chemotherapy and/or radiation therapy, the prognosis is poor. Therefore, an effective combine therapy that enhances the efficacy of chemotherapy and radiation therapy can significantly improve clinical outcomes. Recently, modulated electro-hyperthermia (mEHT), which can selectively maintain tumor cells at 42–43 °C using a high-frequency electromagnetic field (13.56 MHz) to the lesions, has been proposed as a promising combined modality therapy [4,5]. This technique operates based on a complex energy dose control paradigm rather than a straightforward temperature concept. The main targets of mEHT are the intercellular components and cell mem branes of tumor tissues, and it acts selectively on malignant tumor cells with little damage to normal cells [4-6]. mEHT induces tumor cell death by increasing blood flow, suppressing hypoxia, and inhibiting DNA repair in tumors [7,8]. Additionally, when combined with systemic therapy, mEHT can enhance drug concentration within the lesion and increase the sensitivity of chemotherapy and radiation therapy [9,10]. Therefore, mEHT is a promising treatment that can be used in combination with systemic therapy and radiation therapy. This study reviews the clinical outcomes of mEHT in conjunction with chemotherapy and/or radiation therapy [11,12].

mEHT mechanism

Conventional hyperthermia aims to directly kill cancer cells by using temperatures above 39 °C, but this approach has several drawbacks. First, the heterogeneous nature of tumors makes it challenging to deliver and maintain uniform thermal energy [13]. Second, thermal damage causes severe complications to the tumor-surrounding tissue. Third, as temperatures rise above 43 °C, blood flow within the tumor decreases, potentially reducing the effectiveness of chemotherapy and/or radiation therapy [14]. Consequently, mEHT has emerged as an innovative method (Fig. 1). It selectively delivers thermal energy only to the tumor cell membrane and extracellular matrix, using temperatures below 43 °C, thereby minimizing the impact on surrounding tissues and addressing

the limitations of traditional hyperthermia. mEHT selectivity for cancer cells was confirmed in vitro, and severe malignancy increases the degree of damage caused by mEHT [6]. Among the biological effects of mEHT, the most clinically useful are improving the perfusion and oxygenation conditions and interfering with the DNA repair mechanism of tumors [15-17]. Based on these characteristics, mEHT is being used as a combined therapy to enhance the effects of chemotherapy and radiation therapy.

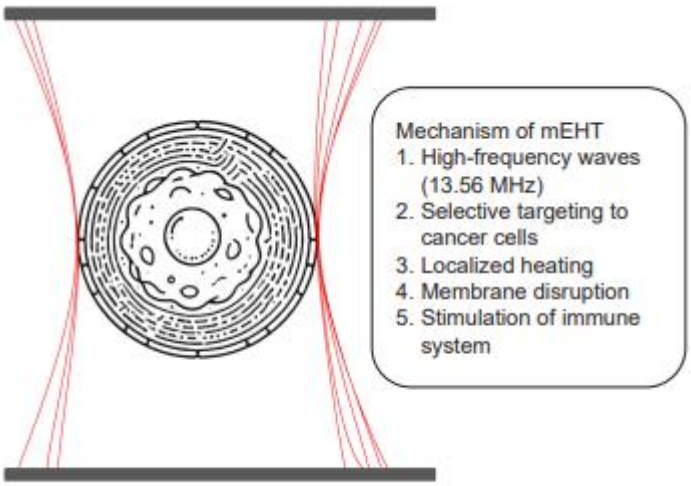

Fig. 1. Mechanism of modulated electro-hyperthermia (mEHT).

mEHT in combination with radiation therapy

Theoretically, mEHT is an excellent radiosensitizer. Conventional radiation therapy often causes hypoxic regions within tumors during treatment [18]. mEHT can not only increase tumor perfusion and oxygen supply, but also increase the tumor apoptotic effect of hyperthermic cells themselves on hypoxic cells, leading to improved efficacy of radiation therapy [19,20]. In addition, the local control rate could be improved by suppressing DNA repair in tumor cells by radiation therapy [20,21]. Since hyperthermia is highly effective on S phase cells, which are resistant to radiation therapy from a cell cycle perspective, concurrent therapy is more effective [22]. mEHT is a useful combined treatment to consider for cancer types that are highly resistant to radiation therapy. The prescribed dose is limited by the tolerance of the critical normal tissue surrounding the radiation treatment site, making hyperthermia highly necessary in cases of radiation retreatment. Since radiation continues to affect lesions even after treatment termination, mEHT could be highly effective in sequential treatments within several months post-radiation therapy. However, there is little information on this, and further study is needed.

mEHT in combination with chemotherapy

mEHT increases blood flow and permeability, contributing to an environment that is conducive to drug delivery to tumors [7]. Owing to the effects of mEHT on tumor cells, including cell membrane damage and increased intratumoral stress, cancer cells compromised by this process may become even more susceptible to chemotherapy [23].

Based on these theoretical foundations, studies on clinical outcomes where hyperthermia was combined with systemic chemotherapy for various cancer types have demonstrated improved clinical results [24-26]. In clinical practice, we often encounter cases where reduced doses of chemotherapy are necessary for patients with poor performance status due to advanced age or concomitant diseases, or for patients who experience severe side effects from chemotherapeutic agents. We believe that mEHT is an effective combination treatment option that can compensate for reduced doses of chemotherapy.

Safety of mEHT

mEHT uses a heating temperature of approximately 42°C, which is lower than that used in conventional hyperthermia treatments, and side effects from heat exposure are relatively few and minor [27]. A common complication from heat exposure is mild erythema in the skin adjacent treated area [5]. Although it is rare, skin burns can occur if the heat power is intense or not properly monitored. In addition to the potential for thermal damage to the surrounding normal tissue at the treatment site, there is an occasional risk of fat necrosis due to minor damage to subcutaneous adipose tissue [28]. Some patients experience mild discomfort, pain, or a burning sensation during or after treatment due to local heating, but most recover without any intervention. Currently, serious side effects from mEHT alone are very rare, although minor side effects may occur. Since these side effects can be managed and minimized through careful supervision by the treating physician, the authors recommend treatment in an outpatient clinic at least once a week. Regarding systemic symptoms, hyperthermia can cause fatigue and tiredness, particularly when used in conjunction with chemotherapy or radiation therapy. Overall, most side effects associated with hyperthermia are manageable in clinical practice or are minor enough for patients to tolerate. Hyperthermia therapy has an antitumor effect on its own, but it is primarily used as a cancer treatment with the expectation of a synergistic effect when combined with chemotherapy and radiation therapy. Therefore, whether the incidence of serious side effects changes when hyperthermia is administered in combination with chemotherapy and radiation therapy is a crucial factor in determining clinical treatment strategies. Several studies have reported that mEHT has a low correlation with toxicity and demonstrates good safety [29-32]. A case report has claimed that hyperthermia helps maintain patient performance status and reduces chemotherapy toxicity [33]. However, several studies have reported an increased incidence of hematologic toxicity in patients who received hyperthermia, suggesting that hyperthermia may enhance the side effects of chemotherapy [34,35]. Although the safety of mEHT is higher than that of conventional hyperthermia [27], further evidence regarding toxicity associated with the treatment should be revealed through multiple well-designed randomized clinical trials.

Previously published studies on hyperthermia

A small number of randomized clinical trial and systematic review have been conducted using hyperthermia in patients with solid tumors, and the characteristics and oncological outcomes of these studies are summarized in Tables 1 and 2 [16,29,36-55]. Hyperthermia is regarded as an effective palliative treatment for cancer patients and can be utilized either as a monotherapy or in combination with other treatments. A randomized phase III trial by Chi et al. [55] demonstrated

that combining hyperthermia with radiotherapy in patients receiving palliative treatment for painful bone metastases extended the duration of pain relief and enhanced the overall pain control rate. Some studies have shown that hyperthermia enhances the therapeutic effect when combined with both chemotherapy and radiation therapy. The results of the EORTC 32961-ESHO 95 trial [47] suggest that for patients with localized high-risk soft tissue sarcoma, the combination of preoperative chemotherapy and hyperthermia is an effective treatment option. De Haas-Kock et al. [46] compared the efficacy of concurrent hyperthermia and radiation therapy with radiation therapy alone in the treatment of locally advanced rectal cancer. The results demonstrated that hyperthermia improved overall survival (hazard ratio, 2.06; 95% confidence interval [CI], 1.33–3.17; p=0.001), and increased complete tumor response rates (relative risk, 2.81; 95% CI, 1.22–6.45; p=0.01).

Future direction

Hyperthermia may have an energy dose-dependent response, but little information is available on the appropriate dose or treatment schedule (twice a week vs. three times a week) that shows efficacy. It may vary depending on each cancer type, but also the combined treatment method. For example, in radiation therapy, conventional radiation regimens and stereotactic body radiation therapy show significant differences due to their unique treatment mechanisms; therefore, the optimal dose of mEHT to be combined should be explored. Since mEHT is a localized treatment, as with radiation therapy, the treatment dose may differ depending on the treatment site and limitations of treatment dose due to surrounding normal tissue; so well-designed studies must be carried out by dividing the tumor into each location.

Table 1. Summary of oncological outcomes and safety of hyperthermia in meta-analyses and systematic reviews

Author	Article type	Cancer type	Intervention	Total patients	Endpoints	Oncologic outcomes	Survival outcomes	QoL outcomes	Side effects
Datta et al. (2016) [36]	Meta-analysis	Breast	RT vs. HT+RT	627	CR	Improved CR with HT	-	-	Minimal acute and late morbidities
Hu et al. (2017) [39]	Meta-analysis	Esophagus	HT+CCRT vs. CCRT or RT alone	1,519	OS Long-term effects (LR and DM rate) Short-term effects (CR and TER)	HT+CCRT vs. CCRT: Improved CR (OR, 2.00; p<0.00001) and TER (OR, 3.47; p<0.00001) No difference in long-term effects HT+CCRT vs. RT alone: Higher CR (OR, 2.12; p=0.003) and TER (OR, 4.8; p=0.002) Lower LR (OR, 0.39; p=0.0001) and DM (OR, 0.46; p=0.003)	HT+CCRT vs. CCRT: Improved 1-, 3-, 5-, and 7-yr OS (OR 1.79, 1.91, 9.99, 9.49; p<0.05) HT+CCRT vs. RT alone: Improved 1-, 2-, 3-, and 5-yr OS (OR 3.20, 2.09, 2.43, 3.47, p<0.05)	-	HT+CCRT vs. CCRT: Less GI toxicities with HT (OR, 0.43; p<0.00001) HT+CCRT vs. RT alone: No statistical difference in toxicities
Van der Horst et al. (2017) [20]	Systematic review	Pancreas	HT+RT or CT or CCRT	395	Overall response rate OS	Improved overall response rate (43.9% vs. 35.3%)	Improved OS (11.7 mo vs. 5.6 mo)	-	-
De Haas-Kock et al. (2009) [46]	Systematic review	Rectum	HT+RT vs. RT alone	520	Pathologic CR OS Toxicity	Higher CR with HT (RR, 2.81; p=0.01)	Improved 2-yr OS (HR, 2.06; p=0.001) but, disappeared in 3-, 4-, 5-yr OS	-	No difference in acute toxicity
Veltsista et al. (2023) [48]	Systematic review	Soft tissue sarcoma	HT+CT or HT+RT	786/618	-	Increased RT effectiveness with HT	-	-	No significant toxicity of HT
Lutgens et al. (2010) [50]	Systemic Review	Uterine cervix	HT+RT vs. RT alone	487	CR LR OS Grade 3 to 4 acute and late toxicity	Improved CR (RR 0.56; p<0.001) and LR rate (HR 0.48; p<0.001)	Better OS (HR, 0.67; p=0.05)	-	No difference in acute or late grade 3–4 toxicity
Datta et al. (2016) [51]	Meta-analysis	Uterine cervix	HT+RT +/− CT vs. RT+/−CT	1,160	CR LC OS Acute and late grade 3/4 toxicity	Higher CR (+22.1%, p<0.001) and LC (+23.1%, p<0.001) with HT	No significant OS benefit	-	No difference in acute or late toxicities
Yea et al. (2021) [53]	Meta-analysis	Uterine cervix	HT+CCRT vs. CCRT	536	5-yr OS LRFS Acute and late toxicity	No LRFS benefit	Better 5-yr OS (HR, 0.67; p=0.03)	-	No difference in acute and late toxicity

QoL, quality of life; RT, radiotherapy; HT, hyperthermia; CR, complete response; CCRT, concurrent chemoradiotherapy; OS, overall survival; LR, local recurrence; DM, distant metastasis; TER, total effective rate; OR, odds ratio; GI, gastrointestinal; CT, chemotherapy; RR, relative risk; HR, hazard ratio; LC, local control; LRFS, local relapse-free survival.

Table 2. Summary of oncological outcomes and safety of hyperthermia in randomized controlled trials

Author	Article type	Cancer type	Intervention	Total patients	Endpoints	Oncologic outcomes	Survival outcomes	QoL outcomes	Side effects
Loboda et al. (2020) [37]	Phase II RCT	Breast	NACT+HT vs. NACT	200	Tumor response 10-yr OS	Better tumor size reduction with HT Objective response rate increased by 15.9% (p=0.034)	Higher 10-yr OS (p=0.009)	-	-
Klimanov et al. (2018) [38]	Phase II RCT	Breast cancer with liver metastases	HT+CT vs. CT alone	103	Tumor response QoL	Higher PR and SD	-	Improved QoL	-
Kang et al. (2013) [40]	Phase II RCT	Head and neck	HT+CCRT vs. CCRT	154	CR DFS OS	Higher 3-mo CR (81.6% vs. 62.8%; p<0.05) and 5-yr LC rate (96.1% vs. 76.9%)	Better 5-yr DFS (51.3% vs. 20.5%) and 3-yr (85.5% vs. 61.5%), 5-yr OS (68.4% vs. 50.0%)	-	No statistical difference in toxicity
Zhao et al. (2014) [41]	Phase II RCT	Head and neck	HT+CCRT vs. CCRT	83	OS DFS QoL	-	Higher 3-yr OS (73% vs. 53.5%, p=0.048) and PFS (61 mo vs. 38 mo, p=0.048)	Better QoL with HT	-
Ren et al. (2021) [42]	Phase II RCT	Head and neck	HT+ induction CT vs. induction CT alone	120	Clinical response rate of induction CT OS DFS Toxicity	Higher clinical response rates (65.45% vs. 40.00%, p=0.0088)	Improved DFS (HR, 0.57; p=0.035) not OS	-	No difference in adverse events
Dong et al. (2016) [16]	Phase II RCT	Liver	HT+RT vs. RT alone	80	Liver function TER (CR, PR, or SD) Recurrence and mortality rate	Improved liver function and TER (60.0% vs. 47.5%, p<0.001)	Lower 1-yr recurrence (27.5% vs. 40.0%, p<0.001) and mortality rates (12.5% vs. 20.0%, p<0.001)	-	-
Mitsumori et al. (2007) [43]	Phase II RCT	Lung	HT+RT vs. RT alone	80	LRR LPFS OS	No difference in LRR	Better LPFS (p=0.036) with HT No difference in OS	-	No grade 3 late toxicity
Shen et al. (2011) [44]	Phase II RCT	Lung	CT+HT vs. CT alone	80	Response rate QoL Toxicity	No difference in response rate	No survival data reported	Improved QoL with HT (82.5% vs. 47.5%, p<0.05)	Toxicity was not statistically analyzed
Schulze et al. (2006) [45]	Phase II RCT	Rectum	HT+CCRT vs. CCRT	137	GI QoL index	-	-	No difference in QoL	-

(Continued to the next page)

Table 2. Continued

Author	Article type	Cancer type	Intervention	Total patients	Endpoints	Oncologic outcomes	Survival outcomes	QoL outcomes	Side effects
Issels et al. (2018) [47]	Phase III RCT	Soft tissue sarcoma	HT+NACT vs. NACT alone	341	LPFS OS	-	Improved LPFS (HR, 0.65; p=0.002) and OS (HR, 0.73; p=0.04) Prolonged 5-yr (62.7% vs. 51.3%) and 10-yr (52.6% vs. 42.7%) survival rate	-	-
Jones et al. (2005) [49]	Phase II RCT	Superficial skin tumor	HT+RT vs. RT alone	108	CR LC OS	Improved CR (OR, 2.7; p=0.02)	No OS benefit	-	-
Minnaar et al. (2022) [52]	Phase III RCT	Uterine cervix	HT+CCRT vs. CCRT	210	LC Toxicity QoL 2-yr OS	Better 6-mo LC (p=0.003) and 2-yr (HR, 0.67; p=0.017) and 3-yr DFS (HR, 0.70; p=0.035)	No OS benefit (except for FIGO III)	Better QoL (pain reduction) with HT	No difference in toxicity
Van der Zee et al. (2000) [54]	Phase III RCT	Uterine cervix and bladder	HT+RT vs. RT alone	101	CR LC OS	Bladder: Improved CR (55% vs. 39%, p=0.001), not LC Uterine cervix: Improved CR (83% vs. 57%, p=0.003)	Bladder: No OS gain Uterine cervix: Improved 3-yr OS (51% vs. 27%, p=0.009)	-	No difference in acute and late toxicities
Chi et al. (2018) [55]	Phase III RCT	Painful bone metastases	HT+RT vs. RT alone	108	Pain response Time to pain progression Toxicity	Improved pain response (CR, 37.9% vs. 7.1%, p=0.006) Longer time to pain progression (HR, 0.178; p<0.001)	-	-	No grade 3 adverse events in both arms

QoL, quality of life; RCT, randomized controlled trial; NACT, neoadjuvant chemotherapy; HT, hyperthermia; OS, overall survival; CT, chemotherapy; PR, partial response; SD, stable disease; CCRT, concurrent chemoradiotherapy; CR, complete response; DFS, disease-free survival; LC, local control; HR, hazard ratio; RT, radiotherapy; TER, total effective rate; LRR, local response rate; LPFS, local progression-free survival; GI, gastrointestinal; OR, odds ratio.

Conclusion

Theoretically and experimentally, mEHT can play an important role in treating tumors, either alone or in combination with chemotherapy and radiation therapy. Although several studies have reported the clinical use of mEHT, particularly in improving oncological outcomes, further research is still required on the optimized treatment dose or schedule. In some patients, the effect of

hyperthermia is minimal, so it cannot improve the disease state and may only increase the social and economic burden. Therefore, hyperthermia should be applied with appropriate monitoring in selected patients. Since various treatment methods and regimens are used in the treatment of tumors, we believe that multidisciplinary medical consultations are also useful in determining the treatment plan.

Article information

Conflicts of interest
No potential conflict of interest relevant to this article was reported.

Funding
None.

Author contributions
Conceptualization: JY. Investigation: SK, JY, JK, YK, TYK. Supervision: JY, JK, YK, TYK. Writing – original draft: SK, JY. Writing – review & editing: SK, JY. Approval of final manuscript: all authors.

ORCID
Sungmin Kim, https://orcid.org/0000-0003-0225-500X Jesang Yu, https://orcid.org/0000-0002-0469-2660 Jihun Kang, https://orcid.org/0000-0002-2263-9054 Yunkyung Kim, https://orcid.org/0000-0003-0393-7264 Taek Yong Ko, https://orcid.org/0000-0002-0096-0664

References

1. Cunningham D, Allum WH, Stenning SP, Thompson JN, Van de Velde CJ, Nicolson M, et al. Perioperative chemotherapy versus surgery alone for resectable gastroesophageal cancer. N Engl J Med 2006;355:11–20.
2. Schneider BJ, Ismaila N, Altorki N. Lung cancer surveillance after definitive curative-intent therapy: ASCO guideline summary. JCO Oncol Pract 2020;16:83–6.
3. Daly ME, Ismaila N, Decker RH, Higgins K, Owen D, Saxena A, et al. Radiation therapy for small-cell lung cancer: ASCO guideline endorsement of an ASTRO guideline. J Clin Oncol 2021; 39:931–9.
4. Fiorentini G, Szasz A. Hyperthermia today: electric energy, a new opportunity in cancer treatment. J Cancer Res Ther 2006; 2:41–6.
5. Andocs G, Szasz O, Szasz A. Oncothermia treatment of cancer: from the laboratory to clinic. Electromagn Biol Med 2009; 28:148–65.
6. Roussakow SV. Clinical and economic evaluation of modulated electrohyperthermia concurrent to dose-dense temozolomide 21/28 days regimen in the treatment of recurrent glioblastoma: a retrospective analysis of a two-centre German cohort trial with systematic comparison and effect-to-treatment analysis. BMJ Open 2017;7:e017387.
7. Kirui DK, Koay EJ, Guo X, Cristini V, Shen H, Ferrari M. Tumor vascular permeabilization using localized mild hyperthermia to improve macromolecule transport. Nanomedicine 2014; 10:1487–96.

8. Oei AL, Vriend LE, Krawczyk PM, Horsman MR, Franken NA, Crezee J. Targeting therapy-resistant cancer stem cells by hyperthermia. Int J Hyperthermia 2017;33:419–27.
9. Baronzio G, Gramaglia A, Fiorentini G. Hyperthermia and immunity: a brief overview. In Vivo 2006;20(6A):689–95.
10. Hildebrandt B, Wust P, Ahlers O, Dieing A, Sreenivasa G, Kerner T, et al. The cellular and molecular basis of hyperthermia. Crit Rev Oncol Hematol 2002;43:33–56.
11. Kang G, Kim SE. How to write an original article in medicine and medical science. Kosin Med J 2022;37:96–101.
12. Kim DJ, Kil SY, Son J, Lee HS. How to conduct well-designed clinical research. Kosin Med J 2022;37:187–91.
13. Dewhirst MW, Viglianti BL, Lora-Michiels M, Hanson M, Hoopes PJ. Basic principles of thermal dosimetry and thermal thresholds for tissue damage from hyperthermia. Int J Hyperthermia 2003;19:267–94.
14. Griffin RJ, Dings RP, Jamshidi-Parsian A, Song CW. Mild temperature hyperthermia and radiation therapy: role of tumour vascular thermotolerance and relevant physiological factors. Int J Hyperthermia 2010;26:256–63.
15. Datta NR, Ordonez SG, Gaipl US, Paulides MM, Crezee H, Gellermann J, et al. Local hyperthermia combined with radiotherapy and-/or chemotherapy: recent advances and promises for the future. Cancer Treat Rev 2015;41:742–53.
16. Dong Y, Wu G. Analysis of short and long term therapeutic effects of radiofrequency hyperthermia combined with conformal radiotherapy in hepatocellular carcinoma. J BUON 2016;21:407– 11.
17. Skandalakis GP, Rivera DR, Rizea CD, Bouras A, Jesu Raj JG, Bozec D, et al. Hyperthermia treatment advances for brain tumors. Int J Hyperthermia 2020;37:3–19.
18. Moeller BJ, Dewhirst MW. HIF-1 and tumour radiosensitivity. Br J Cancer 2006;95:1–5.
19. Kaur P, Hurwitz MD, Krishnan S, Asea A. Combined hyperthermia and radiotherapy for the treatment of cancer. Cancers (Basel) 2011;3:3799–823.
20. Lee SY, Kim JH, Han YH, Cho DH. The effect of modulated electro-hyperthermia on temperature and blood flow in human cervical carcinoma. Int J Hyperthermia 2018;34:953–60.
21. Elming PB, Sorensen BS, Oei AL, Franken NA, Crezee J, Overgaard J, et al. Hyperthermia: the optimal treatment to overcome radiation resistant hypoxia. Cancers (Basel) 2019;11:60.
22. Schneider CS, Woodworth GF, Vujaskovic Z, Mishra MV. Radiosensitization of high-grade gliomas through induced hyperthermia: review of clinical experience and the potential role of MR-guided focused ultrasound. Radiother Oncol 2020;142:43– 51.
23. Hegyi G, Szigeti GP, Szasz A. Hyperthermia versus oncothermia: cellular effects in complementary cancer therapy. Evid Based Complement Alternat Med 2013;2013:672873.
24. Lee SY, Lee NR, Cho DH, Kim JS. Treatment outcome analysis of chemotherapy combined with modulated electro-hyperthermia compared with chemotherapy alone for recurrent cervical cancer, following irradiation. Oncol Lett 2017;14:73–8.
25. Gadaleta-Caldarola G, Infusino S, Galise I, Ranieri G, Vinciarelli G, Fazio V, et al. Sorafenib and locoregional deep electro-hyperthermia in advanced hepatocellular carcinoma: a phase II study. Oncol Lett 2014;8:1783–7.
26. Wismeth C, Dudel C, Pascher C, Ramm P, Pietsch T, Hirschmann B, et al. Transcranial electro-hyperthermia combined with alkylating chemotherapy in patients with relapsed high-grade gliomas: phase I clinical results. J Neurooncol 2010;98:395–405.

27. Kouloulias VE, Nikita KS, Kouvaris JR, Uzunoglu NK, Golematis VC, Papavasiliou CG, et al. Cytoreductive surgery combined with intraoperative chemo-hyperthermia and postoperative radiotherapy in the management of advanced pancreatic adenocarcinoma: feasibility aspects and efficacy. J Hepatobiliary Pancreat Surg 2001;8:564–70.
28. Herold Z, Szasz AM, Dank M. Evidence based tools to improve efficiency of currently administered oncotherapies for tumors of the hepatopancreatobiliary system. World J Gastrointest Oncol 2021;13:1109–20.
29. van der Horst A, Versteijne E, Besselink MG, Daams JG, Bulle EB, Bijlsma MF, et al. The clinical benefit of hyperthermia in pancreatic cancer: a systematic review. Int J Hyperthermia 2018; 34:969–79.
30. Fiorentini G, Giovanis P, Rossi S, Dentico P, Paola R, Turrisi G, et al. A phase II clinical study on relapsed malignant gliomas treated with electro-hyperthermia. In Vivo 2006;20(6A):721–4.
31. Ohguri T, Imada H, Yahara K, Narisada H, Morioka T, Nakano K, et al. Concurrent chemoradiotherapy with gemcitabine plus regional hyperthermia for locally advanced pancreatic carcinoma: initial experience. Radiat Med 2008;26:587–96.
32. Bakshandeh-Bath A, Stoltz AS, Homann N, Wagner T, Stolting S, Peters SO. Preclinical and clinical aspects of carboplatin and gemcitabine combined with whole-body hyperthermia for pancreatic adenocarcinoma. Anticancer Res 2009;29:3069–77.
33. Yeo SG. Definitive radiotherapy with concurrent oncothermia for stage IIIB non-small-cell lung cancer: a case report. Exp Ther Med 2015;10:769–72.
34. Rao W, Deng ZS, Liu J. A review of hyperthermia combined with radiotherapy/chemotherapy on malignant tumors. Crit Rev Biomed Eng 2010;38:101–16.
35. Kampinga HH. Cell biological effects of hyperthermia alone or combined with radiation or drugs: a short introduction to newcomers in the field. Int J Hyperthermia 2006;22:191–6.
36. Datta NR, Puric E, Klingbiel D, Gomez S, Bodis S. Hyperthermia and radiation therapy in locoregional recurrent breast cancers: a systematic review and meta-analysis. In Phys 2016;94:1073–87.
37. Loboda A, Smolanka I Sr, Orel VE, Syvak L, Golovko T, Dosenko I, et al. Efficacy of combination neoadjuvant chemotherapy and regional inductive moderate hyperthermia in the treatment of patients with locally advanced breast cancer. Technol Cancer Res Treat 2020;19:1533033820963599.
38. Klimanov MY, Syvak LA, Orel VE, Lavryk GV, Tarasenko TY, Orel VB, et al. Efficacy of combined regional inductive moderate hyperthermia and chemotherapy in patients with multiple liver metastases from breast cancer. Technol Cancer Res Treat 2018; 17:1533033818806003.
39. Hu Y, Li Z, Mi DH, Cao N, Zu SW, Wen ZZ, et al. Chemoradiation combined with regional hyperthermia for advanced oesophageal cancer: a systematic review and meta-analysis. J Clin Pharm Ther 2017;42:155–64.
40. Kang M, Liu WQ, Qin YT, Wei ZX, Wang RS. Long-term efficacy of microwave hyperthermia combined with chemoradiotherapy in treatment of nasopharyngeal carcinoma with cervical lymph node metastases. Asian Pac J Cancer Prev 2013;14:7395–400.
41. Zhao C, Chen J, Yu B, Chen X. Improvement in quality of life in patients with nasopharyngeal carcinoma treated with non-invasive extracorporeal radiofrequency in combination with chemoradiotherapy. Int J Radiat Biol 2014;90:853–8.
42. Ren G, Ju H, Wu Y, Song H, Ma X, Ge M, et al. A multicenter randomized phase II trial of hyperthermia combined with TPF induction chemotherapy compared with TPF induction

chemotherapy in locally advanced resectable oral squamous cell carcinoma. Int J Hyperthermia 2021;38:939–47.
43. Mitsumori M, Zeng ZF, Oliynychenko P, Park JH, Choi IB, Tatsuzaki H, et al. Regional hyperthermia combined with radiotherapy for locally advanced non-small cell lung cancers: a multi-institutional prospective randomized trial of the International Atomic Energy Agency. Int J Clin Oncol 2007;12:192–8.
44. Shen H, Li XD, Wu CP, Yin YM, Wang RS, Shu YQ. The regimen of gemcitabine and cisplatin combined with radio frequency hyperthermia for advanced non-small cell lung cancer: a phase II study. Int J Hyperthermia 2011;27:27–32.
45. Schulze T, Wust P, Gellermann J, Hildebrandt B, Riess H, Felix R, et al. Influence of neoadjuvant radiochemotherapy combined with hyperthermia on the quality of life in rectum cancer patients. Int J Hyperthermia 2006;22:301–18.
46. De Haas-Kock DF, Buijsen J, Pijls-Johannesma M, Lutgens L, Lammering G, van Mastrigt GA, et al. Concomitant hyperthermia and radiation therapy for treating locally advanced rectal cancer. Cochrane Database Syst Rev 2009;(3):CD006269.
47. Issels RD, Lindner LH, Verweij J, Wessalowski R, Reichardt P, Wust P, et al. Effect of neoadjuvant chemotherapy plus regional hyperthermia on long-term outcomes among patients with localized high-risk soft tissue sarcoma: the EORTC 62961-ESHO 95 Randomized Clinical Trial. JAMA Oncol 2018;4:483–92.
48. Veltsista PD, Oberacker E, Ademaj A, Corradini S, Eckert F, Florcken A, et al. Hyperthermia in the treatment of high-risk soft tissue sarcomas: a systematic review. Int J Hyperthermia 2023; 40:2236337.
49. Jones EL, Oleson JR, Prosnitz LR, Samulski TV, Vujaskovic Z, Yu D, et al. Randomized trial of hyperthermia and radiation for superficial tumors. J Clin Oncol 2005;23:3079–85.
50. Lutgens L, van der Zee J, Pijls-Johannesma M, De Haas-Kock DF, Buijsen J, Mastrigt GA, et al. Combined use of hyperthermia and radiation therapy for treating locally advanced cervix carcinoma. Cochrane Database Syst Rev 2010;2010:CD006377.
51. Datta NR, Rogers S, Klingbiel D, Gomez S, Puric E, Bodis S. Hyperthermia and radiotherapy with or without chemotherapy in locally advanced cervical cancer: a systematic review with conventional and network meta-analyses. Int J Hyperthermia 2016; 32:809–21.
52. Minnaar CA, Maposa I, Kotzen JA, Baeyens A. Effects of modulated electro-hyperthermia (mEHT) on two and three year survival of locally advanced cervical cancer patients. Cancers (Basel) 2022;14:656.
53. Yea JW, Park JW, Oh SA, Park J. Chemoradiotherapy with hyperthermia versus chemoradiotherapy alone in locally advanced cervical cancer: a systematic review and meta-analysis. Int J Hyperthermia 2021;38:1333–40.
54. van der Zee J, Gonzalez Gonzalez D, van Rhoon GC, van Dijk JD, van Putten WL, Hart AA. Comparison of radiotherapy alone with radiotherapy plus hyperthermia in locally advanced pelvic tumours: a prospective, randomised, multicentre trial. Dutch Deep Hyperthermia Group. Lancet 2000;355:1119–25.
55. Chi MS, Yang KL, Chang YC, Ko HL, Lin YH, Huang SC, et al. Comparing the effectiveness of combined external beam radiation and hyperthermia versus external beam radiation alone in treating patients with painful bony metastases: a phase 3 prospective, randomized, controlled trial. Int J Radiat Oncol Biol Phys 2018;100:78–87.

Integrative Oncology for High-Grade Glioma: A Case Report on the Combined Effects of Oncothermia and Complementary Therapies

Pradeep MK Nair[1], Renganathan Ramalakshmi[1] , Muniappan Devibala[1], Maruthanayagam Saranya[1], Sekar Sivaranjini[1], R Thangavelu[2], Manickam Mahalingam[1]

[1] Department of Integrative Oncology, Mirakle Integrated Health Centre, Pollachi, IND

[2] Department of Modern Medicine, Mirakle Integrated Health Centre, Pollachi, IND

Corresponding author: Pradeep MK Nair, drpradeep18bnys@gmail.com

Citation

Nair, P. MK. et al (2024) Integrative Oncology for High-Grade Glioma: A Case Report on the Combined Effects of Oncothermia and Complementary Therapies

Oncothermia Journal 38, August 2026., 190-200.
https://oncotherm.com/NairPMK_2024_Integrative_Oncology_for_high-grade_glioma

High-grade gliomas are aggressive brain tumors with a poor prognosis despite conventional treatments such as surgery, radiation, and chemotherapy. Integrative oncology, combining conventional and complementary therapies, may offer additional benefits in managing these complex cases. We present a 68-year-old male farmer diagnosed with high-grade glioma in the left medial temporal lobe. The patient presented with severe headache, disturbed sleep, and anxiety, and experienced an episode of fever and seizure. He refused conventional radiation therapy due to concerns about side effects and opted for an integrative medicine protocol. This protocol included oncothermia, high-dose vitamin C therapy, hydrogen inhalation, ozone therapy, magnet therapy, fasting, acupuncture, pulsed electromagnetic field therapy, yoga therapy, hydrotherapy, biologicals, and dietary modifications. The patient underwent 12 sessions of oncothermia over 24 days, combined with other integrative therapies. MRI scans before and after treatment showed a reduction in tumor size from 3.6 x 2.9 x 2.5 cm to 3.4 x 2.7 x 2.5 cm, corresponding to a 12% decrease in volume. Hematological parameters (complete blood count, liver function test, kidney function test, Creactive protein), cancer markers (carcinoembryonic antigen, lactate dehydrogenase), and mental health indices (quality of life, survival rate) also showed significant improvement. The patient experienced no adverse events and reported enhanced quality of life. This case report suggests that an integrative oncology approach, combining oncothermia and various complementary therapies, may be an effective treatment option for high-grade gliomas, particularly for patients intolerant to conventional therapies. Further research, including randomized controlled trials, is necessary to validate these findings and determine the specific contributions of each therapy.

Categories: Integrative/Complementary Medicine

Keywords: complementary therapies, integrative medicine, cancer management, brain tumor treatment, quality of life

Introduction

Gliomas are a diverse group of primary brain tumors arising from glial cells, with glioblastoma being the most common and aggressive subtype. These tumors present significant diagnostic and therapeutic challenges due to their rapid growth, infiltrative nature, and poor prognosis [1]. The incidence of high-grade gliomas (approximately six cases per 100,000 population), increases with age, and they are often associated with a variety of neurological symptoms that can mimic other conditions, complicating early diagnosis. Despite, the availability of standards of care like chemotherapy and radiation, the prognosis and survival rate of high-grade gliomas are very poor [2]. This implicates the need for newer technologies and supportive therapies that can improve the prognosis and survival rate.

In recent years, integrative oncology has emerged as a complementary approach in cancer care, combining conventional treatments with evidence-based complementary therapies to improve patient outcomes and quality of life. This approach is particularly relevant in the management of gliomas, where standard treatments like surgery, radiation, and chemotherapy are often insufficient to achieve long-term control.

In this case report, we present a 68-year-old male who was admitted with complaints of fever and a single episode of seizure. Initial clinical evaluation suggested an infectious or inflammatory process; however, subsequent imaging and histopathological studies revealed a high-grade glioma located in the left temporal lobe. This case explores the potential benefits of integrative oncology in managing high-grade gliomas. By incorporating integrative therapies, such as oncothermia, nutritional support, mind-body practices, and adjunctive use of biologicals, we aim to enhance the patient's quality of life and potentially improve clinical outcomes.

Case Presentation

The patient was a farmer who presented to our integrative medicine setting with complaints of severe headaches, disturbed sleep, and anxiety for two weeks. He was admitted to a multi-specialty hospital following an episode of high-grade fever and a seizure (a single episode for five minutes). Subsequently, he was diagnosed with high-grade glioma in March 2024 at a conventional oncology center, as his magnetic resonance imaging (MRI) indicated a ring-enhancing heterointense mass lesion (1.9 x 1.6 x 2.25 cm) in the left medial temporal lobe with mild surrounding edema (Figure 1). He was advised to undergo a biopsy and radiation therapy; however, he refused, citing concerns about the side effects associated with radiation therapy. He was taking levetiracetam (500 mg) daily, prescribed by the oncologist to prevent any further episodes of seizure.

Figure 1: Changes in the tumor lesion across time point

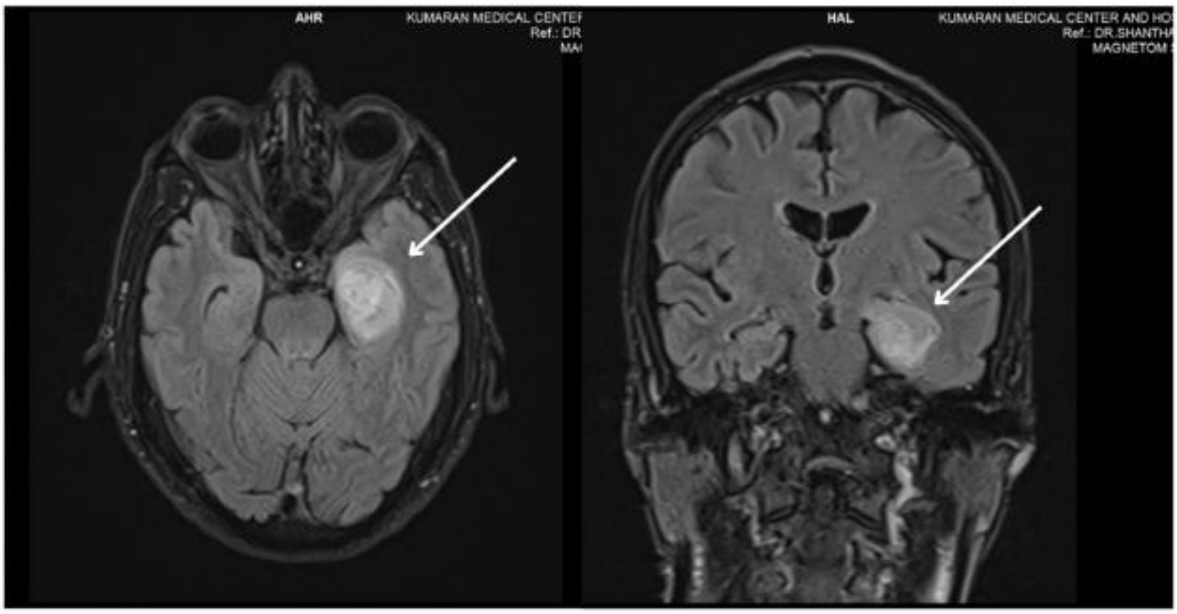

A: Tumor lesion at diagnosis March 2024

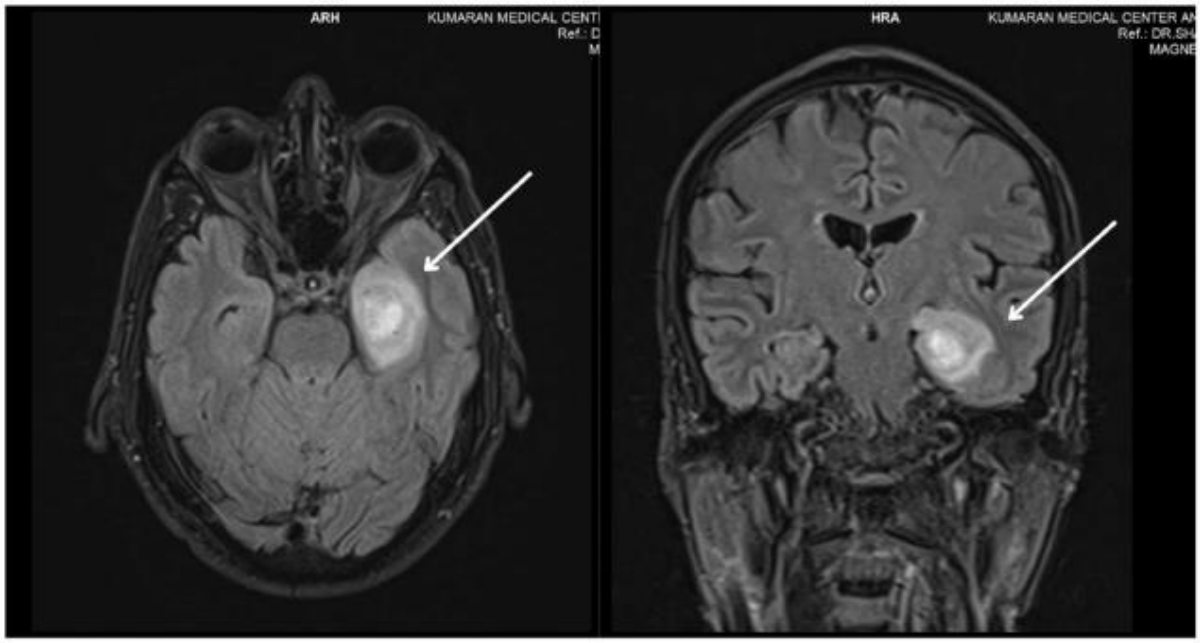

B: Tumor lesion at admission April 2024

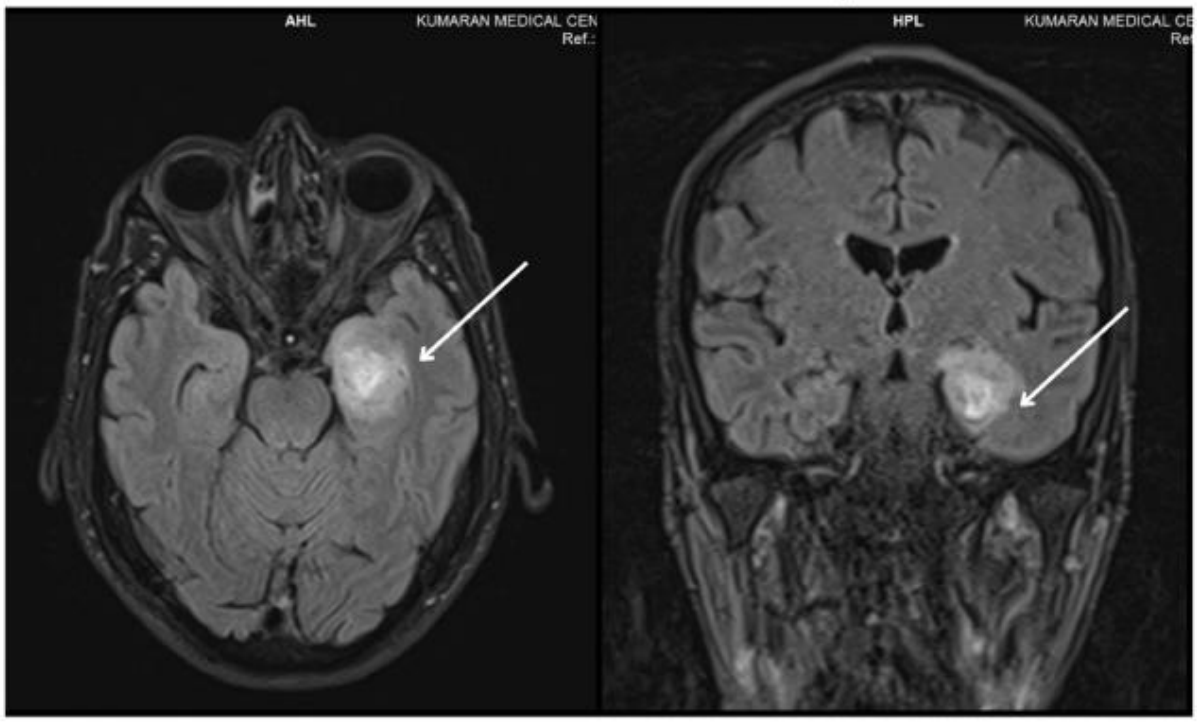

C: Tumor lesion after 12 sittings of integrative medicine protocol

FIGURE 1: Changes in the tumor lesion over various time points. Images (A) and (B) show ill-defined mass lesions with internal necrotic areas, lobulated margins, and internal hemorrhagic areas in the left medial temporal lobe, involving uncus, amygdala, and head of the left hippocampus, measuring 3.6 x 2.9 x 2.5 cm. Image (C) shows T2/fluid-attenuated inversion recovery (FLAIR) heterointense peripherally enhancing lesion measuring 3.4 x 2.7 x 2.5 cm, seen in the left medial temporal lobe with mild surrounding edema.

The patient did not have any other comorbidities or functional disabilities. A positron emission tomography (PET) scan revealed a fluorodeoxyglucose (FDG)-avid peripherally enhancing lesion measuring 2.2 x 1.7 cm in the left medial temporal lobe (maximum standardized uptake value = 13.3) with mild perilesional edema. No other malignant lesions elsewhere in the body were noted. He was admitted as an inpatient in our integrative oncology facility in April 2024. An integrative medicine protocol was planned by a group of physicians, including medical experts from yoga and naturopathy, homeopathy, and medical oncology. The protocol included counseling, oncothermia (modulated electro-hyperthermia), intravenous high-dose vitamin C therapy, ozone therapy, hydrogen therapy, acupuncture, ethylenediaminetetraacetic acid (EDTA) chelation, yoga therapy, hydrotherapy, magnet therapy, Hydrosun therapy (Hydrosun Medizintechnik, Müllheim, Germany), biologicals, and diet therapy. The detailed protocol is outlined in Table 1.

Intervention	Frequency of intervention
Counseling	Daily
Oncothermia (EHY-2030, Oncotherm, Budaörs, Hungary)	Alternate days (a total of 24 sessions was provided with a cooling period of 3 weeks in between each 12 sessions)
High-dose vitamin C therapy	2-3 times per week, the total dose not exceeding 90 grams per week
Ethylenediaminetetraacetic acid (EDTA) chelation	EDTA chelation was performed once in 7 days to remove heavy metal toxins
Ozone therapy	Daily (ozone is administered in the form of rectal insufflation/ear insufflation/saline ozone, and minor autohemotherapy)
Hydrogen inhalation (AT_HO-600 Hydrogen Inhalation Machine, Athena, Mumbai, India)	Daily inhalation of hydrogen for 30 minutes
Diet therapy	The patient was advised to follow a daily diet that is completely millet-based and free of sugar, refined wheat flour, and refined grains. This diet includes carrot, beetroot, and apple juice, as well as fresh vegetable salads and soups. Additionally, a time-restricted feeding schedule of 14:10 was also recommended
Liposomal curcumin therapy	Daily (5-10 ml liposomal curcumin), Mirakle, Coimbatore, India
Pulsed electromagnetic field (PEMF) therapy (PULSATRON at 10 Hz field frequency, Madras Institute of Magnetobiology, Chennai, India)	Daily for 30 minutes, exposed to PEMF using a controlled magnetic field assembly
Probiotic supplementation	Daily (two doses of Liv-Bio Alpha pre and probiotic supplements, Liv Bio Pharma, Poovarany, India)
Co-Q enzyme therapy	Daily (5-15 ml liposomal Co-Q 10 enzyme), Mirakle, Coimbatore, India
Coffee enema	Once a week (three tablespoons of chicory-free coffee is boiled in one liter of water, allowed to cool down, filtered, and then 500 ml is administered through the rectum in the form of an enema)
Hydrosun (Hydrosun 750, Hydrosun Medizintechnik, Müllheim, Germany)	Daily for 20 minutes (Hydrosun light therapy)
Acupuncture	Scalp acupuncture (Jiao Shun-fa School) - motor control area. Other acupuncture points like the large intestine (4), stomach (36), spleen (6), and back - Shu points and Ah-shi points were punctured daily for 30 minutes for 15 days
Yoga therapy	Daily 30-45 minutes (includes pranayama, meditation, and asanas)
Enema	Once a week to relieve constipation
Hot foot bath	As an when there is fatigue and headache
High-dose vitamin D supplementation	Once a week (60000 IU after monitoring the levels of parathyroid hormones and ionized calcium levels)
Injection dexamethasone	8 mg/day administered intravenously for one week to relieve edema
Injection N-acetyl cysteine	200 mg once in a week administered intravenously

TABLE 1: Integreative medicine protocol.

The outcomes of the therapies were assessed through an MRI of the brain taken before and after the session. Furthermore, changes in hematological markers were observed through a complete blood count, liver function test, kidney function test, C-reactive protein, cancer markers such as carcinoembryonic antigen, D- dimer, ferritin, and lactate dehydrogenase, glycemic indices such as glycosylated hemoglobin, and vitamin D levels. Additionally, we used the Edmonton Symptom Assessment Scale (ESAS) [3] to measure changes in symptoms, the European Organization for Research and Treatment of Cancer Quality of Life Questionnaire (EORTC QLQ-C30) to measure quality of life [4], and the Chuang Prognostic Scale to predict survival [5].

The patient was treated as an inpatient and underwent 12 sessions of oncothermia on alternate days, along with other therapies as reported in Table 1, for a total duration of 24 days from April 2024 to May 2024. No adverse events or worsening of symptoms were reported during the treatment. An MRI repeated two weeks after the completion of the treatment revealed a reduction in the size of the lesion from 3.6 x 2.9 x 2.5 cm to 3.4 x 2.7 x 2.5 cm, which corresponds to an approximate 12% decrease in volume (Figure 1). Furthermore, there was a significant improvement in his hematological parameters, cancer markers, and mental health indices (Tables 2-4). The results are tabulated in Table 2. The patient is currently being followed up weekly with one session of oncothermia per week and other integrative medicine therapies for 12 weeks. He is presently stable and symptom-free.

Time points	RBC	Hb	PCV	TC	N	L	E	Platelet	ESR	FE	CEA	LDH	D-dimer	CRP	Weight	BMI kg/m^2
April 2024	5	14.6	43.1	6000	76.9	13.3	0.9	312000	20	48.5	2.57	154	220	2.7	55	21.8
May 2024	4.96	14.7	43.9	6110	59.3	32.1	1.4	265000	6	45	2.15	225	146	0.6	55.5	22

TABLE 2: Changes in complete blood count, cancer markers, and anthropometric profile.
RBC: red blood cells (million/µl); HB: hemoglobin (g/dl); PCV: packed cell volume (%); TC: total leucocyte count (cells/µl); N: neutrophils (%); L: lymphocytes (%); E: eosinophils (%); platelets (cells/µL); ESR: erythrocyte sedimentation rate (mm/HR); Fe: ferritin (ng/ml); CEA: carcinoembryonic antigen (ng/ml); LDH: lactate dehydrogenase (U/L); D-dimer (ng/mL); CRP: C-reactive protein (mg/dL); BMI: body mass index.

Time points	Liver function						HBA1C	Renal function								Vit D
	TB	SGOT	SGPT	ALP	Total protein	Albumin		Urea	Creatinine	eGFR	Uric acid	Na	K	HCO_3	Cl	
April 2024	0.53	11.84	8.61	66.1	6.79	4.20	5.7	13.2	0.54	110	3.34	135	4.1	34.6	101	30
May 2024	0.57	11.79	9.21	61.6	7.03	4.22	5.7	7.13	0.55	109	3.94	137	4.6	35.1	105	29.4

TABLE 3: Changes in safety profiles across time points.
TB: total bilirubin (mg/dL); SGOT: serum glutamic oxaloacetic transaminase (U/L); SGPT: serum glutamic pyruvic transaminase (U/L); ALP: alkaline phosphatase (U/L); HbA1c: glycosylated hemoglobin (%); urea (mg/dL); creatinine (mg/dL); EGFR: estimated glomerular filtration rate (mL/min/1.73m2); uric acid (mg/dL); Na: sodium (mEq/L); K: potassium (mEq/L); Vit D: vitamin D-25-hydroxy vitamin D (ng/ml).

Edmonton Symptom Assessment Scale									EORTC QLQ-C30 Scale			Chuang Survival Score
Nausea	Depression	Anxiety	Drowsy	Appetite	Well-being	Breathlessness	Pain	Tiredness	Global score	Functional score	Symptom score	1.5
0	0	9	8	5	6	0	0	0	58.3	73.3	25.6	
0	0	0	0	0	0	0	0	0	83.3	91.1	0	0

TABLE 4: Changes in quality of life, symptoms, and survival rate scores.
EORTC QLQ-C30: European Organization for Research and Treatment of Cancer Quality of Life Questionnaire.

Discussion

This case highlights the potential benefits of integrative oncology approaches in the management of highgrade gliomas. The patient experienced significant improvements following a comprehensive treatment protocol that included oncothermia and various complementary therapies.

Oncothermia, a form of modulated electro-hyperthermia, has been explored as an adjunctive treatment for various types of cancer, including high-grade gliomas [6]. Studies reported that oncothermia, in combination with chemotherapy and radiotherapy or as a monotherapy, improved tumor control and survival outcomes in patients with advanced cancers [7,8]. In this case, the patient's lesion size was reduced by approximately 12% following oncothermia sessions, indicating a positive response similar to findings in the existing literature.

High-dose vitamin C therapy has been investigated for its potential anticancer properties, including its role in enhancing the effectiveness of other treatments and reducing side effects. A recent review by Renner et al. suggests that high-dose intravenous vitamin C could enhance the cytotoxic effects of chemotherapy in glioblastoma cells. Furthermore, it will selectively induce oxidative stress and induce cytotoxicity in malignant cells [9]. Additionally, Ma et al. suggested that high-dose vitamin C could reduce inflammation and improve the quality of life in cancer patients [10]. The significant improvement in hematological parameters and mental health indices observed in our patient aligns with these findings.

Hydrogen inhalation therapy is an emerging complementary treatment in oncology, known for its antioxidant and anti-inflammatory effects. Previous studies have demonstrated that hydrogen gas can protect cells from oxidative stress and may improve outcomes in various conditions, including cancer [10]. A single case report in 2019 reported complete remission of brain tumor post hydrogen inhalation in a 44- year-old woman [11]. Our patient's improved clinical status and reduced lesion size support the potential benefits of hydrogen inhalation therapy.

Ozone therapy has been explored for its potential benefits in oncology, primarily due to its immunomodulatory and oxidative stress-reducing properties. Hypoxia is considered the hallmark of brain tumors and is associated with tumor progression, as it inhibits antitumor immune responses [12]. Luongo et al. reported that ozone therapy could enhance the effects of traditional cancer treatments by modulating the immune response and reducing tumor hypoxia [13]. Our

patient included ozone therapy as part of the integrative protocol, contributing to the observed clinical improvements.

Diet therapy was another inclusion in this integrative protocol. The patient was advised to follow a lowcarbohydrate diet in a time-restricted manner, ensuring daily fasting for 14 hours. Preclinical studies have shown that time-restricted feeding can slow down tumor growth. This effect is thought to be due to metabolic stress imposed on cancer cells [14], which have a high metabolic demand and are less adaptable to fasting conditions. Acupuncture is widely recognized for its ability to manage pain, reduce stress, and improve overall quality of life in cancer patients. An earlier case report suggested the role of acupuncture in regressing the size of oligodendroglioma in a 54-year-old man [15]. In the current study, we employed acupuncture to reduce headaches, improve cognitive functions, and promote general well-being. Studies suggest that acupuncture may benefit cancer patients by modulating the nervous system to relieve pain, enhancing the immune system, reducing inflammation, improving blood flow, regulating the endocrine system, supporting gastrointestinal function, and enhancing overall quality of life [16].

Magnet therapy is another complementary approach that has been explored for its potential to alleviate symptoms and improve the quality of life in cancer patients. Pulsed electromagnetic field (PEMF) therapy, an advanced form of magnet therapy, has demonstrated beneficial effects in oncology by inhibiting cell proliferation, reducing neovascularization, and exerting cytotoxic effects on cancer cells [17]. Our patient included PEMF therapy in his integrative treatment plan, which may have contributed to his overall clinical improvement. Hydrotherapy measures, such as hot foot baths and enemas, were given to our patient. These naturopathic remedies were provided to relieve fatigue and upregulate gastrointestinal function. Earlier studies have reported the usefulness of hot foot baths in relieving fatigue and improving the quality of life in cancer patients [18]. Our patients reported improvement in energy levels and relief of symptoms, which may be attributed to these therapies. Studies suggest that hydrotherapy may benefit cancer patients by relieving pain, reducing inflammation, enhancing blood circulation, stimulating the immune system, reducing stress, improving emotional well-being, and enhancing sleep quality [19].

Supplemental injections and therapies were also integrated into the patient's regimen. Dexamethasone and N-acetyl cysteine were administered to reduce brain swelling and improve cognitive function. Vitamin D and coenzyme Q10 were included to alleviate mitochondrial dysfunction and reduce fatigue, while Orokinase was used to lower D-dimer levels, addressing hypercoagulability often observed in cancer patients. Additionally, sublingual cannabis and melatonin (5 mg/day) were provided to enhance sleep quality. This comprehensive supplement strategy aimed to target multiple facets of the patient’s condition, contributing to an overall improvement in health status. Hydrosun therapy, also known as hydrotherapy combined with infrared radiation, has garnered attention for its potential therapeutic benefits in various medical conditions, including oncology [20]. In our case, the patient reported significant improvements in energy levels and overall symptom relief following Hydrosun therapy sessions.

The reported outcomes suggest that the combination of these complementary medicine therapies may have synergistic effects, leading to tumor size regression, significant symptomatic relief, and enhanced quality of life for cancer patients. This may be considered the ability of integrative oncological approaches to induce spontaneous regression, suggesting the reversal of cancer cells into normal cells without any conventional therapies [21]. However, it is crucial to note that this

case study represents a single patient's experience, and larger, controlled studies are necessary to establish the efficacy and safety of such integrative approaches in oncology. Additionally, the patient's psychological state and potential placebo effects may have influenced the outcomes. Another limitation of this case report is the difficulty in identifying the individual effects of each therapy included in the integrative treatment protocol. While the overall improvement in the patient's condition is promising, it is challenging to attribute specific outcomes to any single therapy due to the synergistic and cumulative effects of the combined treatments. It is also important to note that this is a preliminary finding, and hence cannot be considered conclusive. Nevertheless, the patient was happy that he was asymptomatic and had resumed his day-to-day activities as before.

Conclusions

In clinical practice, integrative oncology often involves multiple modalities used concurrently, making it complex to isolate the impact of each therapy. This integrative approach, while potentially more effective, complicates the ability to conduct a clear analysis of the efficacy of individual components. Future research should focus on the mechanistic understanding of how these therapies interact and their long-term impact on cancer progression and patient well-being.

Additional Information

Author Contributions

All authors have reviewed the final version to be published and agreed to be accountable for all aspects of the work.

Concept and design: Pradeep MK Nair, Renganathan Ramalakshmi, Muniappan Devibala, Sekar Sivaranjini, Maruthanayagam Saranya, R Thangavelu, Manickam Mahalingam

Acquisition, analysis, or interpretation of data: Pradeep MK Nair, Renganathan Ramalakshmi, Muniappan Devibala, Sekar Sivaranjini

Drafting of the manuscript: Pradeep MK Nair

Critical review of the manuscript for important intellectual content: Pradeep MK Nair, Renganathan Ramalakshmi, Muniappan Devibala, Sekar Sivaranjini, Maruthanayagam Saranya, R Thangavelu, Manickam Mahalingam

Supervision: Pradeep MK Nair, Manickam Mahalingam

Disclosures

Human subjects: Consent was obtained or waived by all participants in this study.

Conflicts of interest: In compliance with the ICMJE uniform disclosure form, all authors declare the following:

Payment/services info: All authors have declared that no financial support was received from any organization for the submitted work.

Financial relationships: All authors have declared that they have no financial relationships at present or within the previous three years with any organizations that might have an interest in the submitted work.

Other relationships: All authors have declared that there are no other relationships or activities that could appear to have influenced the submitted work.

References

1. Frosina G: Recapitulating the key advances in the diagnosis and prognosis of high-grade gliomas: second half of 2021 update. Int J Mol Sci. 2023, 24:6375. 10.3390/ijms24076375
2. Olgun N, Kızmazoğlu D, Özdoğar B, et al.: High-grade glioma of central nervous system: single center treatment experience. J Clin Oncol. 2021, 39: 10.1200/JCO.2021.39.15_suppl.e14040
3. Hui D, Bruera E: The Edmonton Symptom Assessment System 25 years later: past, present, and future developments. J Pain Symptom Manage. 2017, 53:630-43. 10.1016/j.jpainsymman.2016.10.370
4. Cocks K, Wells JR, Johnson C, et al.: Content validity of the EORTC quality of life questionnaire QLQ-C30 for use in cancer. Eur J Cancer. 2023, 178:128-38. 10.1016/j.ejca.2022.10.026
5. Chuang RB, Hu WY, Chiu TY, Chen CY: Prediction of survival in terminal cancer patients in Taiwan: constructing a prognostic scale. J Pain Symptom Manage. 2004, 28:115-22.10.1016/j.jpainsymman.2003.11.008
6. Szasz AM, Arrojo Alvarez EE, Fiorentini G, Herold M, Herold Z, Sarti D, Dank M: Meta-analysis of modulated electro-hyperthermia and tumor treating fields in the treatment of glioblastomas. Cancers (Basel). 2023, 15:880. 10.3390/cancers15030880
7. Szasz A: Current status of oncothermia therapy for lung cancer . Korean J Thorac Cardiovasc Surg. 2014, 47:77-93. 10.5090/kjtcs.2014.47.2.77
8. Jeung TS, Ma SY, Yu J, Lim S: Cases that respond to oncothermia monotherapy. Conf Pap Sci. 2013, 2013:392480. 10.1155/2013/392480
9. Renner O, Burkard M, Michels H, Vollbracht C, Sinnberg T, Venturelli S: Parenteral high-dose ascorbate – a possible approach for the treatment of glioblastoma (review). Int J Oncol. 2021, 58:35. 10.3892/ijo.2021.5215
10. Ma Y, Chapman J, Levine M, Polireddy K, Drisko J, Chen Q: High-dose parenteral ascorbate enhanced chemosensitivity of ovarian cancer and reduced toxicity of chemotherapy. Sci Transl Med. 2014, 6:222ra18. 10.1126/scitranslmed.3007154
11. Chen J, Mu F, Lu T, Du D, Xu K: Brain metastases completely disappear in non-small cell lung cancer using hydrogen gas inhalation: a case report. Onco Targets Ther. 2019, 12:11145-51. 10.2147/OTT.S235195

12. Park JH, Lee HK: Current understanding of hypoxia in glioblastoma multiforme and its response to immunotherapy. Cancers (Basel). 2022, 14:1176. 10.3390/cancers14051176

13. Luongo M, Brigida AL, Mascolo L, Gaudino G: Possible therapeutic effects of ozone mixture on hypoxia in tumor development. Anticancer Res. 2017, 37:425-35. 10.21873/anticanres.11334

14. Nencioni A, Caffa I, Cortellino S, Longo VD: Fasting and cancer: molecular mechanisms and clinical application. Nat Rev Cancer. 2018, 18:707-19. 10.1038/s41568-018-0061-0

15. Kim JS, Lee HJ, Lee SH, Lee BH: Recurrent oligodendroglioma treated with acupuncture and pharmacopuncture. J Acupunct Meridian Stud. 2015, 8:147-51. 10.1016/j.jams.2015.03.004

16. Garcia MK, McQuade J, Haddad R, et al.: Systematic review of acupuncture in cancer care: a synthesis of the evidence. J Clin Oncol. 2013, 31:952-60. 10.1200/JCO.2012.43.5818

17. Vadalà M, Morales-Medina JC, Vallelunga A, Palmieri B, Laurino C, Iannitti T: Mechanisms and therapeutic effectiveness of pulsed electromagnetic field therapy in oncology. Cancer Med. 2016, 5:3128-39. 10.1002/cam4.861

18. Akyuz Ozdemir F, Can G: The effect of warm salt water foot bath on the management of chemotherapyinduced fatigue. Eur J Oncol Nurs. 2021, 52:101954. 10.1016/j.ejon.2021.101954

19. Mooventhan A, Nivethitha L: Scientific evidence-based effects of hydrotherapy on various systems of the body. N Am J Med Sci. 2014, 6:199-209. 10.4103/1947-2714.132935

20. Vaupel P, Piazena H, Müller W, Notter M: Biophysical and photobiological basics of water-filtered infrared-A hyperthermia of superficial tumors. Int J Hyperthermia. 2018, 35:26-36. 10.1080/02656736.2018.1469169

21. Cole WH, Everson TC: Spontaneous regression of cancer: preliminary report . Ann Surg. 1956, 144:366-83. 10.1097/00000658-195609000-00007

Usefulness of a pragmatic integrative medicine approach in the management of breast cancer: A case series with literature review

Pradeep Mk Nair *, Renganathan Ramalakshmi, Muniappan Devibala, Maruthanayagam Saranya, Sekar Sivaranjani, R. Thangavelu, Manickam Mahalingam

Mirakle Integrated Health Centre, Pollachi, India

* Corresponding author: E-mail address: drpradeep18bnys@gmail.com (P.M. Nair).

Citation

Nair, P. MK. et al (2024) Usefulness of a pragmatic integrative medicine approach in the management of breast cancer: A case series with literature review

Oncothermia Journal 38, August 2026., 201-214.
https://oncotherm.com/NairPMK_2024_Usefullness_of_pragmatic_integrative_medicine_approach

Abstract

Complementary and alternative medicine approaches are widely used by breast cancer patients. We present a case series of four patients with breast cancer who underwent a pragmatic integrative medicine protocol in an inpatient integrative oncology setting. The participants were three metastatic and one non-metastatic breast cancer patient who did not undergo any standard cancer therapies. The holistic integrative medicine protocol includes counselling, oncothermia, high-dose vitamin C therapy, ozone therapy, diet therapy, liposomal curcumin therapy, vitamin D supplementation, artesunate injections, probiotic supplementation, Co-Q enzyme therapy, hyperbaric ozone therapy, medical cannabis, coffee enema, colour therapy, sun exposure, and yoga therapy. The treatment duration varied from person to person. All the patients have shown significant improvement in their complete blood cell counts, reduction in their cancer markers. The thermal scan has shown a complete arrest of disease activity in the breast compared to baseline. Further, all the patients have shown improvement in their body weight and expressed a complete revival of subjective wellbeing. The holistic integrative medicine protocol looks promising in the management of breast cancer. However, large-scale randomized control trials are warranted to validate the present findings.

Keywords: Breast cancer, Integrative medicine, Vitamin C therapy, Oncothermia, Case Report

1. Introduction

Breast cancer is one of the most common types of cancers across the globe, accounting for nearly 6.85 lakh deaths and representing 1 in 8 cancer diagnoses [1]. This poses a significant physical, psychological, and economic burden on both the patients and their caregivers. The gold standard of therapeutic recommendations for breast cancer includes surgery, hormonal therapy, chemotherapy, radiation, and immunotherapy. Despite the beneficial effects of these therapies, they are associated with severe side effects [2].On the other side integrative oncology is emerging as a promising avenue that promotes collaborative clinical practice and research in cancer [3]. Furthermore, integrating complementary and alternative medicine (CAM) therapies in the management of breast cancer is becoming popular among patients and caregivers [4]. Homeopathy, traditional Chinese medicine, biological-based practices, energy medicine (Pranic healing, Reikhi), mind-body medicine techniques (yoga, meditation, progressive muscle relaxation) and manipulative and body-based practices are the common CAM therapies used in breast cancer [5]. We report the cases of four patients diagnosed with breast cancer who underwent integrative medicine therapies at an exclusive integrative oncology setting in India.

2. Case presentation

All the patients underwent an integrative medicine protocol (Mirakle ™ protocol) curated by a group of physicians that included experts from yoga, naturopathy, modern medicine, and homoeopathy. The Mirakle™ protocol included counselling, oncothermia, high-dose vitamin C therapy, ozone therapy, diet therapy, liposomal curcumin therapy, vitamin D supplementation, artesunate injections, probiotic supplementation, Co-Q enzyme therapy, hyperbaric ozone therapy (HBOT), medical cannabis, coffee enema, colour therapy, sun exposure, and yoga therapy.

These therapies were used in varying permutations and combinations as per the individual needs of the patient. While the majority of the treatments were administered to all patients with the same frequency, as shown in Table 1, other therapies, such as hyperbaric ozone, yoga, medicinal cannabis, and vitamin D supplements, were combined depending on the patient's condition. Only patients with healthy, large veins were able to receive hyperbaric ozone therapy; patients' physical conditions determined whether yoga therapy was recommended; only patients experiencing excruciating pain were eligible for medical cannabis; and the patient's vitamin D levels determined whether vitamin D supplementation was necessary. All the patients signed an informed consent for sharing their de-identified information.

Patients were selected based on the following criteria: PET CT- confirmed, biopsy-proven carcinoma of the breast, with or without metastasis, any type of breast cancer, and a willingness to undergo integrative medicine therapies. None of the patients in this case series underwent standard conventional therapies due to varying reasons like fear of side effects, lack of confidence, belief in CAM therapies, and economic constraints. The treatment duration varied from patient to patient. Even though all the patients had a confirmatory diagnosis of cancer through a positron emission tomography (PET) scan, we have used a thermography technique[6], which is a non-invasive and sensitive test to screen breast cancer (a thermography camera captures these temperature differences in the breast area, which are then analyzed for abnormalities) along with the other cancer markers, to evaluate the prognosis in these patients from the baseline. We further assessed the subjective well-being of our patients by qualitatively exploring their personal experiences, emotions, and perceptions related to their diagnosis, treatment, and overall quality of life.

2.1. Case 1

The patient was a 49-year-old female of Indian ethnicity, diagnosed with carcinoma of the right breast with metastasis to the right axillary nodes and skeleton. She was diagnosed with carcinoma of the right breast in November 2021 through a biopsy and PET scan. She initially underwent flower therapy and Siddha (a traditional Indian medicine practice) at her hometown, but did not find any relief in her symptoms. She presented to our setting with severe pain in the left hip region associated with difficulty walking in September 2023. Her baseline thermography reports suggested the presence of hyperthermic lesions in her right breast with cellular activity.

She underwent the Mirakle™ protocol for 3 months, where she reported improvement in subjective quality of life, reduction in fatigue, pain, and stability in body weight. Her thermography report from November 2023 has shown regression of the right breast lesion with no cellular activity (Fig. 1). Even though the patient has shown significant subjective improvement in her cancer-related symptoms and well-being, there was a rise in the cancer markers at the end of the third month. The detailed changes in the clinical parameters are tabulated in Table 2. At present, the patient follows the diet regimens and supplements (liposomal vitamin C drink, liposomal curcumin, CoQ-10 enzyme, probiotics, vitamin D) advised at home and is visits the hospital every 15 days for maintenance therapy

Table 1
The Mirakle™ Protocol: An integrative oncology protocol.

Intervention	Frequency of intervention	Role in cancer therapeutics
Counselling	Daily	Yoga and naturopathy based counselling techniques was utilized in our patients to remove the fear of disease, fear of death, build hope and resilience among patients and caregivers.
Oncothermia	Alternate days (A total of 12–24 sessions was provided to the patients depending upon patient's condition and affordability)	Oncothermia uses a modulated radiofrequency which helps in selectively stimulating the programmed cell death of cancer cells and arresting the metastasis.
High dose vitamin C therapy	2–3 times per week, the total dose not exceeding 90 g per week.	It acts as a scavenger of reactive oxygen species (ROS), inhibits the growth of cancer cells, reduces the side effects of conventional therapies, and reduces the symptoms associated with cancers.
Ozone therapy	Daily (Ozone is administered in the form of rectal insufflation/vaginal insufflation/ saline ozone, Minor autohaemotherapy and major autohaemotherapy)*.	Ozone exhibit anti-tumor effect by its anti-oxidant property which promotes tumor cell apoptosis. Furthermore, it improves the oxygen carrying capacity of the cells, acts as an anti-microbial agent, and modulate the immune system.
Diet therapy	Daily (A complete Millet-based, sugar free, maida free, refined grains free diet was advised to our patients. This also includes carrot, beetroot, apple juice, fresh vegetable salads, and soups.)	A low glycemic index diet rich in phytonutrients, vitamins and minerals can help in addressing the macro and micronutrient deficiencies that are common in cancer.
Liposomal curcumin therapy	Daily (5–10 ml liposomal curcumin drink is consumed by all the patients)	Liposomal curcumin induces cytotoxicity, inhibit the cancer cell growth and induce apoptosis.
Vitamin D supplementation	Daily (The doses are decided based on the vitamin D deficiency ranging from 10000 to 60000 IU after monitoring the levels of parathyroid hormones and ionized calcium levels.)	Adequate levels of vitamin D has shown to check the progression, tumorigenesis and alter the cancer cell–microenvironment interaction.
Artesunate injections	Weekly once (The doses starts from 60 g and gradually elevated up to 180 g after monitoring the haemoglobin levels of the patients)	Artesunate induces tumor cell apoptosis and arrests the tumor cell growth.
Probiotic supplementation	Daily (Two doses of Liv-Bio alpha Pre and probiotic supplements are provided to all the patients.)	Upregulating the gut flora improves the diversity of gut microbiota which upregulate the metabolic and immune functions in cancer.
Co-Q enzyme therapy	Daily (5–15 ml liposomal Co-Q 10 enzyme were consumed by all the patients)	Co-Q enzyme upregulate the mitochondrial dysfunction and increase the energy levels of patients.
Hyperbaric oxygen therapy	Once in a month	Hyperbaric oxygen therapy influence the antioxidant activities and inhibits cancer growth.
Medical cannabis	As per need 4–8 drops (Cannaronil- cannabidiol: tetrahydrocannabinol 1:4)	Helps in relieving cancer symptoms pain, anxiety, insomnia as well as inhibit cancer growth and promote apoptosis.
Coffee enema	Thrice in a week	Functions as a detoxifier of liver, promotes antioxidant capacity
Colour therapy	Once in a week (Hydrosun light therapy)	It combines the oriental medicine concept of chakra, chromotherapy and properties of light. It is useful in relieving pain, induce calmness and activate the immune system.
Sun exposure	Daily 10–20 minutes (between 10 am to 3 pm)	Sun exposure helps in upregulating the vitamin D levels, improves mood and cognition.
Yoga therapy	Daily 30–45 minutes (Includes pranayama, meditation and asanas)	Yoga helps in improving the mental health, builds resilience and also helps in regaining homeostasis.

* The choice of treatments varies from patient to patient

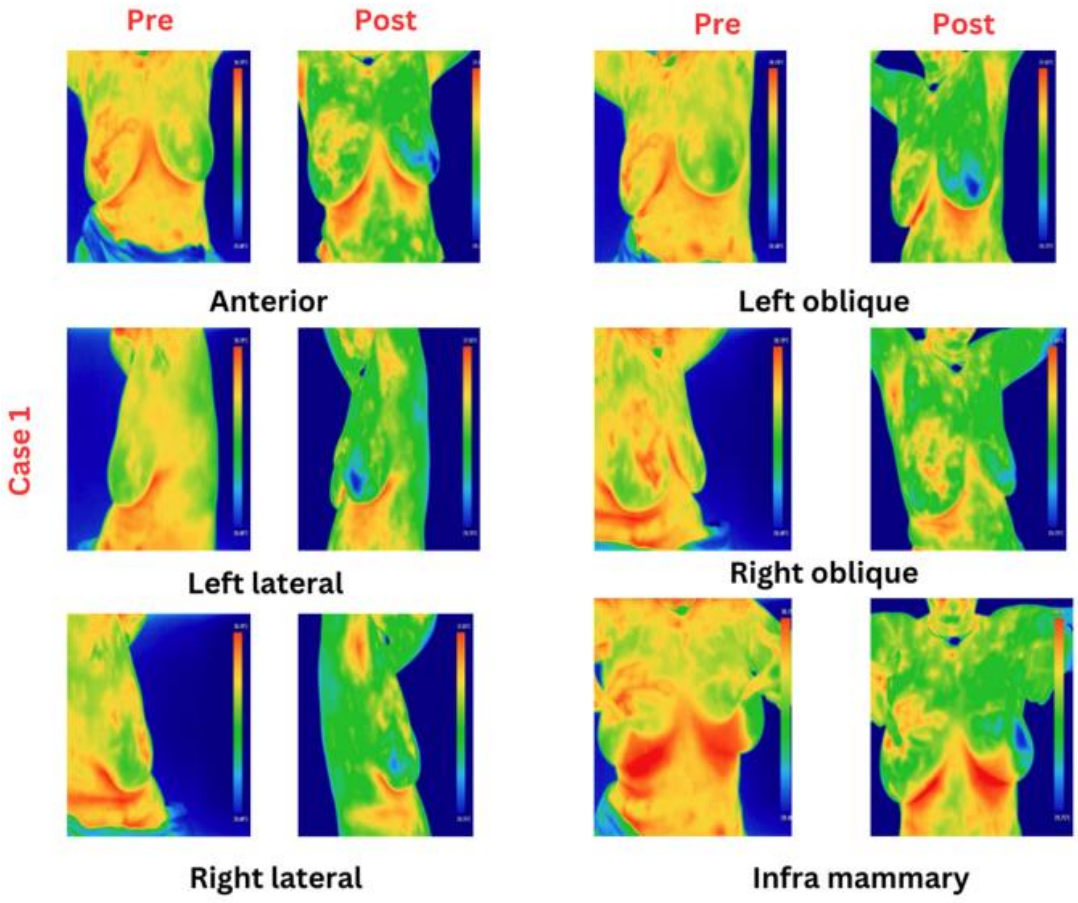

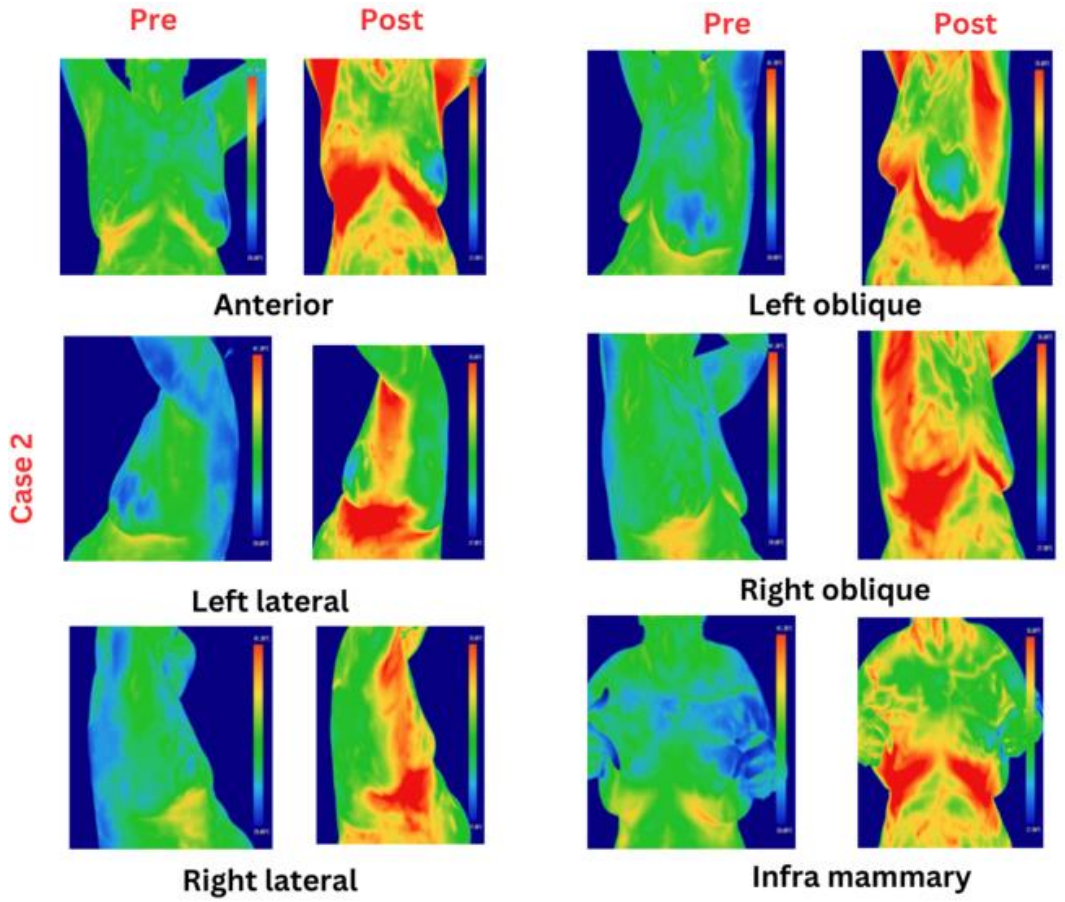

Fig. 1. Changes in the thermal scan before and after the treatment.

2.2. Case 2

The patient was a 76-year-old female of Indian ethnicity, diagnosed with carcinoma of the right breast with axillary node metastasis in December 2021.She visited our hospital in January 2022 with severe pain in the right breast, both shoulders, and a freely mobile hard mass in the right breast. She was a known case of rheumatoid arthritis and type 2 diabetes mellitus, for which she was taking metformin 500 mg twice daily. Her baseline thermography report suggested small hyperthermic lesions in the right breast and large hyperthermic lesions in the left breast with irregular borders. She underwent the Mirakle™ protocol as an inpatient for 4 months at different intervals since January 2022.

Besides this, during the intervals of her inpatient stay, she visited the hospital for maintenance therapies once every 15 days with regular supplements, as mentioned in Case 1. Her thermograph report in June 2023 was similar to that of the baseline report with respect to the breast. The lymph nodes appeared normal in the follow-up thermograph (Fig. 1). Nevertheless, the patient expressed complete relief from her pain, fatigue, and improvement in quality of life. We have observed a significant reduction in the cancer markers across the past year, suggesting reduced disease progression (Table 2). Currently, she is visiting the hospital once a month and continuing the maintenance therapy.

Table 2
Changes in the biochemical markers across time points.

Time points		RBC	Hb	PCV	TC	N	L	E	RDW-CV	Platelets	ESR	FE	CEA	Ca 15.3	LDH	D-DIMER	hs-CRP	Weight
P1	Baseline	3.7	9.1	27	6410	56.5	33.2	1.5	13.1	401	35	7.5	2.18	33.26	172	1600	1.7	66.7
	3rd month	3.61	8.9	26.7	7890	63.1	31.6	1.5	15	394	50	20.7	2.1	61.65	170	2471	0.6	64.7
P2	Baseline	4.06	10	26.9	9910	58	34	3	13.6	413	25	16.8	3.3	43.9	273	1590	10.63	62.9
	1st month	3.97	10.4	28.1	7	46	45	4	14.3	276	28	NE	4.1	37.1	251.7	1120	6.35	59.3
	3rd month	3.88	11.1	29.1	5.6	56	34	4	12.3	287	26	72.9	3.8	32.7	480.63	1910	4.85	60.2
	6th month	3.6	10.9	28.6	6.7	60	32	3	13.7	255	28	NE	NE	29.3	332.4	850.6	2.7	63.9
	12th month	4.16	10.8	31.9	8.43	60	34	2	12.9	392	22	NE	NE	19.33	207	NE	12.85	67.5
	18th month	4.36	11.3	33.4	12400	58.5	32.8	1.2	12.1	444	50	NE	NE	20.53	208	1019	13.5	67
P3	Baseline	4.43	12.6	33.8	9400	76	19	2	12.5	251	23	39.3	3.8	59.9	350.6	260	1.54	71.8
	1st month	4.65	13.5	36.1	7700	66	25	4	12.8	257	36	49.1	4.3	56.6	520.97	285	1.15	69
	3rd month	4.26	12.1	32.3	8900	67	27	2	12.3	244	20	40	2.87	42.6	324.49	310	5.2	67.3
	6th month	4.45	12.9	37.9	7630	64.3	26.1	3	14.8	336	25	69.4	4.1	24.17	274.1	310	1.62	65.8
P4	Baseline	4.53	11.8	36.4	9600	64	30	2	15.2	243	40	125.2	2.81	12.99	158	504	3.1	64.1
	3rd month	4.36	11.4	33.6	8120	55.8	34.7	2.6	11.1	293	12		1.78	10.48	155	206	2.8	64.4

P-Patient; RBC- Red Blood Cells (million/cu mm); Hb- haemoglobin (g/dL); PCV- Packed Cell volume (%); TC- Total Count (cells/cu mm); N- Neutrophils (%); L-Lymphocytes(%); E-Eosinophils(%); RDW-CV- Red Cell distribution width (%); ESR- Erythrocyte sedimentation rate (mm); FE- Ferritin(ng/ml); CEA- Carcinoembryonic antigen (ng/ml); Ca 15.3- Cancer antigen 15.3 (U/ml);; LDH- Lactate Dehydrogenase (U/L); D-DIMER (ng/ml); hs-CRP- High sensitive C-reactive protein (mg/L); Weight (Kg); NE- Not evaluated

2.3. Case 3

The patient was a 69-year-old female of Indian ethnicity, diagnosed with carcinoma of the left breast with nodal metastasis in December 2021. She presented to the hospital on January 2022 with pain in the left breast, inverted nipples, and an enlarged left breast. She was a known case of hypertension and was taking calcium channel blockers and beta blockers for it. The initial thermography report has shown hyperthermic lesions in her left breast with cellular activity. She took the Mirakle™ protocol for 3 months as an inpatient at different intervals, followed by visiting as an outpatient once a month since June 2022. During the course of treatment, she had persistent pricking pain in her left breast and upper limbs, as well as disturbances in sleep. Her thermograph report from June 2023 has shown complete remission of the lesion from her left breast (Fig. 2). We noted a subsequent reduction in her cancer markers (Table 2), an improvement in her subjective quality of life, and a complete reduction of symptoms. She is currently taking maintenance therapy once a month.

2.4. Case 4

A 58-year-old female of Indian ethnicity, diagnosed with carcinoma of the left breast in May 2023 visited our setting in June 2023. She did not have any specific complaints related to her disease except for severe fatigue. She was a known case of type 2 diabetes mellitus and is taking metformin for the same. Her baseline thermography report has shown a hyperthermic patch over the upper quadrant of the left breast with an irregular border and cellular activity. She underwent the Mirakle™ protocol for 3 months as an outpatient, where the therapies were scheduled every alternate day. Within two weeks of the initiation of the protocol, the patient expressed remarkable improvement in her energy levels; however, the lump was still palpable in her left breast. By the end of the third month, we noticed that there were no palpable lumps, and the thermography report also showed that there were no hyperthermic patches or cellular activity in her breasts (Fig. 2), indicating remission. Further, her cancer markers have also shown a significant reduction (Table 2). Her therapy frequency was reduced to once a week for one month, and at present she is taking maintenance therapy once a month. The detailed timeline of events is presented in Fig. 3.

3. Discussion

This case series discusses the usefulness of a comprehensive integrative medicine protocol in the management of breast cancer. All the patients responded well to the therapies provided and have shown improvement in their symptoms and cancer markers. No adverse events were reported by any of the patients. These therapies were intended to promote cancer cell death, upregulate

mitochondrial function, reduce tissue hypoxia, improve mental health and quality of life, and reduce symptoms. The integrative medicine therapies used in this protocol have Table been shown to have potential anti-tumor effects. Oncothermia, which uses a modulated radiofrequency current, has been shown to target and destroy cancer cells by disrupting the extracellular membrane of cancer cells. It induces programmed cell death; however, it does not affect normal cells [7]. Earlier studies have also shown oncothermia to be beneficial in treating different types of cancer [8,9].

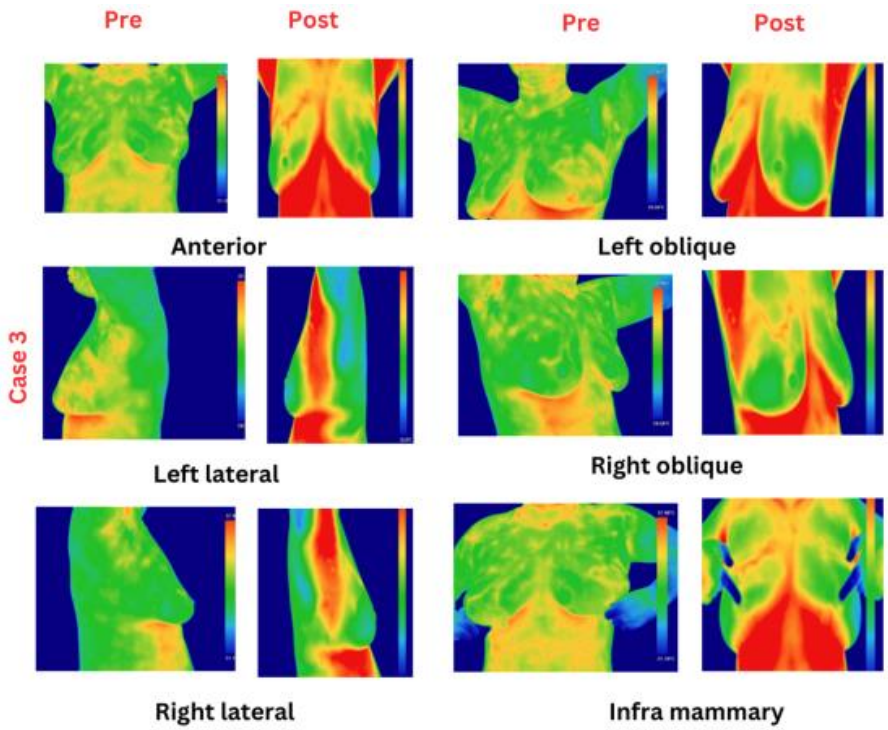

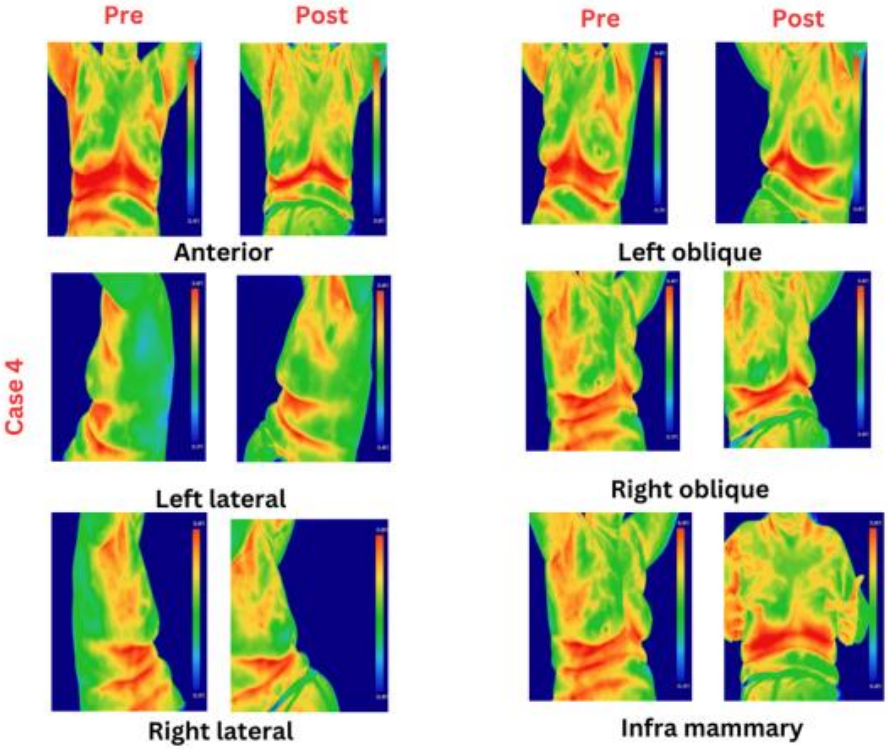

Fig. 2. Changes in the thermal scan before and after the treatment.

This is the first study to report the use of oncothermia in breast cancer patients. This study also reports the use of high-dose vitamin C as a potential anti-cancer therapy. The doses were tolerated well by all the patients without any adverse events. The role of vitamin C as an anti-cancer agent has been reported in earlier studies as well [10]. Vitamin C in higher doses suppresses the invasion and metastases of breast cancer cells by inhibiting epithelial-mesenchymal transition [11]. The role of ozone therapy in cancer is presently being studied through in vitro and clinical studies. Ozone applications have been shown to improve tissue oxygenation, reduce oxidative stress, stimulate mitochondria, and promote and modulate immune function[12,13].

Fig. 3. Timeline of events.

While whole grain consumption has been suggested in the management of cancer, millets may be the most appropriate choice owing to their high nutrient content, lack of acid-forming properties, and glutenfree status in comparison to other grains[14,15]. It is paramount that adequate nutrition is provided to cancer patients from the right source. We observed significant improvements in body weight and physical wellbeing among study participants, which may be attributed to adequate nourishment through millets in addition to the other therapies. In vitro and in vivo studies suggest curcumin exhibits an anti-cancer effect in breast cancer by accelerating programmed cell death, modulating the inflammatory process, inhibiting angiogenesis, and inhibiting cancer metastases[16]. A liposomal based curcumin was used in this study, as liposomal curcumin increases the bioavailability of curcumin and possesses significant pro-apoptotic and inhibitory effects on cancer cells[17].

Vitamin D deficiency is considered a risk factor for breast cancer and is also associated with its poor prognosis. Combining vitamin D supplementation with other breast cancer therapies has been thought to have potential anticancer activity by influencing intracellular mechanisms like cell differentiation, proliferation, programmed cell death, and epithelial-mesenchymal transition [18]. All

the patients in the current case series presented with vitamin D deficiency, and the supplementation of the same might have contributed to the better prognosis. In addition to this, we also recommended 10–15 minutes of sun exposure to all the participants, as sun exposure is found to be protective against breast cancer, which is further associated with vitamin D synthesis in response to sun exposure [19].

Artesunate injections have been an integral part of this protocol. Artesunate is a derivative of Artemisia annua, which has been shown to possess potential anticancer effects such as promoting apoptosis, autophagy, improving redox balance, inhibiting angiogenesis, and inducing ferroptosis [20]. Prebiotics and probiotics were used as part of this protocol since gut dysbiosis is thought to play a significant role in the development and metastasis of breast cancer [21]. Probiotic use is recommended as an effective approach to enhance immunomodulation and quality of life in patients with breast cancer [22]. Further, coenzyme Q10 was consumed by the participants of this study. Coenzyme Q10 is an important component in the mitochondrial electron transport chain, whose deficiency will result in mutations of mitochondrial DNA and subsequent mitochondrial dysfunction. Studies have shown a depletion in the coenzyme Q10 among breast cancer patients and recommend its supplementation as a prognostic strategy [23].

Cancer cells thrive in a hypoxic environment, as it helps in angiogenesis and further metastasis. Furthermore, this induces structural and functional damage to the adjacent healthy cells[24]. As discussed earlier, ozone therapy helps in addressing tissue hypoxia. Besides this, we have also used HBOT, a more powerful tissue oxygenation method, with our patients. There are reports suggesting the usefulness of HBOT as an adjuvant in the management of breast cancer[25,26]. HBOT augments tissue functions by improving the oxygen supply, reducing inflammation, reinstating the redox balance, and promoting apoptosis [27].

Managing the psychological burden and pain associated with cancer remains one of the primary challenges in cancer therapeutics. In our protocol, we primarily use yoga therapy and medical cannabis preparations to manage pain, insomnia, anxiety, depression, and stress among our patients. A mixture of cannabidiol and tetrahydrocannabinol was used in our patients primarily to control pain and upregulate their mental health status. Earlier studies recommend the use of cannabis in breast cancer as it improves mental health symptoms, forbids cancer cell progression, promotes apoptosis, and arrests tumor angiogenesis [28–30]. Yoga is known to reduce pain, fatigue, improve the quality of life, and increase physical activity among patients with breast cancer [31,32].

A coffee enema was given to all the patients in this study as a detoxification measure. Coffee enemas are reported to detoxify the liver by enhancing the activity of antioxidants such as glutathione and Stransferase activity[33,34]. There are reports on the adverse effects associated with coffee enema as well[35]. However, we did not find any adversities associated with coffee enema among our participants. Nevertheless, this needs to be validated through large-scale studies. Colour healing is one of the most common methods used in complementary and alternative medicine settings. Colour therapy has been reported to alleviate cancer-related symptoms like insomnia, pain, fatigue, poor appetite, nausea, and mood disturbances [36]. Our participants also reported improvements in their symptoms and mental health status, which may be attributed to the use of colour therapy as well.

This is the first case series reporting the pragmatic use of an array of CAM therapies in the management of breast cancer. There are substantial limitations in the present report that warrant future large-scale studies. The use of multiple treatments, all of which have potential anticancer effects, limits our ability to understand the specific role of each therapy. Nevertheless, the primary intention was to holistically support the patients with all the possible CAM approaches. Besides the cancer-related markers, this study did not use any conventional imaging techniques like PET scans or CT (computed tomography) scans. Even though a thermal scan is considered a reliable technique for detecting breast cancer, evidence suggests it could be used only as a supplementary diagnostic technique alongside a mammogram[6,37,38]. Furthermore, our patients were not ready to take a PET/CT scan or mammogram. This might be considered a limitation, as it can affect the reliability of the outcomes presented. Another limitation of this study is that we did not assess the changes in quality of life using any established quality of life instruments. This study did not collect any data beyond the cancer-related markers, which may be considered a limitation.

All patients in this case series did not receive any standard medical care. Even though there are favourable outcomes, there are probabilities that the patient may or may not have minimal residual disease. A PET scan would have ideally revealed if there was any minimal residual disease. Since our patients refused to undergo a PET scan or mammogram, the authors do not have enough evidence to comment on this aspect. This needs to be investigated in future randomized controlled studies.

The study design, being a case series, limits the generalizability of the present findings, which is a limitation. One of the primary limitations of this case series is the small sample size, which inherently restricts the power of any statistical analysis. While case series are valuable for generating hypotheses and exploring potential benefits of treatments, they lack the robustness required to establish definitive cause-and-effect relationships. The absence of a control group further limits the ability to draw firm conclusions about the efficacy of the interventions studied. Consequently, the findings should be interpreted with caution, and further research with larger, controlled studies is necessary to validate these observations. Nevertheless, this report offers promising directions for research and clinical practice in integrative oncology.

4. Patient perspective

All the patients were happy that they could improve their quality of life and achieve considerable control over their condition with an integrated approach. They opined that involving them in the decisionmaking process of treatment planning gave them confidence to continue the therapies.

Ethics approval and consent to participate

The ethical approval was waived by the institutional ethics committee of Mirakle Integrated Health centre. All the participants signed an informed consent to share their de-identified information.

Consent for publication

All the participants consented to publish their reports.

Funding

None

CRediT authorship contribution statement

Manickam Mahalingam: Writing – review & editing, Resources, Project administration, Methodology, Funding acquisition, Conceptualization. Thangavelu R: Resources, Project administration, Investigation, Conceptualization. Sekar Sivaranjini: Project administration, Methodology, Formal analysis, Data curation, Conceptualization. Maruthanayagam Saranya: Project administration, Investigation, Data curation, Conceptualization. Muniappan Devibala: Project administration, Methodology, Investigation, Data curation, Conceptualization. Renganathan Ramalakshmi: Project administration, Investigation, Data curation, Conceptualization. Pradeep MK Nair: Writing – review & editing, Writing – original draft, Visualization, Validation, Supervision, Software, Resources, Project administration, Methodology, Investigation, Funding acquisition, Formal analysis, Data curation, Conceptualization.

Declaration of Competing Interest

The authors declare that they have no known competing financial interests or personal relationships that could have appeared to influence the work reported in this paper.

Data Availability

Data will be made available on request.

Acknowledgements

None

References

[1] M. Arnold, E. Morgan, H. Rumgay, A. Mafra, D. Singh, M. Laversanne, et al., Current and future burden of breast cancer: global statistics for 2020 and 2040, Breast 66 (2022 Dec) 15–23.

[2] G.J. Dobos, P. Voiss, I. Schwidde, K.E. Choi, A. Paul, B. Kirschbaum, et al., Integrative oncology for breast cancer patients: introduction of an expert-based model, BMC Cancer 12 (2012 Nov) 539.

[3] M. Frenkel, L.G. Balneaves, Integrative oncology: an essential feature of highquality cancer care, J. Alter. Complement Med [Internet] 24 (9–10) (2018 Sep 27) 855–858. Available from: 〈 https://www.liebertpub.com/doi/10.1089 /acm.2018.29053.mfl〉 .

[4] C.M. Witt, M.J. Cardoso, Complementary and integrative medicine for breast cancer patients–evidence based practical recommendations, Breast 28 (2016) 37–44.

[5] Intervention types CAM-Cancer [Internet]. [cited 2023 Nov 9]. Available from: 〈htt ps://cam-cancer.org/en/intervention-types-0〉

[6] M.B. Rakhunde, S. Gotarkar, S.G. Choudhari, Thermography as a breast cancer screening technique: a review article, Cureus (2022 Nov 8) cited 2023 Nov 10];14 (11). Available from: /pmc/articles/PMC9731505/.

[7] G. Hegyi, G.P. Szigeti, A. Sz´ asz, Hyperthermia versus oncothermia: cellular effects in complementary cancer therapy, Evid. Based Complement Altern. Med. (2013) [cited 2023 Oct 16];2013.

[8] T.S. Jeung, S.Y. Ma, J. Yu, S. Lim, Cases that respond to oncothermia monotherapy, Conf. Pap. Med 2013 (2013 May 29) 1–12.

[9] A. Szasz, Current status of oncothermia therapy for lung cancer, Korean J. Thorac. Cardiovasc Surg. 47 (2) (2014) 77 [cited 2023 Nov 15];.

[10] F. Bottger, ¨ A. Vall´es-Martí, L. Cahn, C.R. Jimenez, High-dose intravenous vitamin C, a promising multi-targeting agent in the treatment of cancer, J. Exp. Clin. Cancer Res 40 (1) (2021) 1–44. 〈 https://jeccr.biomedcentral.com/articles/10.1186/s 13046-021-02134-y〉 (Available from).

[11] Zeng L.H., Wang Q.M., Feng L.Y., Ke Y.D., Xu Q.Z., Wei A.Y., et al. High-dose vitamin C suppresses the invasion and metastasis of breast cancer cells via inhibiting epithelial-mesenchymal transition. Onco Targets Ther [Internet]. 2019 Sep 10 [cited 2023 Nov 15];12:7405–13. Available from: https://www.dovepress. com/high-dose-vitamin-c-suppresses-the-invasion-and-metastasis-of-breast-c-peerreviewed-fulltext-article-OTT.

[12] J. Baeza-Noci, R. Pinto-Bonilla, M. Malatesta, B. Cisterna, M. Costanzo, Systemic review: ozone: a potential new chemotherapy, Int J. Mol. Sci. Vol 22 (2021) 11796. 〈https://www.mdpi.com/1422-0067/22/21/11796/htm〉 (Available from).

[13] M. Luongo, A.L. Brigida, L. Mascolo, G. Gaudino, Possible therapeutic effects of ozone mixture on hypoxia in tumor development, Anticancer Res 37 (2017) 425–436.

[14] S. Saini, S. Saxena, M. Samtiya, M. Puniya, T. Dhewa, Potential of underutilized millets as Nutri-cereal: an overview, J. Food Sci. Technol. 58 (12) (2021 Dec 1) 4465 [cited 2023 Nov 22];.

[15] M. Xie, J. Liu, R. Tsao, Z. Wang, B. Sun, J. Wang, Whole grain consumption for the prevention and treatment of breast cancer, Nutrients 11 (8) (2019 Aug 1) [cited 2023 Nov 22];.

[16] X. Song, M. Zhang, E. Dai, Y. Luo, Molecular targets of curcumin in breast cancer, Mol. Med Rep. 19 (1) (2019) 23–29.

[17] T. Feng, Y. Wei, R.J. Lee, L. Zhao, Liposomal curcumin and its application in cancer, Int J. Nanomed. 12 (2017 Aug 21) 6027 [cited 2023 Oct 20];.

[18] J. Vanhevel, L. Verlinden, S. Doms, H. Wildiers, A. Verstuyf, The role of vitamin D in breast cancer risk and progression, Endocr. Relat. Cancer 29 (2) (2022 Feb 1) R33–R55. 〈 https://erc.bioscientifica.com/view/journals/erc/29/2/ERC-21-0182. xml〉. cited 2023 Nov 22];.

[19] C.M. Nazario, R.V. Rosario-Rosado, M. Schelske-Santos, I. Mansilla-Rivera, F. A. Ramírez-Marrero, J. Nie, et al., Sun exposure is associated with reduced breast cancer risk among women living in the caribbean: the atabey study in puerto rico (Available from:), Cancer Epidemiol. Biomark. Prev. 31 (2) (2022 Feb 1) 430–435, https://doi.org/10.1158/1055-9965.EPI-21-0932.

[20] X. Yang, Y. Zheng, L. Liu, J. Huang, F. Wang, J. Zhang, Progress on the study of the anticancer effects of artesunate, Oncol. Lett. 22 (5) (2021 Nov 1) [cited 2023 Nov 23].

[21] J. Zhang, Q. Xie, X. Huo, Z. Liu, M. Da, M. Yuan, et al., Impact of intestinal dysbiosis on breast cancer metastasis and progression, Front Oncol. [Internet] 12 (2022 Nov 7) 1037831 [cited 2023 Nov 23].

[22] M.S. Thu, T. Ondee, T. Nopsopon, I.A.K. Farzana, J.L. Fothergill, N. Hirankarn, et al., Effect of probiotics in breast cancer: a systematic review and meta-analysis, Biology 12 (2) (2023 Feb 1) 280 [cited 2023 Nov 23];.

[23] O. Portakal, Oz ¨ Ozkaya, ¨ M. Erden Inal, B. Bozan, M. Kos¸an, I. Sayek, Coenzyme Q10 concentrations and antioxidant status in tissues of breast cancer patients, Clin. Biochem. 33 (4) (2000 Jun 1) 279–284.

[24] Y. Zhang, H. Zhang, M. Wang, T. Schmid, Z. Xin, L. Kozhuharova, et al., Hypoxia in breast cancer—scientific translation to therapeutic and diagnostic clinical applications, Front Oncol. 11 (2021 Mar) 652266 [cited 2023 Nov 24];11.

[25] U.M. Carl, J.J. Feldmeier, G. Schmitt, K.A. Hartmann, Hyperbaric oxygen therapy for late sequelae in women receiving radiation after breast-conserving surgery, Int J. Radiat. Oncol. Biol. Phys. 49 (4) (2001 Mar 15) 1029–1031. 〈http://www.redjo urnal.org/article/S0360301600015157/fulltext〉 (Available from).

[26] J.H. Koo, S.H. Song, H.S. Oh, S.H. Oh, Comparison of the short-term effects of hyperbaric oxygen therapy and complex decongestive therapy on breast cancerrelated lymphedema: a pilot study, Medicine 99 (11) (2020 Mar 23) E19564. 〈https://journals.lww.com/md-journal/fulltext/2020/03130/comparison_of_the_ short_term_effects_of_hyperbaric.91.aspx〉 (Available from).

[27] I. Moen, L.E.B. Stuhr, Hyperbaric oxygen therapy and cancer - a review, Target Oncol. 7 (4) (2012 Dec 2) 233–242. Available from: 〈https://link.springer.com/art icle/10.1007/s11523-012-0233-x〉.

[28] M.M. Caffarel, C. Andradas, E. Mira, E. P´erez-Gomez, ´ C. Cerutti, G. Moreno-Bueno, et al., Cannabinoids reduce ErbB2-driven breast cancer progression through Akt inhibition, Mol. Cancer [Internet] 9 (1) (2010 Jul 22) 1–11. Available from: 〈https://molecular-cancer.biomedcentral.com/articles/10.1186/1476-4598-9-19 6〉.

[29] R. Zafar, D. Sulak, J. Brambila, D. Nutt, A. Schlag, Raising awareness: The implementation of medical cannabis and psychedelics used as an adjunct to standard therapy in the treatment of advanced metastatic breast cancer, Drug Sci. 8 (2022 Sep 22). Available from: 〈 https://journals.sagepub.com/doi/10.1177/2 0503245221114323〉.

[30] M.P. Davis, Cannabinoids for symptom management and cancer therapy: the evidence, J. Natl. Compr. Cancer Netw. 14 (7) (2016 Jul 1) 915–922. 〈https://p ubmed.ncbi.nlm.nih.gov/27407130/〉 (Available from).

[31] F. Siedentopf, I. Utz-Billing, S. Gairing, W. Schoenegg, H. Kentenich, I. Kollak, Yoga for patients with early breast cancer and its impact on qualityof life – a randomized controlled trial, Geburtshilfe Frau 73 (4) (2013) 311 [cited 2023 Nov 24];.

[32] J.W. Carson, K.M. Carson, L.S. Porter, F.J. Keefe, H. Shaw, J.M. Miller, Yoga for women with metastatic breast cancer: results from a pilot study, J. Pain. Symptom Manag. 33 (3) (2007 Mar 1) 331–341.

[33] The Gerson Therapy [Internet]. [cited 2023 Oct 23]. Available from: 〈https://gers on.org/how-it-works/〉.

[34] C.H. Lo, Traditional chinese medical analysis, Integr. Cancer Ther. 1 (1) (2002 Mar) 55–56. 〈https://journals.sagepub.com/doi/abs/10.1177/1 534735402001001 10〉. cited 2023 Nov 24];1(.

[35] A.H. Lee, S. Kabashneh, C.P. Tsouvalas, U. Rahim, M.Y. Khan, M. Anees, et al., Proctocolitis from coffee enema, ACG Case Rep. J. 7 (1) (2020 Jan) e00292. Available from: 〈https://journals.lww.com/acgcr/fulltext/2020/01000/proctoco litis_from_coffee_enema.8.aspx

[36] J.L. Roseman-Halsband, Is color and light therapy an effective complementary therapy for oncology patients? An analysis of one practitioner's anecdotal experiences. Alter. Complement Ther. 24 (3) (2018 Jun 1) 121–128. Available from: 〈https://www.liebertpub.com/doi/10.1089/act.2018.29165.jlr〉.

[37] A. Mashekova, Y. Zhao, E.Y.K. Ng, V. Zarikas, S.C. Fok, O. Mukhmetov, Early detection of the breast cancer using infrared technology – a comprehensive review, Therm. Sci. Eng. Prog. 27 (2022 Jan 1) 101142.

[38] M. Gautherie, Thermopathology of breast cancer: measurement and analysis of in vivo temperature and blood flow, Ann. N. Y Acad. Sci. 335 (1) (1980 Mar 1) 383–415. Available from: 〈https://onlinelibrary.wiley.com/doi/full/10.1111/j.1 749-6632.1980.tb50764.x

Oncotherm
HYPERTHERMIC IMMUNO-ONCOLOGY

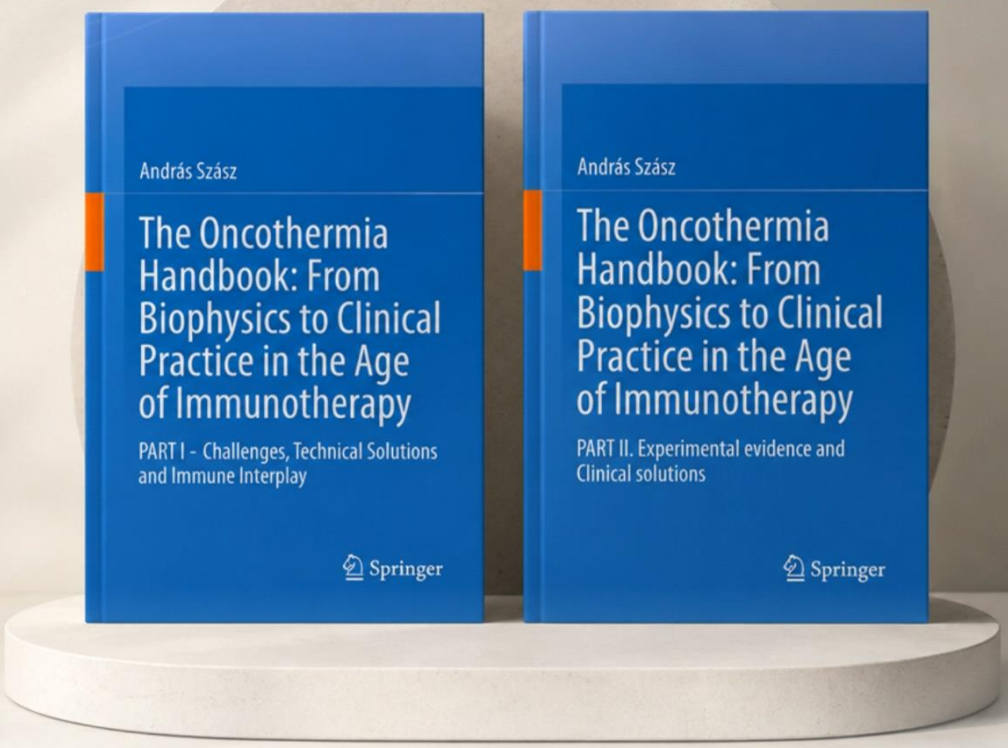

Now Available

The Oncothermia Handbook by Prof. András Szász

Volume I
Biophysics to Clinical Practice

The first volume introduces the theoretical framework of oncothermia, covering its biophysical principles, biological mechanisms of action, and the scientific rationale behind the treatment. It also places oncothermia within the broader context of contemporary cancer therapy.

Volume II
Experimental and Clinical Evidence

The second volume focuses on experimental research, clinical studies, treatment outcomes, and practical applications across various cancer types. It highlights the growing body of evidence supporting oncothermia and discusses future perspectives for clinical practice.

More information

https://oncotherm.com/the-oncothermia-handbook-released/

EHY-2030

Loco-regional modulated electro-hyperthermia (mEHT) device

The EHY-2030 is Oncotherm's latest development for the loco-regional treatment of tumors. The newly designed device includes the Smart Electrode system and the integrated Patient Management System (PMS) and a user-friendly touch screen display with full system control. The new RF generator with impulse mode increased peak power has been developed with a new intelligently controlled step motor tuning system for rapid impedance matching to achieve shorter tuning-time.

The EHY-2030 device is a CE-marked medical device, and is intended for professional use.

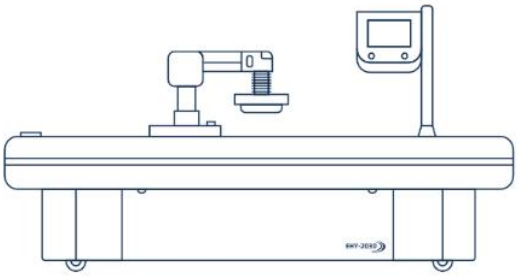

Oncotherm
HYPERTHERMIC IMMUNO-ONCOLOGY

Oncotherm Kft. | Gyár utca 2. | 2040 Budaörs, HUNGARY
+36 23 555 510 | info@oncotherm.org | www.oncotherm.com